ABSTRACT

Title of Document: **MOLECULAR MECHANISMS UNDERLYING CADHERIN-6B INTERNALIZATION IN PREMIGRATORY CRANIAL NEURAL CREST CELLS DURING THEIR EPITHELIAL-TO-MESENCHYMAL TRANSITION**

Rangarajan Padmanabhan, Doctor of Philosophy, 2015

Directed by: **Lisa Taneyhill, Assistant Professor, Department of Animal and Avian Sciences**

The generation of migratory cells from immotile precursors occurs frequently throughout development and is crucial to the formation and maintenance of a functioning organism. This phenomenon, called an epithelial-to-mesenchymal transition (EMT), involves the disassembly of intercellular adhesions and cytoskeletal rearrangements in order to promote migration. Importantly, aberrant EMTs and cell migration can lead to devastating human conditions including cancer metastasis and fibrosis. How cells accomplish EMT to become migratory is still an unanswered question in the biomedical field. To this end, we use chick neural crest cells as an *in vivo* model to elucidate the molecules and pathways that regulate EMT and migration. Neural crest cells are a population of embryonic cells that are originally stationary within the dorsal neural tube but later migrate to form a variety of adult derivatives, such as the craniofacial skeleton, skin pigment cells and portions of the heart. To facilitate EMT, chick premigratory neural crest cells lose intercellular contacts mediated, in part, by the transmembrane cell adhesion protein Cadherin-6B (Cad6B). While *Cad6B* mRNA is transcriptionally repressed in premigratory neural crest cells, loss of Cad6B protein does not directly follow and instead occurs ~90 minutes later, just prior to migration. This rapid depletion of Cad6B is all the more striking given that the half-life of most cadherins, including Cad6B, is ~6-8 hours *in vitro*. As such, unique post-

translational mechanisms must exist to remove Cad6B from premigratory neural crest cell plasma membranes to facilitate neural crest EMT. Since cadherins are known to be downregulated through internalization mechanisms (e.g., endocytosis, macropinocytosis) in other *in vitro* systems, the hypothesis of this dissertation is that Cad6B is internalized, and that this process plays a critical function to enable neural crest EMT. To this end, we document the existence of Cad6B cytoplasmic puncta in cultured cells, cultured neural crest cells and transverse sections of chick embryos. We subsequently identified a p120-catenin binding motif in the Cad6B cytoplasmic tail and demonstrated its functionality through site-directed mutagenesis, revealing a role in enhancing Cad6B internalization and reducing the stability of membrane-bound Cad6B. Furthermore, we uncover for the first time that Cad6B is removed from premigratory cranial neural crest cells through cell surface internalization events that include clathrin-mediated endocytosis and macropinocytosis. Both of these processes are dependent upon the function of dynamin, and inhibition of Cad6B internalization abrogates neural crest cell EMT and migration. Collectively, our findings provide a molecular blueprint for how cadherins are dynamically regulated during the formation of migratory cell types required for normal embryonic development and tissue repair as well as those generated during human diseases and cancers. Importantly, our research is multi-disciplinary, integrating cell biology and physiology to reveal how a cellular event, the active downregulation of a membrane protein, results in a physiological event, neural crest EMT and migration.

MOLECULAR MECHANISMS UNDERLYING CADHERIN-6B INTERNALIZATION IN PREMIGRATORY CRANIAL NEURAL CREST CELLS DURING THEIR EPITHELIAL-TO-MESENCHYMAL TRANSITION

By

Rangarajan Padmanabhan

Dissertation submitted to the Faculty of the Graduate School of the
University of Maryland, College Park, in partial fulfillment
of the requirements for the degree of
Doctor of Philosophy
2015

Advisory Committee:
Dr. Lisa Taneyhill (Chair)
Dr. Iqbal Hamza
Dr. Tom Porter
Dr. Stephen Wolniak
Dr. Alexandra Bely, Dean's Representative

Acknowledgements

This endeavor of Graduate School, which started in August 2007, is finally coming to an end 7.5 years later. The journey has been long, and because of that very reason has witnessed significant changes in my personality, character, and the way I see and interact with the world. The loneliness, frustration, anxiety, and the monetary insecurity of Graduate School changed my attitudes and my perspectives of the world like no other earlier phase. It will take the same amount of time in the "normal world" to regain much my old self. To begin with, I thank Biology for being interesting and being the single exclusive factor I was able to weather all the negativity associated with this journey. Biology is beautiful in my mind, in its most poetic sense. I can't imagine doing anything else that would keep me self-motivated for 7.5 years!

People have come and left, and memories have been formed and changed in this voyage. On top of providing great company after a tiring day, these personalities have shaped my attitudes one way or the other: Kiran, Siddharth, Ramanand, Ranjan, Umang, Bhaven, and Sesha being the most noteworthy of them in the chronological order. I wish I can stay in touch with them for this lifetime. And while I thank the friends who have come and left, I have to thank the ones that were always with me- Giridhar Thiagarajan. Being the most unlikely people who can become friends, our friendship has somehow endured 12 years thus far, and I hope this continues for a lifetime.

Coming on to the academic part of this endeavor, I am very thankful to Lisa for everything. When I left Dr. Perez's lab with an MS, unable to mesh with the science of infectious diseases, Lisa took her chances on me. Being her first graduate student, I've enjoyed most of her attention and mentoring, and I leave with a very positive experience.

She has been a mentor for both science and non-science. She always critically oversaw my ideas and data, only to make it better at the end of the day. Her style of communication, time-management, professionalism, and people-management are all lessons that I will carry long and far. Thanks to her rigorous oversight, my writing has become much better than what it was 5 years ago. Being a mother and an assistant professor, she taught me that I can never get away saying I have too much to do and don't have enough time.

This story wouldn't have come to its current shape without the guidance of my committee members Dr. Alexa Bely, Dr. Iqbal Hamza, Dr. Tom Porter, and Dr. Steve Wolniak. Their suggestions and thoughtful criticisms during my committee meetings has steered my project away from problematic hurdles to a meaningful completion. In addition, I also thank Dr. Wolniak for his time and assistance in microscopy, and Dr. Porter for helping me apply and secure several graduate school fellowships.

I thank all the past and present members of the Taneyhill lab who have provided all their friendship and support over the years. Thanks to Chyong-Yi, Andy, Ankita, Sharon, Rachel, and Shen, the lab was a very pleasant place to be spending most of the waking hours in a day. They have not only graciously lent their ears to my frustrated rants, but also have been great conversationalists on anything under the sky. Thanks to Lisa's management style, the lab always felt like a congenial place rather than it's opposite. Thanks to Andy for his insightful thoughts on my data, for they have been tremendously helpful a lot of times. In summary, life would have been very miserable the last 5 years if not for such a wonderful lab.

As I thank the lab, I have to thank the wonderful faculty and staff at the Department of Animal and Avian Sciences. Thanks to the small size and a wonderful Chair, the

Department of Animal and Avian Sciences has always felt like a family. Dr. Keefer has been a wonderful graduate chair and has always supported me in my (successful) attempts to obtain graduate scholarships and fellowships. I should also thank Kim and the wonderful sweet ladies at the business office- Sheryl, Sandra, and Janice for their tremendous assistance in getting the innumerable paperwork done in this process. I sincerely thank Dr. Ashley Franklin, a graduate student alumni of the department for her help in performing statistics on my data.

I finally would like to thank my family for their patience, confidence and support in making this happen. Coming this far from a middle-class Indian family is not easy, and if not for their patience, this wouldn't have happened. Especially, if not for my brother and my sister-in-law and their financial support for the family, I couldn't have gone too far showing my almost-empty pockets. Thanks to my family for believing in me and letting me do what I wanted to do, in spite of dire financial struggles 7 years back. And finally, thanks to my lovely wife Shruthi. Although she entered my life only in the last year of my graduate school, her help in this short period of time has been immense. She has not only compromised her time that I should have been spending for/with her, but also spent several late nights in the lab and at the confocal sleeping on the chairs while I was working to finish up my experiments. Her enormous support during the time I was writing this dissertation is unforgettable. She learned to live on my frugal graduate student budget, asking for the smallest of things and finding joy in the cheapest of gifts. In summary, she was always there for me, in my happy and unhappy times, and if not for her, this last year would have been really difficult.

Table of contents

List of Figures

Chapter 1

Chapter 2

Chapter 3

Chapter 4

Chapter 5

Appendices

List of Tables

Abbreviations

Cad6B	Cadherin6B
EMT	Epithelial-to-Mesenchymal Transition
NT6B	Antibody that recognizes N-terminal end of Cad6B
CT6B	Antibody that recognizes C-termial end of Cad6B
HA	Hemagglutinin
GFP, RFP	Green and Red Fluorescent Protein
CHO	Chinese Hamster Ovary
wtCad6B-HA	wild-type Cad6B
LI645AA-HA	Cad6B mutant wherein LI at position 645 substituted with AA
EED666AAA-HA	Cad6B mutant wherein EED at position 666 substituted with AAA
SEM	Standard Error of Mean
CHX	Cycloheximide
TX100	TritonX-100
CSK	Cytoskeleton
ADAM	A Disintegrin And Metalloprotease

Chapter 1. Literature Review

Parts of this Introduction were adapted from the following published book chapter:

Taneyhill LA and Padmanabhan R. (2013)

Chapter 3: The Cell Biology of Neural Crest Cell Delamination and EMT (pp. 51-66).

In: **Neural Crest Cells: Evolution, Development and Disease**. Edited by P. Trainor.

Elsevier, Inc., Taramani, Chennai, India.

1.1. The Neural Crest: An Overview

Neural crest cells are an embryonic, multipotent cell population that played a crucial role in vertebrate evolution. It is thought that William His discovered neural crest cells in 1868, but the actual term was later coined by Arthur Milnes Marshall in line with the anatomical origins of these cells (Hall, 2008). Neural crest cells have been a subject of fascination for embryologists and cell biologists and have been used to investigate embryonic cell induction, specification, commitment, delamination, migration, cell fate determination. Neural crest cells are also known as the fourth germ layer, considering the wide range of adult derivatives that arise from these cells: neurons and glia of sensory, autonomic and enteric ganglia, smooth muscle cells, melanocytes, medullary secretory cells, and bone and cartilage cells. For this reason and the fact that they possess some regenerative capacity, neural crest cells have been considered for use for stem cell-based therapies (Crane and Trainor, 2006).

Apart from their multipotency, the appearance of neural crest cells is synonymous with the appearance and evolution of vertebrates. The transition from protochordate body to a vertebrate body plan has been associated with an increasing ability to actively acquire food. The primitive chordates, including the cephalochordates and urochordates, were filter feeders that fed by taking in water through a primitive, non-muscularized ciliated pharynx and filtered whatever food particles came through it (Hall, 2009; Douarin NM, 2014). The shift from passive filter feeders to active predation (vertebrates) required several features, including a muscularized pharynx to push food (which later led to the development of jaws and the craniofacial skeleton), ectodermal placodes (to sense food in different aspects, such as smell, sight and sound, and a brain to integrate these signals), and pharyngeal breathing

characterized by gill capillaries. Of these vertebrate innovations, neural crest cells were responsible for the evolution of a muscularized pharynx and nervous systems to integrate placodal signals. Thus, neural crest cells were important in the evolution of vertebrates from their proto-chordate ancestors (Hall, 2009; Douarin NM, 2014).

Several diseases have been associated with abnormal development of neural crest cells and neural crest cell derivatives, and are referred to as neurocristopathies (Bolande, 1997). Some of the most common birth defects linked to aberrations in neural crest cell formation include Waardenburg-Shah syndrome (aganglionic megacolon, hypopigmentation and deafness), Hirschsprung disease (megacolon, hypopigmentation and deafness), DiGeorge syndrome (thymic hypoplasia, craniofacial and heart defects), and Treacher-Collins syndrome (cleft palate, micrognathia and deafness) (Etchevers et al., 2006; Jones et al., 2008; Passos-Bueno et al., 2009; Keyte and Hutson, 2012). Furthermore, tumors such as melanoma (melanocytes), neuroblastoma (sympathoadrenal cells), and pheochromocytoma (chromaffin cells of the adrenal medulla) are of neural crest origin (Kerosuo and Bronner-Fraser, 2012; Theveneau and Mayor, 2012; Mayor and Theveneau, 2013).

Neural crest cells can be grouped into four categories based primarily upon their axial level of origin in the embryo. These include cranial, vagal and sacral, cardiac, and trunk, and neural crest cells from each domain have distinct migratory characteristics and form specific adult structures upon differentiation (Sauka-Spengler and Bronner, 2010). Cranial neural crest cells migrate dorsolaterally to give rise to most of the craniofacial skeleton, cranial neurons and glia and connective tissues of the face (Fig. 1.1). Vagal and sacral neural crest cells generate the parasympathetic or enteric ganglia of the gut, while

cardiac neural crest cells (not shown in the figure) form the endothelium of the aortic arch arteries and the septum between the aorta and the pulmonary artery. Trunk neural crest cells will differentiate to give rise to melanocytes, sensory and sympathetic neurons, Schwann cells, and adrenomedullary cells (Sauka-Spengler and Bronner, 2010)

1.2. Neural Crest Cell Induction

Neural crest cell progenitors are induced at the border of the neural plate through signals from the neuroectoderm, which will form the future brain and spinal cord, the non-neural ectoderm, which will form the future epidermis, and the mesoderm. During neurulation (Fig. 1.1), an indentation forms along the midline as the neural plate invaginates and concomitantly the edges (which contain the neural crest cell progenitors) elevate to form the neural folds. At the end of neurulation, the elevating neural folds fuse in the dorsal midline creating the hollow neural tube, which eventually pinches off and separates from the overlying ectoderm. Neural crest cells now lie at the dorsal region of the neural tube, where they are referred to as premigratory neural crest cells. These cells lose intercellular contacts, delaminate (detach) and migrate away from the neural tube (Sauka-Spengler and Bronner-Fraser, 2008) to form the varied derivatives described above.

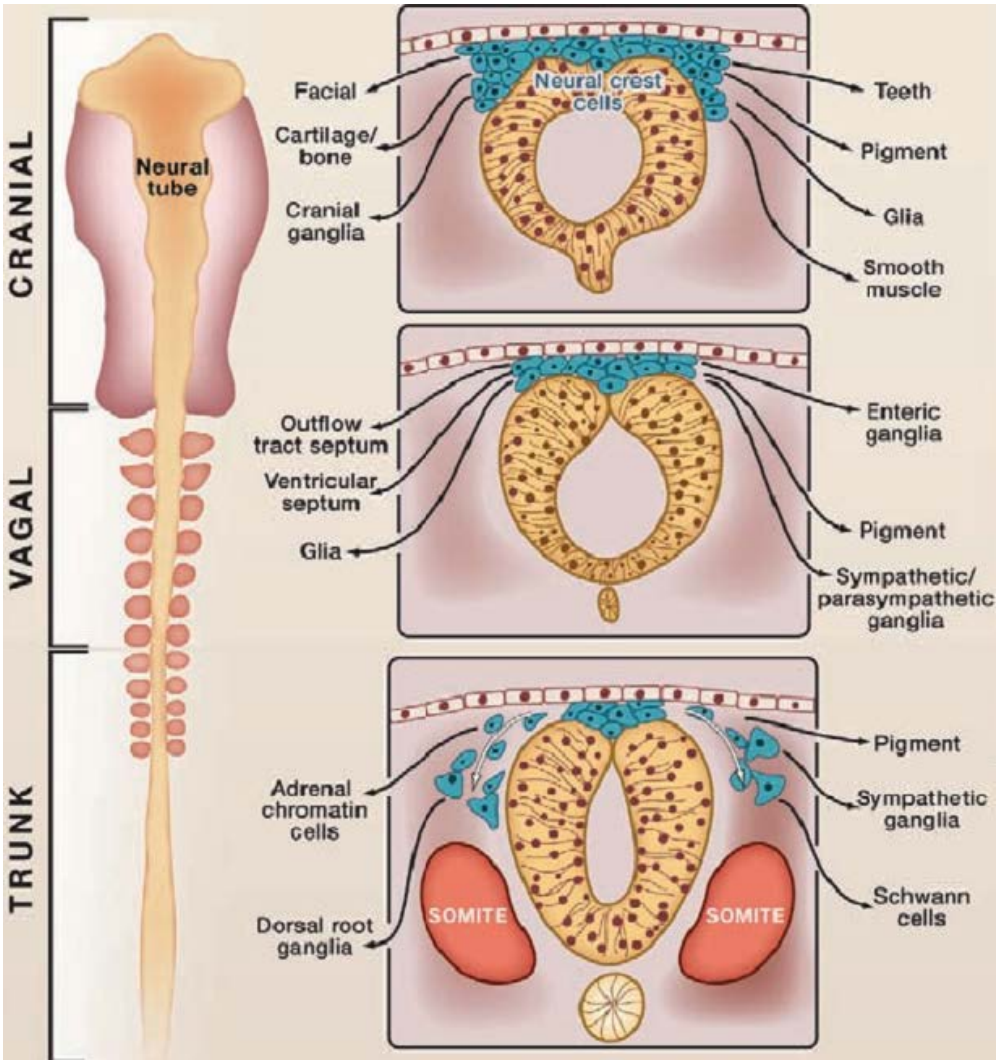

Figure 1.1. Neural crest cells form a variety of adult derivatives. Shown on the left is a cartoon diagram of a developing human embryo (dorsal view), with the cranial region (rostral) at the top and the tail region (caudal) at the bottom. Based on the adult derivatives and the axial region of the embryo from which they originate, neural crest cells can categorized as cranial, vagal (including cardiac) and trunk. Shown on the right are transverse sections at the appropriate axial region in the whole-mount image on the left, with neural crest cells in blue residing at the dorsal region of the hollow neural tube as well as a list of the different adult derivatives that arise from those neural crest populations. Image reproduced from (Sauka-Spengler and Bronner, 2010).

Although the overall steps in neural crest cell formation are conserved, the exact sequence varies between species. In mouse and *Xenopus*, cranial neural crest cell delamination occurs while the neural tube is still open (Nichols, 1981; Sadaghiani and Thiebaud, 1987), while in aves it occurs concurrent with neural fold fusion (Duband and Thiery, 1982; Theveneau et al., 2007) (Fig.1.2). Furthermore, cephalic and trunk neural crest cell populations fundamentally differ in their formation and delamination from the neural tube, and the implications of this are only recently coming to light. While cranial neural crest cells delaminate *en masse*, trunk neural crest cells delaminate progressively (Thiery et al., 1982; Erickson and Weston, 1983; Sadaghiani and Thiebaud, 1987; Jesuthasan, 1996; Davidson and Keller, 1999; Duband, 2010; Krispin et al., 2010), leaving the neural tube one by one over an extended period of time (Fig. 1.2). The molecular differences between cranial and trunk neural crest cell delamination and EMT are very intriguing, and studies are required to elucidate the evolutionary rationale and the molecular mechanism(s) underlying these differences.

Figure 1.2. Neural crest cell EMT varies temporally and spatially in different species. (A) The dorsal region of a vertebrate embryo at the early neurula stage, with neural crest cells shown in green at the border of the open neural plate (blue). (B) *Xenopus* cephalic neural crest cells delaminate between stages 16 and 18 while the neural tube is still open. (C) Similar to *Xenopus,* mouse cephalic neural crest cells delaminate at the open neural plate stage. (D) Chick cephalic neural crest cells undergo massive EMT after neural tube closure. (E) Delamination of chick or mouse rostral trunk neural crest cells occurs one by one in a drip-like fashion, and migration begins as neural crest cells leave the neural tube. The premigratory neural crest cell domain and neural crest cells are shown in green, and red round cells represent mesenchymal neural crest cells or neural crest cells undergoing EMT. The neural plate/tube is in blue, the non-neural ectoderm is in yellow, and the mesoderm and its derivatives are in pink. Two things that are noticeable in the figure are that (1) delamination and EMT are distinct events (see Section 2.2) and (2) cephalic neural crest cells undergo *en masse* EMT, as compared to trunk neural crest cells which undergo progressive EMT. Image reproduced from (Theveneau and Mayor, 2012).

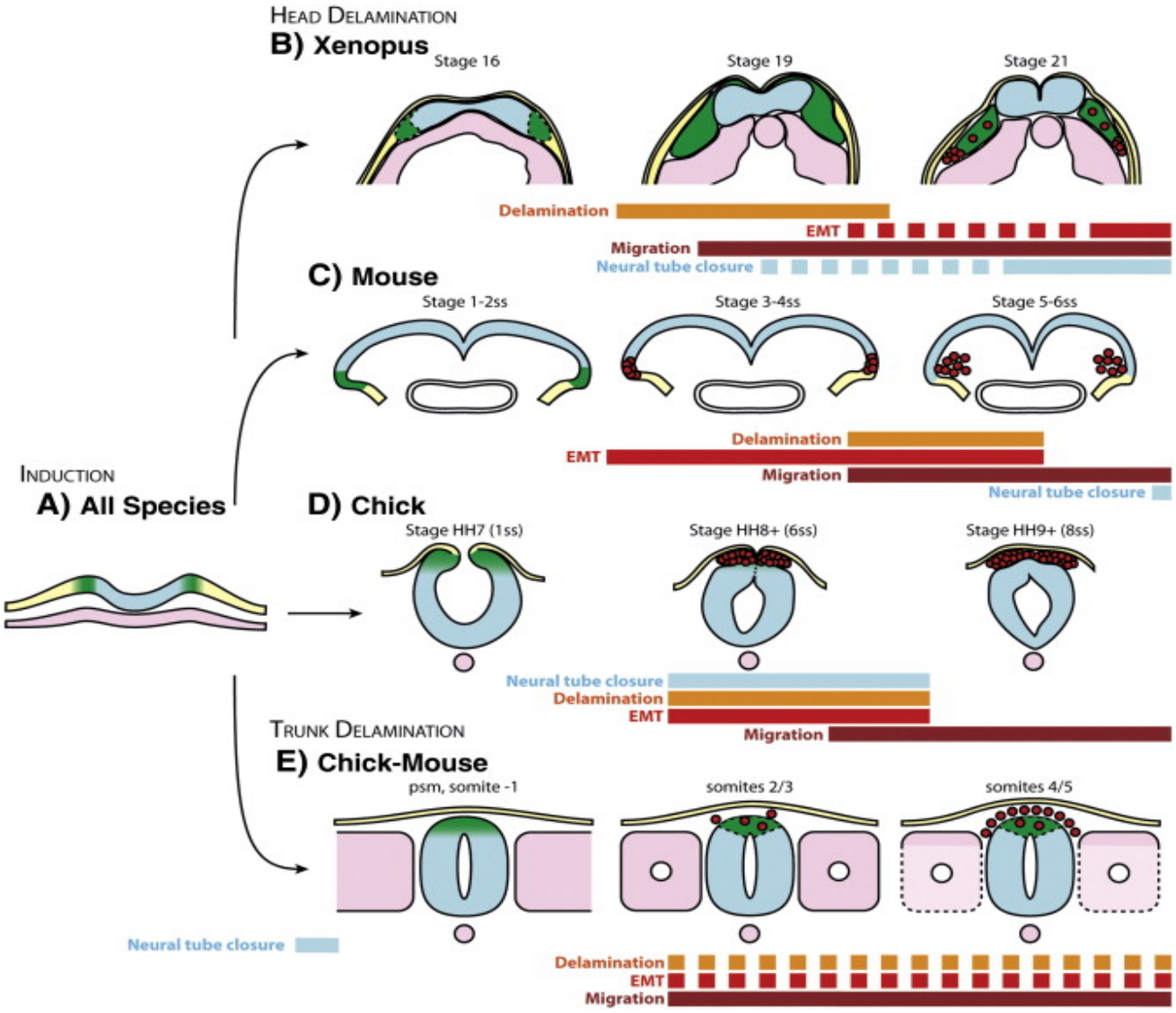
HEAD DELAMINATION
B) Xenopus
Stage 16
Stage 19
Stage 21
Delamination
EMT
Migration
Neural tube closure
C) Mouse
Stage 1-2ss
Stage 3-4ss
Stage 5-6ss
Delamination
EMT
Migration
Neural tube closure
INDUCTION
A) All Species
D) Chick
Stage HH7 (1ss)
Stage HH8+ (6ss)
Stage HH9+ (8ss)
Neural tube closure
Delamination
EMT
Migration
TRUNK DELAMINATION
E) Chick-Mouse
psm, somite -1
somites 2/3
somites 4/5
Neural tube closure
Delamination
EMT
Migration

Neural crest cells are generated by complex signals that function to induce them at precise spatiotemporal locations. Chiefly, these signals include Bone Morphogenetic Protein (BMP), Fibroblast Growth Factors (FGFs), and vertebrate homologues of the Drosophila Wingless proteins (Wnts). BMPs play a crucial role in specifying prospective neural crest cells. In *Xenopus* embryos, high levels of BMP will lead to non-neural ectoderm, low levels give rise to neuroectoderm (Wilson and Hemmati-Brivanlou, 1995), and intermediate levels permit the formation of neural plate border cells (LaBonne and Bronner-Fraser, 1998; Marchant et al., 1998). In the chick, both BMP4 and BMP7 are expressed in the ectoderm, and each individually is necessary and sufficient for neural crest cell induction (Liem et al., 1995; Liem et al., 1997), suggesting that a single upstream activator can use either BMP4 or BMP7 as a downstream inducing factor. This requirement was further refined by work from Ragland and Raible who showed that during gastrulation and neurulation, BMP inhibition and activation, respectively, is required to specify neural crest cell precursors (Ragland and Raible, 2004), indicating that the role of BMPs in chick neural crest specification is more complex than previously thought. Moreover, prior studies have shown that BMP signaling alone cannot account for neural crest cell induction *in vivo* or *in vitro*, and that other signaling pathways are also involved (LaBonne and Bronner-Fraser, 1998; Garcia-Castro et al., 2002).

In keeping with this, FGFs and Wnts have also been implicated in neural crest cell induction. Inhibiting FGF signaling significantly hampers neural crest cell induction in *Xenopus* and the chick (Mayor et al., 1997; Villanueva et al., 2002). Similarly, Wnt inhibition suppresses expression of neural crest cell markers, while active Wnt is required for neural crest cell induction in the chick, *Xenopus* and zebrafish (Saint-Jeannet et al.,

1997; LaBonne and Bronner-Fraser, 1998; Deardorff et al., 2001; Garcia-Castro et al., 2002; Lewis et al., 2004; Wu et al., 2005; Steventon et al., 2009). Both of these signaling pathways, including crosstalk between them, are required for neural crest cell induction (Mayor et al., 1995; Mayor et al., 1997; Hong et al., 2008). Therefore, neural crest cell induction is complex and likely requires the convergence of multiple environmental cues.

1.3. Neural Crest Cell Specification

The combined signaling cues described above converge and induce a set of genes called the neural plate border specifiers, which sets apart neural plate border cells from other border progenitors by conferring on them the competence to respond to neural crest–specifying signals and allocating them as neural crest cell precursors. These factors include protein products of *Zic1, Msx1, Msx2, Dlx3, Dlx5, Pax3* and *Pax7* (Fig.1.3). Although knowledge on the order and downstream effects of activation of these genes is sparse, considerable information is available regarding how distinct signaling pathways activate neural plate border specifier genes (for reviews see (Sauka-Spengler and Bronner-Fraser, 2008; Betancur et al., 2010)). Nevertheless, work carried out in lamprey embryos has provided some insight into the temporal order of activation of these genes due to the slow development of these organisms (Nikitina et al., 2008). From these studies, *Msx* and *AP2α* reside at the top of the cascade, with border specifiers such as *Msx, Pax3/7* or *Zic* and early neural crest specifiers such as *AP2α*, *n-Myc* or *Id* feeding back and cross-regulating one another (Nikitina et al., 2008).

Once neural plate border cells have been primed by the expression of neural plate border specifiers, prospective neural crest cells commence the process of specification into

bona fide neural crest cells. This is noted by expression of a new set of genes, including *Snail1, Snail2, Sox8, Sox9, Sox10, FoxD3, AP-2, Twist, c-Myc*, and *Id* family members (Sauka-Spengler and Bronner-Fraser, 2008; Betancur et al., 2010) (Fig. 1.3). These genes regulate a variety of downstream targets that enable neural crest cells to segregate and delaminate from the neuroepithelium (a process referred to as the epithelial-to-mesenchymal transition, or EMT), migrate away from the neural tube and cease migration and differentiate at their destination sites. Additionally they play important roles in controlling population size and the cell cycle (Betancur et al., 2010) (see below). The role of *Snail* and *Twist* genes, both of which are involved in EMT, will be discussed in detail later, but the functions of *SoxE* and *FoxD3* will be briefly described here.

The SoxE transcription factor family, which includes *Sox8, Sox9* and *Sox10*, has well-established roles in neural crest cell development (Nelms BL, 2010). Knockdown of *Sox8, Sox9* or *Sox10* in *Xenopus* results in the loss of expression of several neural crest cell specifier genes, including *Snail2, FoxD3* and *Twist* (O'Donnell et al., 2006). In zebrafish and mouse, neural crest cell specification is not perturbed after Sox10 knockdown, but neural crest cells fail to migrate and eventually undergo apoptosis (Dutton et al., 2001; Reiprich et al., 2008). In the chick, Sox9 functions in neural crest cell progenitor formation, delamination and in the development of specific neural crest cell derivatives (Cheung et al., 2005; Sakai et al., 2005). Similarly, the winged-helix transcription factor FoxD3 is an important regulator of neural crest cell development in all vertebrates. In the mouse embryo, FoxD3 is required for maintenance of multipotency (Lister et al., 2006) and controls cell survival (Teng et al., 2008). In zebrafish, *FoxD3* homozygous mutants show increased apoptosis in a subpopulation of migratory hindbrain neural crest cells (Stewart

et al., 2006). Overexpression of FoxD3 in the chick embryo dorsal neural tube (containing the premigratory neural crest cells) expands the neural crest cell domain, as demonstrated by ectopic induction of migratory neural crest cell markers (Sasai et al., 2001).

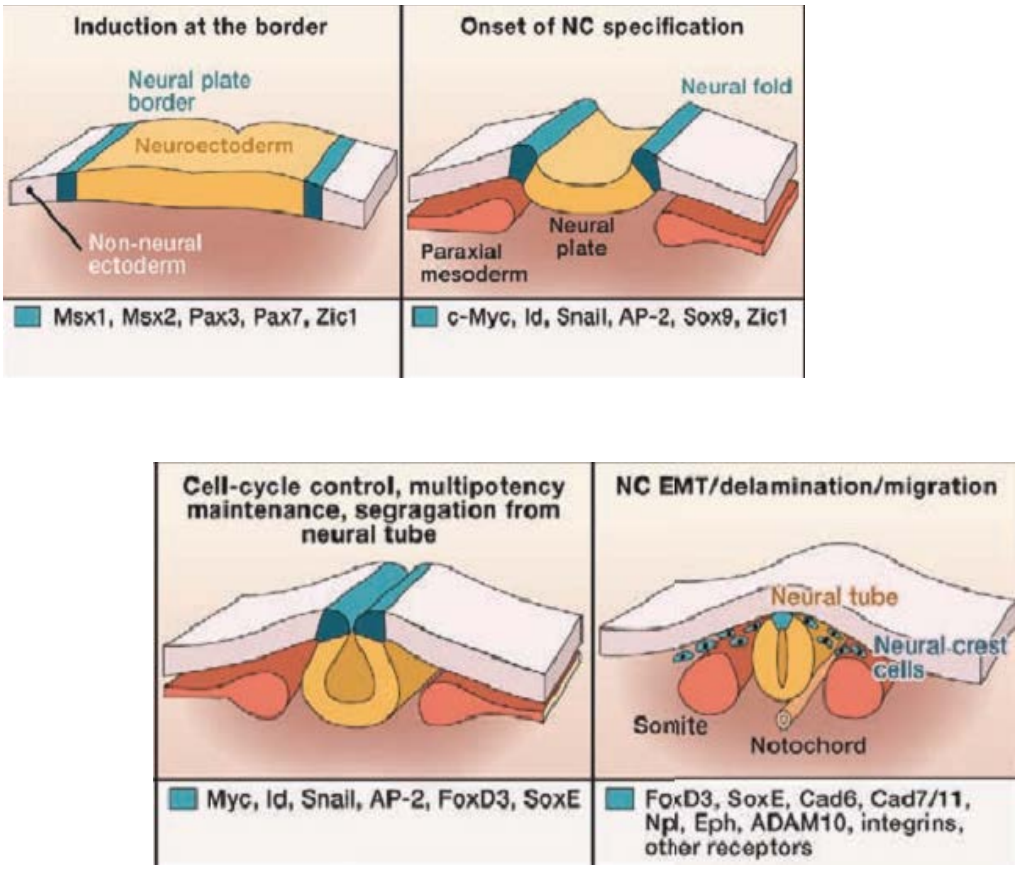

Figure 1.3. The neural crest gene regulatory network is responsible for the induction, specification, EMT, migration and differentiation, of neural crest cells. Neural crest cell induction at the neural plate border is mediated by FGF from the underlying mesoderm as well as Wnts from the mesoderm and adjacent non-neural ectoderm (epidermis). These signals result in the expression of neural plate border specifiers such as Pax3 and Zic1 in a manner that is dependent upon intermediate levels of BMP. Pax3 and Zic1 act synergistically to upregulate other downstream neural crest cell specifiers in the neural folds such as Snail, FoxD3 and members of the SoxE transcription factors. Genes controlling later migration and differentiation are not shown. Image reproduced from (Sauka-Spengler and Bronner, 2010).

1.4. The Epithelial-to-Mesenchymal Transition of Neural Crest Cells

Epithelial cells are tightly associated to one another, exhibit apical-basal polarity and are anchored to the basement membrane, thereby providing a penetrable barrier and maintaining structural integrity (Hay, 2005). Mesenchymal cells, in contrast, are loosely associated with one another and the surrounding tissue, exhibit a front-to-back polarity required for locomotion and are capable of diverse morphological movements (Hay, 2005). Collectively, EMT is defined as the process by which stationary epithelial cells undergo a series of molecular and morphological changes to become migratory mesenchymal cells (Fig.1.4). EMT occurs throughout embryonic development and adult tissue homeostasis (Hay, 1995; Hay, 2005; Thiery et al., 2009) and has been categorized into three types based on the biological context in which the EMT occurs. Type I EMT occurs during implantation, embryo formation and organ development, while type II EMT takes place during wound healing, tissue regeneration and organ fibrosis. Type III EMT is exhibited by cancerous cells when they metastasize (Kalluri and Weinberg, 2009). Although EMT occurs in distinct tissues and at various times during development and disease, many of the cell biological changes and molecular mechanisms underscoring EMT are conserved (Thiery et al., 2009; Kerosuo and Bronner-Fraser, 2012) (Fig.1.4). This section will detail the molecular and cellular changes associated with EMT as they apply to neural crest cells.

Figure 1.4. The Epithelial-to-Mesenchymal Transition is characterized by the expression of distinct molecular markers. Cartoon diagram of the transition of polarized epithelial cells into mesenchymal cells, with each phase of EMT characterized by the expression of distinct molecular markers. Epithelial cells express junctional components (cadherins, occludins, desmoplakins, claudins), polarity proteins (par and crumb), basement membrane proteins (laminin), and cytoskeletal proteins (cytokeratins), which provide structural integrity for this framework. Morphogens such as TGFβ, BMPs, HGF/SF, FGF, Wnt, and Notch activate transcription factors such as Snail, Zeb, Twist, and Fox, which suppress the expression of a variety of molecules involved in maintaining the epithelial nature of cells. As the epithelial cells become mesenchymal, they express a new repertoire of adhesion, cytoskeletal and matrix components that enable them to actively migrate in a foreign environment. Epithelial cells are depicted in beige, cells undergoing EMT in green and mesenchymal cells in blue. Green solid bars, basement membrane; purple lines, fibrillar extracellular matrix. Image reproduced from (Duband, 2010; Kowalczyk AP, 2014)

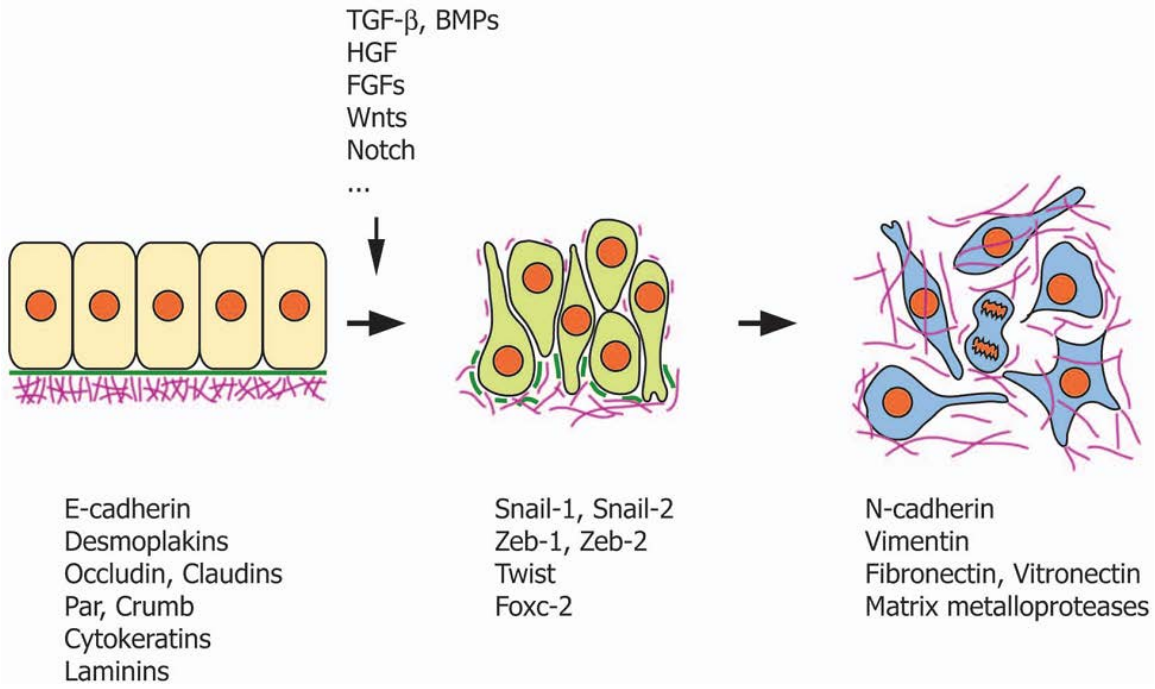

1.5. The Transcriptional Control of Neural Crest Cell EMT

Neural crest cell EMT is orchestrated by the aforementioned transcription factors in Sections 1.2 and 1.3, which all cause significant changes within neural crest cells to enable them to lose cell-cell adhesion, delaminate and emigrate from the neural tube. *Snail* genes are zinc finger transcription factors that were the first to be identified as important players during neural crest cell EMT (Nieto et al., 1994). Indeed, Snail proteins are involved in a wide variety of EMTs during development as well is in diseases characterized by aberrant cell migration (Nieto, 2002). While chick and mouse premigratory neural crest cells express *Snail2* and *Snail1*, respectively, both *Snail* genes are expressed in *Xenopus* premigratory neural crest cells (Swanson, 1989; Thisse et al., 1993; Hewlett et al., 1994; Schnatwinkel et al., 2004). Gain-of-function experiments reveal that *Snail1* in *Xenopus* and *Snail2* in chick are sufficient to induce greater numbers of migrating neural crest cells, whereas knockdown severely decreases neural crest cell migration (Hewlett et al., 1994; Nieto et al., 1994; LaBonne and Bronner-Fraser, 2000). *Cadherins* have been identified as one of the major transcriptional targets of Snail proteins in various systems, including that of neural crest cells and cancers (Batlle et al., 2000; Cano et al., 2000; Taneyhill et al., 2007; Wheelock et al., 2008). In chick premigratory cranial and trunk neural crest cells, Snail2 represses the expression of the premigratory neural crest cell cadherin *cadherin6B* (*Cad6B*) (Taneyhill et al., 2007). Snail proteins transcriptionally repress target genes by binding to E box sequences within their promoters. Specifically, Snail2, together with PHD12 and Sin3A/HDAC, deacetylates lysines on histone H3 within the *Cad6B* promoter, thereby repressing *cad6B* transcription (Taneyhill et al., 2007; Strobl-Mazzulla and Bronner, 2012). The tight junction genes *claudin-3, claudin-4, claudin-7,* and *occludin* are

also targets of Snail transcription factors (Ikenouchi et al., 2003). The function of Snail proteins is not necessarily restricted to transcriptional regulation of junction proteins. Snail1, together with Sox5, upregulates *rhoB*, which plays an important role in neural crest cell EMT by coordinating the rearrangement of the actin cytoskeleton and the formation of focal adhesions and stress fibers (Perez-Alcala et al., 2004).

Additional transcription factors downstream of neural plate border specifier genes control neural crest cell EMT. For example, overexpression of FoxD3 in trunk neural crest cells downregulates N-cadherin while concomitantly upregulating expression of Cadherin-7 and β1 integrin, both of which are expressed in migrating neural crest cells (Cheung et al., 2005; Liang et al., 2014). More recently, FoxD3 has been shown to transcriptionally repress *Tspan18*, whose expression is required for the post-translational downregulation of Cad6B in cranial neural crest cells (Fairchild et al., 2014). Sox10 overexpression also induces *β1 integrin* while inhibiting *N-cadherin* expression (Cheung et al., 2005). Mouse knockouts of *Zeb-2*, another transcription factor expressed in premigratory neural crest cells, have severe deficits in cranial neural crest cell migration along with persistence of E-cadherin (Van de Putte et al., 2003). Recently, Rogers et al. (2013) identified a role for Sip1/Zeb-2 in chick cranial neural crest cell EMT, where Zeb-2 promotes an E-cadherin to N-cadherin switch during EMT (see Section 1.6.2.1 on "Cadherins in Neural Crest Cell EMT") (Rogers et al., 2013). The transcription factor Twist is strongly expressed in migrating cranial, but not trunk, neural crest cells (Hopwood et al., 1989; Soo et al., 2002; Germanguz et al., 2007), and is found downstream of Snail1 (Linker et al., 2000). Importantly, Twist represses *E-cadherin* in several cell types *in vitro* (Vandewalle et al., 2005), and although direct demonstration of Twist activity has not been shown, it is likely

to play a similar role in neural crest cells. Overexpression of c-Myb, another transcription factor present in chick premigratory and migratory neural crest cells, induces expression of *Snail2* and leads to ectopic EMT of neuroepithelial cells in explant cultures (Karafiat et al., 2005; Vandewalle et al., 2005). *Id-2* is another transcription factor expressed in cranial but not trunk premigratory neural crest cells. Ectopic expression of Id-2 in the non-neural ectoderm converts these cells to a neural crest cell-like fate as identified by expression of HNK-1 (labels migratory neural crest cells) (Lee et al., 2013) and the loss of epithelial features (Martinsen and Bronner-Fraser, 1998).

Although the information described thus far focuses exclusively on individual transcription factors, there is extensive cooperation and feedback among them to regulate neural crest cell specification and EMT. For example, in *Xenopus* cranial neural crest cells, Snail1 can enhance its own expression and induce expression of *Snail2, Twist, FoxD3*, and *Ets-1* (Hewlett et al., 1994). In turn, FoxD3 is able to induce itself and *Snail2, Twist, Ets-1, Sox2*, and *NCAM* in *Xenopus* (Sasai et al., 2001). In chick cranial neural crest cells, Sox9 induces *Snail2* but not *FoxD3* (Cheung et al., 2005; Sakai et al., 2006). The promoter regions of *Xenopus Snail2* and *Sox9* both contain binding sites for Lef/Tcf transcription factors, suggesting that they may be regulated by canonical Wnt signaling (Vallin et al., 2001; Bagheri-Fam et al., 2006). Similarly, *Sox10* enhancer sequences isolated from chick cranial neural crest cells possess binding sites for Sox9, Ets-1 and c-Myb, and mutation of these sites abolishes cranial *Sox10* transcription (Betancur et al., 2010). Thus, the genetic network controlling neural crest cell induction, specification and EMT is very complex and involves regulation and cross-control at multiple levels.

1.6. The Cell Biology of Neural Crest Cell EMT

From a cell biological standpoint, neural crest cell EMT can be divided into distinct phases, including cellular delamination, emigration and migration. Although the terms are loosely defined and are often used interchangeably (and thus incorrectly), they do possess distinct characteristics (Fig. 1.2). Delamination is the phase in which cellular adherens and tight junctions are dismantled and neural crest cells round up as they express mesenchymal markers and prepare to leave the neural tube. Emigration refers to the active exiting of neural crest cells from the neural tube prior to their emergence into the embryonic milieu. Migration occurs when neural crest cells have left the confines of the neural tube and have moved into the surrounding embryo tissue and extracellular matrix as they head to their target destinations. This introduction will focus solely on the delamination phase of neural crest cells. The delamination phase consists of three components: the presence of an appropriate substratum for migration, the loss of intercellular adhesion and the acquisition of migratory competence. Reviews on the appropriate substratum for neural crest cell migration and the acquisition of migratory competence are available at (Wilson and Hemmati-Brivanlou, 1995). Loss of intercellular adhesion in epithelial cells requires dismantling of adherens and tight junctions (Fig. 1.5). These junctions constitute the fundamental components that maintain premigratory neural crest cells in an epithelial state, as outlined below.

Figure 1.5. Epithelial sheets (cells) are characterized by intact cellular junctions and apicobasal polarity. Epithelial cells consist of cellular junctions, including adherens, tight and gap junctions; polarity complexes (par proteins); and desmosomes. Adherens junctions are comprised of nectin and cadherin transmembrane proteins, and tight junctions contain the occludin, JAM and claudin transmembrane proteins. Desmosomes and gap junctions are discussed elsewhere (Mese et al., 2007; Kowalczyk AP, 2014). These junctional proteins are bound by several cytoplasmic proteins that link them to the actin cytoskeleton, thus providing structural integrity to the epithelial sheet. Image reproduced from (Sleeman and Thiery, 2011).

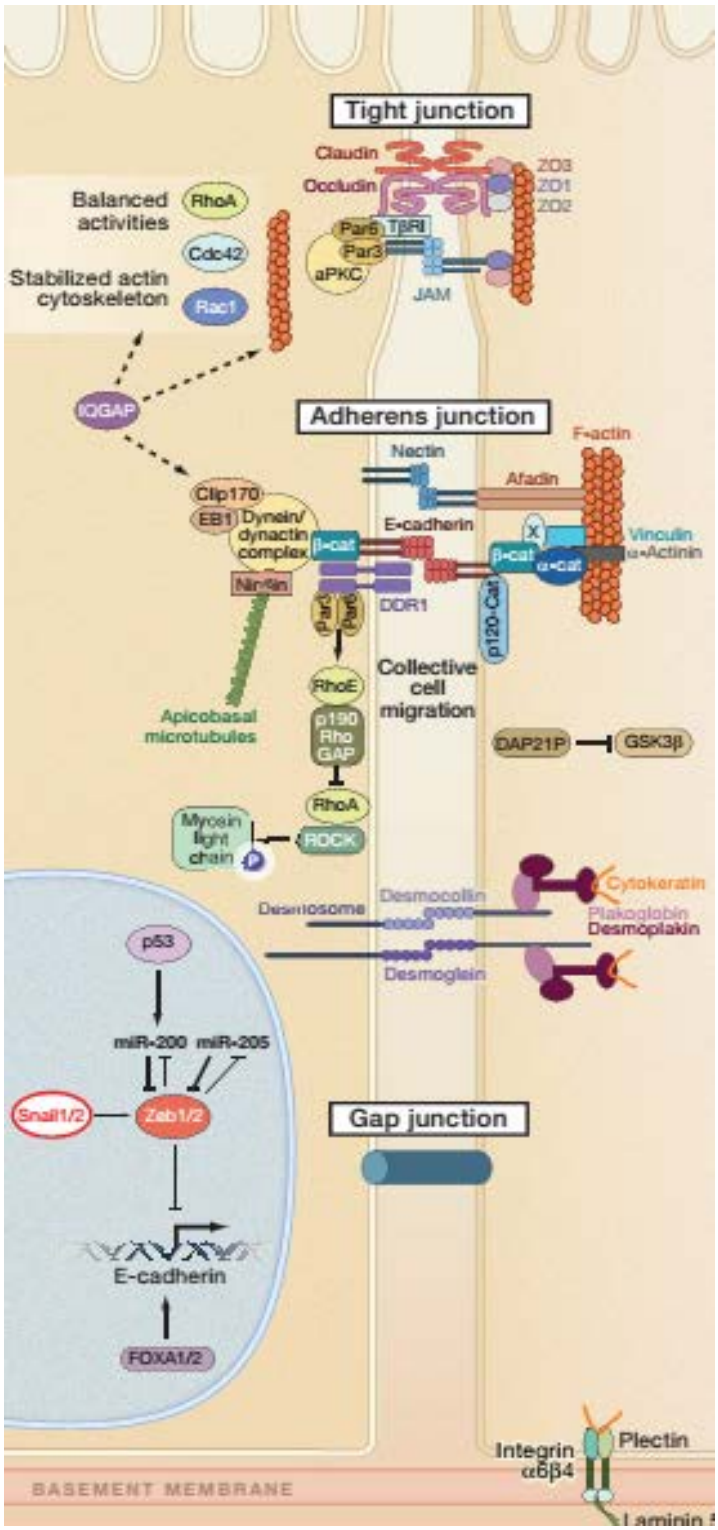
Tight junction
Claudin
Occludin
ZO3
ZO1
ZO2
Balanced activities
RhoA
Cdc42
Rac1
Stabilized actin cytoskeleton
Par6
TβRI
Par3
aPKC
JAM
IQGAP
Adherens junction
F-actin
Nectin
Afadin
Clip170
EB1
Dynein/ dynactin complex
E-cadherin
β-cat
α-cat
Vinculin
α-Actinin
Nin/Lin
DDR1
p120-Cat
Collective cell migration
RhoE
Apicobasal microtubules
p190 Rho GAP
DAP21P
GSK3β
RhoA
Myosin light chain
ROCK
Cytokeratin
Desmocollin
Desmosome
Plakoglobin
Desmoplakin
Desmoglein
p53
miR-200
miR-205
Snail1/2
Zeb1/2
Gap junction
E-cadherin
FOXA1/2
Integrin α6β4
Plectin
BASEMENT MEMBRANE

1.6.1. Neural Crest Cell Tight Junctions

Tight junctions or zonula occludens, present at the most apical surface of the membrane, regulate the diffusion of solutes through the plasma membranes of apposing cells with size and charge selectivity, and prevent the diffusion of transmembrane proteins between the apical and basolateral membranes (Furuse, 2010). Tight junctions consist of membrane-bound and cytoplasmic proteins. Claudins constitute the key transmembrane proteins for tight junction formation and function, creating tight junctions through homophilic interactions with claudins of apposing cells (Ikenouchi et al., 2005; Furuse, 2010). Apart from claudins, occludin, tricellulin and JAM-A are the other transmembrane proteins of the tight junctions (Furuse, 2010). ZO-1, ZO-2 and ZO-3 are the major cytoplasmic proteins that interact with the cytoplasmic domain of these transmembrane proteins (Stevenson et al., 1986; Gumbiner et al., 1991; Haskins et al., 1998). Cingulin is another cytoplasmic protein concentrated relatively far from the tight junctions (Citi et al., 1988) that also interacts with ZO proteins (Cordenonsi et al., 1999; D'Atri et al., 2002). Cingulin and ZO proteins interact with the actin cytoskeleton and provide structural integrity for tight junctions (Fanning et al., 1998; Wittchen et al., 1999; D'Atri and Citi, 2001). Recent work in chick, described below, has shed light on the function of tight junction proteins in neural crest cell EMT.

In the chick, claudin-1 is observed in the apical region of the forming neural tube but is downregulated in the cranial dorsal neural folds (and premigratory neural crest cells) well prior to neural crest cell delamination. Migratory neural crest cells are also devoid of claudin-1 protein (Fishwick et al., 2012) (Fig. 1.6). Morpholino-mediated knockdown and overexpression of claudin-1 results in the presence of greater or fewer numbers of

migratory neural crest cells, respectively, but does not affect expression of important neural crest cell molecular markers such as Cad6B and laminin. Instead, the number of premigratory cranial neural crest cells is altered (Fishwick et al., 2012). Taken together, these results suggest that the observed effects on EMT are not through the basal lamina or other junctional proteins but instead through the number of neural crest cell precursors available to migrate (Fishwick et al., 2012).

Expression of another tight junction protein in the chick, cingulin, is similar to that of claudin-1, except that cingulin continues to be diffusely expressed throughout the apical neural tube even after neural crest cell EMT (Wu et al., 2011). Morpholino-mediated knockdown of cingulin increases the number of migratory neural crest cells. Surprisingly, cingulin overexpression also expands the migratory neural crest cell population and is associated with nuclear localization and ectopic delamination of neuroepithelial cells. Interestingly, RhoA levels vary with cingulin in the ventrolateral neural tube, with cingulin knockdown or overexpression increasing or decreasing RhoA levels, respectively. Exogenous cingulin has no influence on RhoA levels in the dorsal neural tube, however, suggesting that the enhanced neural crest cell migration phenotype observed upon cingulin overexpression and knockdown is probably independent of cingulin-mediated RhoA modulation within the premigratory neural crest cell population (Wu et al., 2011). Neither cingulin knockdown nor overexpression causes any changes in the expression of Cad6B, claudin-1 and ZO-1, suggesting that the influence of cingulin on other junctional components is minimal (Wu et al., 2011).

1.6.2. Neural Crest Cell Adherens Junctions

Termed zonula adherens in polarized epithelial cells, adherens junctions form the "adhesion belt" by interacting with circumferential F-actin, thereby linking cells into a continuous sheet and separating the apical and basolateral membranes. In addition, they provide a penetrable barrier and protect the epithelial sheet against external hazards (Hay, 2005). Adherens junctions consist of transmembrane cadherin and nectin/afadin molecules (Takai et al., 2008; Meng and Takeichi, 2009), the latter of which will not be discussed but detailed reviews are available at (Takai et al., 2008; Ridenour et al., 2014).

1.6.2.1. Cadherins

Cadherins are Ca^{2+}-dependent integral membrane proteins that mediate cell-cell adhesion through the formation of homophilic interactions with cadherins on adjacent cells (Pokutta et al., 1994; Overduin et al., 1995). Cadherins link adherens junctions to the actin cytoskeleton through intracellular interactions with β-catenin, and subsequently α-catenin (Yonemura, 2011), thereby providing mechanical and structural support to epithelial cells. In addition to the binding site for β-catenin, many cadherin cytoplasmic tails also possess a binding site for p120-catenin (Kourtidis et al., 2013). The cadherin family is extremely diverse and is divided broadly into two different types based upon their adhesive properties and phylogenic relationships. Type I cadherins consist of cadherins-1 to -5, commonly referred as E-, N-, C-, P-, and R-cadherin, respectively, and type II cadherins constitute cadherin-6 and higher (Oda and Takeichi, 2011). In addition to the *trans* interaction between cadherins on different cells, the cadherin extracellular domain is also capable of

lateral *cis* interactions in the plasma membrane of a given cell, thereby forming cadherin dimers that form the basic adhesive unit (Brieher et al., 1996).

Cadherins are crucial components for normal embryonic development and pathogenesis. During development, both small and large cellular rearrangements are associated with spatiotemporal changes in cadherin expression (Takeichi, 1991). Homozygous deletion of *E-cadherin* (Larue et al., 1994) or *N-cadherin* (Radice et al., 1997) causes embryonic lethality in mice. Altering cadherin expression in embryonic cells (Detrick et al., 1990; Fujimori et al., 1990), expressing a non-adhesive mutant of cadherin (Radice et al., 1997), or blocking cadherin function with inhibitory antibodies (Bronner-Fraser et al., 1992) leads to loss of adhesion, dispersion of cells and therefore serious morphological defects or loss of tissue architecture. Cadherins also function in tissue homeostasis. For example, VE-cadherin (Vascular Endothelial cadherin; cadherin-5) regulates the exchange of oxygen and carbon dioxide across the endothelial lining of pulmonary alveolae and the transendothelial transport of fluid and proteins (Giannotta et al., 2013). Furthermore, cadherin mutations or aberrant cadherin expression is frequently associated with the onset of esophageal, gastric and colon cancers (van Roy, 2014). Importantly, a change from E-cadherin to N-cadherin expression, termed "cadherin switching," has been documented in numerous tumors of epithelial origin, including melanoma, breast, prostate, bladder, and squamous cell carcinoma. It is postulated that cadherin switching replaces an epithelial cadherin with a mesenchymal cadherin, although the switching mechanisms are not clear (Wheelock et al., 2008). Thus, cadherin regulation plays a key role in determining cellular and tissue homeostasis.

1.6.2.2. Cadherins in Neural Crest Cell EMT

Much of the investigation on the expression and regulation of junctional proteins of neural crest cells has focused on cadherins. Chick premigratory cranial neural crest cells express at least three cadherins: Cad6B, N-cadherin and E-cadherin (Hatta and Takeichi, 1986; Duband et al., 1988; Nakagawa and Takeichi, 1995; Nakagawa and Takeichi, 1998; Dady et al., 2012) (Fig.1.6). Expression of E-cadherin is high in prospective neural crest cells prior to neurulation, but as neurulation progresses, E-cadherin is gradually reduced and only retained until early stages of neural crest cell delamination. N-cadherin protein, however, is expressed during neurulation but is lost before EMT in premigratory cranial neural crest cells (Dady et al., 2012; Rogers et al., 2013). On the other hand, in the trunk, only *N-cadherin* transcripts are downregulated, and expression of protein persists until EMT (our unpublished data). Cad6B expression is considered to be a definitive and unique marker of premigratory neural crest cells. In the crania, Cad6B expression begins in the apposing neural folds, gradually increases as premigratory neural crest cells prepare for EMT, and is completely downregulated as neural crest cells undergo EMT and migrate (Nakagawa and Takeichi, 1995; Nakagawa and Takeichi, 1998; Taneyhill, 2008). In the trunk, Cad6B levels (mRNA and protein) are qualitatively much higher compared to that of the midbrain (our unpublished data). The significance and the molecular mechanism behind this differing expression pattern are unknown at this time. In addition, why premigratory neural crest cells express multiple cadherins simultaneously is still not clear. One hypothesis is that prospective neural crest cells segregate from the newly formed neural tube through an N-cadherin to Cad6B switching event, and that differential

expression prevents mixing of neural crest cells and other neuroepithelial cells (Nakagawa and Takeichi, 1995; Nakagawa and Takeichi, 1998).

Once neural crest cells initiate migration, they express two other cadherins, Cadherin-7 and Cadherin-11 (Nakagawa and Takeichi, 1998; Chalpe et al., 2010). *Xenopus* cephalic and trunk neural crest cells do not express Cad6B and Cadherin-7, but express Cadherin-11, whose expression pattern seems to be the sum total of Cad6B and Cadherin-7 expression within the chick embryo (Vallin et al., 1998). Mouse neural crest cells express Cadherin-6, the mouse orthologue of chick Cad6B, and, like Cadherin-11 in *Xenopus*, its expression appears to be the sum of chick Cad6B and Cadherin-7 (Inoue et al., 1997). In zebrafish, trafficking of N-cadherin is important in the normal migration of zebrafish neural crest cells (Piloto and Schilling, 2010).

During neural crest cell EMT, cadherins undergo both transcriptional and post-translational downregulation. Sip1/Zeb-2, a zinc finger transcriptional repressor, downregulates E-cadherin in emigrating neural crest cells but maintains N-cadherin levels in the neural tube of the chick embryo (Fig. 1.6). Knockdown of Sip1 reduces the number of neural crest cells undergoing EMT and is associated with enhanced expression of E-cadherin in emigrating neural crest cells and reduced expression of N-cadherin in the neural tube (Bolande, 1997). Similar to E-cadherin, Cad6B also undergoes transcriptional and post-translational downregulation (Fig. 1.6). As mentioned previously (Section 2.1), *Cad6B* expression in chick cranial and trunk neural crest cells is repressed by Snail2 (Taneyhill et al., 2007). The downregulation of Cad6B protein from the plasma membrane of premigratory cranial neural crest cells, however, occurs through the activity of several proteases, including the metalloproteinases A Disintegrin and Metalloprotease

Figure 1.6. Junctional molecules in chick cranial neural crest cells are dynamically modulated during EMT. The top panel shows transverse cross-sections through the midbrain of a 5 somite stage (ss, left) and a 6ss (right) chick embryo showing the premigratory (left) and migratory neural crest cells (right). The bottom panel shows the magnified image of a neural crest cell and the junctional molecular components with demonstrated expression patterns and if available, molecular mechanisms associated with their regulation. The basal lamina that surrounds the neural tube on its basolateral surface is not shown but is absent in the dorsal region of the neural tube prior to cranial neural crest cell emigration. Image modified from (Taneyhill LA, 2014).

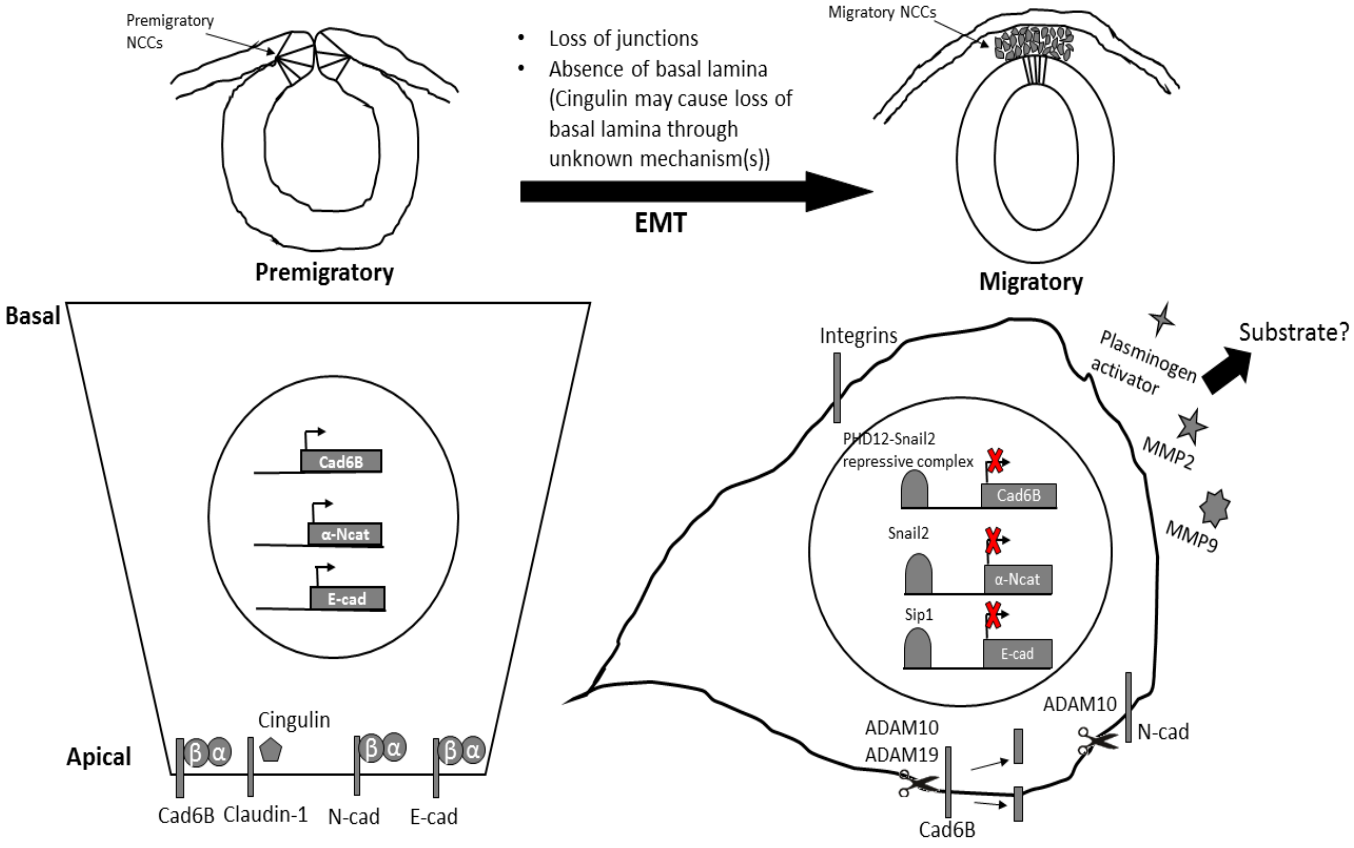

(ADAM) ADAM10 and ADAM19, followed by γ-secretase (Schiffmacher et al., 2014), and through internalization (Padmanabhan, Ph.D. thesis). This proteolysis releases N- and C-terminal fragments (NTF, CTF1, CTF2) and thus likely decreases cell-cell adhesion by relieving intercellular adhesion. However, the released fragments may play other signaling roles in modulating neural crest cell EMT (Schiffmacher and Taneyhill, unpublished data). ADAM-mediated proteolysis of cadherins also occurs in the chick during trunk neural crest cell EMT. Shoval et al. (2007) showed that BMP signaling activates ADAM10, which proteolytically cleaves the N-cadherin extracellular domain. CTF2, one of the released cytoplasmic domain fragments, then translocates to the nucleus and directly or indirectly stimulates transcription of genes important for modulating neural crest cell EMT such as *cyclin D1*. Downregulation of *cad6B* is crucial in the chick midbrain because overexpression and knockdown of Cad6B inhibits and augments neural crest cell emigration, respectively (Coles et al., 2007). Cad6B is regulated differently in chick trunk neural crest cells, however, with *cad6B* expression triggering premigratory neural crest cell de-epithelialization and knockdown decreasing the number of migratory neural crest cells (Park and Gumbiner, 2010; Park and Gumbiner, 2012). This occurs through a non-canonical LIM kinase/cofilin Wnt signaling pathway, and ectopic expression of LIM kinase (with Sox9) triggers ectopic EMT of trunk neural crest cells (Park and Gumbiner, 2012). This observed difference with respect to Cad6B function in the chick head and trunk may be due to (1) differences in the properties of head and trunk neural crest cells and (2) the metric used to determine effects on neural crest cell migration. Cad6 facilitation of EMT is also observed in zebrafish hindbrain neural crest cells (Dixon et al., 2006). These cells lose N-cadherin but upregulate Cad6 prior to EMT. Moreover, Cad6 promotes

detachment of neural crest cell "tails" by altering the spatiotemporal localization of Rho GTPase and through accumulation of F-actin in the tail region. Finally, Cad6 knockdown alters the subcellular distribution of active Rho, which is known to promote localized actomyosin contraction crucial for apical neural crest cell detachment (Dixon et al., 2006). Another example whereby cadherins facilitate EMT is the role of Cadherin-11 in *Xenopus* neural crest cells. Similar to Cad6B, knockdown and overexpression of Cadherin-11 in *Xenopus* neural crest cells augments or prevents neural crest cell migration, respectively (Borchers et al., 2001). Overexpression of ADAM13 was found to rescue the latter phenotype, and *ADAM13* knockout embryos have elevated Cadherin-11 levels. Interestingly, this proteolytic cleavage occurs throughout cranial neural crest cell migration, unlike that of the chick in which ADAM10-mediated proteolytic cleavage occurs only within premigratory cranial neural crest cells (Borchers et al., 2001). Following ADAM13-mediated proteolysis, the membrane-bound cytoplasmic fragment of Cadherin-11 localizes to the filopodia of migratory neural crest cells and associates with Trio, a small GTPase guanine exchange factor (Kashef et al., 2009) that activates Rho, Rac and Cdc42 *in vitro* (Bateman and Van Vactor, 2001). Consistent with this observation, overexpression of Trio or constitutively active Rho, Rac and Cdc42 is sufficient to restore neural crest cell spreading and migration in Cadherin-11 knockdown embryos, suggesting that the membrane-anchored, cytoplasmic fragment of Cadherin-11 is crucial for the activation of these small GTPases *in vivo* (Kashef et al., 2009). These observations point to a new, emerging theme in cadherin regulation in which a fine balance between intracellular and membrane-bound cadherin levels regulate neural crest cell EMT.

1.6.2.3. Mechanisms of Cadherin Downregulation

Cells employ multiple mechanisms to modulate cadherin protein levels at the plasma membrane, further to repressing their expression transcriptionally: (1) Phosphorylation and dephosphorylation of cadherins (reviewed in (Fujita et al., 2002)), (2) Interaction of cadherins with small GTPases such as Rho, Rac and Cdc42 (reviewed in (Watanabe et al., 2009)), (3) Cadherin endocytosis and sequestration (reviewed in (Chiasson CM, 2008)), and (4) Shedding/proteolysis of the cadherin extracellular domain (reviewed in (Hayashida et al., 2010)). The rest of this section will focus on proteolysis and endocytosis as mechanisms of downregulation of cadherins from the plasma membranes of cells.

1.6.2.3.1. Proteolysis

The first of a series of studies demonstrating proteolysis of the ectodomain of cadherins was from Wheelock et al. (Wheelock et al., 1987). The authors purified an 80 kilodalton (kD) E-cadherin soluble fragment from serum-free medium conditioned by MCF-7 cells. This soluble fragment caused scattering of epithelial cells in culture, suggesting that it was able to interfere with cell adhesion *in vitro* (Wheelock et al., 1987).

Cadherin ectodomain shedding occurs through ADAM/Matrix Metalloprotease (MMP)-mediated cleavage of the cadherin extracellular domain to release the NTF. In many instances, this is followed by γ-secretase-mediated proteolytic cleavage of the remaining, membrane-bound C-terminal intracellular domain (CTF1) at the juxtamembrane region to release the intracellular fragment CTF2 (Marambaud et al., 2002; Marambaud et al., 2003). ADAMs and MMPs belong to the metzincin zinc-dependent metalloprotease superfamily and cleave a variety of substrates in the extracellular matrix

during embryogenesis, adult tissue homeostasis and metastasis. Typical substrates for ADAMs include growth factors, cytokines, receptors, and cell-adhesion molecules (White JM, 2005), while traditional substrates of MMPs include extracellular matrix components as well as a range of membrane-bound proteins (Rodriguez et al., 2010). The link between the degradation of extracellular matrix by ADAMs/ MMPs and cancer cell invasion has been clearly established from earlier studies on tumor metastasis (Fingleton, 2006). Numerous reports show that knockdown or inhibition of MMPs (by synthetic and natural inhibitors) decreases cell invasion, whereas increased cell invasion is observed upon MMP activation (reviewed in (Fingleton, 2006)). γ-secretase is a membrane-bound protein complex composed of at least four subunits: presenilin (possesses the active site), nicastrin, anterior pharynx-defective 1, and presenilin enhancer 2. γ-secretase has generated much interest recently because it cleaves APP to generate amyloid-β peptide, the primary component of amyloid plaques characteristic of Alzheimer's disease (reviewed in (Beel and Sanders, 2008))

ADAM/MMP- and γ-secretase-mediated proteolytic cleavage of the cadherin extracellular and intracellular domains is usually accompanied by the loss of intercellular adhesion. For example, MMP-7 cleaves E-cadherin during wound healing within the injured lung epithelium (McGuire et al., 2003), allowing cells to move to heal the injured site, and MMP-3 cleaves E-cadherin in mammary epithelial cells, resulting in EMT (Lochter et al., 1997). ADAM10 processes both E-cadherin (Maretzky et al., 2005) and N-cadherin (Reiss et al., 2005) in epithelial cells to decrease cell-cell adhesion as well as VE-cadherin in umbilical vein endothelial cells, promoting transmigration (Schulz et al., 2008). γ-secretase has been shown to cleave both E-cadherin and N-cadherin at their

juxtamembrane regions to release intracellular fragments that play signaling roles (Marambaud et al., 2002; Marambaud et al., 2003). In addition to a function in EMT, cadherin proteolysis is involved in several non-EMT developmental processes. N-cadherin cleavage during chick retinal development releases a truncated extracellular domain that promotes cell adhesion and neurite development (Wilkie and Morriss-Kay, 2001). Similarly, ADAM10-mediated E-cadherin proteolysis in response to Eph/ephrin signaling plays a role in cell sorting of epithelial tissues during development (Orpen et al., 2003). Furthermore, as discussed in the previous section (Section 3.1), cadherin proteolysis plays an important function in regulating cadherin levels during and after neural crest cell EMT.

1.6.2.3.2. Endocytosis and Degradation

1.6.2.3.2.1. Overview

Cadherin endocytosis occurs both constitutively and under conditions in which cell adhesion is compromised. The degree of endocytosis and the fate of the endocytosed cadherin are dependent on the amount of cell-cell contact and presence of extracellular signals that trigger endocytosis. Upon endocytosis, cadherins are either recycled back to the plasma membrane or degraded in the lysosomes (Fig. 1.7). In the case of E-cadherin in MDCK cells, the internalized pool of cadherin is rapidly recycled to the cell surface (Le et al., 1999). VE-cadherin in endothelial cells, however, undergoes a certain level of constitutive endocytosis and lysosomal degradation (Xiao et al., 2003b; Xiao et al., 2003a).

Figure 1.7. Multiple mechanisms regulate cadherin endocytosis. Cadherins undergo both clathrin-dependent and clathrin-independent internalization. p120-catenin plays a critical role in regulating cadherin endocytosis through the clathrin-mediated pathway. Upon endocytosis, cadherins are recycled back to the plasma membrane or degraded in lysosomes. Image reproduced from (Kowalczyk and Nanes, 2012).

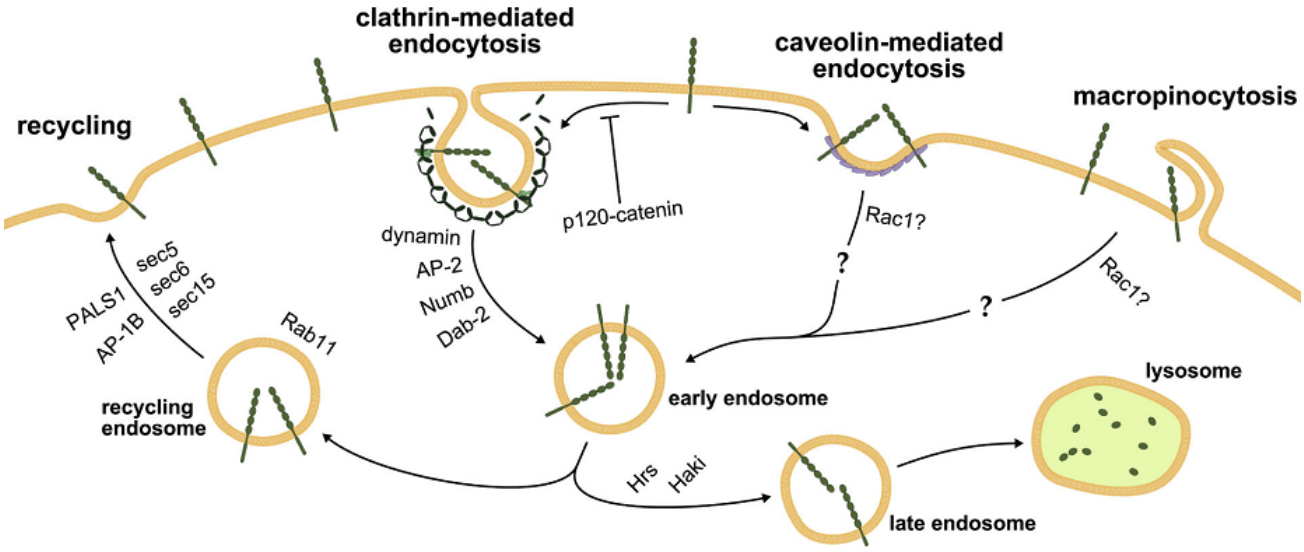

Cadherin endocytosis can directly influence the adhesive state of cadherins *in vitro* and *in vivo*. For example, using ATP depletion or hypertonic sucrose treatment to inhibit endocytosis, E-cadherin adhesive dimers were stabilized in the absence of endocytosis *in vitro*, leading to a dramatic increase in the amount of adhesive dimers and a parallel decrease in the pool of cadherin monomers (Troyanovsky, 2005). Similarly, inhibition of E-cadherin endocytosis enhances epithelial cell adhesion *in vivo* in *Drosophila* embryos (Harris and Tepass, 2008; Leibfried et al., 2008; Wirtz-Peitz and Zallen, 2009). Consistent with these observations, non-adhesive cadherin molecules that are able to flow within the plane of the plasma membrane were shown to enter endocytic routes *in vitro* (Le et al., 1999; Izumi et al., 2004; Miyashita and Ozawa, 2007a). Cadherin endocytosis is also dependent on the adhesive state of the cell. For instance, endocytosis increases in cells lacking stable cell-cell contacts, such as in pre-confluent monolayers or following disruption of cell junctions by Ca^{2+} depletion (Kartenbeck et al., 1991; Ivanov et al., 2004).

In addition to playing roles in adherens junction homeostasis, cadherin endocytosis can elicit cellular responses such as EMT. During EMT induced by v-Src activation, v-Src stimulates phosphorylation-dependent ubiquitination of E-cadherin, which is then trafficked through the endosomes to the lysosome for degradation through a pathway that requires hepatocyte growth factor-regulated tyrosine kinase substrate and the GTPases Rab5 and Rab7 (Palacios et al., 2005). In another study, Src-stimulated phosphorylation of the E-cadherin juxtamembrane domain recruits Hakai, an E3 ubiquitin ligase that monoubiquitinates E-cadherin and marks it for trafficking to lysosomes (Fujita et al., 2002) (Fig. 1.7). This process of cadherin ubiquitination, followed by degradation, has been hijacked by pathogenic viruses. For example, Kaposi's Sarcoma-associated herpesvirus

protein K5, another E3 ubiquitin ligase, ubiquitinates and downregulates VE-cadherin and enhances endothelial permeability (Qian et al., 2004; Mansouri et al., 2008). In addition, increased endocytosis has been associated with some cancers. A mouse model of squamous cell carcinoma exhibits augmented E-cadherin endocytosis (Goodman, 2003), and cytoplasmic localization of E-cadherin is associated with poor survival in nasopharyngeal cancer (Xie et al., 2010)

1.6.2.3.2.2. Clathrin-dependent Endocytosis of Cadherins

Cadherins undergo endocytosis through both clathrin-dependent and -independent pathways (Fig. 1.7). For example, E-cadherin in MDCK cells undergoes constitutive endocytosis and recycling in a clathrin-dependent manner (Le et al., 1999). Similarly, in T84 cells, Ivanov *et al.* observed clathrin-dependent internalization of the entire apical junctional complex into an intracellular compartment enriched in syntaxin-4 upon Ca^{2+} depletion (Ivanov et al., 2004). In endothelial cells, VE-cadherin is internalized through a clathrin-dependent manner and is trafficked through early and late endosomes to the lysosome, where it undergoes degradation (Xiao et al., 2003a; Xiao et al., 2005).

The clathrin-dependent endocytosis pathway is the most well characterized mechanism of endocytosis. Here, cargo proteins are recruited into clathrin-coated pits in the plasma membrane through recognition of distinct sorting motifs in their cytoplasmic domains by adaptor proteins. Prior work has revealed that cadherins possess sorting or endocytic motifs in their cytoplasmic domains, including a tyrosine-based sorting signal (YXXØ consensus in which X is any amino acid and Ø is a hydrophobic residue) (Canfield et al., 1991; Jadot et al., 1992) and a dileucine motif ([DE]XXXL[LI] consensus)

(Bonifacino and Traub, 2003). In MDCK cells, the dileucine motif is required for endocytosis of E-cadherin, and mutation of the dileucine motif at amino acids 587-588 results in E-cadherin accumulation at the basolateral surface (Miranda et al., 2001) and a significant reduction in endocytosis (Miyashita and Ozawa, 2007a). Mutating the region possessing the dileucine motif of N-cadherin decreases N-cadherin endocytosis in hippocampal neurons (Tai et al., 2007). Interestingly, VE-cadherin does not possess this dileucine motif, but its cytoplasmic tail is able to mediate clathrin-dependent endocytosis when attached to an unrelated transmembrane protein, indicating that cadherins may contain other as of yet identified endocytic motifs (Xiao et al., 2005). As mentioned above, these motifs are recognized by cytoplasmic adaptor protein, which serve as a scaffold for both clathrin and the cargo to which they bind. AP-2 is the most common adaptor protein, binding to clathrin, phospholipids and other proteins. (Benmerah and Lamaze, 2007; Rappoport, 2008) (Fig.1.7). Importantly, it is responsible for the recognition of cargo proteins through their cytoplasmically-localized sorting motifs, including the tyrosine and the dileucine motif described above (Bonifacino and Traub, 2003). AP-2 co-immunoprecipitates with the VE-cadherin cytoplasmic tail during clathrin- and dynamin-dependent endocytosis of VE-cadherin (Chiasson et al., 2009), and with the E-cadherin cytoplasmic tail during E-cadherin endocytosis in MCF-7 cells (Liem et al., 1997). In addition to AP-2, other adaptor proteins have been implicated in clathrin-mediated endocytosis of cadherins, such as β-arrestin in VEGF-stimulated endocytosis of VE-cadherin (Gavard and Gutkind, 2006), and Numb in radial glial (Liem et al., 1995) and epithelial (Lewis et al., 2004; Ragland and Raible, 2004) cells (Fig. 1.7), which directly binds to and regulates E-cadherin endocytosis.

1.6.2.3.2.3. Clathrin-independent Endocytosis of Cadherins

Clathrin-independent mechanisms of protein internalization, which include caveolae-dependent pathways, lipid raft-mediated pathways and macropinocytosis, are now recognized as increasingly important pathways of transmembrane protein trafficking (Fig. 1.7). In response to EGF treatment, E-cadherin in A431 cells is internalized through a pathway that requires caveolin-1 (Lu et al., 2003). In keratinocytes, E-cadherin is endocytosed through a caveolin-mediated pathway upon Rac activation (Akhtar and Hotchin, 2001). The desmosomal cadherin Desmoglein-3, the target of the autoimmune disease Pemphigus Vulgaris, is internalized through a lipid raft-dependent, but clathrin- and dynamin-independent, pathway (Delva et al., 2008).

In addition to clathrin-, caveolin- and lipid raft-dependent endocytic pathways, macropinocytosis-mediated cadherin internalization has also been observed (Fig. 1.7). In isolated MCF-7 cells, E-cadherin is internalized by ARF6- and dynamin-dependent macropinocytosis (Paterson et al., 2003). In epithelial cells, EGF induces macropinocytosis of the E-cadherin-catenin complex from ruffling cell membranes, which then undergo SNX1-dependent recycling back to the plasma membrane (Bryant et al., 2007). In another case of E-cadherin recycling, reggies/flottilins mediate E-cadherin macropinocytosis and junction formation by regulating EGFR phosphorylation and endocytosis in A431 cells (Solis et al., 2012). Thus, the existence of multiple internalization pathways to modulate cadherin levels points towards a fine tuned system that is highly dependent on cellular context.

1.6.2.3.2.4. Regulation of Cadherin Endocytosis by p120-catenin and Rho GTPases

Of the three catenins, p120-catenin has the most significant influence on cadherin endocytosis. p120-catenin, a member of the armadillo family of proteins, binds to the juxtamembrane domain of cadherins and serves as an inhibitor of cadherin turnover by functioning as a "set-point" for cadherin expression levels (Kourtidis et al., 2013) (Fig. 1.7). Experiments in a colon carcinoma cell line were the first to reveal the importance of p120-catenin in that the epithelial nature of these cells could be restored upon exogenous expression of p120-catenin. This occurs through an increase in the E-cadherin half-life and protein levels without changes to *E-cadherin* transcripts, suggesting that p120-catenin could stabilize cadherin protein levels. Subsequent studies showed that p120-catenin binds to the cadherin cytoplasmic tail and that loss of p120-catenin augments cadherin endocytosis (Davis et al., 2003; Xiao et al., 2003b). Interestingly, expressing cadherin mutants that compete for p120-catenin binding results in endocytosis of the endogenous cadherin, while cadherin mutants that cannot bind to p120-catenin lack this activity (Davis et al., 2003; Xiao et al., 2003b; Xiao et al., 2005). This suggests that p120-catenin could serve as a master regulator of cadherin levels in cells, and competition to bind to p120-catenin could determine the cadherin expressed on the plasma membrane in cells that express two different cadherins. Indeed, exogenous expression of R-cadherin causes endocytosis and downregulation of endogenous E- and P-cadherins in A431 cells (Maeda et al., 2006), and exogenous VE-cadherin similarly affects N-cadherin (Ferreri et al., 2008). Subsequent studies have focused on the mechanism of action of p120-catenin, which is thought to serve as a physical mask and prevent the recognition of endocytosis sorting motifs by adaptor proteins of the clathrin-mediated endocytosis pathway (Miyashita and

Ozawa, 2007a; Chiasson et al., 2009; Ishiyama et al., 2010). Recently, the crystal structure of the E-cadherin-p120-catenin complex was solved, and it reveals that the p120-catenin-E-cadherin interface contains both static and dynamic binding regions, supporting competitive binding of cadherins or of endocytic adaptor proteins (Ishiyama et al., 2010).

The Rho family of small GTPases, including RhoA and Rac, plays important roles in cadherin endocytosis through regulation of the cadherin/catenin complex or intracellular trafficking steps. Activation of Rac1 has both stimulatory and inhibitory effects on cadherin endocytosis, depending on the cell type examined. In endothelial cells, VE-cadherin is refractory to regulation by Rho or Rac activity; however, when expressed in CHO cells, inhibition of Rho or Rac induces VE-cadherin endocytosis from junctions (Braga et al., 1999). Similarly, inhibition of Rho or Rac causes endocytosis and degradation of E-cadherin and P-cadherin (Braga et al., 1999). In L-cells, E-cadherin endocytosis is regulated by Rho but not Rac (Braga et al., 1999).

1.6.2.3.2.5. Regulation of Cadherin Endocytosis by Growth Factors

Given their fundamental importance in homeostasis, cadherins are not only regulated by intracellular processes but also by extracellular signals that include the hepatocyte growth factor (HGF), epithelial growth factor (EGF), vascular endothelial growth factor (VEGF), fibroblast growth factor (FGF), and transforming growth factor β (TGFβ) signaling pathways (reviewed in (Kowalczyk and Nanes, 2012)). Treatment of cells with HGF, which stimulates cell motility, causes endocytosis of both the HGF receptor and associated E-cadherin (Kamei et al., 1999) through a clathrin-mediated pathway that employs the Numb adaptor (Wang et al., 2009). Similarly, VEGF, which disrupts endothelial cell-cell

junctions and causes vasculogenesis and angiogenesis, functions through Src-mediated phosphorylation of VE-cadherin. This leads to the recruitment of β-arrestin and subsequent clathrin-mediated endocytosis of VE-cadherin (Gavard and Gutkind, 2006). Interestingly, VE-cadherin can reciprocally influence the endocytosis of the VEGF receptor. In confluent cells, VE-cadherin associates with the VEGF receptor and not only prevents VEGF receptor internalization but also redirects it from the lysosomal to a recycling pathway (Grazia Lampugnani et al., 2003). Treatment of cells with EGF, on the other hand, causes E-cadherin internalization through a caveolin-mediated (Lu et al., 2003) or a macropinocytic (Bryant et al., 2007) pathway. Similar to VE-cadherin, E-cadherin-EGF receptor interactions also prevent endocytosis of EGF receptor (Bremm et al., 2008).

1.7. Rationale and objectives

In the developing chick embryo midbrain, Cad6B transcripts and protein expression begin at the 3 and 4 somite stages (ss), respectively, just as neural crest cells are segregating from the ectoderm and the non-neural ectoderm (there is 90 minutes between each somite stage) (Hamburger and Hamilton, 1992) (Fig. 1.8). The expression of the transcripts and protein gradually increases in premigratory cranial neural crest cells and at the 6ss, when neural crest cells undergo delamination, Snail2-mediated transcriptional repression of *cad6B* occurs (Taneyhill et al., 2007). By the 7ss, as neural crest cells undergo EMT, *cad6B* transcripts are completely repressed, and levels of Cad6B protein, surprisingly, are also significantly reduced (Taneyhill et al., 2007; Schiffmacher et al., 2014) (Fig. 1.8). Cad6B has a half-life of 5.5 hours *in vitro* (Schiffmacher et al., 2014), however, suggesting that this substantial loss of Cad6B protein from premigratory cranial neural crest cells may occur through active post-translational mechanisms to remove Cad6B from these cells. Studies by Schiffmacher *et al.* (2014) revealed that Cad6B undergoes proteolysis and separation of the extracellular and the intracellular domains mediated by ADAM10, ADAM19 and γ-secretase enzymes (Schiffmacher et al., 2014). Nevertheless, we note Cad6B localized to cytoplasmic puncta in premigratory and early migratory cranial neural crest cells, indicative of a potential role for Cad6B internalization as cranial neural crest cells undergo EMT. The possibility that internalization of Cad6B plays an important role during EMT is not without precedence, as discussed earlier in this Introduction, but has never been demonstrated in an *in vivo* EMT. As such, the aim of this dissertation is to investigate if and how Cad6B undergoes internalization in chick premigratory cranial neural crest cells during EMT.

Figure 1.8. Cad6B protein downregulation occurs rapidly after *mRNA* downregulation. Cad6B protein expression (green) is restricted to premigratory neural crest cells in the dorsal neural tube (arrows, top panel), begins at 4ss, and correlates with the expression profile of *cad6B* transcripts (arrows, bottom panel, *in situ* hybridization for cad6B mRNA). During EMT (7ss), Cad6B mRNA and protein undergo rapid downregulation, partially enabling neural crest cell EMT (Schiffmacher et al., 2014).

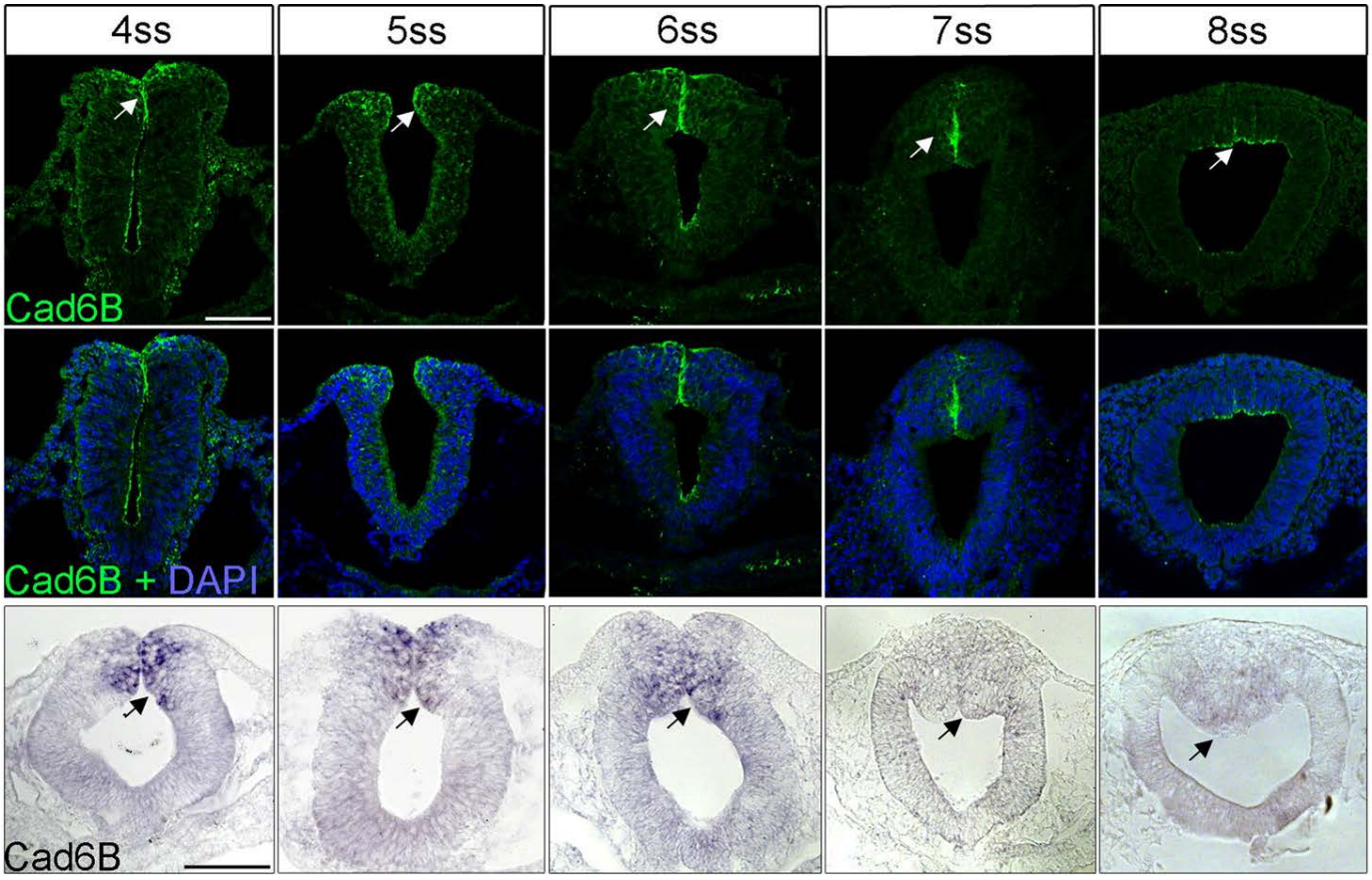

Chapter 2. Materials and Methods

2.1. Chick embryos

Fertilized chicken eggs were obtained from B & E Farms (York, PA, USA) and incubated at 38°C in humidified incubators (EggCartons.com, Manchaug, MA, USA). Embryos were staged by the number of pairs of somites (somite stage, ss) according to Hamburger-Hamilton (Hamburger and Hamilton, 1992).

2.2. *Neural crest cell explant preparation*

Neural crest cell explants were prepared as described in (Coles et al., 2007; Taneyhill et al., 2007; Jhingory et al., 2010). Dorsal neural folds (containing premigratory neural crests cells) from the midbrain region of chick embryos were dissected out of the embryo using tungsten needles in PB-1 standard medium and then placed into chamber slides coated with a 1:100 dilution (1µg/mL) of poly-L-lysine (P5899, Sigma, St. Louis, MO, USA) and fibronectin (356008, Corning, NY, USA). Cultures were incubated in serum-free Dulbecco's Modified Eagle's Medium (DMEM, 10-013-CV, CellGro, Manassas, VA, USA) supplemented with a 1:100 dilution of N-2 (17502-048, Life Technologies, Carlsbad, CA, USA) at 37˚C for varying time periods to observe effects on neural crest cell EMT.

2.3. Cloning of Cad6B mutants

Full-length Cad6B cloned in pCIG (Coles et al., 2007) was sub-cloned into pCI-H2B-RFP (gift from Dr. M. Bronner) along with a hemagglutinin (HA) epitope tag at the Cad6B C-terminal end through standard cloning procedures. To create the endocytic mutants, Cad6B in the pCI-H2B-RFP vector was mutagenized using the QuikChange II XL Site-Directed

Mutagenesis Kit (200521, Agilent Technologies, Santa Clara, CA, USA). The primer sequences for cloning are:

LI645AA-HA Forward: 5' GAG ACG GCA AAG GAA AAA AGA GCC TGC GGC TAT TTC CAA AGA AGA CAT CAG AGA C 3'

LI645AA-HA Reverse: 5' CTC TGC CGT TTC CTT TTT TCT CGG ACG CCG ATA AAG GTT TCT TCT GTA GTC TCT G 3'

EED666AAA-HA Forward: 5' AAT GAT GAA GGT GGT GGA GCG GCA GCC ACC CAG GCA TTT GAT ATC 3'

EED666AAA-HA Reverse 5' TTA CTA CTT CCA CCA CCT CGC CGT CGG TGG GTC CGT AAA CTA TAG 3'

Primers were chemically synthesized and PAGE-purified by Integrated DNA Technologies, Coralville, Iowa, USA. All clones were sequenced ensure sequence accuracy.

2.4. FlpIn cell culture and reagents

CHO cells stably expressing a single integrated copy of wild-type and various endocytic mutants of Cad6B were created as described previously using the FlpIn system (K6010-02, R75807, Life Technologies, Carlsbad, CA, USA; (Schiffmacher et al., 2014)). Briefly, HA-tagged wild-type or mutant Cad6B was directionally sub-cloned from the pCI-H2B-RFP vector (above) into the pcDNA5/FRT expression vector and co-transfected at a 1:9 ratio with the pOG44 plasmid into FlpIn-CHO cells (R758-07, Life Technologies, Carlsbad, CA, USA). 24 hours posttransfection, media was replaced with antibiotic-free F12 media, and then another 24 hours later, cells were trypsinized and plated at 20–25%

confluency in F12 media supplemented with 1 mM L-glutamine and 600µg/ml hygromycin to select for individual clones of positive transfectants (cells were subsequently grown in this medium). Fresh medium was added every 2 days until small colonies of stable cells were observed. Individual colonies were aseptically transferred to 96 well plates and cultured to confluency. Colonies were then sequentially passaged into 48-, 24-, and 12-well plates. Colonies were screened for Cad6B expression by immunohistochemistry and immunoblotting, and those with maximum transfection efficiency were eventually passaged to 10-cm plates, and grown in a humidified incubator (with 5% CO_2 and 95% air) at 37˚C in Ham's F12 growth media supplemented with 10% fetal bovine serum (S11150, Atlanta Biologicals, Flowery Branch, GA, USA), 600µg/mL hygromycin (30-240-R, CellGro, Manassas, VA, USA), 1mM L-glutamine (25-005, CellGro, Manassas, VA, USA), and 1:100 dilution of 1:1 penicillin-streptomycin (30-002-CI, CellGro, Manassas, VA, USA).

2.5. Immunohistochemistry

Embryos were collected at the 6ss and 7ss and fixed in 4% paraformaldehyde (PFA) for 30 minutes at room temperature. The embryos were permeabilized in fresh Tris-buffered saline (TBS) containing 0.2% TX-100 (TBST) and blocked in TBST buffer containing 5% fetal bovine serum for one hour at room temperature. Immunofluorescence was performed on whole embryos overnight at 4˚C with Cad6B primary and anti-mouse Cad6B secondary antibodies as in (Jhingory et al., 2010; Schiffmacher et al., 2014). To observe Cad6B protein in explants, explants were fixed by serial dilution of the explant media with 4% PFA for 20 minutes at room temperature, permeabilized with fresh TBST, blocked with

5% FBS in TBST, and incubation with the Cad6B primary antibody overnight at 4°C and with secondary antibody for three hours at room temperature. For immunostaining of cell lines, cells were fixed in either 4% PFA for 20 minutes at room temperature or in cold 5% ethanol/95% acetic acid for 20 minutes at -20°C. For cells fixed in 4% PFA, permeabilization was carried out with TBST, and immunofluorescence was performed as for the explants. For cells fixed in ethanol/acetic acid, immunofluorescence was performed similarly as for explants but in TBS buffer without detergents.

The following primary antibodies and concentrations were used in the experiments following fixation by conditions provided in the next section. Cad6B (1:100 in whole-mount and 1:250 on sections and cells: Cad6B (CCD6B-1, Developmental Studies Hybridoma Bank, OH, USA; referred to as NT6B in the text), caveolin-1 (1:500; ab2910, Abcam, Cambridge, England), HA (1:750; 3F10, Roche, Basel, Switzerland), clathrin (1:750; ab21679, Abcam, Cambridge, England), Na^+K^+ATPase (1:750; ab76020, Abcam, Cambridge, UK), p120-catenin (1:500; sc-373751; Santa Cruz Biotechnology, Santa Cruz, CA, USA), β-catenin (1:500; AHO0462, Life Technologies, Carlsbad, CA, USA), GFP (1:1000; R10367, Life Technologies, Carlsbad, CA, USA), FoxD3 (1:500; kind gift from Dr. David Raible (Department of Biological Structure, University of Washington, Seattle, WA, and K-cad (1:200; ab64917, Abcam, Cambridge, UK; referred to as CT-6B in the text). Alexa Fluor488-conjugated phalloidin (Life Technologies, Carlsbad, CA, USA) was used at 1:50. Appropriate fluorescently-conjugated secondary antibodies (AlexaFluor 488, 594, 647; Life Technologies, Carlsbad, CA, USA) were used at the following concentrations: Cad6B (1:250 in whole-mount and 1:500 on cells), HA (1:1000), clathrin

(1:1000), Na^+K^+ATPase (1:1000), p120 (1:1000), β-catenin (1:1000), GFP (1:1500), and K-cad (1:750).

2.6. In ovo electroporation and FoxD3 cell counts

Cad6B wild-type and mutant expression constructs were introduced into premigratory midbrain neural crest cells in developing 3ss chick embryos using a modified version of *in ovo* electroporation (Itasaki et al., 1999) procedure. Constructs were injected at a concentration of 3μg/μl into the neural tube lumen and two 30-ms pulses at 25 V were applied across the embryo for unilaterally introducing the constructs into one side of the neural tube (Jhingory et al., 2010; Wu et al., 2011; Wu and Taneyhill, 2012). Embryos were incubated at 37˚C until they grew to 6-7ss, harvested, fixed, and processed for immunofluorescence as described below. The embryos were subsequently embedded in 20% gelatin in 1X phosphate-buffered saline (PBS), cryostat-sectioned at 14 μm, and mounted for imaging. In midbrain regions where neural crest cell migration had commenced, 5–7 serial images were captured for at least 8 embryos that had exogenous Cad6B expression in the dorsal neural tube. Every DAPI- and FoxD3-positive nuclei in the migratory streams on both the electroporated and non-electroporated side was counted and recorded to detect population effects of expressing exogenous Cad6B. The fold differences were averaged over the number of sections in which cells were counted, and the standard error of the mean was calculated and compared for embryos electroporated with wild-type Cad6B. Significance of results was established using the unpaired Student's *t* test, as in (Coles et al., 2007; Jhingory et al., 2010).

2.7. Cad6B antibody feeding assays

The feeding assay was performed *in vivo* as in (Arancibia-Carcamo IL, 2006) with the following modifications. The hollow neural tube lumen of 5ss embryos was filled with CCD6B-1 antibody after electroporation with an expression construct coding for membrane-GFP to label plasma membranes (a kind gift from Dr. Paul Kulesa, Stowers Institute of Medical Research, Kansas, MO). After incubation for a few hours to allow for EMT to occur, the embryos were fixed and immunofluorescence was performed for Cad6B and GFP as described above (Fig. 2.1).

The feeding assay was performed *in vitro* as in (Arancibia-Carcamo IL, 2006) with minor modifications. FlpIn-CHO cells stably expressing wild-type Cad6B were washed with 3X ice-cold fresh PBS^{2+} (PBS supplemented with 1.5mM $MgCl_2$ and 0.2mM $CaCl_2$) to slow down cellular processes and incubated with a 1:50 dilution of NT6B antibody in cell culture media at 4˚C for an hour to allow for the NT-6B antibody to recognize Cad6B. The cells were washed with 3X ice-cold PBS^{2+} to remove excess antibody, replaced with warm media, and incubated at 37˚C for an hour to permit internalization to occur. Following this, the cells were brought back to 4˚C and subjected to 3X acid wash with a low pH buffer (0.1M glycine, pH 2.0) for 5 minutes at 4˚C. The cells were washed 2X with PBS, fixed, permeabilized, and immunofluorescence was performed as described above.

Figure 2.1. Cad6B antibody feeding assay *in vivo*. Cad6B antibody recognizes and binds to endogenous Cad6B protein. The Cad6B antibody-Cad6B complex should be processed in the same way as endogenous Cad6B protein. Membrane GFP serves as a marker of individual cellular membranes (green lines in the premigratory neural crest cell region). NCCs, neural crest cells.

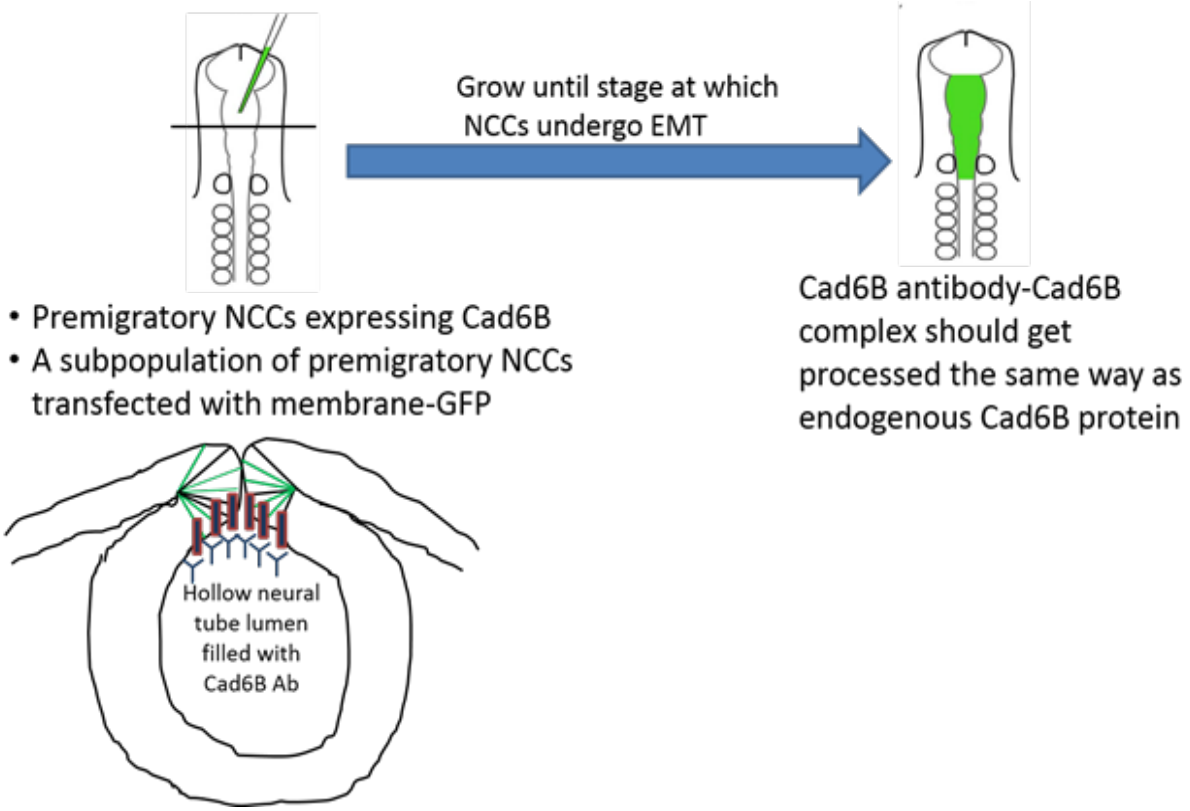

To perform the feeding assay *ex vivo,* cranial dorsal neural folds from 5ss embryos were explanted as described above into one well of a 4-well chamber slide and incubated at 37˚C for 90 minutes to allow the tissue to attach to the chamber slide. The media was serially diluted with ice-cold fresh PBS^{2+}, and the explants were incubated at 4˚C for 5 minutes. PBS^{2+} was then serially diluted with ice-cold explant media containing a 1:50 dilution of CCD6B-1 antibody and incubated at 4˚C for an hour. Following serial dilution with ice-cold PBS^{2+} to remove excess antibody, fresh warm explant media was serially added to the explants and incubated at 37˚C for three hours to allow for EMT and cellular processes such as internalization to occur. The explants were brought back to 4˚C to slow down cellular processes and following serial dilution of the explant media with ice-cold PBS^{2+}, non-internalized antibody (bound to the plasma membranes) was removed by treatment with a low pH buffer as described above for 15 minutes at 4˚C temperature. The explants were then fixed, permeabilized, and immunofluorescence was performed as described above (Fig. 2.2).

Figure 2.2. Cad6B antibody feeding assay *ex vivo*. Similar to feeding assay in vivo (Fig. 8), the Cad6B antibody-Cad6B complex gets processed in the same way as endogenous Cad6B protein (red). Internalized Cad6B-Cad6B antibody complex and membrane-bound Cad6B is differentiated by means of an antibody that recognizes the C-terminal end of Cad6B (green). Thus, green immunofluorescence denotes membrane-bound Cad6B, while yellow immunofluorescence denotes internalized Cad6B.

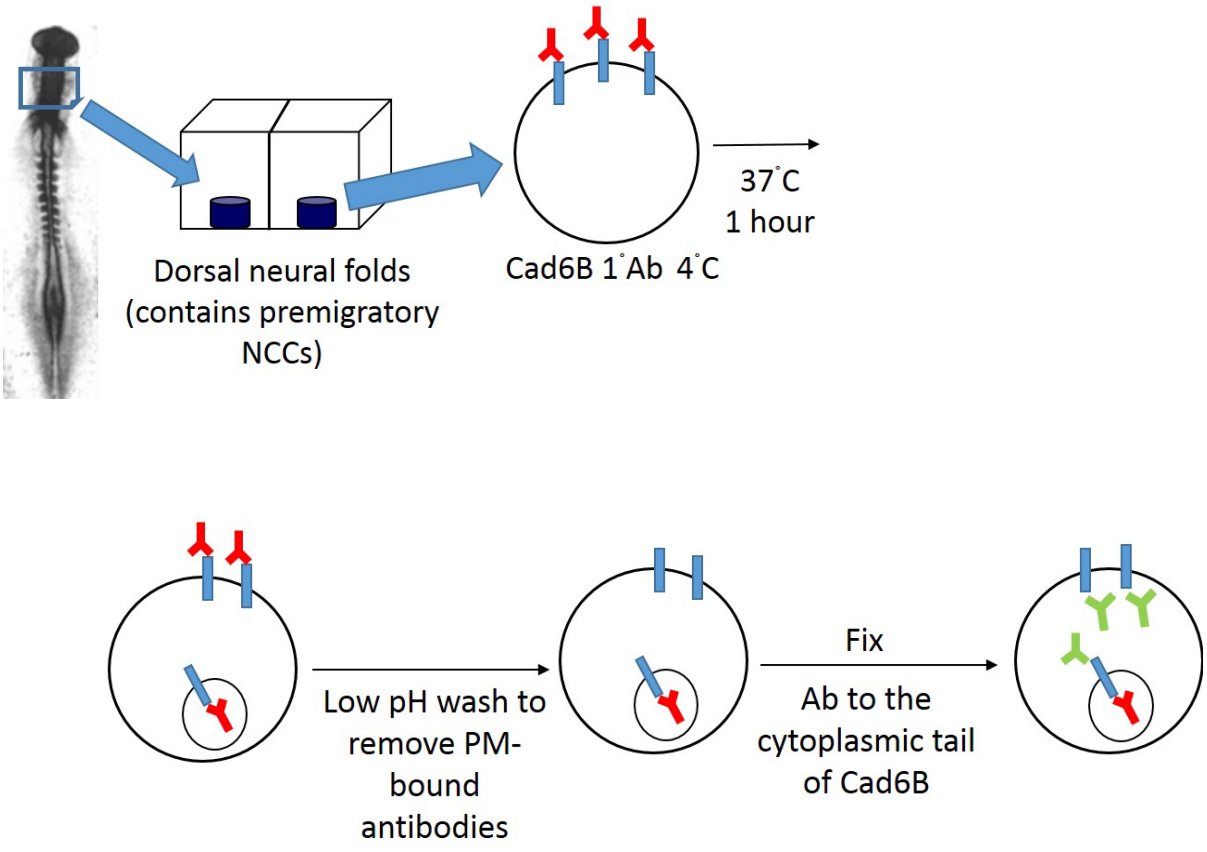

2.8. Protein extraction and immunoblotting

Protein extraction and immunoblotting was performed as described in (Schiffmacher et al., 2014). FlpInCHO cells expressing wild-type or mutant Cad6B were scraped in ice-cold PBS^{2+} and pelleted with low-speed centrifugation at 2300rpm for 5 minutes at 4˚C. The PBS^{2+} was completely removed and the cell pellets were stored at -80˚C until required. For cell lysis, 2X volume of lysis buffer (50mM Tris, pH 8.0, 150mM NaCl, 1% IGEPAL CA-630) supplemented with cOmplete Protease Inhibitor Cocktail (Roche, Basel, Switzerland) and 1 mM PMSF was added to the cell pellets on ice and subjected to gentle vortexing every 5 minutes for a total lysis time of 30 minutes at 4˚C. The lysate was subjected to high-speed centrifugation at 14000rpm for 15 minutes at 4˚C in order to separate the debris, and the protein concentration was quantified by Bradford assay (Thermo Scientific, Rockford, IL). Equivalent amounts of protein per sample were boiled at 95°C for 5 minutes in 4X reducing Laemmli sample buffer and centrifuged at maximum speed for 5 min at room temperature. The lysates were processed by SDS–PAGE electrophoresis in 1.5mm-thick 7.5% PAGE gels at 100V for 2 hours at room temperature. The gels were rinsed in water and soaked in cold 1X transfer buffer (1X running buffer without SDS) along with pre-cut PVDF membranes for 20 minutes at 4°C. The separated proteins were transferred on to the PVDF membranes in 1X transfer buffer at 100V for 1 hour in ice-cold conditions. Membranes were blocked in 5% non-fat milk in PBS supplemented with 0.1% Tween (PBS-Tween) for 30 minutes at room temperature and incubated overnight at 4°C with the following primary antibodies diluted in the blocking solution: Cad6B (1:80, CCD6B-1), β-actin (1:1000; sc-47778, Santa Cruz Biotechnology, Santa Cruz, CA, USA), p120-catenin (1:1000; sc-373751; Santa Cruz Biotechnology, Santa Cruz, CA, USA), and HA (1:2500;

3F10, Roche, Basel, Switzerland). Non-specifically bound antibodies were washed off with PBS-Tween 3X for 10 mins at room temperature. Membranes were subsequently incubated with species- and isotype-specific horseradish peroxidase-conjugated secondary antibodies (40ng/ml; Jackson ImmunoResearch, West Grove, PA, USA) in blocking solution for 1 hour at room temperature. Following 3X 10 minutes antibody washes with PBS-Tween, antibody detection was performed using the Supersignal West Pico or Femto chemiluminescent substrates (Thermo Pierce Scientific, Waltham, MA, USA) by mixing the substate and the enhancer solutions at a ratio of 1:1 and laying it on the membrane for 5 mins at room temperature. Following removal of excess substrate:enhancer solution, protein bands on the PVDF membrane were visualized using the ChemiDoc XRS system (Bio-Rad, Hercules, CA, USA). Immunoblot band volumes (intensities) were calculated from unmodified immunoblot images using Image Lab software (Bio-Rad, Hercules, CA, USA) and analyzed by repeated measures analysis of variance assuming a compound symmetric covariance matrix for time and an unstructured covariance matrix for band intensity based on AIC values within the PROC MIXED procedure in SAS statistical software (SAS Institute, Cary, NC). Levels were deemed significantly different when $p < 0.05$ based on Fisher's LSD multiple mean comparison test. Confidence intervals were calculated for the cytoskeleton (CSK) extraction assays and were deemed statistically significant if the confidence intervals did not overlap.

2.9. Magnetic beads co-immunoprecipitation

For reversible co-immunoprecipitation, cells from four 10cm plates were scraped in ice-cold PBS^{2+} and centrifuged at 2300rpm for 5 minutes at 4˚C. The PBS^{2+} was completely

removed, and 4X volume of lysis buffer (50mM Tris, pH 8.0, 150mM NaCl, 0.5% IGEPAL CA-630) supplemented with cOmplete Protease Inhibitor Cocktail (Roche, Basel, Switzerland) and 1mM PMSF was added to the cell pellets, pooled, and lysed gently on a rotator platform for 30 minutes at 4˚C. The lysate was then subjected to high- speed centrifugation at 14000rpm for 15 minutes at 4˚C in order to separate the debris from the supernatant. The supernatant was separated into two halves and each half was pre-cleared individually with a mixture of 40µL each of protein A and protein G beads. Antibody pre-clearing was performed by adding 2µg of mouse IgG for the p120 immunoprecipitation and 2ug rat IgG for the HA immunoprecipitation for one hour at 4˚C. Protein concentration was then determined by a Bradford assay (Thermo Scientific, Rockford, IL). Two micrograms of p120 and HA antibody was added to 1.5 and 1.2mg of appropriate pre-cleared lysates for immunoprecipitation, respectively, and the antigen-antibody complexes were allowed to form overnight at 4˚C in the rotator platform. On the next day, the antigen-antibody complexes were captured on protein A/G magnetic beads (88804, Thermo Scientific, Rockford, IL) for one hour at room temperature. Following 3X washes with 1X lysis buffer at room temperature, the beads were boiled at 95°C for 5 minutes in 4X reducing Laemmli sample buffer and centrifuged at maximum speed for 5 min at room temperature. The lysates were processed by SDS–PAGE electrophoresis in 1.5mm-thick 4% PAGE gels at 100V for 2 hours at room temperature and transferred to PVDF membranes as described earlier. Antibody addition and detection was performed as described previously.

2.10. Cell surface biotinylation

Four 6cm plates of confluent layers of FlpInCHO cells stably expressing wild-type or endocytic mutants of Cad6B were brought to 4˚C to significantly slow down cellular processes and washed twice with ice-cold PBS^{2+} for 5 minutes at 4˚C (Fig. 2.3). After removing all traces of PBS^{2+}, 1mL of freshly-prepared solution of EZ-Link Sulfo-NHS-Biotin (21326; Thermo Scientific, Waltham, MA, USA) dissolved in ice-cold PBS^{2+} was added to the cells at a concentration of 1mg/mL, and was incubated on a rocking platform at low speed for 30 minutes at 4˚C. After removal of the biotin solution, excess biotin was quenched with by washing 3 times, 5 minutes each, with ice-cold PBS^{2+} supplemented with 100mM glycine and 0.5% BSA at low speed on the rocking platform. After rinsing off the residual quenching buffer with ice-cold PBS^{2+}, cells were scraped off the dish from one of the plates in ice-cold PBS^{2+}, pelleted at 2300rpm for 5 minutes at 4˚C, and set aside as positive control for the "Total Surface" fraction. Biotin was then stripped off of cells from another plate by washing cells 3 times, 10 minutes each, at 4˚C using a stripping buffer (75mM NaCl, 75mM NaOH, 50mM L-glutathione (0399, Amresco, Solon, OH, USA) supplemented with 1% BSA) at low speed on a rocking platform, followed by scraping the cells in ice-cold PBS^{2+}, centrifugation, and the cell pellets set aside as negative control (T=0). Warm growth media (see above) was added to the cells in the remaining two plates, and cells were incubated at 37˚C for 60 minutes and 180 minutes, respectively, to allow for the resumption of cellular processes, including endocytosis.

Figure 2.3. Cad6B biotinylation assays *in vitro*. Cells expressing Cad6B are biotinylated at cold and incubated for various times at physiological temperature to allow for internalization. Following release of non-internalized biotin, cells are lysed and biotinylated proteins are immunoprecipitated with streptavidin. The amount of immunoprecipitated protein is a direct indicative of the endocytosed fraction.

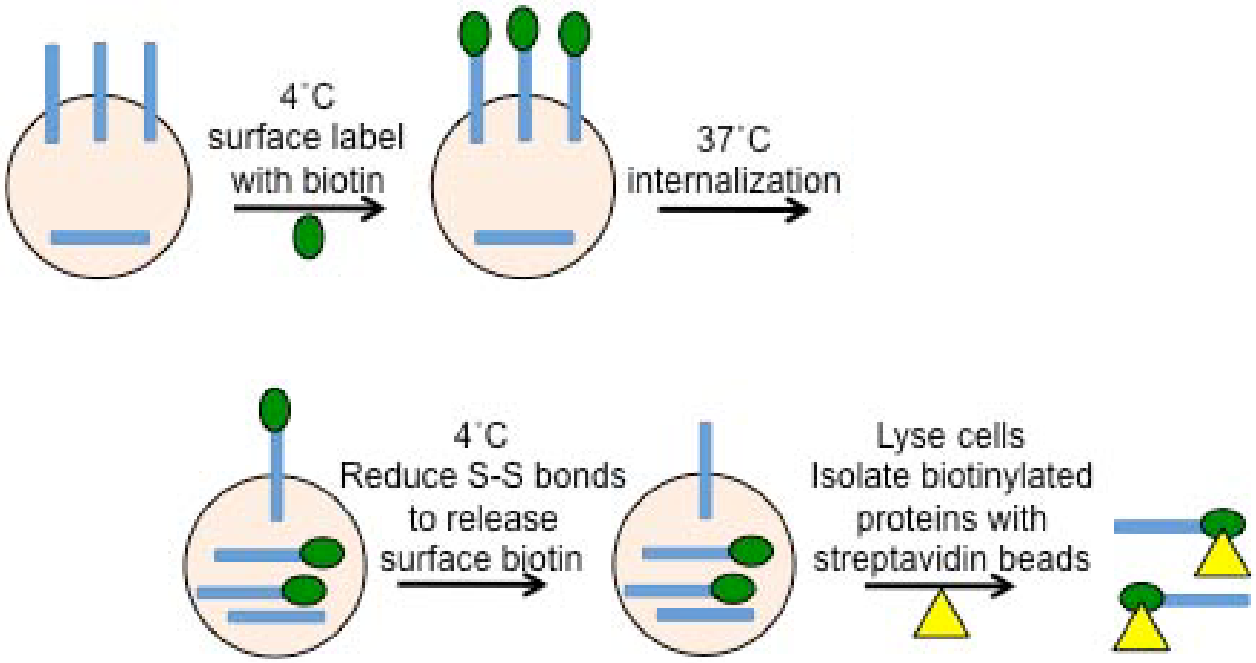

At the indicated time points, cells were brought back to 4˚C, rinsed 2X with ice-cold $PBS^{2+,}$ and any remaining biotin from cell surface-bound, non-endocytosed proteins was removed with the biotin stripping conditions as described above (Fig. 2.3). All the cell pellets were stored at -80˚C until ready for use. Cell pellets were thawed on ice and was lysed and subjected to a Bradford protein analysis with the protocol as described above in the immunoblotting section. Meanwhile, Streptavidin-Agarose resin (20347, Thermo Scientific, Waltham, MA, USA) was pre-blocked by rinsing the beads 3X with a 4% BSA solution, and replaced with 1X lysis buffer. Streptavidin-Agarose resin was incubated at a volume equivalent to 0.33µL per µg protein lysate with 175 (for wtCad6B-HA and LI645AA-HA cell lysates) or 200µg (for EED666AAA-HA lysate) of total protein lysate (in a total volume of 400µL) in a rotating-platform overnight at 4˚C to immunoprecipitate biotin-labeled proteins (Fig. 2.3). The following day, non-specific interactions were removed by rinsing the beads three times with 1X lysis buffer through gentle tube inversion. Freshly prepared 2X Laemmli sample buffer was added to the resin, and samples were boiled at 95˚C for 5 minutes and loaded onto a 7.5% PAGE gel. Electrophoresis, immunoblotting, and band intensity quantification for Cad6B was performed as described above.

2.11. TX-100 extraction of soluble and insoluble proteins

Sixty microliters of ice-cold cytoskeleton extraction buffer (CSK) (50mM NaCl, 10mM Pipes pH 6.8, 3mM $MgCl_2$, 0.5%Triton X-100, 300mM sucrose), supplemented with 1.2mM PMSF (36978; Thermo Pierce, Waltham, MA, USA) and 1X dilution of cOmplete Protease Inhibitor Cocktail (04693124001; Roche, Basel, Switzerland), was added to equal

numbers of FlpIn-CHO cells expressing wild-type or mutant Cad6B in 12-well dishes and incubated on a rocking platform for 30 minutes at 4˚C with occasional manual mixing. The extraction buffer was collected, centrifuged at maximum speed for 5 minutes at 4˚C, and the supernatant was designated as the TX-100 soluble fraction. The cells remaining on the plate were scraped and pelleted in ice-cold PBS^{2+}, and 2X Laemmli sample buffer was directly added to the cell pellet. Following brief pulses of sonication to shear genomic DNA, the lysate was centrifuged at maximum speed for 5 minutes at 4˚C, and designated as the TX-100 insoluble fraction. Following addition of 6X Laemmli sample buffer to the TX-100 soluble fraction, both the TX-100 insoluble and soluble fractions were boiled at 95°C for 5 minutes and all the lysates were loaded on to a 7.5% PAGE gel and subjected to SDS-PAGE electrophoresis as describe above. Immunoblotting and band intensity quantification as also performed described above.

2.12. Inhibitor treatment of explants

Cranial neural folds containing premigratory neural crest cells were directly explanted onto 4-well chamber slides containing 0.5% (vol/vol) DMSO, Dynasore (100uM; 304448-55-3, Adipogen, San Diego, CA, USA), Latrunculin A (100nM; L5163, Sigma-Aldrich, St. Louis, MO, USA), or EIPA (50uM; 3378, Tocris Bioscience, Sunnyvale, CA, USA) dissolved in 500µL neural crest explant media. The explants were incubated for 3 hours at 37˚C to allow for the neural crest cells to undergo EMT, and were fixed by serial dilution of the explant media with 4% PFA five times and incubating for 10 minutes at room temperature. Following removal of the fixative and a brief rinse with TBS, the explants were permeabilized with TBST and processed for immunofluorescence as described

previously. To quantify the size of the putative macropinocytic vesicles, each vesicle (n = 18) was visualized in 3D using the Zen software (Zeiss), and vesicle length was measured at its greatest extent using the Measurement tool provided in the software.

2.13. Confocal microscopy

All images were acquired with the LSM Zeiss 710 microscope (Carl Zeiss Microscopy, Thornwood, NY, USA) at the Imaging Core Facilty, University of Maryland, College Park. Where possible, the laser power, gain, and offset were kept consistent for the different channels throughout experiments. The pinhole was always set to one airy unit. The z-section optical images were acquired between 0.25-0.4μm per optical section and reconstituted in 3D composites using the Zen software (Zeiss).

Chapter 3. Cad6B is internalized in premigratory cranial neural crest cells *in vivo* and in cultured cells in *vitro*

Parts of this section were adapted from the following article under re-review at the Journal of Cell Science:

Padmanabhan R, Taneyhill LA (2015). Cadherin-6B undergoes macropinocytosis and clathrin-mediated endocytosis during cranial neural crest cell EMT.

3.1. Summary

In chick premigratory cranial neural crest cells, Cad6B is proteolytically processed by ADAM10, ADAM19 and γ-secretase (Schiffmacher et al., 2014). Nevertheless, Cad6B is also observed as puncta in premigratory neural crest cells and in cultured cells, suggesting that Cad6B could get internalized through endocytosis (or other mechanisms) during cranial neural crest cell EMT. The hypothesis that internalization of Cad6B could play an important role during EMT is not without precedence, as described in Chapter 1, Section 3.2, but such findings for cadherins have never been described for an *in vivo* EMT. To confirm that the observed Cad6B cytoplasmic puncta were due to internalization/endocytosis rather than exocytosis, we performed Cad6B antibody feeding assays *in vivo*, using an antibody against the Cad6B extracellular domain, to follow the processing of endogenous Cad6B protein. The antibody feeding assays showed the presence of Cad6B antibody-Cad6B complexes in the cytoplasm of premigratory cranial neural crest cells, suggesting that Cad6B could be internalized. To rule out the possibility that addition of Cad6B antibody could be stimulating Cad6B internalization, the antibody feeding assays were performed with the inclusion of an acid wash to remove any non-internalized (membrane-bound) Cad6B. Together with the preceding results, these data reveal that addition of Cad6B antibody does not stimulate Cad6B internalization, strongly suggesting that the Cad6B cytoplasmic puncta observed in wild-type embryos, in cultured cells and in the feeding assays are of endocytic nature.

3.2. Results

3.2. Generation of a stable cell line for biochemical analysis of Cad6B

Prior work demonstrated that the transcription factor Snail2 represses *cad6B* transcription in chick premigratory cranial neural crest cells prior to EMT (Taneyhill et al., 2007). Cad6B protein levels, however, are rapidly reduced over a span of ninety minutes (the developmental time frame for the addition of one somite pair in the chick embryo) during EMT (Hamburger and Hamilton, 1992) (Fig. 1.8). Since cadherins generally possess long half-lives (Ireton et al., 2002; Pujuguet et al., 2003; Pon et al., 2005), the loss of the majority of Cad6B protein within ninety minutes raised the possibility that additional mechanisms besides transcriptional repression and steady-state protein turnover were in place. To substantiate this possibility, we first determined the stability of Cad6B *in vitro* by creating a Cad6B stable cell line.

A cell line stably expressing wild-type Cad6B (tagged with a hemagglutinin (HA) epitope at the C terminus) from a single genomic locus was generated using CHO cells as the parent cell line (FlpInwtC6B-HA). Single-copy expression of Cad6B was important to minimize any deleterious effects that might occur due to Cad6B overexpression (Levenberg et al., 1999; Bryant et al., 2005), and CHO cells were chosen because they do not express any endogenous cadherins (Hong et al., 2010). Immunofluorescence for Cad6B was performed on fixed FlpInwtC6B-HA cells with an antibody that recognizes the N terminal, extracellular domain of Cad6B (this antibody will now be referred to as NT6B) and HA to determine if the transgene was properly expressed. FlpInCHO cells stably transfected with the empty expression vector had no detectable immunofluorescence for Cad6B (Fig. 3.1A-A”), while FlpInwtC6B-HA cells exhibited Cad6B immunofluorescence

on the plasma membranes of apposing cells (Fig. 3.1C", arrows) and in what appear to be cytosolic puncta (Fig. 3.1C", arrowheads). Cad6B (NT6B) was also at times observed to be negative for HA immunoreactivity, suggesting these could be the N-terminal fragments post-proteolysis by unknown proteases in the FlpInCHO cell lines (Fig. 3.1C", caret), consistent with our prior results (Schiffmacher et al., 2014). These data demonstrate that Cad6B-HA localizes to the correct location as other cadherins *in vitro* and endogenous Cad6B in embryos (see Fig. 3.4 below) (Breviario et al., 1995; Nakagawa and Takeichi, 1995; Navarro et al., 1998; Taneyhill et al., 2007; Schiffmacher et al., 2014). We also performed immunoblotting for Cad6B (NT6B) in lysates prepared from FlpInwtC6B-HA cells and compared the relative molecular weight of Cad6B-HA to endogenous Cad6B expressed by embryos *in vivo*. As shown in Fig. 3.1D, Cad6B-HA expressed by the FlpInwtC6B-HA cells and by embryos is approximately the same molecular weight, indicating that Cad6B-HA is biosynthesized and localizes similarly in this cell line as observed *in vivo*. Additionally, we notice an additional ~100kDa band recognized by the Cad6B (NT6B) antibody, which could be a proteolytic product of Cad6B (Schiffmacher et al., 2014) and thus the identity of the Cad6B (NT6B)-positive HA-negative puncta seen upon immunofluorescence in these cells (Fig. 3.1C-C'''').

Figure 3.1. Cad6B in the FlpInwtC6B-HA cells is observed in the correct sub-cellular pattern and is expressed at the appropriate molecular weight. Immunofluorescence performed for NT6B (green) and HA (red) on FlpInCHO cells stably transfected with empty vector (A-A") and FlpInwtC6B-HA cells (B-B") (n = 30). (C-C") are higher magnification views of the boxed region in (B"). Arrows and arrowheads represent Cad6B (NT6B) and HA co-staining at the membrane and cytoplasm, respectively. Caret in (C") represents NT6B-positive but HA-negative puncta that are occasionally observed. Panels represent the 3D composite of 17 Z-stack images (0.25 μm/optical slice) acquired with a confocal microscope. (D) Immunoblotting for Cad6B (NT6B) in lysates prepared from 12-16ss embryos and FlpInwtCad6B-HA cells (Cad6B bands in the last two lanes will be discussed in the next chapter). The band at ~100kDa is presumed to be a proteolytic product of Cad6B due to the action of endogenous proteases in CHO cells, as observed in (Schiffmacher et al., 2014). Immunoblotting for β-actin was performed as a loading control. Scale bars: 10μm.

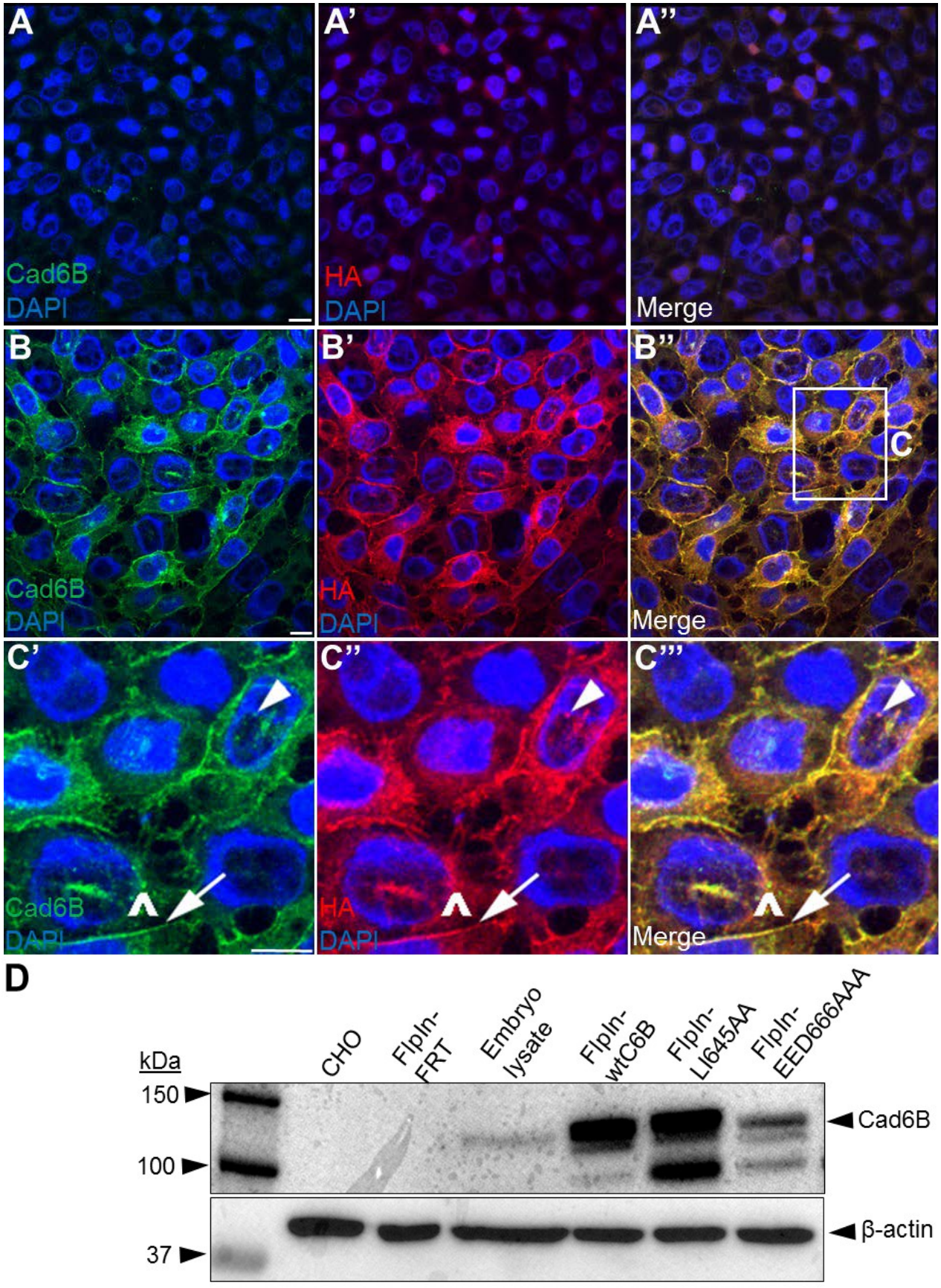
A
A'
A''
Cad6B
DAPI
HA
DAPI
Merge
B
B'
B''
C
Cad6B
DAPI
HA
DAPI
Merge
C'
C''
C'''
Cad6B
DAPI
HA
DAPI
Merge
D
kDa
CHO
FlpIn-FRT
Embryo lysate
FlpIn-wtC6B
FlpIn-LI645AA
FlpIn-EED666AAA
150
100
37
Cad6B
β-actin

3.3. Cad6B is stable for 5.5 hours in vitro

As mentioned above, the loss of the majority of Cad6B protein within ninety minutes in premigratory cranial neural crest cells is suggestive of either Cad6B turnover through additional mechanisms or that Cad6B possesses a short half-life. To address the latter possibility, the stability of Cad6B was determined *in vitro* by examining Cad6B-HA levels over time upon inhibition of *de novo* protein synthesis with addition of cycloheximide. Our results reveal that Cad6B-HA is stable for 5.5 hours in FlpInwtC6B-HA cells (Fig. 3.2). This is in agreement with what has been observed for E-cadherin (4-6 hours; (Ireton et al., 2002; Pujuguet et al., 2003)) and N-cadherin (6 hours; (Pon et al., 2005)) *in vitro*, suggesting that other mechanisms likely operate to remove Cad6B from the plasma membranes of premigratory neural crest cells.

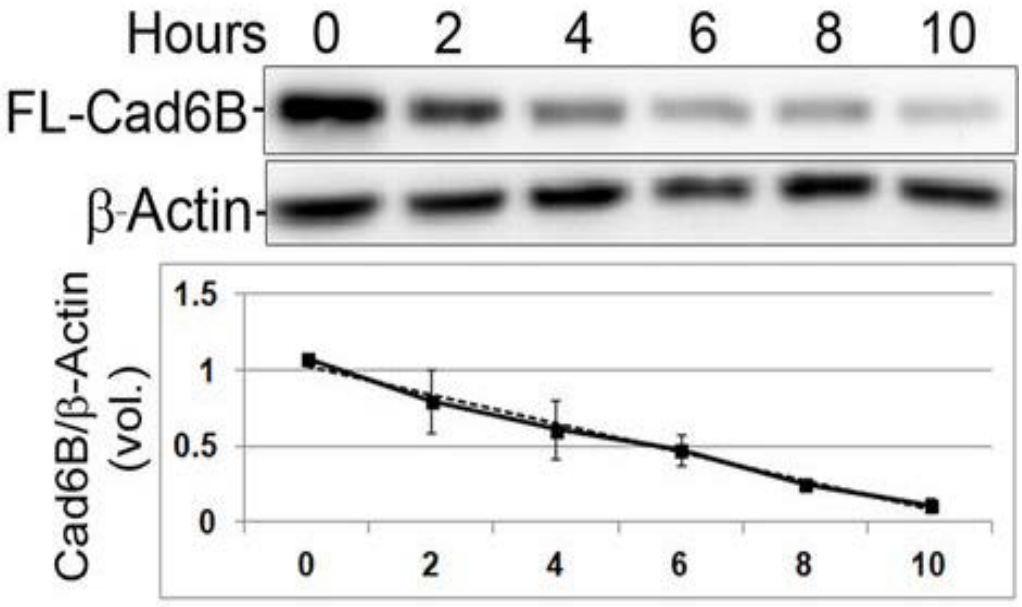

Figure 3.2. Cad6B is stable for 5.5 hours in FlpInwtC6B-HA cells. FlpInwtC6B-HA cells were treated with cycloheximide for different periods, lysed and subjected to SDS-PAGE electrophoresis. Immunoblotting was performed using Cad6B (NT6B) and β-actin (loading control) antibodies, and a representative blot is shown (top). Densitometric band intensities of Cad6B and β-actin from three independent replicates were quantified and plotted on a graph (below). Image reproduced from (Schiffmacher et al., 2014).

3.4. Cad6B localizes to the cytoplasm in vitro

To explore the possibility that Cad6B might undergo internalization via endocytosis, we performed immunofluorescence for Cad6B (NT6B) and several markers of the endosomal and lysosomal compartments (Appendix 1). Most of these latter antibodies (raised against human antigens in mouse and rabbit) did not recognize their cognate antigens in chick tissue (data not shown; Appendix 1), except for clathrin (discussed in further detail in Chapter 5). As an alternative, we obtained endosomal/lysosmal marker-fluorescent protein fusion constructs (a kind gift from Dr. Iqbal Hamza, University of Maryland, College Park) and expressed them in chick embryos at trace levels (Appendix 2). Although we noted that certain endosomal marker-fusion proteins co-localized with Cad6B-HA *in vivo*, we were unable to validate this observation upon performing immunofluorescence against endogenous antigens in chick tissue (Appendix 2). Moreover, several constructs were ubiquitously expressed leading to spurious co-localization with Cad6B-HA (Appendix 2), forcing us to return to our previous approach using antibodies against endogenous proteins. For this reason, Na^+K^+ATPase, a marker of the plasma membrane (Van Dyke, 2004), was chosen for use in future assays, as it was one of the few antigens for which successful immunostaining could be performed. Since Na^+K^+ATPase plays an important role in the acidification of endosomes (Cain et al., 1989; Fuchs et al., 1989; Feldmann et al., 2007) and localizes to Rab5-positive endosomes (Feldmann et al., 2007), we reasoned that cytosolic Na^+K^+ATPase could serve as a marker for the early endosomal compartment. Through confocal microscopy analysis of Z-stack images, we observe Cad6B-HA (NT6B) on the plasma membrane and in the cytoplasm in apparent puncta, where it partially co-localizes with Na^+K^+ATPase (Fig. 3.3A-A", arrowheads; carets represent puncta in which

Cad6B-HA and Na^+K^+ATPase do not co-localize). These results suggest that Cad6B-HA is internalized and localizes to the cytoplasm in this cell line.

Figure 3.3. Cad6B localizes to the cytoplasm *in vitro*. (A-A") FlpInwtC6B-HA cells were fixed and immunostained for NT6B (green) and Na^+K^+ATPase (red). Cad6B-HA (NT6B) partially co-localizes with Na^+K^+ATPase in several cytoplasmic puncta (arrowheads in A"; carets represent puncta in which Cad6B-HA and Na^+K^+ATPase do not co-localize) (n = 3). Panels represent the 3D composite of 20 Z-stack images (0.35 μm/optical slice) acquired with a confocal microscope. Scale: 10μm. Image reproduced from (Padmanabhan R, Taneyhill LA, under re-review at J Cell Sci).

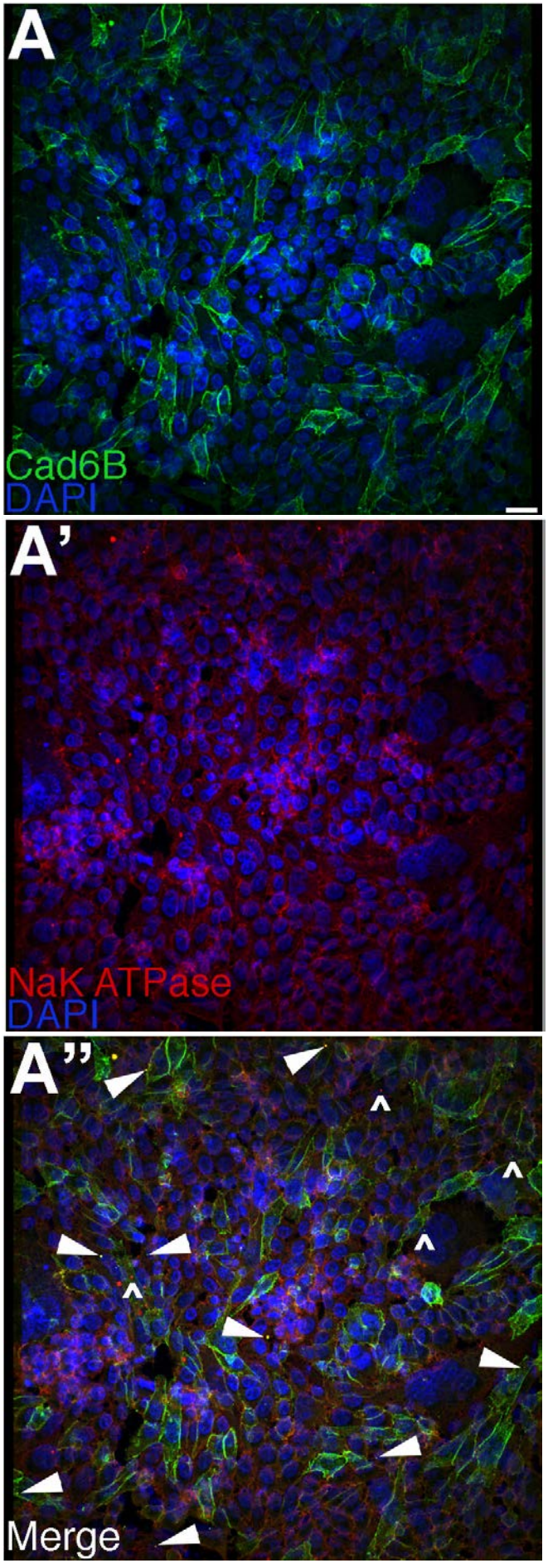
A
Cad6B
DAPI
A'
NaK ATPase
DAPI
A''
Merge

3.5. Cad6B is observed in the cytoplasm of premigratory and early migratory neural crest cells (in vivo) and in neural crest cell explants (ex vivo)

To ascertain whether internalization plays a role in the post-translational downregulation of Cad6B *in vivo*, we performed immunohistochemistry for endogenous Cad6B (NT6B) and Na^+K^+ATPase on 6 and 7ss embryos, when premigratory cranial neural crest cells begin to reduce Cad6B levels during EMT (Taneyhill et al., 2007; Schiffmacher et al., 2014). In addition to Cad6B marking cell membranes (Fig. 3.4A-A'', arrow), we observe Cad6B (NT6B) co-localizing with Na^+K^+ATPase in cytoplasmic puncta within premigratory cranial neural crest cells (Fig. 3.4A", arrowheads). These results indicate that Cad6B (NT6B) may be internalized in these precursor cells prior to and/or during EMT. To further address this question, we conducted cranial neural crest cell explant assays (Taneyhill et al., 2007) and examined Cad6B (NT6B) in neural crest cells undergoing EMT *ex vivo* in culture. Immunostaining with the NT6B antibody reveals several puncta in the cytosol of emigrating neural crest cells (the Na^+K^+ATPase antibody did not recognize its cognate antigen in this *ex vivo* system), strongly suggesting that Cad6B (NT6B) may be internalized in premigratory neural crest cells undergoing EMT and in early migratory neural crest cells in the chick head (Fig. 3.4B-B', arrowheads).

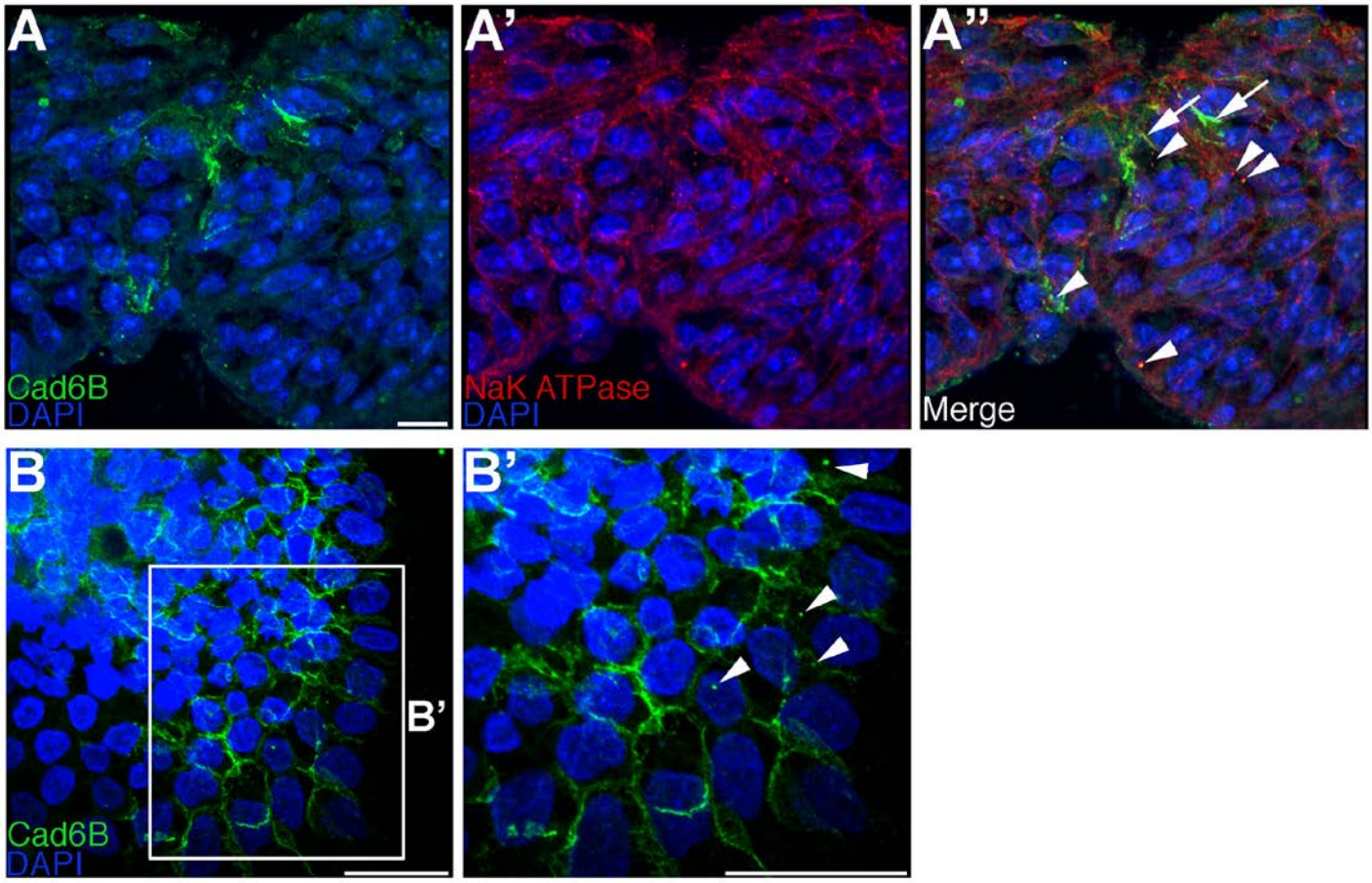

Figure 3.4. Cad6B localizes to the cytoplasm of neural crest cells undergoing EMT *in vivo* and *ex vivo*. (A-A") Embryos possessing neural crest cells initiating EMT were harvested, fixed and immunostained for Cad6B (NT6B; green) and Na^+K^+ATPase (red). Cad6B co-localizes with Na^+K^+ATPase on the plasma membrane (arrows) as well as in cytoplasmic puncta (arrowheads) (n = 20 transverse sections from at least 10 embryos). (B-B') Cranial dorsal neural folds possessing premigratory neural crest cells were explanted onto chamber slides, allowed to undergo EMT for 3 hours (longer incubation time results in significant reduction of immunofluorescence due to natural loss of Cad6B in explants), fixed, and immunostained for NT6B (n = 3 explants). The antibody against Na^+K^+ATPase did not recognize their cognate antigen in the explant system. (B') is a higher magnification view of the boxed region in (B). Cad6B (NT6B) localizes to the cytoplasm (arrowheads in B'), similar to what is observed *in vitro* and *in vivo*. Panels represent the 3D composite of 20 (A-A") and 23 Z-stack images (B-B") (0.25 µm/optical slice) acquired with a confocal microscope at 63x magnification. Scale bars: 10µm. Image reproduced from (Padmanabhan R, Taneyhill LA, under re-review at J Cell Sci).

3.6. Cad6B antibody feeding assays demonstrate Cad6B in the cytosol of delaminating neural crest cells in vivo

Although suggestive of an internalization event, Cad6B cytoplasmic puncta could also be due to exocytosis, as *cad6B* transcripts (and protein) persist until the 6ss in premigratory cranial neural crest cells (Taneyhill et al., 2007; Schiffmacher et al., 2014). To differentiate between internalization events and exocytosis, we performed Cad6B antibody feeding assays (Arancibia-Carcamo IL, 2006) in which we introduced the NT6B antibody into the lumen of embryos electroporated with a membrane GFP construct (to label premigratory neural crest cell plasma membranes; a gift from Dr. Paul Kulesa, Stowers Institute of Medical Research, Kansas City, MO, USA) (Fig. 3.5B-C"). We reasoned that since the NT6B antibody recognizes the lumen-exposed, extracellular domain of Cad6B, the NT6B-Cad6B complex would be processed in the same way as endogenous Cad6B protein when premigratory cranial neural crest cells undergo EMT. As a control, we introduced an antibody to RFP into a separate set of embryos and performed the same experiment. RFP antibody-fed embryos fail to show any discernable immunofluorescence for Cad6B (Fig. 3.5A-A"), indicating that addition of an unrelated antibody does not non-specifically stimulate internalization of Cad6B. In embryos fed with the NT6B antibody, however, we note NT6B-Cad6B in several cytosolic puncta (Fig. 3.5C", arrowheads) within the confines of a membrane GFP-expressing delaminating neural crest cell (Fig. 3.5C", arrow), as discerned by confocal imaging. These data indicate that the Cad6B-containing puncta observed *in vivo* and *ex vivo* are likely to be of endocytic rather than exocytic nature.

Figure 3.5. Cad6B feeding assays demonstrate that Cad6B puncta are endocytic rather than exocytic in nature. RFP (A-A") or NT6B (B-B") antibody was introduced into the lumen of embryos electroporated with a membrane GFP construct. Embryos were incubated to allow for EMT to occur, fixed and then immunostained to detect RFP antibody-Cad6B or NT6B antibody-Cad6B complexes (red) and GFP (green) (n = 6 from 3 different embryos). (C-C") are high magnification images of the boxed region in (B). Embryos fed with RFP antibody fail to elicit any detectable immunofluorescence with a secondary antibody to detect Cad6B (A-A"). Internalized NT6B antibody-Cad6B complexes (C", arrowheads) are seen in the cytoplasm within the confines of the GFP-expressing plasma membrane (C", arrow) of a delaminating neural crest cell. Panels (B-C") represent the 3D composite of 22 Z-stack images (0.25 µm/optical slice) acquired with a confocal microscope at 63x magnification. Scale bars: 10µm. Image modified from (Padmanabhan R, Taneyhill LA, under re-review at J Cell Sci).

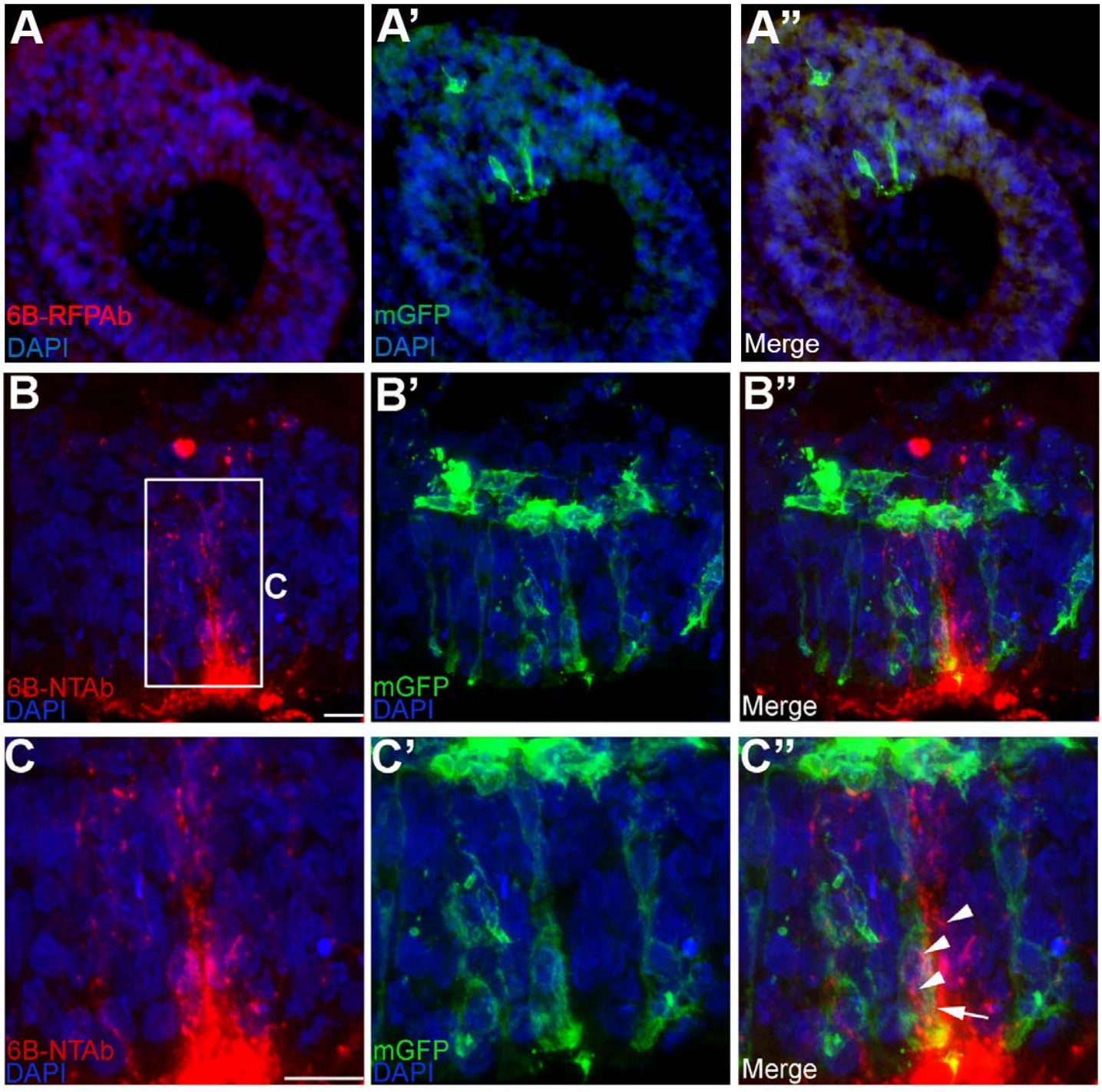
A
6B-RFPAb
DAPI
A'
mGFP
DAPI
A''
Merge
B
C
6B-NTAb
DAPI
B'
mGFP
DAPI
B''
Merge
C
6B-NTAb
DAPI
C'
mGFP
DAPI
C''
Merge

3.7. Addition of Cad6B antibody does not stimulate Cad6B internalization

Although our current data reveal that Cad6B is internalized both *in vitro* and *in vivo*, binding of the NT6B antibody to Cad6B protein exposed on cell membranes could have artificially stimulated internalization of Cad6B-NT6B complexes. To eliminate this possibility, we performed the same antibody assay *in vitro* (Fig. 3.6A-B") and *ex vivo* in explants (Fig. 3.7C-D") with the inclusion of an acid wash protocol. Following addition of the NT6B antibody, cells were washed with a low pH buffer, which strips off any plasma membrane-bound NT6B antibodies but does not disturb internalized complexes (Arancibia-Carcamo IL, 2006). The cells were then fixed, permeabilized and immunofluorescence performed to detect the NT6B antibody (through addition of secondary antibody alone) and the HA tag at the C terminal end of Cad6B. Cad6B that remains on the plasma membrane is recognized only by the HA antibody, while internalized NT6B-Cad6B complexes are recognized by both the HA and NT6B antibodies (see Fig. 2.2, Materials and Methods). When the assay was performed at 4˚C to slow down cellular processes, most of the NT6B antibody was stripped off (Fig. 3.6A) without affecting overall membrane distribution of Cad6B, as noted by the continued presence of Cad6B on the plasma membrane detected by HA immunoreactivity (Fig. 3.6A", arrows). Performing the assay at 37˚C led to the appearance of several internalized NT6B-Cad6B cytoplasmic puncta (Fig.3.6B", arrowheads) but did not stimulate global internalization of Cad6B protein, as indicated by retained plasma membrane HA (Cad6B) immunoreactivity (Fig. 3.6B", arrows).

The same assay was then performed *ex vivo* in explants (Figs. 3.7C-C" and 3.7D-D") to corroborate these *in vitro* observations. Here plasma membrane-bound Cad6B was

distinguished from internalized NT6B-Cad6B complexes with an antibody that recognizes the C terminus of endogenous Cad6B (CT6B). Explants remaining at 4˚C and subjected to the low pH wash resulted in the removal of virtually all NT6B antibody bound to non-internalized (plasma membrane-localized) Cad6B without affecting general Cad6B membrane distribution, as shown by the CT6B antibody immunoreactivity (Fig. 3.7B', B", arrows). Incubating the explants at 37˚C, however, led to the appearance of several NT6B-Cad6B cytosolic puncta (Fig. 3.7D", arrowheads) and the persistence of some membrane-bound Cad6B (Fig. 3.7D", arrows). These data suggest that addition of the Cad6B antibody (NT6B) does not stimulate significant internalization of Cad6B and corroborates our earlier observation that the puncta are likely of endocytic rather than exocytic nature. Collectively, our observations reveal that Cad6B is internalized in cultured cells and in premigratory cranial neural crest cells during EMT.

Figure 3.6. Cad6B antibody feeding assays in the presence of an acid wash demonstrate that the NT6B antibody does not stimulate internalization of Cad6B *in vitro*. The NT6B antibody was added to the media of FlpInwtC6B cells (A-A" and B-B") and incubated for an hour. The cells were then washed with a low pH buffer, fixed and immunostained with the NT6B and HA antibodies (n = 4). At 4˚C, little to no internalized NT6B-Cad6B complexes are observed, with most (if not all) Cad6B immunofluorescence localized to the plasma membrane (A", arrows). At 37˚C, internalized NT6B-Cad6B complexes are observed in the cytoplasm (B", arrowheads), and Cad6B immunofluorescence is still noted on the plasma membrane (B", arrows). All images represent a single optical slice acquired with a confocal microscope. Inset boxes in (A-A", B-B") show the original image at 63x, with the asterisks in (A, B) indicating the location of the higher magnification field of view shown in the main panels. Scale bars: 10μm. Image reproduced from (Padmanabhan R, Taneyhill LA, under re-review at J Cell Sci).

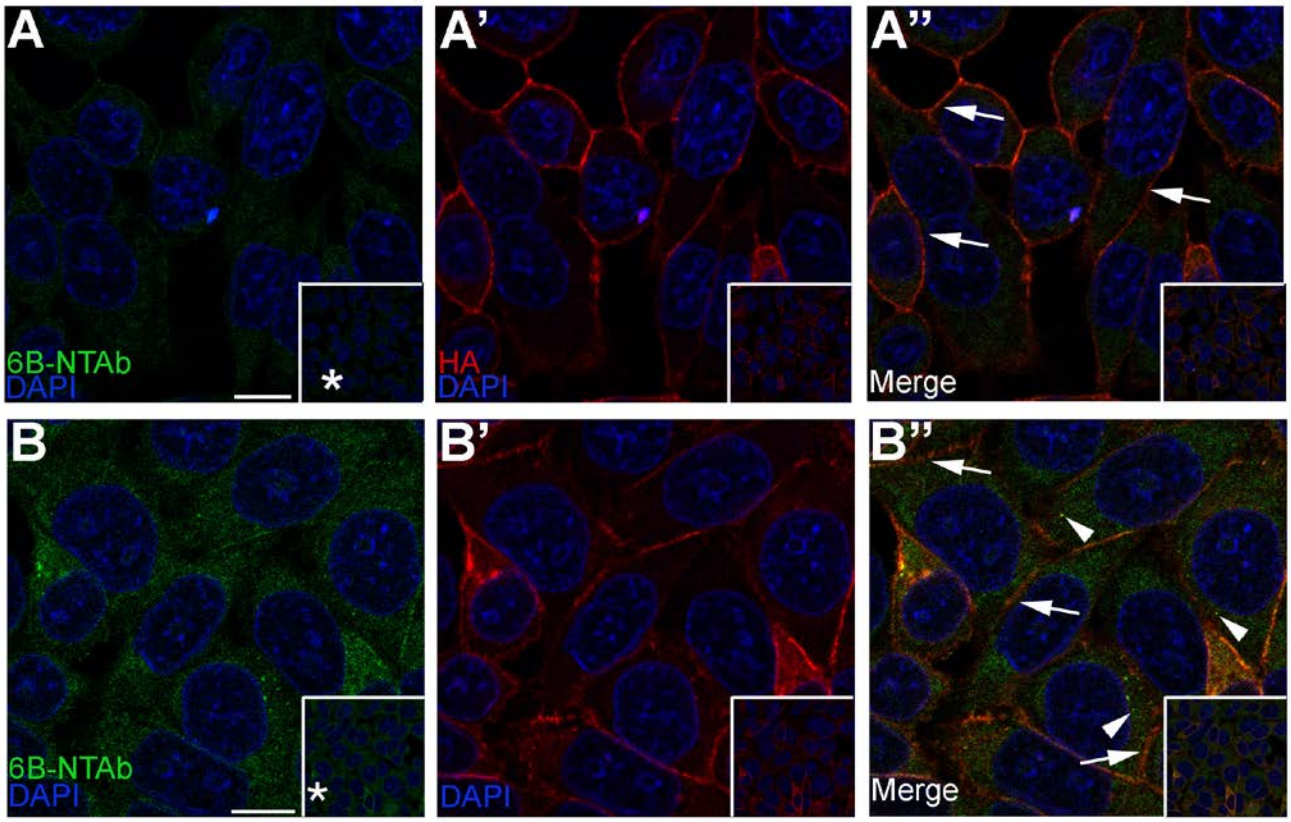
A
6B-NTAb
DAPI
*
A'
HA
DAPI
A''
Merge
B
6B-NTAb
DAPI
*
B'
DAPI
B''
Merge

Figure 3.7. Cad6B antibody feeding assays in the presence of an acid wash demonstrate that the NT6B antibody does not stimulate internalization of Cad6B *ex vivo*. The NT6B antibody was added to the media of dorsal neural fold explants containing premigratory cranial neural crest cells (A-A" and B-B"), and the explants were incubated for to allow for EMT to occur. Explants were then washed with a low pH buffer, fixed and immunostained with the NT6B and CT6B antibodies (Fig. 2.2) (n = 2 explants). At 4˚C, little to no internalized NT6B-Cad6B complexes are observed, with most (if not all) Cad6B immunofluorescence localizing to the plasma membrane (A", arrows). At 37˚C, internalized NT6B-Cad6B complexes are noted in the cytoplasm (B", arrowheads), but some Cad6B immunofluorescence is still observed on the plasma membrane (B", arrows). All images represent the 3D composite of 61 (A-A") and 124 Z-stack images (B-B") (0.25 µm/optical slice) acquired with a confocal microscope at 63x magnification. Inset boxes in (B-B") show the original image at 63x, with the asterisks in (B) indicating the location of the higher magnification field of view shown in the main panels. Scale bars: 10µm. Image reproduced from (Padmanabhan R, Taneyhill LA, 2015, under re-review at J Cell Sci).

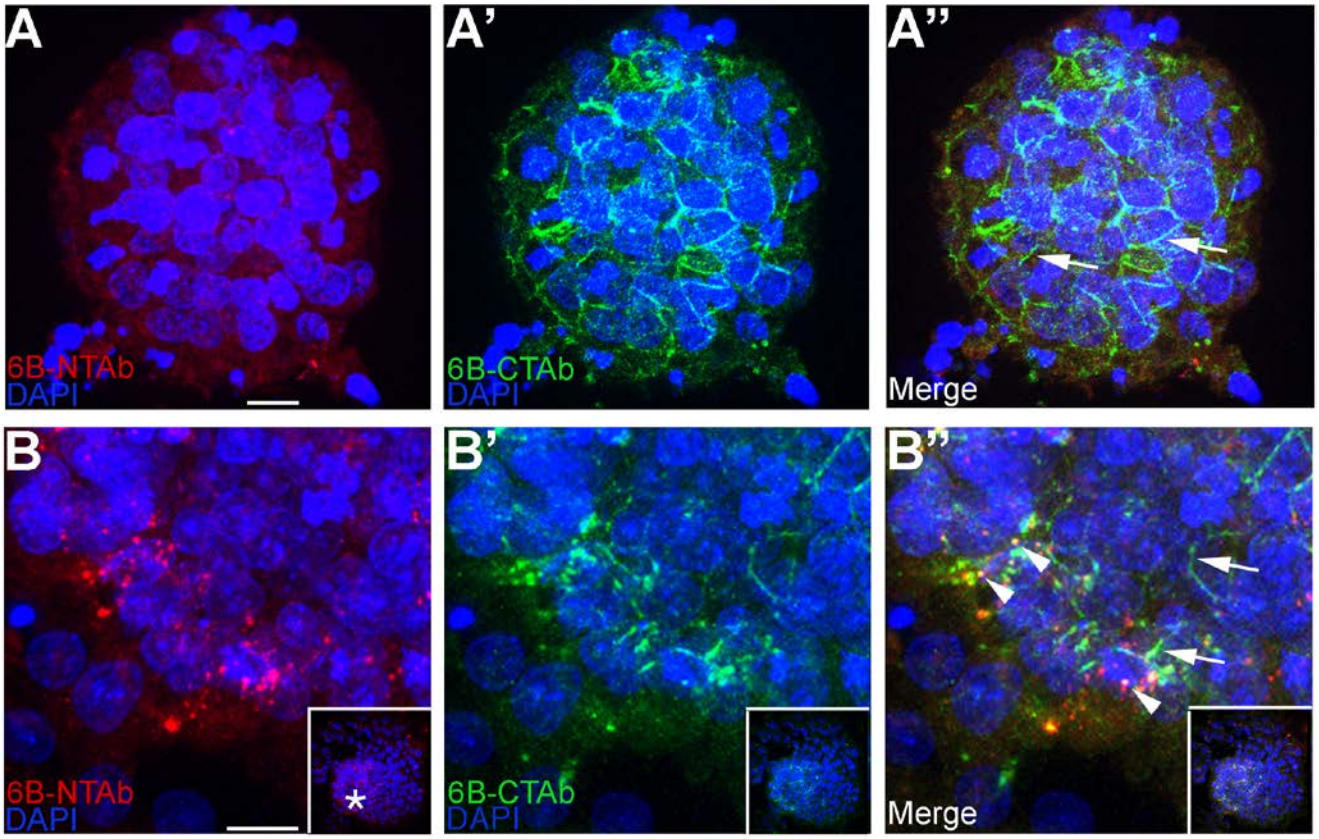
A
6B-NTAb
DAPI
A'
6B-CTAb
DAPI
A''
Merge
B
6B-NTAb
DAPI
*
B'
6B-CTAb
DAPI
B''
Merge

3.8. Discussion

EMT is a highly dynamic and tightly regulated process that is mediated by multiple mechanisms (see Introduction, Section 1.4). Endocytosis is one such mechanism, in which the internalization of growth factor receptors, cell junction proteins, integrins, and/or polarity proteins all facilitate EMT. Aberrant endocytosis of one or more of these molecules is now recognized as an emerging feature of cancer (Mosesson et al., 2008). Intrigued by the finding that Cad6B is observed in cytosolic puncta in premigratory and emigrating cranial neural crest cells, we wondered if Cad6B could be internalized (possibly through endocytosis) in premigratory neural crest cells as they undergo EMT. As described in the Introduction (Section 1.4.2.2.2), Cad6B is unique in its exclusive expression by the premigratory neural crest cell population and its reduction during EMT. Rapid loss of Cad6B protein (Taneyhill et al., 2007) suggests that other mechanisms besides transcriptional repression exist to remove Cad6B post-translationally from the plasma membranes of premigratory neural crest cells. Indeed, Cad6B-HA is stable for 5.5 hours *in vitro* through cycloheximide-inhibition assays, supporting our hypothesis for a potential role for post-translational downregulation of Cad6B during EMT, and internalization of Cad6B through endocytosis could be one such means by which this occurs. Although the half-life of a protein can be more accurately determined through pulse-chase immunoprecipitation of radiolabeled proteins, cycloheximide inhibition still provides a reasonable estimate of the half-life of Cad6B protein (Zhou 2004). Furthermore, cadherin endocytosis during EMT has been demonstrated *in vitro* (Fujita et al., 2002; Lu et al., 2003; Gavard and Gutkind, 2006; Kowalczyk and Nanes, 2012), and is thus not without precedent.

A definitive indicator of Cad6B endocytosis would have been a demonstration of the co-localization of cytoplasmic Cad6B puncta with known markers of endosomal compartments and the lysosome, such as Rab4, Rab7 and LAMP-1. Since antibodies for these markers failed to recognize their cognate antigens under various experimental conditions in the chick embryo (Appendix 1), and approaches to express endosomal and lysosomal marker-fusion proteins proved futile (Appendix 2), Na^+K^+ATPase, a generic plasma membrane marker, was chosen. In addition to serving as a marker of the plasma membrane and thus delineating cell boundaries, Na^+K^+ATPase plays an important role in the acidification of endosomes (Cain et al., 1989; Fuchs et al., 1989; Feldmann et al., 2007) and localizes to Rab5-positive endosomes (Casciola-Rosen and Hubbard, 1992; Feldmann et al., 2007), facilitating a reasonable extrapolation that cytosolic Na^+K^+ATPase serves to denote the early endosomal compartment. Immunofluorescence experiments revealed that Cad6B-HA (NT6B) cytosolic puncta noted in FlpInwtC6B-HA cells co-localize with Na^+K^+ATPase (and both proteins also co-localize at the membrane), both *in vitro* (Fig. 3.3) and *in vivo* (Fig. 3.4). These results suggest not only that Cad6B-HA could undergo internalization and localize to the early endosome, but also that the puncta are present within the vicinity of the plasma membrane (Fig. 3.3), indicating that these cytoplasmic puncta could represent *bona fide* internalized Cad6B molecules (Fig. 3.3).

We also observed several NT6B-positive, Na^+K^+ATPase-negative and NT6B-negative, Na^+K^+ATPase-positive puncta (Fig. 3.3, carets), raising questions as to their identities. Since the early endosome serves as an initial sorting compartment (Jovic et al., 2010), these puncta could represent later events in the endosomal pathway, where Cad6B (NT6B) and/or Na^+K^+ATPase are routed differently, either recycled back to the plasma

membrane or trafficked to the lysosome for degradation. Indeed, Na^+K^+ATPase-positive vesicles undergo both clathrin- and caveolin-mediated endocytosis and subsequently localize to the late endosome (Liu et al., 2004; Liu et al., 2005; Periyasamy et al., 2005). Further proof for the presence of intracellular Cad6B puncta came from experiments performed in neural crest cell explant cultures, in which endogenous Cad6B (NT6B)-containing puncta localize within the confines of Cad6B (NT6B)-positive neural crest cell plasma membranes (Fig. 3.4).

To ascertain the nature of these puncta (endocytic versus exocytic), *in vivo* Cad6B antibody feeding assays were performed, which showed cytosolic localization of NT6B-Cad6B complexes within cells expressing membrane GFP (Fig. 3.5). Antibody feeding assays have been widely used to study trafficking and endocytosis of a variety of transmembrane proteins (Arancibia-Carcamo IL, 2006), including cadherins (Paterson et al., 2003; Xiao et al., 2003b; Tai et al., 2007). Importantly, this assay rests on the fundamental assumption that the addition of the antibody does not stimulate endocytosis of the antigen. Although studies have shown that antibody addition does not increase endocytosis in the case of other cadherins (Paterson et al., 2003; Xiao et al., 2003b; Tai et al., 2007), this had yet to be shown for Cad6B, thus necessitating the use of the same assay (acid wash, Fig.3.6 and 3.7). If the NT6B antibody were stimulating internalization of Cad6B, its addition would likely result in gross internalization of Cad6B. Since a significant portion of Cad6B was still retained/localized to the plasma membrane, these results instead suggest that such stimulation of Cad6B internalization was not occurring, in agreement with what is observed for other cadherins. Moreover, performing the assay at 4˚C did not result in any cytoplasmic NT6B-Cad6B complexes, indicating that the

observed puncta are not due to non-specific "antibody-trapping" inside the cells. Taken together, the *in vitro* and *ex vivo* feeding experiments validate the results obtained in the *in vivo* Cad6B antibody feeding assay. Interestingly, although the Cad6B antibody feeding assays were performed identically, a striking difference was observed in the number of cytosolic NT6B-Cad6B puncta *in vitro* (Fig. 3.6B") compared to *ex vivo* (roughly 10-fold; Fig. 3.7B"). This disparity could be attributed to a variation in the rates of Cad6B protein internalization (i.e., Cad6B basal turnover rates *in vitro* versus *en masse* Cad6B internalization in explant cultures during EMT in response to extrinsic and intrinsic signals). Furthermore, this difference supports our initial hypothesis that additional mechanisms controlled by such signals must operate to rapidly remove Cad6B from the plasma membranes of premigratory neural crest cells for EMT to occur. In addition, the size of the Cad6B cytoplasmic puncta observed *in vivo, ex vivo* and *in vitro* vary considerably. The larger complexes observed *ex vivo* and *in vivo* could represent one or more internalized compartments merging together as multi-vesicular bodies, indicating that additional mechanisms operating solely in neural crest but not cultured cells may be in place to internalize Cad6B. Collectively, our observations reveal that Cad6B undergoes internalization in cultured cells and in premigratory cranial neural crest cells *in vivo* and *ex vivo*.

Although convincing, additional experiments could be performed to further validate that the NT6B antibody does not stimulate Cad6B internalization: (1) After addition of the NT6B antibody, the neural fold explants could be incubated for a shorter time period (less than the current 3.5 hours used herein) to investigate whether there is a decrease in the number of NT6B-Cad6B complexes. (2) The assay could be performed

using tissue that is negative for Cad6B. (3) An antibody against another neural crest cadherin, such as E-cadherin or N-cadherin, could be fed to dorsal neural fold explants to determine if another cadherin antibody can affect Cad6B localization. (4) Cad6B in the midbrain could be knocked down through morpholinos and then the NT6B antibody could be fed. (5) The feeding assays could be performed following inhibition of endocytic pathways (e.g., through use of Latrunculin A; see Chapter 5).

Another important observation from our experiments was the relatively few NT6B-positive Cad6B puncta *in vivo* (and *ex vivo* to a certain extent). If Cad6B is downregulated through internalization, it is perplexing that only few Cad6B (NT6B) puncta are observed *in vivo* and *ex vivo*. Moreover, the NT6B-antibody feeding assays (discussed below) reveal a large number of NT6B-Cad6B antibody complexes in emigrating neural crest cells as compared to native NT6B immunofluorescence performed on embryos. This difference could be partially explained by the conservative image acquisition settings employed, wherein only large fluorescence emitters are captured and not their faint counterparts. As such, increasing the photomultiplier sensitivity (gain) of the confocal microscope will enable visualization of additional NT6B puncta, albeit with increased background. Indeed, enhancing the signal of the images post-image acquisition reveals several faint NT6B-positive immunofluorescence puncta (data not shown). Another explanation is the dynamic nature of Cad6B protein downregulation, involving both proteolysis and internalization. Our results indicate that neural crest cells possess different degrees of Cad6B downregulation in the same transverse section of a chick midbrain, wherein some neural crest cells still harbor Cad6B on the membrane while some have started to remove Cad6B (Fig. 3.4 illustrates this very well). This, coupled with the occurrence of ADAM-mediated

proteolysis (Schiffmacher et al., 2014), could translate into very few cells actively internalizing Cad6B at a given time point in the chick midbrain. Moreover, with the coordination between ADAM-mediated proteolysis and internalization being unknown, a possibility exists that subpopulations of premigratory neural crest cells may employ solely proteolysis or internalization to remove Cad6B from their plasma membranes. As such, these factors could explain the occurrence of only a few Cad6B puncta *in vivo* on chick premigratory neural crest cells.

Chapter 4. Cad6B possesses a functional endocytosis motif in its cytoplasmic domain that mediates its internalization *in vitro*

Parts of this section were adapted from the following article under re-review at the Journal of Cell Science:

Padmanabhan R, Taneyhill LA (2015). Cadherin-6B undergoes macropinocytosis and clathrin-mediated endocytosis during cranial neural crest cell EMT.

4.1. Summary

Although strongly suggestive of internalization, the identification of cytosolic Cad6B-containing puncta through immunostaining and antibody feeding assays necessitated additional biochemical experiments to demonstrate this removal of Cad6B from cellular plasma membranes. To this end, we identified and mutated putative endocytosis motifs within Cad6B and examined their effects on Cad6B localization and biochemical properties *in vitro*. Multiple sequence alignment of the Cad6B cytoplasmic domain with the cytoplasmic domains of other type II cadherins revealed the conservation of two putative endocytosis motifs, a dileucine motif and p120-catenin binding motif, which function to promote or inhibit endocytosis, respectively. Site-directed mutagenesis was performed to change critical residues in these motifs to alanine, and these mutants were expressed stably from a single genomic locus in FlpInCHO cells. Experiments were then performed to examine Cad6B-HA distribution, including its localization with respect to its catenin-binding partners, and to biochemically characterize the different Cad6B mutants. We hypothesized that mutation of the dileucine motif would decrease Cad6B endocytosis, leading to increased cell surface Cad6B and possibly its associated catenins, while alterations to the p120-catenin binding motif would augment Cad6B endocytosis and decrease Cad6B (and potentially catenin) membrane localization, causing increased intracellular distribution of all molecules.

In keeping with our hypothesis, mutation of the p120-catenin binding motif to alanine resulted in Cad6B-HA localization primarily to the cytosol, enhanced internalization of Cad6B-HA *in vitro*, decreased the ability of Cad6B-HA to form stable cell-cell adhesions, and reduced the overall stability of Cad6B. Surprisingly, there was no

loss of ability of this mutant to interact with p120-catenin. Furthermore, mutation of the EED residues resulted in enhanced cytoplasmic distribution of α- and p120-catenin, but not of β-catenin. Interestingly, mutation of the dileucine motif did lead to increased presence of Cad6B-HA and β-catenin on the plasma membrane but did not elicit any significant effects on the distribution of α- and p120-catenin or on Cad6B-HA internalization, stability and cell-cell adhesion. These observations reveal that Cad6B internalization, likely through endocytosis, is negatively regulated by a functional p120-catenin binding motif *in vitro*. In order to address the question whether Cad6B endocytosis is critical for neural crest cell EMT *in vivo*, we expressed wtCad6B-HA and the endocytosis mutants in premigratory neural crest cells and analyzed for effects on neural crest cell EMT. Unlike our expectation, expression of wtCad6B-HA and the endocytosis mutants did not additionally affect neural crest migration *in vivo*.

4.2. Results

4.2. Generation of putative Cad6B endocytosis mutants

Several cadherins possess motifs within their C terminal intracellular domains that regulate their internalization and degradation (Xiao et al., 2005; Miyashita and Ozawa, 2007b; Miyashita and Ozawa, 2007a; Tai et al., 2007; Hong et al., 2010; Kowalczyk and Nanes, 2012; Nanes et al., 2012). We compared the amino acid sequence of the cytoplasmic domain of Cad6B to that of several type II cadherins through the ClustalW algorithm (http://www.ebi.ac.uk/Tools/msa/clustalw2/), and identified two conserved motifs that could potentially regulate internalization of Cad6B given their function in the endocytosis of other cadherins (Fig. 4.1, yellow highlight). Mutation of the dileucine motif negatively influences endocytosis (Miyashita and Ozawa, 2007a; Hong et al., 2010), whereas mutations in the p120-catenin binding motif promote endocytosis due to the inability of p120-catenin to bind to and mask the dileucine motif (Ireton et al., 2002; Xiao et al., 2003b; Xiao et al., 2005; Miyashita and Ozawa, 2007a; Ishiyama et al., 2010; Nanes et al., 2012). To investigate whether these two motifs regulate the internalization of Cad6B through endocytosis, we performed site-directed mutagenesis to create two Cad6B mutant constructs, LI645AA-HA and EED666AAA-HA. These constructs were expressed independently from a single genomic locus (tagged with the HA epitope at the C terminus) in CHO cells using the FlpIn system described in Chapter 3, generating the FlpInLI645AA-HA and the FlpInEED666AAA-HA mutants, respectively.

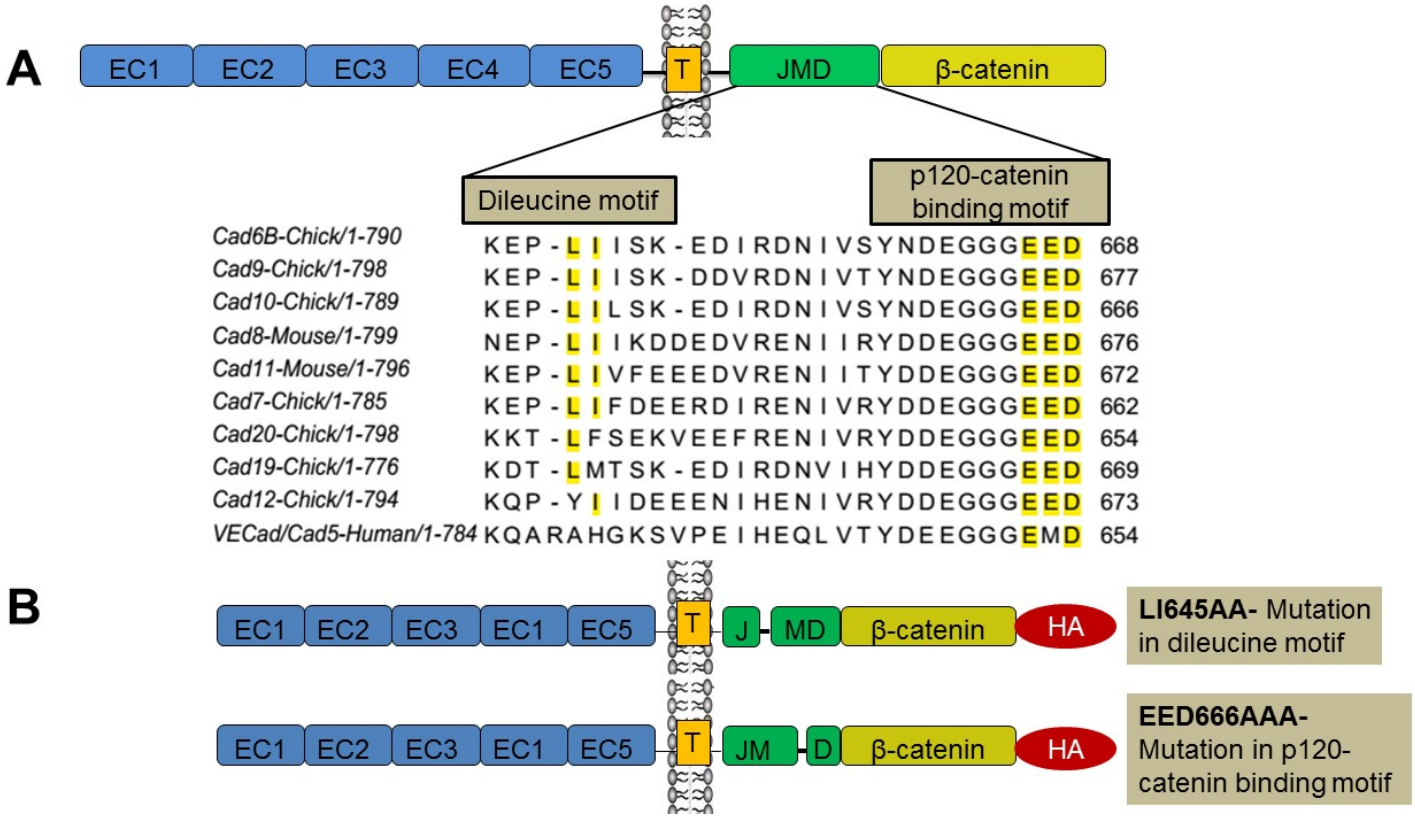

Figure 4.1. Cad6B possesses putative endocytosis motifs in its cytoplasmic tail at the juxtamembrane region. (A) A portion of the ClustalW multiple sequence alignment of the Cad6B juxtamembrane domain with those from other type II cadherins. The multiple sequence alignment output was then exported into Jalview2 (Waterhouse et al., 2009), manually edited and is represented here. The putative dileucine motif (which in these type II cadherins is a leucine-isoleucine motif) and the p120-catenin binding motif are highlighted in yellow. (B) Cartoon of the Cad6B putative endocytosis motif mutants. EC, Extracellular domain; T, Transmembrane domain; JMD, Juxtamembrane domain; β-catenin, β-catenin binding domain; HA, Hemagglutinin tag cloned into the mutants. Image modified from (Padmanabhan R, Taneyhill LA, under re-review at J Cell Sci).

4.3. Putative endocytosis motif mutants of Cad6B exhibit distinct intracellular localization

To validate that the mutant expression constructs express a full-length protein similar to wild-type Cad6B in FlpInwtC6B-HA cells and embryos, immunoblotting was performed on lysates prepared from the two mutant cell lines, FlpInwtC6B, empty vector control, and 13-16ss whole embryos (Fig. 4.2A). Cad6B expressed by embryos and the FlpInLI645AA-HA, FlpInEED666AAA-HA and FlpInwtC6B-HA cell lines is approximately the same molecular weight, indicating that Cad6B-HA protein is synthesized normally and not grossly altered by mutations within putative endocytosis motifs (Fig. 4.2A). We noticed, however, that the levels of Cad6B-HA expressed by each of these mutant cell lines varied compared to cells expressing wtCad6B-HA. We associate this difference with variations in the degree of transfection we obtained for each construct in CHO cells with respect to the percentage of transfected cells expressing the transgene (Fig. 4.2B-D’’’), especially noticeable in cells expressing the EED666AAA-HA construct (less transfected) (Fig. 4.2D’’’)

Figure 4.2. Cad6B mutants in FlpInwtC6B-HA cells are expressed at the appropriate molecular weight and exhibit varying transfection efficiencies. (A) Immunoblots of Cad6B (NT6B) and β-actin with lysates from control cells, 12-16ss embryos, FlpInwtCad6B-HA, FlpInLI645AA-HA and FlpInEED666AAA-HA cells. The band at ~100kDa is presumed to be a proteolytic product of Cad6B as a result of the activity of unknown endogenous proteases in CHO cells. β-actin is shown as an internal loading control. (B-D) 40x images of FlpIn cells stably expressing wtCad6B-HA (B-B"), LI645AA-HA (C-C"), and EED666AAA-HA (D-D") constructs and immunostained for NT6B (green) and HA (yellow) (n = 3). Panels represent the 3D composite of 22-25 Z-stack images (0.25 μm/optical slice) acquired at 63x magnification with a confocal microscope. Scale bar: 5μm.

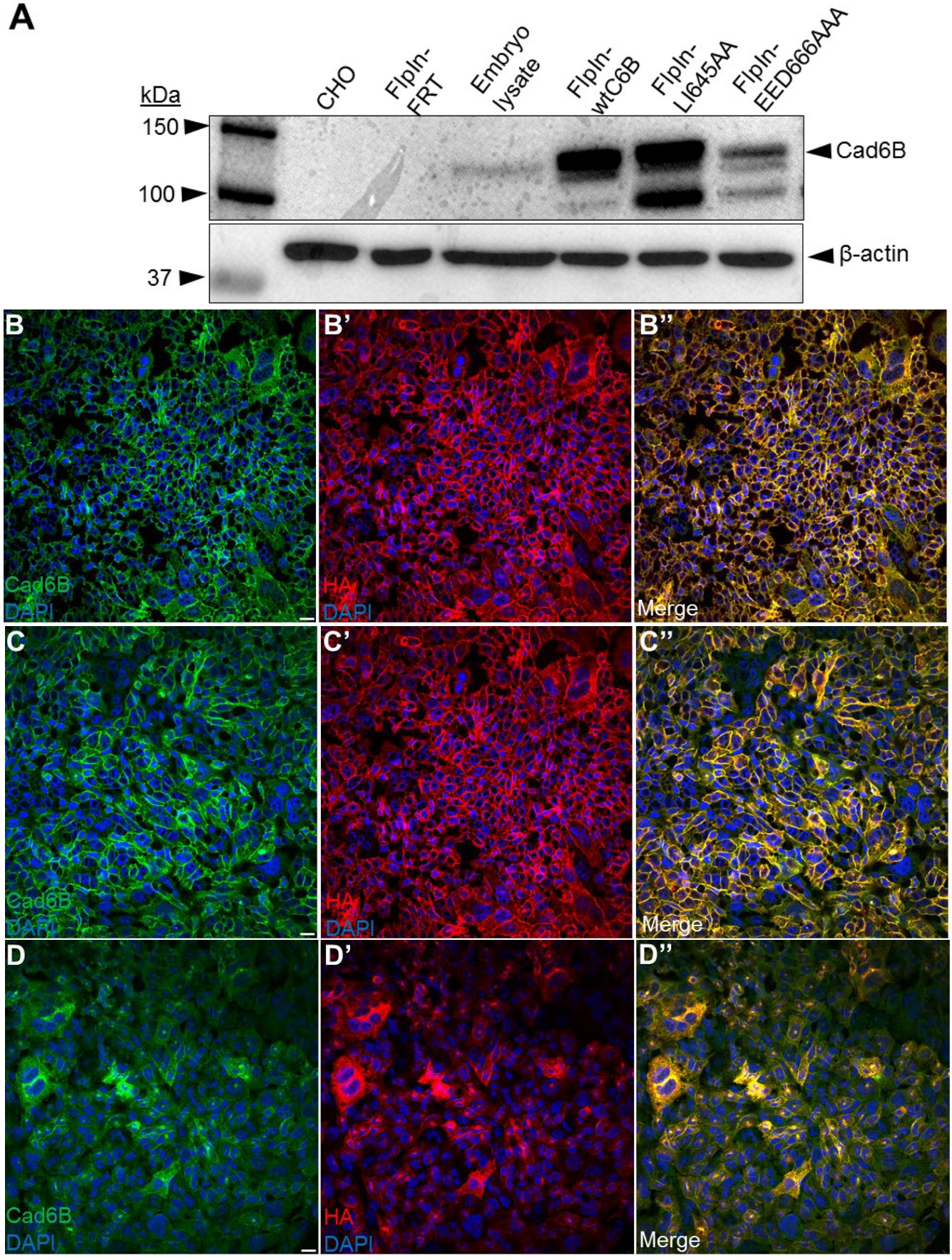
A
kDa
CHO
FlpIn-FRT
Embryo lysate
FlpIn-wtC6B
FlpIn-LI645AA
FlpIn-EED666AAA
150
100
37
Cad6B
β-actin
B
B'
B''
Cad6B
DAPI
HA
DAPI
Merge
C
C'
C''
Cad6B
DAPI
HA
DAPI
Merge
D
D'
D''
Cad6B
DAPI
HA
DAPI
Merge

To determine the effects of the mutations on Cad6B distribution, immunofluorescence was performed with antibodies to the Cad6B extracellular (NT6B) and intracellular (HA) domains, along with an antibody to Na^+K^+ATPase (Figs. 4.3-4.5). As shown in Figs. 4.4 and 4.5, both mutants express Cad6B but they possess different localization patterns. Compared to wild-type Cad6B (FlpInwtC6B-HA) (Fig. 4.3A-A’’’, B-B’’’, arrows and arrowheads), the LI645AA-HA mutant localizes preferentially to the plasma membrane (Fig. 4.4A-A’’’ and B’-B’’’’, arrows). Interestingly, the EED666AAA-HA mutant exhibits increased presence in the cytoplasm relative to wild-type Cad6B-HA, indicating that those mutated residues may modulate Cad6B distribution (Fig. 4.5A-A’’’ and B’-B’’’’, arrowheads).

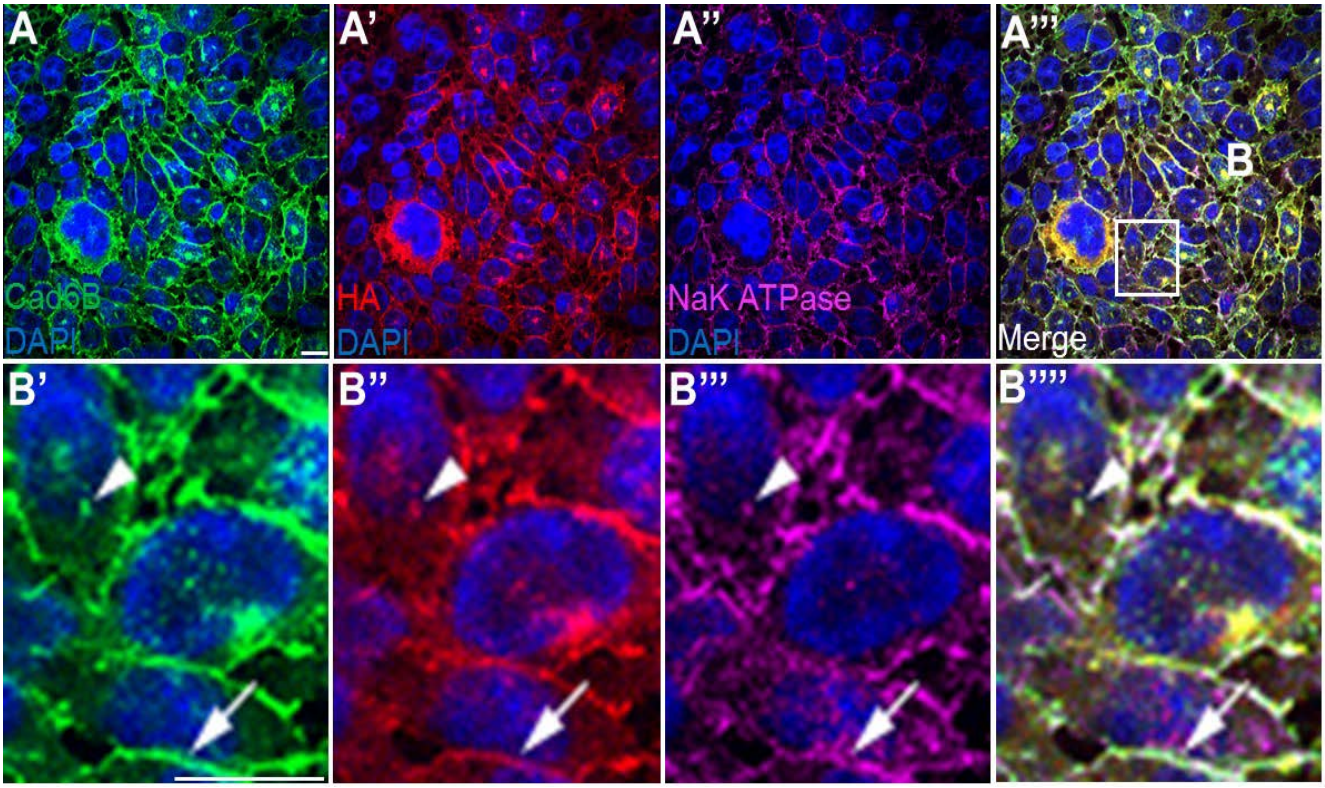

Figure 4.3. Wild-type Cad6B localizes to the membrane and cytoplasm. FlpInCHO cells stably expressing wtCad6B-HA were fixed and immunostained for NT6B (green), HA (red), and Na+K+ATPase (purple) (n = 5). (B'-B'''') is a higher magnification view of the boxed region in (A'''). Arrows and arrowheads point to co-localization of Cad6B (NT6B), HA and Na+K+ATPase at the plasma membrane and in the cytoplasm, respectively. Panels represent the 3D composite of 13 Z-stack images (0.25 µm/optical slice) acquired at 63x magnification with a confocal microscope. Scale bars: 10µm.

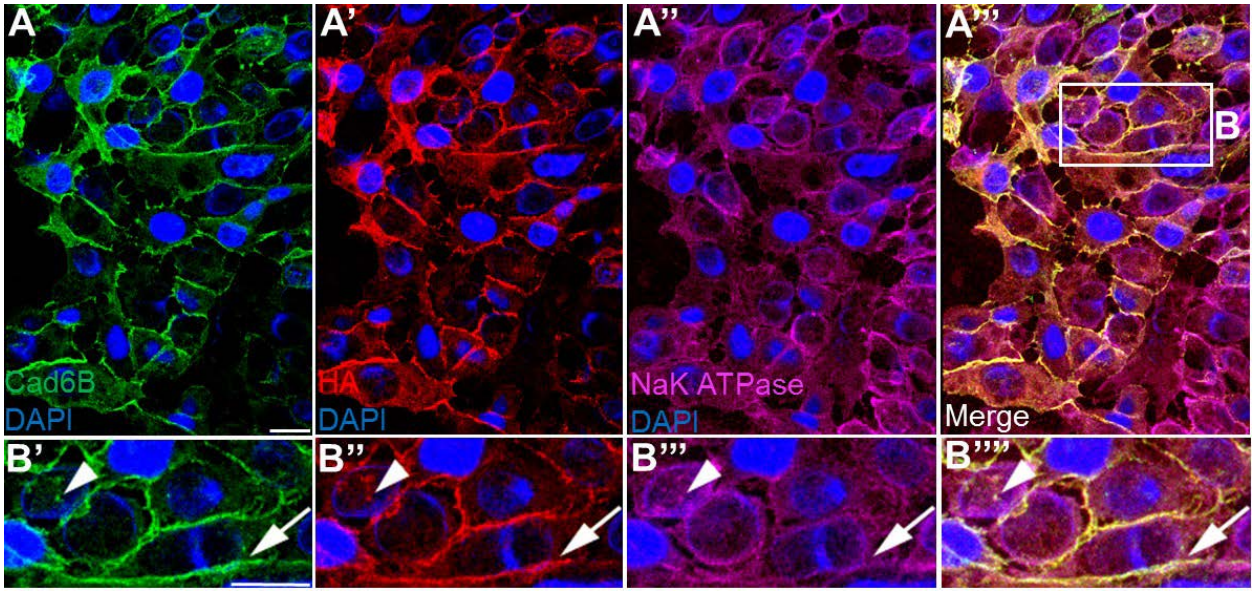

Figure 4.4. The Cad6B LI645AA-HA-HA mutant shows increased plasma membrane localization. FlpInCHO cells stably expressing the LI645AA-HA Cad6B mutant were fixed and immunostained for NT6B (green), HA (red) and Na^+K^+ATPase (purple) (n = 5). (B'-B'''') is a higher magnification view of the boxed region in (A'''). Arrows and arrowheads point to co-localization of Cad6B (NT6B), HA and Na^+K^+ATPase at the plasma membrane and in the cytoplasm, respectively. Panels represent the 3D composite of 16 Z-stack images (0.25 µm/optical slice) acquired at 63x with a confocal microscope. Scale bars: 10µm.

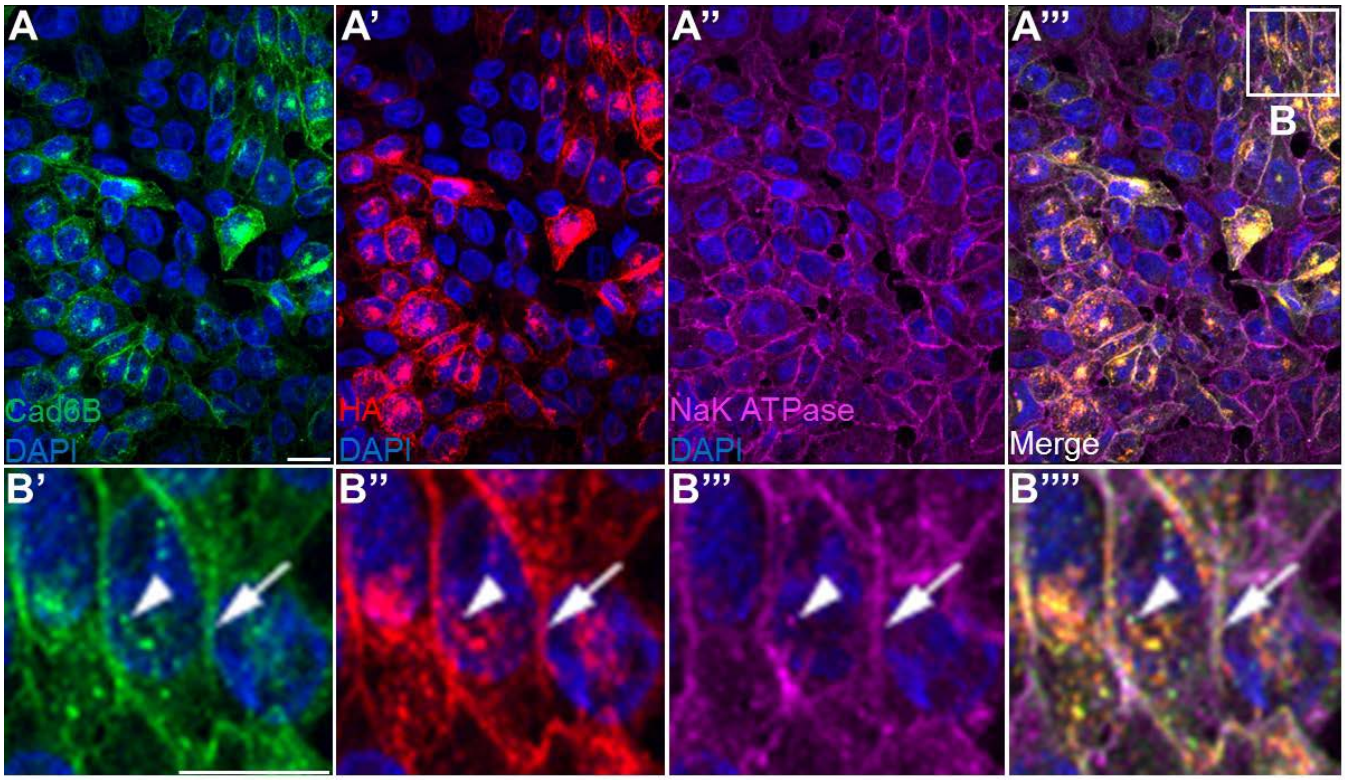

Figure 4.5. The Cad6B EED666AAA-HA mutant exhibits enhanced localization to the cytosol. FlpInCHO cells stably expressing the EED666AAA-HA mutant were fixed and immunostained for NT6B (green), HA (red) and Na^+K^+ATPase (purple) (n = 5). (B'-B'''') is a higher magnification view of the boxed region in (A'''). Arrows and arrowheads point to co-localization of Cad6B (NT6B), HA and Na^+K^+ATPase at the plasma membrane and in the cytoplasm, respectively. Panels represent the 3D composite of 25 Z-stack images (0.25 µm/optical slice) acquired at 63x magnification with a confocal microscope. Scale bars: 10µm.

4.4. Mutation of the EED and LI residues alters the distribution of catenins bound to the cytoplasmic domain of Cad6B

Plasma membrane-localized cadherins are normally bound directly to both p120-catenin and β-catenin and indirectly to α-catenin through motifs within their cytoplasmic domains (see Literature Review, 1.6.2.3.2.1). To ascertain the effects of mutating the LI and EED amino acids on the localization (and thus the Cad6B-bound state) of α-, β- and p120-catenin, immunofluorescence was performed on the FlpInwtC6B-HA and two mutant cell lines using antibodies against the Cad6B extracellular domain (NT6B), β-catenin, α-catenin, and p120-catenin (Figs. 4.6-4.9). Mutation of the LI motif does not qualitatively alter the distribution of α- and p120-catenin (Figs. 4.6C-D''' and 4.8 C-D'''', respectively), as confirmed by the observation that the LI645AA-HA mutant co-localizes with catenins on the plasma membrane and in the cytoplasm. Nonetheless, mutation of these residues does appear to affect the localization of β-catenin, as it is observed preferentially on the membrane in the FlpInLI645AA-HA cells (Fig. 4.7C-D'''') compared to wild-type Cad6B-HA (Fig. 4.7A-B''''). Conversely, mutation of the EED motif qualitatively affects the distribution of α- and p120-catenin, but not of β-catenin. β-catenin localization in FlpInEED666AA-HA cells is similar to that observed for wild-type Cad6B-HA-expressing cells, localizing both to the plasma membrane and the cytoplasm (Figs. 4.7A-B'''', E-F'''', arrows and arrowheads). Although Cad6B (NT6B) and β-catenin co-localize at the plasma membrane in the FlpInEED666AAA-HA cells, we also note Cad6B (NT6B)-positive, β-catenin-negative puncta in the cytoplasm (Fig. 4.7F'''', caret), suggesting a loss or reduction in this interaction, at least in the cytoplasm. Furthermore, α-catenin in the FlpInEED666AAA-HA cells are observed diffusely throughout the cytoplasm and on the

plasma membrane, co-localizing all along with the EED666AAA-HA mutant (Fig. 4.6E-F’’’). The most striking effect of mutating the EED residues is seen with the p120-catenin where its observed diffusely throughout the cytoplasm and below the limit of detection by this assay on the plasma membrane (Fig. 4.8E-F’’’’). This distribution of p120-catenin is in keeping with our hypothesis that mutation of the EED amino acids should alter the ability of p120-catenin to interact, and thus co-localize with, Cad6B-HA on the plasma membrane.

Figure 4.6. Mutation of EED666AAA-HA motif alters the distribution of αE-catenin. FlpInCHO cells stably expressing wtCad6B-HA (A-B’’’), the LI645AA-HA mutant (C-D’”) and the EED666AAA-HA mutant (E-F’”) were fixed and immunostained for HA (Cad6B, red) and αE-catenin (αE-cat, green; note: we were unable to perform co-immunofluorescence with the Cad6B (NT6B) antibody because it is the same isotype as the αE-catenin antibody) (n = 3). (B’-B’’’, D-D’’’ and F-F’’’) are higher magnification views of the boxed regions in (A’’), (B’’) and (C’’), respectively. Arrows and arrowheads in (B’’’, D’’’ and F’’’) indicate co-localization of Cad6B (HA) and αE-catenin at the plasma membrane and in the cytoplasm, respectively. Panels represent the 3D composite of 17 (A-B’’’), 17 (C-D’’’), and 15 (D-E’’’) Z-stack images (all at 0.25 μm/optical slice) acquired at 63x magnification with a confocal microscope. Scale bars: 10μm.

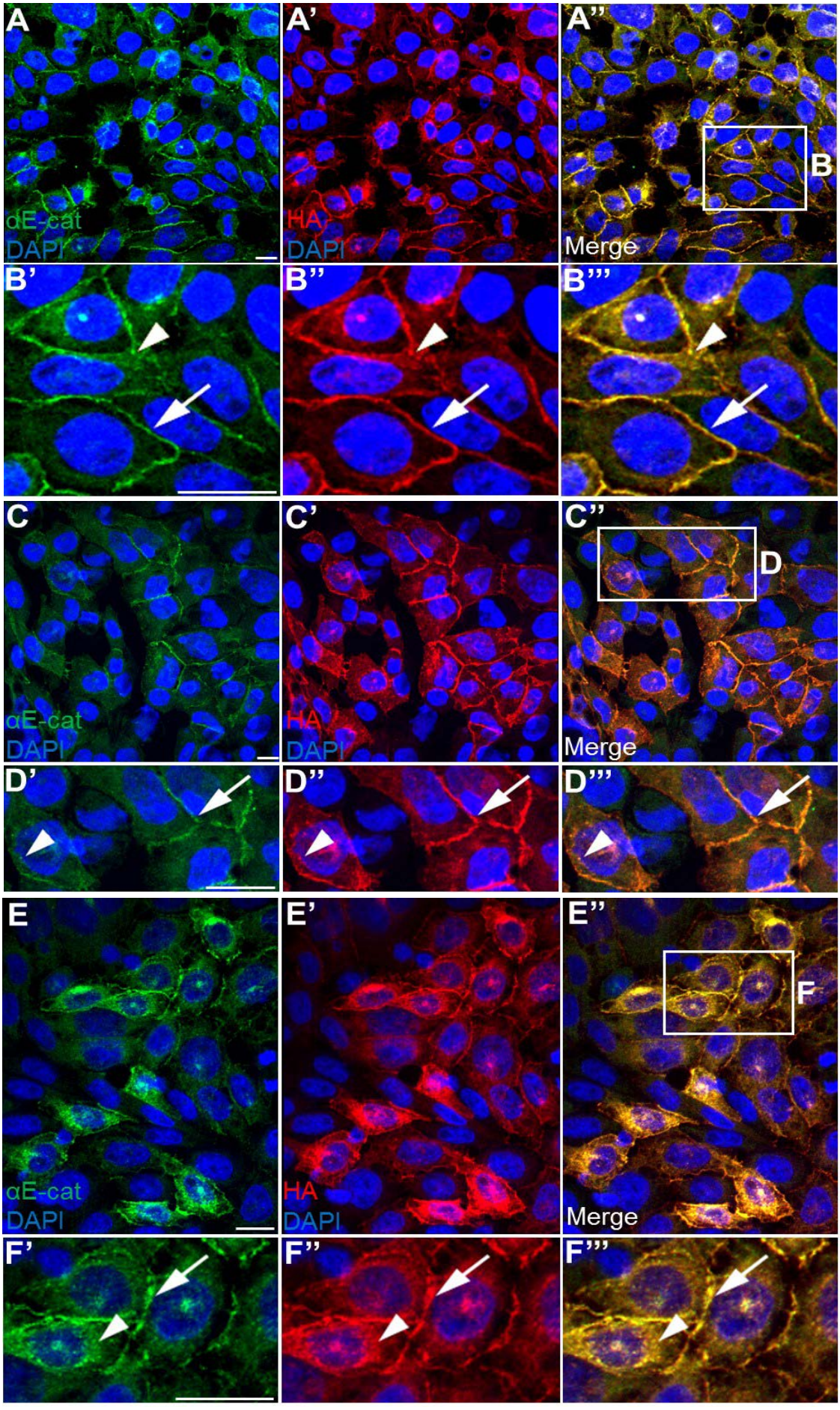
A
αE-cat
DAPI
A'
HA
DAPI
A''
B
Merge
B'
B''
B'''
C
αE-cat
DAPI
C'
HA
DAPI
C''
D
Merge
D'
D''
D'''
E
αE-cat
DAPI
E'
HA
DAPI
E''
F
Merge
F'
F''
F'''

Figure 4.7. β-catenin exhibits enhanced localization to the plasma membrane in FlpInLI645AA-HA cells. FlpInCHO cells stably expressing wtCad6B-HA (A-B’’’), the LI645AA-HA mutant (C-D’’’) and the EED666AAA-HA mutant (E-F’’’) were fixed and immunostained for Cad6B (NT6B; green), HA (purple), and β-catenin (red) (n = 3). (B’-B’’’, D-D’’’ and F-F’’’) are higher magnification views of the boxed region in (A’’), (B’’) and (C’’), respectively. Arrows and arrowheads in (B’’’, D’’’ and F’’’) indicate co-localization of Cad6B (NT6B), HA and β-catenin at the plasma membrane and in the cytoplasm, respectively. Carets in (F’’’) represent Cad6B-positive, β-catenin-negative puncta in FlpInEED666AAA-HA cells, representing either endocytosed Cad6B-HA proteins post β-catenin dissociation or proteolytic products of Cad6B. Panels represent the 3D composite of 23 (A-B’’’’), 24 (C-D’’’’), and 23 (E-F’’’’) Z-stack images (all at 0.25 μm/optical slice) acquired at 63x magnification with a confocal microscope. Scale bars: 10μm.

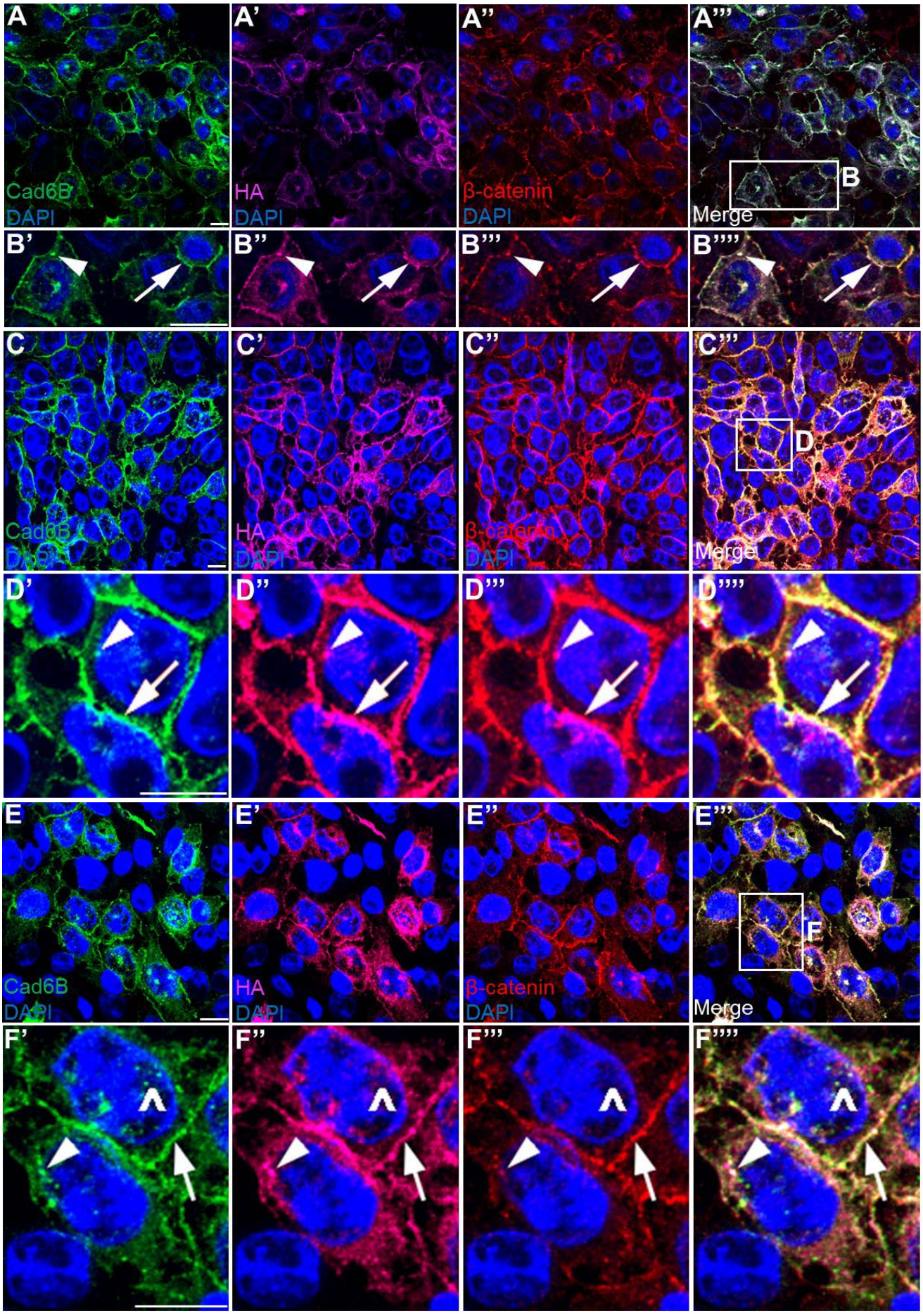
A
A'
A''
A'''
Cad6B
DAPI
HA
DAPI
β-catenin
DAPI
Merge
B
B'
B''
B'''
B''''
C
C'
C''
C'''
Cad6B
DAPI
HA
DAPI
β-catenin
DAPI
Merge
D
D'
D''
D'''
D''''
E
E'
E''
E'''
Cad6B
DAPI
HA
DAPI
β-catenin
DAPI
Merge
F
F'
F''
F'''
F''''

Figure 4.8. p120-catenin exhibits primarily cytosolic distribution in FlpInEED666AAA-HA cells. FlpInCHO cells stably expressing wtCad6B-HA (A-B’’’’), the LI645AA-HA mutant (C-D’’’’) and the EED666AAA-HA mutant (E-F’’’’) were fixed and immunostained for Cad6B (NT6B; green), HA (red), and p120-catenin (purple) (n = 3). (B’-B’’’, D-D’’’ and F-F’’’) are higher magnification views of the boxed region in (A’’’), (B’’’) and (C’’’), respectively. Arrows and arrowheads in (B’-B’’’’) and (D’-D’’’’) indicate co-localization of Cad6B (NT6B), HA and p120-catenin at the plasma membrane and in the cytoplasm respectively. Carets in (B’-B’’’’) and (D’-D’’’’) represent Cad6B (NT6B)-positive p120-catenin negative puncta. Large patches of fluorescence in (E-F’’’’) could either represent the endoplasmic reticulum/golgi or the lysosomes. Panels represent the 3D composite of 22 (A-B’’’’), 24 (C-D’’’’) and 21 (E-F’’’’) Z-stack images (0.25 μm/optical slice) acquired at 63x magnification with a confocal microscope. Scale bars: 10μm.

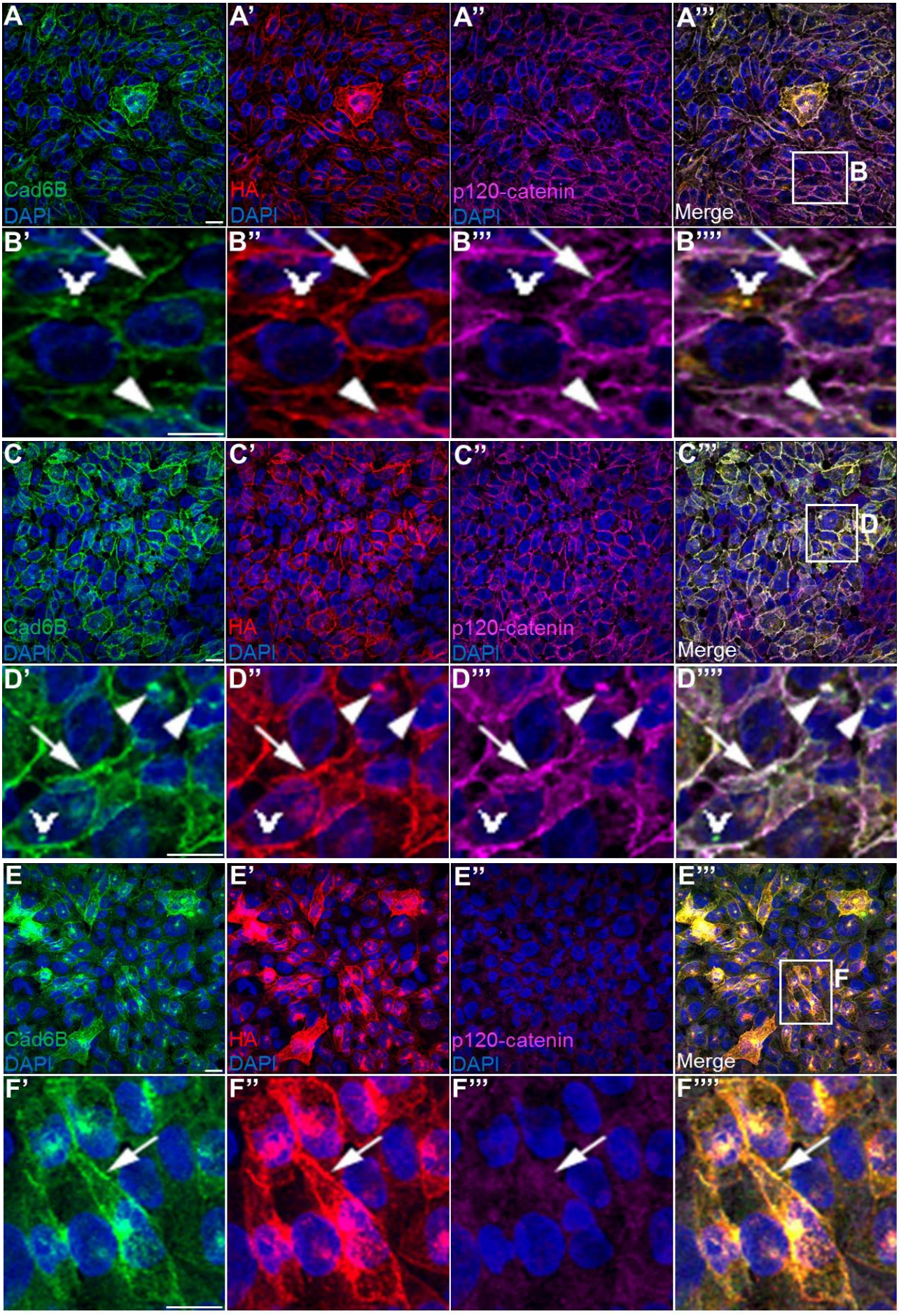
A
Cad6B
DAPI
A'
HA
DAPI
A''
p120-catenin
DAPI
A'''
B
Merge
B'
B''
B'''
B''''
C
Cad6B
DAPI
C'
HA
DAPI
C''
p120-catenin
DAPI
C'''
D
Merge
D'
D''
D'''
D''''
E
Cad6B
DAPI
E'
HA
DAPI
E''
p120-catenin
DAPI
E'''
F
Merge
F'
F''
F'''
F''''

4.5. The p120-catenin-Cad6B interaction is not affected in the FlpInEED666AAA-HA mutant

The reduced membrane localization of p120-catenin in the FlpInEED666AAA-HA cell line suggests an inability of p120-catenin to interact with this mutant form of Cad6B. To test this hypothesis, Cad6B was immunoprecipitated from lysates of FlpInwtC6B-HA and FlpInEED666AA-HA cells using an antibody to the C terminal HA tag. SDS-PAGE and immunoblotting on the immunoprecipitated lysates with the p120-catenin antibody, however, revealed no effect on the ability of p120-catenin to interact with the EED666AAA-HA Cad6B mutant (Fig. 4.9). CHO cells express two isoforms of p120-catenin, isoform 1 and isoform 3 (isoform 1 is longer than isoform 3 by 101 amino acids) (Wang et al., 2013), and wild-type and mutant Cad6B both interact efficiently with the higher molecular weight p120-catenin isoform (Fig. 4.9, left panel). Similarly, p120-catenin immunoprecipitated equally well from lysates of FlpInwtC6B-HA and FlpInEED666AAA-HA cells when the reciprocal experiment was performed (p120-catenin immunoprecipitation and immunoblotting for HA) (Fig. 4.9, right panel). These data demonstrate that although the EED residues of the p120-catenin binding domain in Cad6B-HA are not critical for the Cad6B-HA-p120-catenin biochemical interaction, they are important for the proper localization of p120-catenin to the plasma membrane.

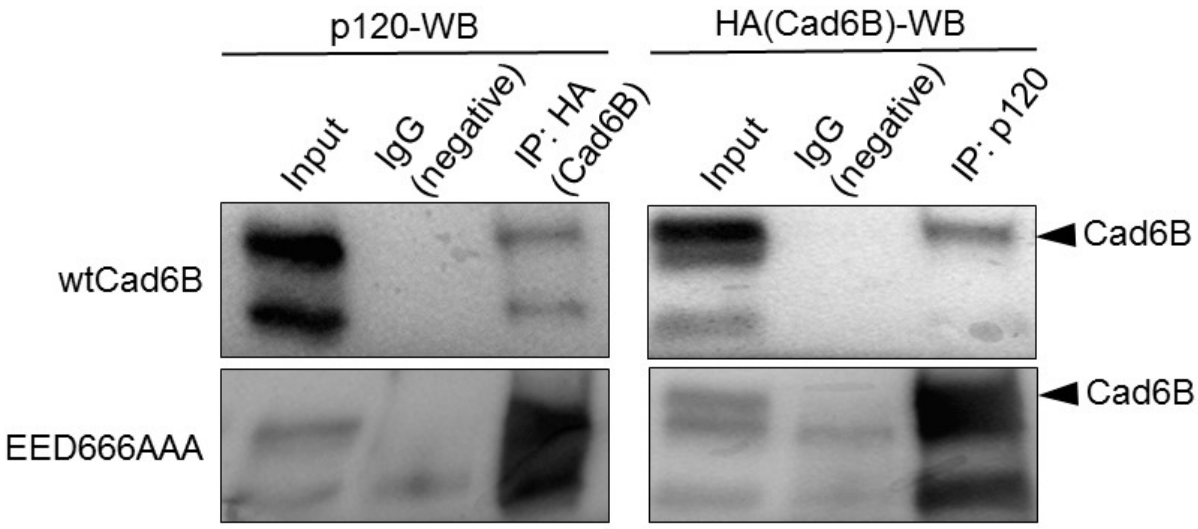

Figure 4.9. The EED mutation does not abrogate the interaction of Cad6B with p120-catenin. FlpInwtCad6B-HA and EED666AAA-HA cells were lysed and immunoprecipitated with an antibody to HA to detect Cad6B followed by immunoblotting for p120-catenin (left panel) (n = 1). The converse experiment was performed (p120-catenin immunoprecipitation and immunoblotting for HA) and is shown on the right (n = 1). Arrowheads denote full-length Cad6B. Mutation of the EED residues does not appear to affect the interaction of p120-catenin with Cad6B-HA.

4.6. The Cad6B EED666AAA-HA mutant is deficient in forming stable associations with the actin cytoskeleton

The higher intracellular distribution of Cad6B in the EED666AAA-HA mutant implies that this mutant Cad6B might possess a reduced ability to localize to the plasma membrane and form intercellular contacts. To investigate this, we analyzed the proportion of Cad6B-HA anchored to the actin cytoskeleton, as cadherins dynamically interact with the actin cytoskeleton to modulate cell-cell adhesion (see Literature Review, Section 1.6.2.1), and any decrease in cytoskeletal association would be a read-out of the amount of functional cadherin present on the plasma membrane. To this end, a low percentage TX100-containing buffer was employed to separate cytoskeleton-associated (TX100-insoluble) from cytoplasmic (TX100-soluble) proteins in the FlpInwtC6B-HA and two putative endocytosis mutant cell lines, and the separated pools were subjected to SDS-PAGE electrophoresis and immunoblotting with the NT6B antibody to note Cad6B distribution (Fig. 4.10A). Although possessing enhanced membrane localization (Fig. 4.4B-B"), the LI645AA-HA mutant did not show a difference in its Cad6B actin-anchored proportion compared to wild-type Cad6B-HA, in line with observation that αE-catenin, which plays an important role in anchoring cadherins to the cytoskeleton (Yonemura, 2011), exhibits a "wild-type" localization pattern in the FlpInLI645AA-HA cells (Figs. 4.6A-B''', C-D'''). With the EED666AAA-HA mutant, however, we observe a statistically significant reduction in the proportion of actin-anchored Cad6B (Fig. 4.10B, $p < 0.05$) compared to the LI645AA-HA mutant or wild-type Cad6B-HA, in keeping with our observation that αE-catenin is diffusely distributed in the cytoplasm in this mutant (Fig. 4.6E" and F'''). These results corroborate our immunofluorescence data (Fig. 4.5) and substantiate our

hypothesis that the FlpInEED666AAA-HA cells are deficient in forming stable cell-cell adhesions.

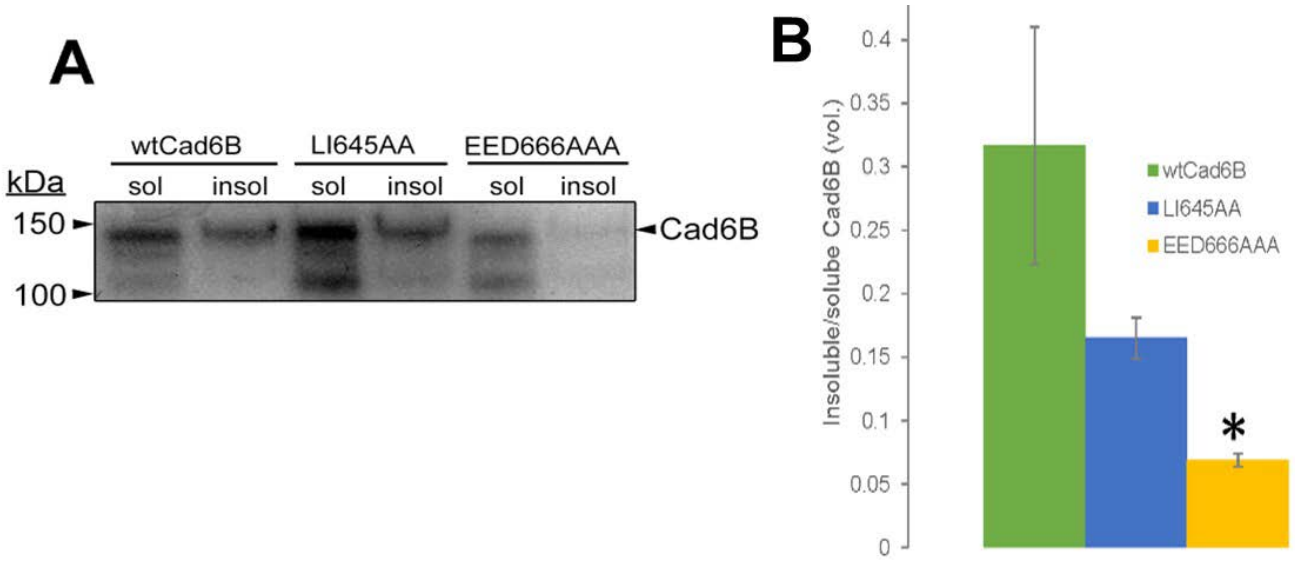

Figure 4.10. The Cad6B EED666AAA-HA mutant is deficient in forming stable associations with the actin cytoskeleton. Equal numbers of FlpInwtC6B, FlpInLI645AA-HA and FlpInEED666AAA-HA cells were extracted with a buffer containing 0.5% TX100 to separate TX100-soluble and TX100-insoluble fractions, and the separated pools were subjected to SDS-PAGE electrophoresis. Immunoblotting was performed with the NT6B antibody to identify Cad6B. Sol, TX100-soluble fraction; Insol, TX100-insoluble fraction (cytoskeleton-associated). (B) Densitometric ratios of insoluble/soluble Cad6B bands evaluated from triplicate blots. Error bars represent ± standard error of mean (SEM), and the asterisk denotes statistical significance where the confidence intervals do not overlap. Image modified from (Padmanabhan R, Taneyhill LA, under re-review at J Cell Sci).

4.7. The Cad6B EED666AAA-HA mutant undergoes increased internalization in vitro

In cultured cells, cadherins that are unable to interact with the actin cytoskeleton are rapidly endocytosed (Ivanov et al., 2004; Izumi et al., 2004), indicating that the EED666AAA-HA mutant may undergo enhanced internalization. To investigate the steady state internalization of wild-type Cad6B-HA and the EED666AAA-HA and LI645AA-HA mutants, biotinylation assays were performed. Although wild-type-HA and the LI645AA-HA mutant form of Cad6B do not show significant differences in internalization, the EED666AAA-HA mutant undergoes rapid internalization by 60 minutes post-biotinylation (Figs. 4.11A and B, $p < 0.05$), confirming that this motif normally negatively regulates Cad6B internalization. Surprisingly, however, the levels of internalized Cad6B in the EED666AAA-HA mutant decrease at 180 minutes post-biotinylation (Fig. 4.11B), suggesting the potential presence of other mechanisms to turnover this internalized Cad6B.

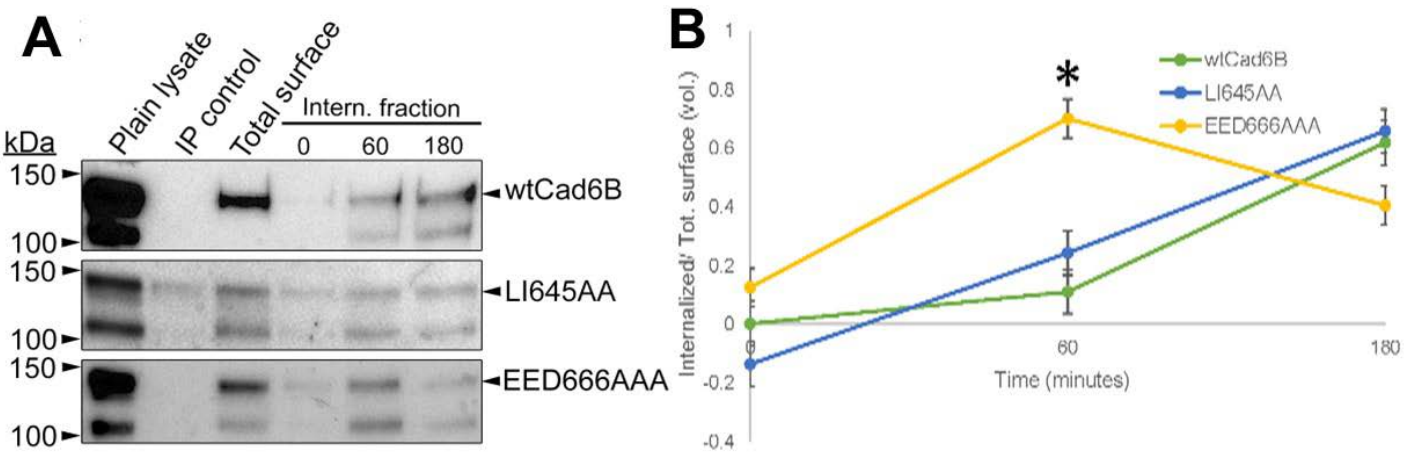

Figure 4.11. The Cad6B EED666AAA-HA mutant undergoes enhanced internalization in biotinylation assays *in vitro*. (A) FlpInwtC6B-HA, FlpInLI645AA-HA and FlpInEED666AAA-HA cells were surface-biotinylated at 4˚C and incubated at 37˚C for 0, 60, and 180 minutes. Following glutathione stripping, cells were lysed and internalized biotin was immunoprecipitated with streptavidin-agarose beads. Immunoprecipitates were subjected to SDS-PAGE electrophoresis followed by immunoblotting with the NT6B antibody. Separately, cells were harvested after the initial biotinylation step without stripping (Total surface). (B) Graphical representation of densitometric ratios of the proportion of internalized Cad6B protein with respect to the total surface biotinylated protein ("Total surface") from triplicate blots. Error bars represent ± SEM, and the asterisk denotes a statistically significant difference determined using the Fishers LSD test. Image reproduced from (Padmanabhan R, Taneyhill LA, under re-review at J Cell Sci).

4.8. The Cad6B EED666AAA-HA mutant is inherently unstable in vitro

The decreased levels of the EED666AAA-HA mutant Cad6B observed 180 minutes post-biotinylation (Figs. 4.11A and B) denotes that this mutation negatively impacts Cad6B stability and may make it more susceptible to degradation. To address this possibility, we inhibited *de novo* protein synthesis through cycloheximide treatment of the wild-type Cad6B-HA and mutant cell lines and then analyzed levels of Cad6B protein over time. Compared to wild-type Cad6B-HA and the LI645AA-HA mutant, the EED666AAA-HA mutant undergoes a rapid and statistically significant reduction in total Cad6B levels, particularly by 180 minutes. These results reveal that the EED residues contribute to the stability of *de novo* synthesized Cad6B (Figs. 4.12A and B, $p < 0.001$).

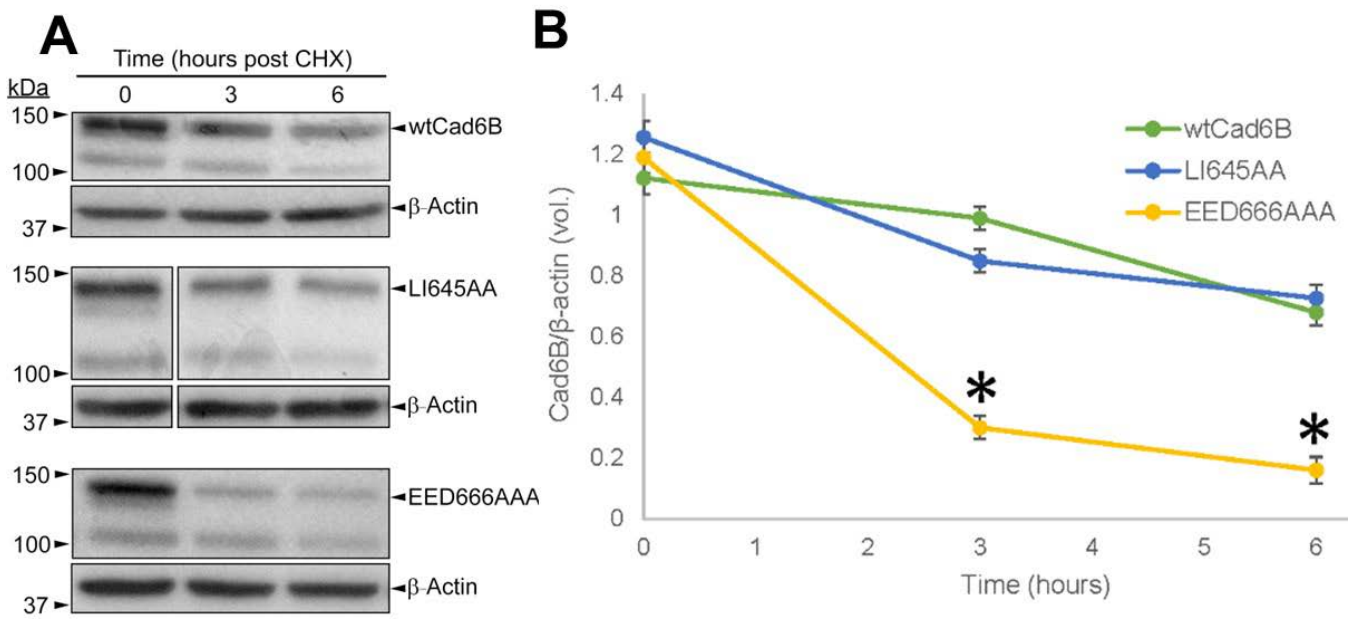

Figure 4.12. The EED666AAA-HA mutant is inherently unstable *in vitro*. (A) FlpInwtCad6B-HA, FlpInLI645AA-HA and FlpInEED666AAA-HA cells were treated with cycloheximide (CHX) for 0, 3, and 6 hours, lysed and subjected to SDS-PAGE electrophoresis. Immunoblotting was performed with the NT6B and β-actin antibodies. (B) Graphical representation of the quantification of densitometric ratios of Cad6B/actin from triplicate blots. Error bars represent ± SEM, and the asterisks denote a statistically significant difference determined using the Fishers LSD test. Image reproduced from (Padmanabhan R, Taneyhill LA, under re-review at J Cell Sci).

4.9. Mutations in Cad6B endocytosis motifs do not additionally impact neural crest cell EMT

Given that Cad6B possesses a functional p120-catenin binding motif that negatively regulates Cad6B internalization *in vitro*, we then investigated if Cad6B internalization plays a role in neural crest cell EMT and emigration from the neural tube. We hypothesized that if Cad6B internalization (potentially through endocytosis) is critical for neural crest cell EMT, introduction of the Cad6B EED666AAA-HA mutant (increased Cad6B internalization) should enhance EMT by stimulating precocious loss of endogenous (and exogenous) Cad6B when compared to wild-type Cad6B-HA overexpression. Although the Cad6B dileucine motif mutant (LI645AA-HA) had no significant effects on Cad6B internalization *in vitro*, we surmised that it, too, could have effects on neural crest cell EMT when introduced into its native environment in the chick embryo. Initial efforts to express these endocytosis mutants *in vivo* in the absence of endogenous Cad6B (with knockdown of endogenous Cad6B mediated by a Cad6B morpholino) proved futile because of the mosaic nature of electro-transfection (electroporation) and the inability to successfully electroporate cells with both the morpholino and expression construct (Appendix 3). As such, wild-type and mutant Cad6B-HA constructs were introduced in the presence of endogenous Cad6B in premigratory neural crest cells. Embryos were incubated until EMT and early migration stages and then immunostained for FoxD3, a marker of premigratory and migratory neural crest cells. The influence of each construct was determined by counting the number of FoxD3-positive cells on the electroporated versus the contralateral control side of the embryo in at least five serial transverse sections in a minimum of three embryos.

In agreement with prior work (Coles et al., 2007), we find that expression of wild-type Cad6B-HA decreases the number of migratory neural crest cells (Fig. 4.13B’’’, arrow; fold differences quantified in Fig. 4.14). Expression of the LI645AA-HA mutant, however, results in a similar reduction in the number of neural crest cells undergoing EMT when compared to wild-type Cad6B (Figs. 4.13C’’’, arrow; 4.14). Surprisingly, expression of the EED666AAA-HA mutant failed to rescue neural crest cell EMT, with this construct showing a similar general trend on EMT (but not statistically significant) as observed for overexpression of wild-type and the LI645AA-HA mutant form of Cad6B (Fig. 4.13D’’’, arrow; Fig. 4.14). We also note a general decrease in the number of neural crest cells undergoing EMT on either side of the neural tube upon introduction of any form of Cad6B when compared to electroporation of the empty vector (Fig. 4.14). This suggests that general overexpression of Cad6B could have both cell and non-cell autonomous effects on neural crest cell EMT.

Figure 4.13. Expression of EED666AAA-HA mutant *in vivo* does not qualitatively influence neural crest cell EMT and migration. Empty expression vector (A-A’’’), wild-type Cad6B (B-B’’’), LI645AA-HA (C-C’’’), or EED666AAA-HA (D-D’’’) expression constructs were introduced unilaterally into premigratory neural crest cells, and embryos were harvested at stages when neural crest cells are undergoing EMT. Immunostaining was performed on whole embryos for RFP (marking electroporated cells), HA (exogenous Cad6B) and FoxD3 (marking premigratory and migratory neural crest cells), followed by transverse sectioning to reveal effects on neural crest cell EMT. Shown here is one representative transverse section of embryos electroporated with the empty vector or the Cad6B-HA expression constructs. Arrows in (A’’’) denote normal neural crest migration on the electroporated side, and arrows in (B’’’, C’’’, and D’’’) denote a reduction in the number of emigrating and migrating neural crest cells on the electroporated side. Scale bar: 10μm.

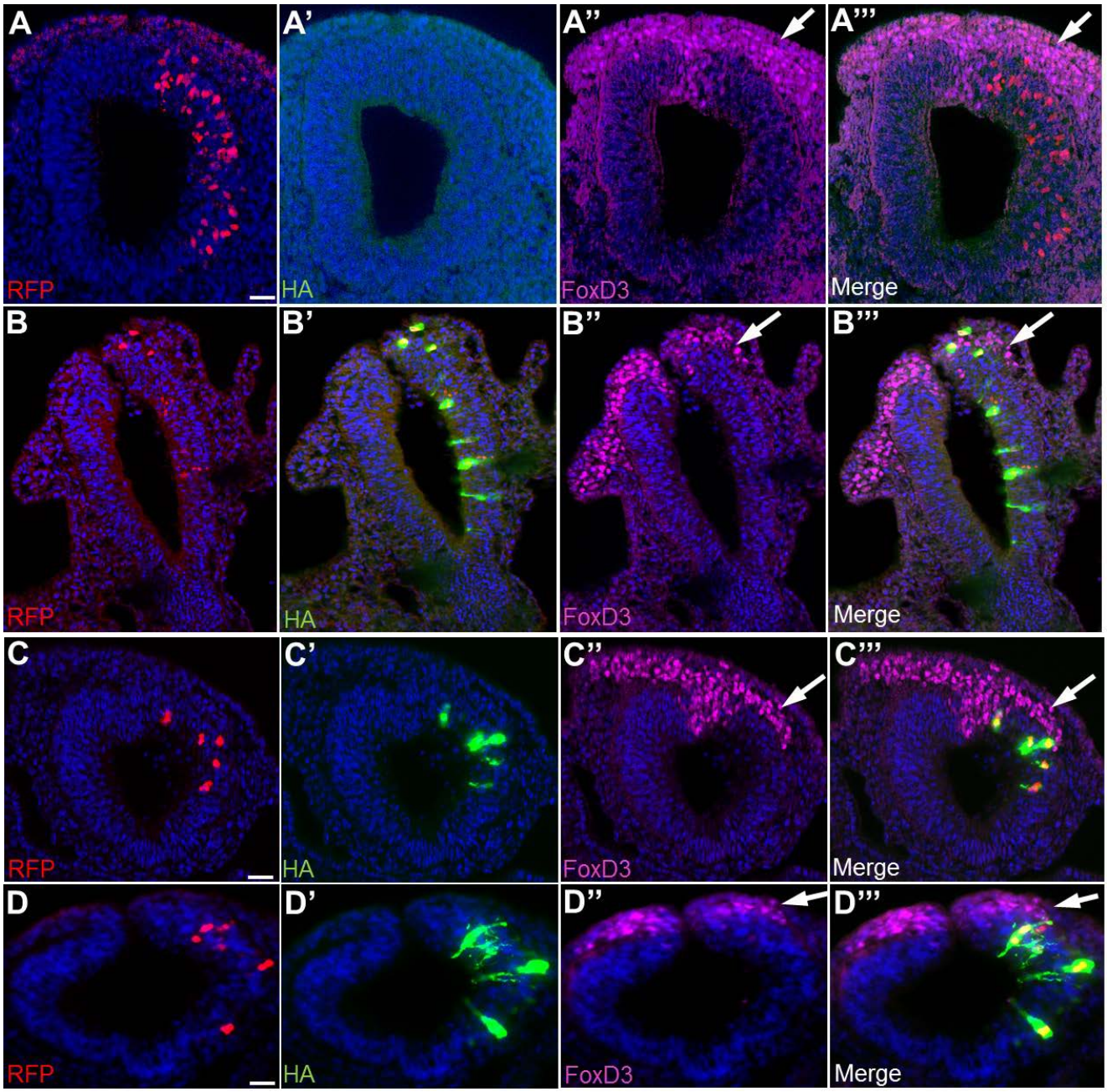
A
A'
A''
A'''
RFP
HA
FoxD3
Merge
B
B'
B''
B'''
RFP
HA
FoxD3
Merge
C
C'
C''
C'''
RFP
HA
FoxD3
Merge
D
D'
D''
D'''
RFP
HA
FoxD3
Merge

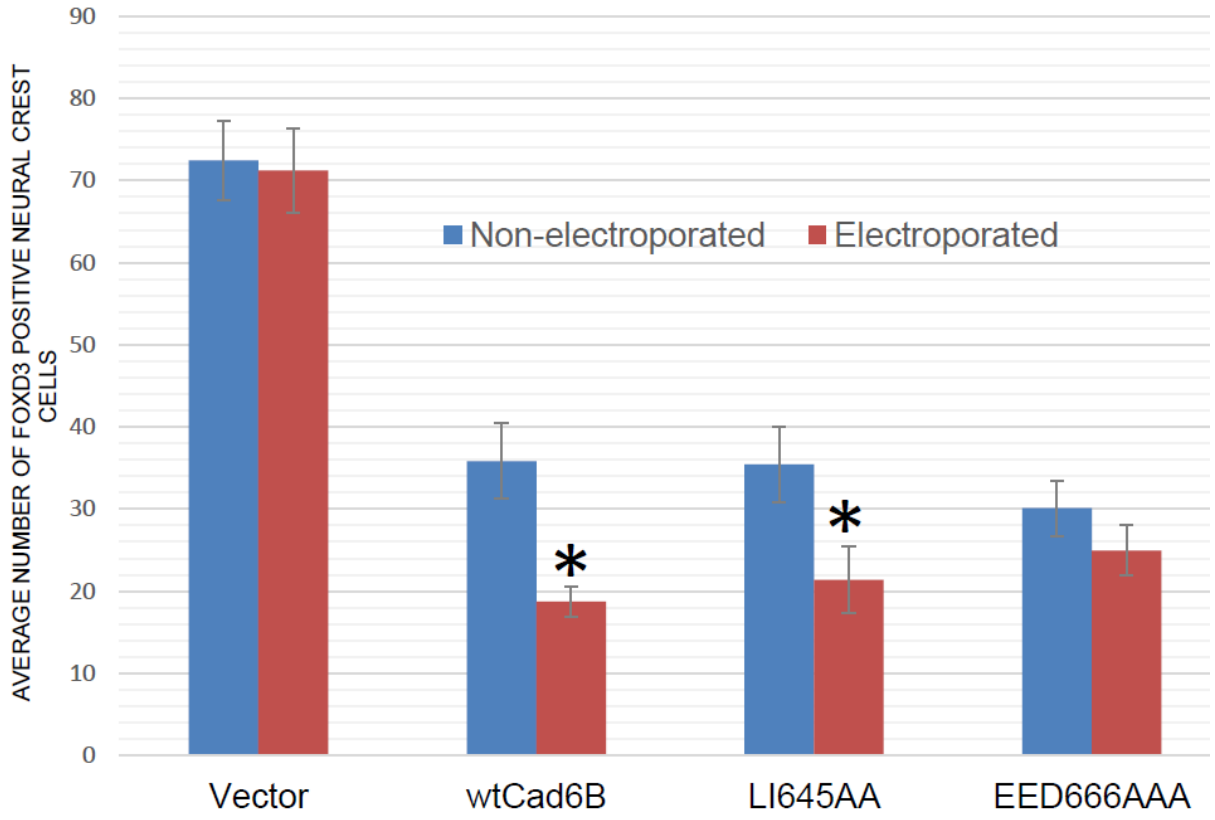

Figure 4.14. Expression of the EED666AAA-HA mutant *in vivo* does not quantitatively influence neural crest cell EMT and migration. FoxD3-positive migratory neural crest cells were counted from at least four serial transverse on the non-electroporated contralateral control side (blue) and the side electroporated with the empty vector or the Cad6B constructs (red). The counts were averaged and graphically represented here. The number of embryos analyzed for each construct is as follows: Vector, 6; wtCad6B-HA, 3; LI645AA-HA, 6; and EED666AAA-HA, 6. Error bars represent ± SEM, and asterisk represents a statistically significant difference ($p<0.05$) as determined by the unpaired Student's t-test (Jhingory et al., 2010; Wu and Taneyhill, 2012).

4.11. Discussion

Through co-localization studies and antibody feeding assays, we demonstrated that Cad6B localizes to the cytoplasm of premigratory cranial neural crest cells through internalization (Chapter 3). Substantiating this observation, however, requires biochemical evidence, as immunofluorescence-based assays are at best qualitative in nature. To characterize Cad6B internalization biochemically, we exploited an *in vitro* approach using single-copy stable cell lines expressing Cad6B-HA mutants due to the technical limitations associated with the chick embryo, namely the inability to generate stable Cad6B mutants in the absence of endogenous wild-type Cad6B. For this dissertation, we created Cad6B mutants that were likely to be deficient in internalization due to the known roles of these mutations in affecting endocytosis of other cadherins. As such, any differences in Cad6B internalization would imply that the putative endocytosis motifs are in fact functional in mediating Cad6B internalization. If Cad6B internalization is critical for neural crest cell EMT, introducing mutants with altered endocytosis capabilities should affect neural crest cell EMT *in vivo*. For example, a Cad6B mutant that undergoes enhanced or reduced internalization should increase or decrease the number of neural crest cells undergoing EMT, respectively.

The plasma membrane localization of cadherins is regulated by distinct endocytosis motifs within the cadherin cytoplasmic domain (Xiao et al., 2005; Miyashita and Ozawa, 2007b; Miyashita and Ozawa, 2007a; Tai et al., 2007; Hong et al., 2010; Ishiyama et al., 2010; Kowalczyk and Nanes, 2012; Nanes et al., 2012). A comparison of the Cad6B cytoplasmic domain sequence to those found in other type II cadherins revealed the presence of two conserved motifs that have been shown to regulate endocytosis of other cadherins *in vitro*: A LI (dileucine motif) at position 645 and a DEGGGEED (p120-catenin

binding motif) at position 666. These two motifs are important because p120-catenin binding masks the LI motif and thus negatively regulates endocytosis. Additional residues that could affect Cad6B internalization include a lysine at position 642 (Hong et al., 2010) and two generic tyrosine-based endocytosis signals (YDSL, position 738 and YDYL, position 765) within the β-catenin-binding domain. Based on the interrelationship between the LI645 and DEGGGEED666 residues in the internalization of other cadherins, the LI645AA-HA and EED666AAA-HA mutants were created through site-directed mutagenesis and expressed stably from a single genomic locus in FlpInCHO cells. The generation of Cad6B lysine and tyrosine motif mutants was left for future experimentation.

Immunofluorescence experiments revealed that, compared to wild-type Cad6B-HA, the LI645AA-HA mutant exhibits enhanced localization to the plasma membrane. This was corroborated by our observation that β-catenin is primarily observed on the plasma membrane in this cell line. The distribution pattern of p120-catenin and α-catenin, however, is not perturbed. The lack of a significant difference in the proportion of cytoskeleton-bound LI645AA-HA compared to wild-type Cad6B-HA provides biochemical evidence to support this more qualitative observation by immunostaining. As anticipated, p120-catenin is not localized differently in these mutant cells compared to the wild-type Cad6B cell line. In summary, from immunofluorescence observations, the mutation of the LI residues appears to only affect localization of β-catenin.

Contrary to LI645AA-HA, the relative cytoplasmic localization of the EED666AAA-HA mutant is higher as compared to wild-type Cad6B-HA, and concomitantly exhibits reduced membrane localization. These data indicate that the EED residues, which comprise a portion of the p120-catenin binding domain (DEGGGEED),

have a functional role in regulating the localization of Cad6B. Indeed, mutation of the EED residues causes a re-distribution of α- and p120-catenin, but not of β-catenin, from the plasma membrane to the cytoplasm. The persistence of membrane β-catenin in these cells (similar to that of wild-type cells) and the reciprocal observation upon mutation of the LI residues is quite interesting, and suggests that the LI residues potentially play a role in the either the affinity or stability of the Cad6B-β-catenin interaction. The mechanism behind the re-distribution of α-catenin to the cytoplasm and the co-localization with EED666AAA-HA Cad6B is somewhat perplexing and is in keeping with the fact that the molecular basis for the α-catenin-cadherin interaction is still not well understood (Miller et al., 2013).

On the other hand, p120-catenin localizes more diffusely in the cytosol in the EED666AAA-HA mutant, with less immunoreactivity observed on the plasma membrane and co-localizing with Cad6B, compared to what is observed in the wild-type and LI645AA-HA mutant cell lines. The lack of co-localization with Cad6B-HA suggested a reduced interaction with the EED666AAA-HA mutant. Surprisingly, immunoprecipitation experiments revealed no loss in the ability of p120-catenin to interact with the EED666AAA-HA mutant (Fig. 4.9). This is unlike what is observed with E-cadherin (Miyashita and Ozawa, 2007a) where there is a complete loss of interaction, and suggests that the EED residues in Cad6B-HA are only required for proper localization p120-catenin but not its biochemical interaction with Cad6B-HA. A possible explanation is that the localization and/or stabilization of p120-catenin on the membrane could be mediated by an unknown factor(s) that serves as a scaffold for the creation of the p120-catenin-Cad6B interaction. This factor could require the EED residues and the region around it for

maintaining the stability of the p120-catenin-Cad6B complex only at the plasma membrane but not in the cytoplasm. In this instance, our immunoprecipitation experiments would be detecting this cytoplasmic Cad6B-p120-catenin complex. Such an interpretation of our results is in keeping with our observation that the EED-HA mutant Cad6B is localized predominantly in the cytoplasm. Furthermore, the EED666AAA-HA Cad6B mutant is less stable, undergoes enhanced endocytosis, and has impaired interactions with the actin cytoskeleton *in vitro* (see below). These observations collectively suggest that the mutation of the EED residues (and its indirect effects on p120-catenin localization) critically affects Cad6B function *in vitro*. Indeed, p120-catenin is a known regulator of cadherin endocytosis, performing its function by "masking" the dileucine motif present very near to it (Miyashita and Ozawa, 2007a; Ishiyama et al., 2010; Nanes et al., 2012). Dissociation of p120-catenin from the cadherin cytoplasmic domain exposes the dileucine motif, which in turn is recognized by adaptor proteins of the clathrin-mediated endocytic pathway and leads to cadherin endocytosis (Miyashita and Ozawa, 2007a; Ishiyama et al., 2010; Nanes et al., 2012). As such, it is likely that the dileucine motif in the EED666AAA-HA Cad6B mutant is continuously exposed, thereby causing constitutive and rapid endocytosis of plasma membrane Cad6B, as noted for E-cadherin (Xiao et al., 2003b; Miyashita and Ozawa, 2007a). These observations could be validated by performing site-directed mutagenesis experiments of putative Cad6B-binding sites of p120-catenin and observing for changes in Cad6B internalization. Interestingly, we also note Cad6B cytoplasmic puncta negative for β-catenin in the FlpInEED666AAA-HA cells, which could be internalized Cad6B (NT6B) molecules post-β-catenin dissociation.

In addition to preferential localization to the cytoplasm, the EED666AAA-HA Cad6B mutant is deficient in forming stable cell-cell adhesive interactions due to the decreased proportion of actin-anchored Cad6B. The increased endocytosis of this Cad6B mutant could translate into fewer opportunities for the mutant to form stable interactions with the actin cytoskeleton, as observed for other cadherins in this *in vitro* assay (Collinet and Lecuit, 2013). Alternatively, association with p120-catenin could be required for cadherins to interact with the actin cytoskeleton (Hoshino et al., 2005), such that the reduction of p120-catenin binding in this mutant in turn leads to enhanced endocytosis. These possibilities are not mutually exclusive and could in fact be occurring simultaneously, further augmenting Cad6B endocytosis.

Although the EED666AAA-HA Cad6B mutant undergoes rapid endocytosis initially, the internalized protein levels rapidly drop at 180 minutes post-biotinylation. Such results suggest that the absence of these residues may decrease the stability of this particular Cad6B mutant protein. In agreement with this, cycloheximide assays demonstrate that the EED666AAA-HA Cad6B mutant is less stable compared to both wild-type Cad6B-HA and the LI645AA-HA mutant (Fig. 4.10). Interestingly, loss of p120-catenin binding to endogenous cadherins (through expression of dominant negative cadherin mutants that function by titrating away p120-catenin) drives endocytosis and degradation of these endogenous cadherins (Kintner, 1992; Zhu and Watt, 1996; Nieman et al., 1999; Xiao et al., 2003b; Xiao et al., 2003a). Knockdown of p120-catenin similarly causes internalization and degradation of E-cadherin, while inhibition of lysosomal degradation through chloroquine treatment rescues this loss (Davis et al., 2003). Our work

now shows that p120-catenin plays a critical role in regulating the stability and endocytosis of another cadherin, Cad6B, in cultured cells.

A surprising observation in this study, however, is that the dileucine motif in Cad6B plays a minimal role in regulating Cad6B stability or membrane localization. This motif (normally masked by p120-catenin) binds several proteins required for clathrin-mediated endocytosis (Ishiyama et al., 2010), and thus mutation of this motif was hypothesized to negatively affect Cad6B endocytosis. On the contrary, mutation of the LI residues in Cad6B-HA does not significantly affect Cad6B internalization or its association with the actin cytoskeleton but does affect β-catenin distribution. This is in contrast with what has been observed with E-cadherin (Miyashita and Ozawa, 2007b) and N-cadherin (Tai et al., 2007). A more detailed molecular analysis of this motif in Cad6B provides insight into this observation. First, the LI motif, corresponding to the consensus (DE)XXXL(LI) (Bonifacino and Traub, 2003), is present in the form of QRKKEPLIIS in Cad6B. The existence of acidic residues at position -4 and -5 from the first leucine is critical for the endocytosis and targeting of other proteins to the late endosomes or lysosomes (Pond et al., 1995; Sandoval et al., 2000; Bonifacino and Traub, 2003; Pandey, 2009). Cad6B instead possesses the basic residues arginine and lysine in these positions, and these amino acids may provide the reasoning behind the lack of effect on internalization upon mutation of the LI residues. Second, the lysine at position 748 of E-cadherin was recently shown to control E-cadherin endocytosis *in vitro*, and complete loss of E-cadherin endocytosis was only observed when both the dileucine motif and lysine residue were mutated (Hong et al., 2010). Because Cad6B has a conserved lysine in a similar position (position 642), mutating it along with the LI motif may be necessary to block Cad6B endocytosis. Third, the -5 to -

8 positions upstream of the LI motif of Cad6B and several other type II cadherins are characterized by the presence of several arginine and glutamate residues. The glucose transporter GLUT4 similarly has two arginine residues -4 and -5 upstream of its dileucine motif (RRTPSLL), and substitution of these arginines with glutamate impairs its internalization and sorting to storage compartments (Sandoval et al., 2000). Conversely, substitution of the aspartate-glutamate pair (DERAPLI) of the lysosomal membrane protein LIMP-II with two arginines also impairs internalization and lysosomal targeting (Sandoval et al., 2000). Taken together, these contrasting examples suggest that Cad6B internalization may be additionally dependent on unknown residues upstream of its dileucine motif. Finally, Cad6B may just possess a different combination of endocytosis motifs protected by p120-catenin binding, as observed for VE-cadherin (Nanes et al., 2012), which lacks the dileucine motif altogether. Instead, the amino acids DEE (corresponding to DEG at position 650 in Cad6B) within the core-binding region of p120-catenin plays the role of the dileucine motif in VE-cadherin (Nanes et al., 2012). Similarly, p120-catenin could be masking a different motif in Cad6B and preventing its internalization, as our data suggest that mutation of the p120-catenin binding domain (EED666AAA-HA mutant) augments Cad6B endocytosis *in vitro*. Further mutational analyses of the region preceding the p120-catenin binding domain of Cad6B will be required to accurately identify the region masked by p120-catenin.

Although Cad6B possesses YDSL and YDYL motifs (YXXØ consensus) at position 738 and 765, respectively, these motifs are unlikely to play a role in Cad6B endocytosis because of their distance from the transmembrane domain. Purely endocytic- and lysosomal-targeting YXXØ signals are most often situated 10–40 and 6-9 residues

from the transmembrane domain, respectively, but not at the C terminus of proteins (Bonifacino and Traub, 2003). The YDSL and YDYL motifs of Cad6B are present nearly 100-140 amino acids away from the transmembrane domain and lie within the putative β-catenin binding region of Cad6B, suggesting that these residues could also be masked from cytosolic adaptor proteins by β-catenin. Nevertheless, considering that these residues are conserved across all type II cadherins, novel functions may exist for them in the context of cadherin internalization.

The role of the LI and EED motif with respect to Cad6B function and localization raises interesting questions particularly regarding the ability of these motifs to influence neural crest cell EMT *in vivo*. If Cad6B modulation through internalization is critical for neural crest cell EMT, introducing a Cad6B mutant that undergoes enhanced internalization (EED666AAA-HA) should result in increased numbers of neural crest cells undergoing EMT. Conversely, expressing a mutant with reduced internalization should decrease the number of neural crest cells undergoing EMT. Although the LI645AA-HA mutant is internalized in a similar fashion to wild-type Cad6B-HA *in vitro*, we hypothesized that this mutant might behave differently *in vivo* in regulating neural crest cell EMT. Our initial strategy to study the function of these mutants in a Cad6B-depleted background proved technically challenging due to the mosaic nature of electroporation (Appendix 3), and thus instead these mutants were expressed in the presence of endogenous Cad6B. This method has been used previously to successfully study Cad6B function in neural crest cells (Coles et al., 2007; Park and Gumbiner, 2010; Park and Gumbiner, 2012).

Our experimental observations regarding the effects of Cad6B endocytosis mutants on neural crest cell EMT have actually disproved our initial hypotheses (at least when

introduced in the presence of endogenous Cad6B). We find that expression of the Cad6B EED666AAA-HA or LI645AA-HA mutant does not rescue or further impede cranial neural crest cell EMT, respectively. There are several reasons for why are *in vivo* observations are not in complete agreement with what we note *in vitro*. First, all of the constructs were expressed in premigratory cranial neural crest cells possessing endogenous Cad6B. As described earlier, expression of cadherin mutants that can compete for p120-catenin binding leads to the endocytosis of the endogenous cadherin (Davis et al., 2003; Xiao et al., 2003b; Xiao et al., 2005). Our *in vitro* studies revealed that although the p120-catenin-EED666AAA-HA biochemical interaction is not affected, the localization of p120-catenin is perturbed, suggesting that p120-catenin can still be recruited to *de novo* synthesized EED666AAA-HA, only to be dissociated rapidly. Moreover, the localization of p120-catenin upon expression of the EED666AAA-HA mutant *in vivo* is unknown, and this may or may not replicate what is observed *in vitro*, as p120-catenin is potentially bound by cadherins other than Cad6B in the neural tube (see Literature Review, Section 1.6.2.2 for cadherins expressed in the neural tube and premigratory neural crest cells). Additional experiments are underway to investigate the localization of p120-catenin upon expression of wtCad6B-HA and the EED666AAA-HA mutant in order better explain this observation. Taken together, constitutive expression of EED666AAA-HA *in vivo* could be hypothesized to only weakly compete for p120-catenin binding at the plasma membrane and thus cause no effects on the membrane localization endogenous Cad6B. Nevertheless, since the EED666AAA-HA Cad6B mutant occasionally localizes to the plasma membrane both *in vitro* (Fig. 4.5) and *in vivo* (Fig. 4.13 D-D’’’), these transient localizations to the plasma membrane, combined with membrane-bound endogenous Cad6B, could be sufficient to

cause an overall reduction in neural crest cell EMT, as seen previously after wild-type Cad6B-HA overexpression (Coles et al., 2007). Thus, novel strategies (e.g. CRISPR) that can completely knockout endogenous Cad6B in premigratory neural crest cells are required in order to fully discern the effects of these Cad6B endocytosis mutants *in vivo* in the absence of any competing endogenous Cad6B.

In addition, the lack of spatiotemporal control over the expression of the Cad6B-HA mutant constructs could negatively impact the ability to investigate construct function *in vivo*. Endogenous Cad6B expression in neural crest cells is tightly regulated both spatially and temporally (Chapter 1, Section 1.6.2.2), so this must be taken into consideration for any experimental manipulations. Although we controlled for the temporal expression by harvesting embryos as cranial neural crest cells were undergoing EMT (6 and 7ss), it is possible that we have not allowed sufficient time for expression and function of the mutant constructs. This is due to the fact that we target premigratory neural crest cells at the 3ss and then harvest embryos 5-6 hours later when neural crest cells are undergoing EMT. Furthermore, the large size of the expression constructs (~10kb) could also negatively impact the ability of the DNA to enter cells of the neural tube and thus affect electroporation efficiency, as observed in our own experiments (Fig. 4.13). Future experiments will include introducing Cad6B mutant constructs earlier, but these assays can only be performed after the function of Cad6B at these even earlier embryonic stages has been determined (i.e., in wild-type embryos). Methods to introduce *cad6B* mRNA into premigratory neural crest cells could also be a strategy to circumvent this issue. Third, we lack the ability to properly control expression of exogenous Cad6B-HA. Endogenous *cad6B* is transcriptionally regulated by the Snail2 repressor (and likely by other

transcription factors as well), but the promoter driving exogenous *cad6B* in our constructs lacks any *cad6B* regulatory elements and is instead constitutively active, as we detect some migratory cranial neural crest cells expressing exogenous Cad6B-HA (data not shown). Driving the expression of exogenous *cad6B* and its mutants from a minimal *cad6B* promoter would be one way to overcome this limitation but requires additional work to identify these regulatory regions. Finally, our work indicates that Cad6B-HA partially co-localizes with clathrin *in vitro* and *in vivo*, suggestive of a role for clathrin-mediated endocytosis in Cad6B internalization (see Chapter 5). Our own studies, however, reveal that this pathway may not in fact be the primary mechanism of Cad6B internalization *in vivo*, and that alternative mechanisms are likely functioning. These pathways for internalization, and the data to support their existence, are discussed in the next chapter.

Chapter 5. Cad6B undergoes clathrin-mediated endocytosis and macropinocytosis *in vivo*

Parts of this section was adapted from the following article under re-review at the Journal of Cell Science:

Padmanabhan R, Taneyhill LA (2015). Cadherin-6B undergoes macropinocytosis and clathrin-mediated endocytosis during cranial neural crest cell EMT.

5.1. Summary

Cad6B undergoes internalization and possesses a functional p120-catenin binding motif in its cytoplasmic domain. Since we were unable to determine the importance of Cad6B internalization in neural crest cell EMT through the introduction of endocytosis mutants *in vivo*, we undertook an *ex vivo* approach, treating neural crest cell explants with chemical inhibitors to various internalization pathways. Furthermore, we sought to determine the pathway through which Cad6B is internalized, and in doing so identified that Cad6B partially co-localizes with clathrin *in vitro* and *in vivo,* suggesting that Cad6B is endocytosed through the clathrin-mediated pathway. Interestingly, though, we observed intracellular puncta positive for Cad6B, p120-catenin and β-catenin *in vitro* and *in vivo*, indicating that internalization of entire adherens junctions might be occurring through a process called macropinocytosis. To test whether clathrin-mediated endocytosis and macropinocytosis of Cad6B occur in neural crest cells, pharmacological inhibitors of these processes (Dynasore, a dynamin inhibitor, and Latrunculin A and EIPA, both macropinocytosis inhibitors) were employed and Cad6B distribution was documented in neural crest cell explants. While addition of Latrunculin A results in retention of Cad6B on the membrane, addition of EIPA and Dynasore causes the accumulation of large vesicles in the cytoplasm of neural crest cells undergoing EMT and starting to migrate. Furthermore, although correlative, the reduction in EMT upon inhibition of macropinocytosis and clathrin-mediated endocytosis suggested that Cad6B internalization through macropinocytosis is critical for neural crest cell EMT. These data suggest that Cad6B undergoes macropinocytosis and clathrin-mediated endocytosis through a dynamin-dependent pathway in neural crest cells.

5.2. Results

We have demonstrated that Cad6B is internalized and possesses a functional p120-catenin binding motif in its cytoplasmic domain, but its mechanism of internalization is still not clear. In this chapter, we now investigate the pathway(s) of Cad6B internalization *in vitro* and *in vivo* and explore the role of this internalization during neural crest EMT. Cadherins are known to be internalized through multiple pathways, including clathrin-dependent and –independent (e.g., caveolin) endocytosis and macropinocytosis (Le et al., 1999; Akhtar and Hotchin, 2001; Paterson et al., 2003; Bryant et al., 2005; Palacios et al., 2005; Xiao et al., 2005; Bryant et al., 2007; Toyoshima et al., 2007). Detecting co-localization of Cad6B with molecular markers of endosomal compartments would provide insight into pathways mediating Cad6B internalization. As mentioned in Chapter 4, however, we faced challenges in detecting co-localization of Cad6B with several endogenous (Appendix 1) and exogenous (Appendix 2) molecular markers of endosomal compartments *in vivo*. Nonetheless, we were able to detect the co-localization of endogenous clathrin with Cad6B *in vivo*, and the observations are detailed below.

5.2. Cad6B co-localizes with clathrin in vitro and in vivo

To determine the pathway by which Cad6B is internalized and endocytosed, we performed immunohistochemistry for Cad6B-HA (NT6B), caveolin-1 and clathrin in our cultured cell lines. We note that intracellular Cad6B (NT6B) does not co-localize with caveolin-1 (Appendix 2, Figs. A2.3 and A2.4), but partially co-localizes with clathrin *in vitro* (Fig. 5.1A-A", arrowheads). This co-localization was corroborated by examining Cad6B-HA (NT6B) and clathrin sub-cellular distribution in the LI645AA-HA (Fig. 5B-B", arrowheads) and EED666AAA-HA (Fig. 5C-C", arrowheads) mutant cell lines. Intriguingly, though, all cell lines show some intracellular puncta that are Cad6B(NT6B)-positive but devoid of clathrin immunoreactivity (Fig. 5.1A", B", C", carets).

Figure 5.1. Cad6B partially co-localizes with clathrin *in vitro.* FlpIn cells expressing wtCad6B-HA (A-A"), LI645AA-HA (B-B") and EED666AAA-HA (C-C") constructs were fixed, and immunofluorescence was performed for NT6B (green) and clathrin (red) (n = 3 from each cell line). Arrowheads in (A", B", C") show Cad6B (NT6B) and clathrin co-localization, and carets point to Cad6B (NT6B) puncta that do not co-localize with clathrin. Panels represent the 3D composite of 9 (A-A"), 11 (B-B"), and 11 (C-C") Z-stack images (0.25 μm/optical slice) acquired at 63x magnification with a confocal microscope. Inset boxes show the original image at 63x, with the asterisks in (A-C) indicating the location of the higher magnification field of view shown in the main panels. Scale bars: 10μm. Image reproduced from (Padmanabhan R, Taneyhill LA, under re-review in J Cell Sci).

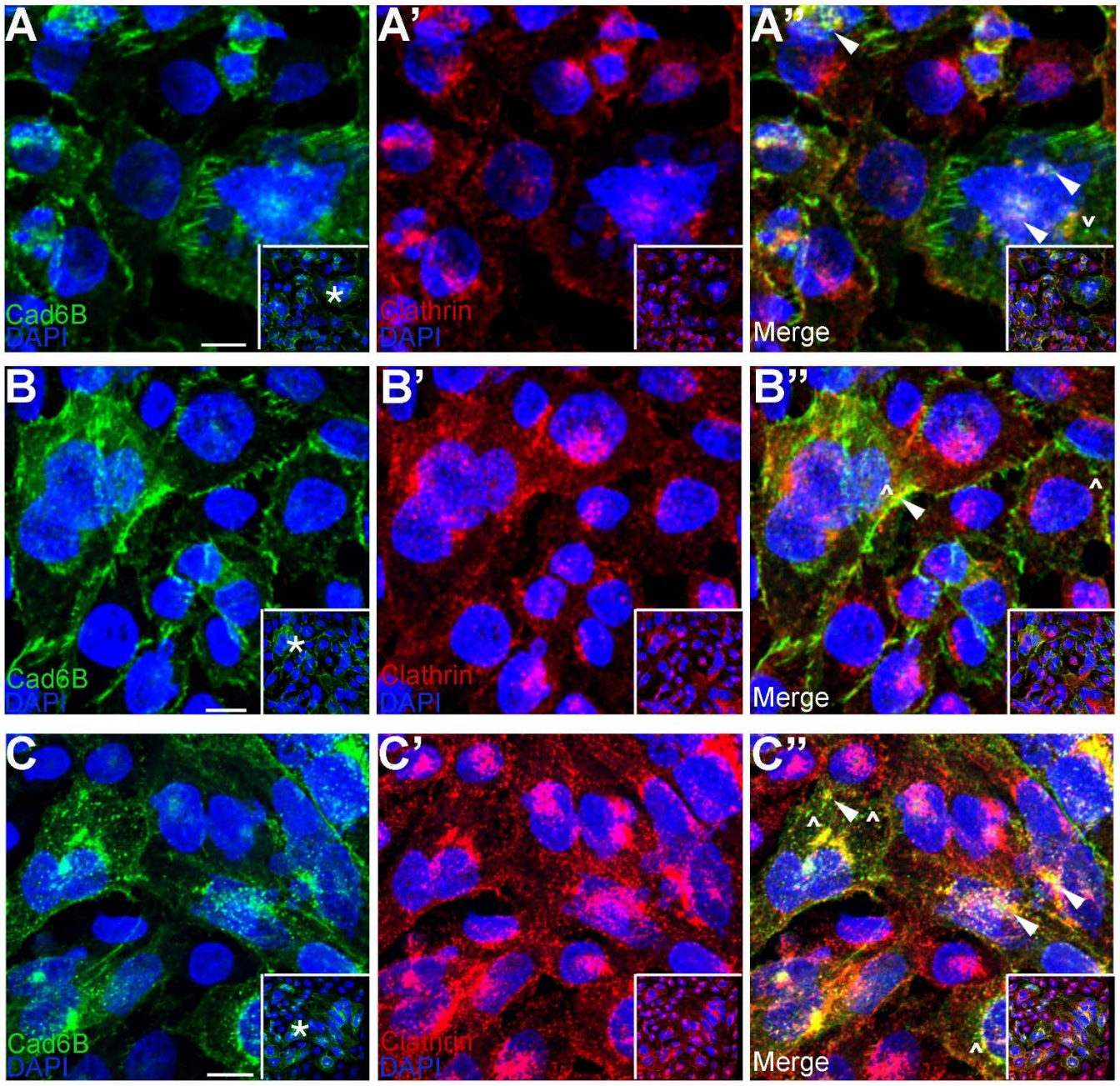
A
Cad6B
DAPI
A'
Clathrin
DAPI
A''
Merge
B
Cad6B
DAPI
B'
Clathrin
DAPI
B''
Merge
C
Cad6B
DAPI
C'
Clathrin
DAPI
C''
Merge

To confirm these findings *in vivo*, embryos at stages where premigratory cranial neural crest cells are actively undergoing EMT were dissected, fixed and immunofluorescence was performed for Cad6B and clathrin (Fig. 5.2). As observed *in vitro*, Cad6B (NT6B) co-localizes with clathrin *in vivo* (Fig. 5.2B-B", arrowheads). Once again, though, we note some Cad6B (NT6B)-positive puncta that lack clathrin (Fig. 5.2B", carets). Taken together, these data suggest that Cad6B undergoes clathrin-mediated endocytosis *in vitro* and *in vivo* as premigratory cranial neural crest cells are undergoing EMT. The presence of clathrin-negative, Cad6B (NT6B)-positive puncta, however, is indicative of additional mechanism(s) by which Cad6B could be internalized.

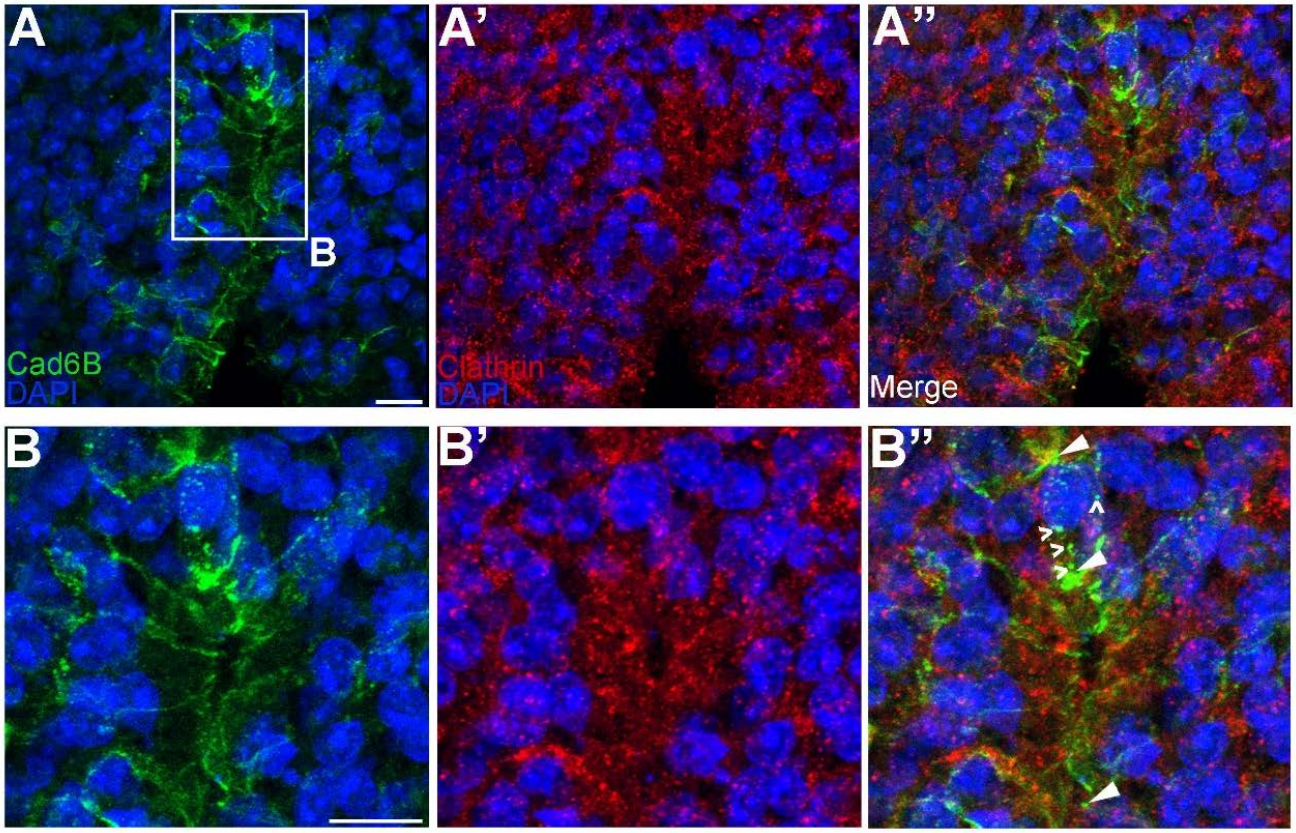

Figure 5.2. Cad6B partially co-localizes with clathrin *in vivo*. (A-A") Embryos in which neural crest cells are actively undergoing EMT were harvested, fixed and immunostained for Cad6B (NT6B; green) and clathrin (red) (n = 5 from 3 embryos). (B-B") is a higher magnification view of the boxed region in (A). Panels represent the 3D composite of 41 Z-stack images (0.25 µm/optical slice) acquired at 63x maginification with a confocal microscope. Arrowheads in (B") represent areas of Cad6B (NT6B) and clathrin co-localization, and carets indicate Cad6B (NT6B)-positive, clathrin-negative puncta. Scale bars: 10µm. Image reproduced from (Padmanabhan R, Taneyhill LA, under re-review in J Cell Sci).

5.3. Intracellular Cad6B puncta are at times positive for p120-catenin and β-catenin in vitro and in vivo

Our cell line data revealed that Cad6B (NT6B) puncta co-localize with either p120-catenin (Fig. 4.8B’’’’, D’’’’, F’’’’, arrows) or β-catenin (Fig. 4.7B’’’’, D’’’’, and F’’’’, arrows and arrowheads). When triple immunostaining was performed for Cad6B (NT6B), p120-catenin and β-catenin on chick cranial transverse sections, we observe that Cad6B (NT6B)-positive intracellular puncta occasionally co-localize with both p120-catenin and β-catenin in the cytoplasm (Fig. 5.3B’-B’’’’, arrowhead). Nevertheless, we also observe puncta that are positive for Cad6B (NT6B) and β-catenin but not p120-catenin (Fig. 5.3D-D’’’’, arrowhead). Endocytosis, however, relies upon the removal of the p120-catenin protein, as its binding normally serves to inhibit endocytosis, and its loss signals for cadherin endocytosis *in vitro* (Davis et al., 2003; Xiao et al., 2003a; Hoshino et al., 2005). Our *in vivo* co-localization data for Cad6B, β-catenin and p120-catenin suggest that, in some instances, whole complexes containing Cad6B and associated catenins are internalized rather than individual Cad6B molecules Moreover, considering that Cad6B is proteolytically processed by ADAM proteases, it is unlikely that the proteolysed extracellular fragment is not released into the explant media, further substantiating the likelihood that these NT6B- and p120-catenin-positive immunofluorescence puncta could represent full-length Cad6B protein. This process could be occurring through macropinocytosis, which involves the internalization of large volumes of plasma membrane (Falcone et al., 2006) and has been shown to regulate cadherin levels *in vitro* (Paterson et al., 2003; Bryant et al., 2007; Sharma and Henderson, 2007; Solis et al., 2012). Collectively, these results indicate the existence of at least two mechanisms (clathrin-

mediated endocytosis and macropinocytosis) by which premigratory cranial neural crest cells reduce levels of cell surface Cad6B to initiate and proceed through EMT.

Figure 5.3. Cad6B-positive cytoplasmic puncta at times co-localize with p120-catenin and β-catenin *in vivo*. Embryos in which neural crest cells are actively undergoing EMT were harvested, fixed and immunostained for Cad6B (NT6B; green), β-catenin (red) and p120-catenin (purple). (B'-B'''') and (D-D'''') are higher magnification views of the boxed region in (A''') and (C'''), respectively. The arrow represents membrane-bound Cad6B (NT6B), and the arrowhead in (B'-B'''') points to a punctum that is also positive for both β-catenin and p120-catenin (n = 1). Arrowhead in (D'-D'''') points to a Cad6B (NT6B)-containing intracellular punctum that is positive for Cad6B (NT6B) and β-catenin, but not p120-catenin (n = 3 from 3 embryos). Panels represent the 3D composite of 29 (A-B'''') and 53 (C-D'''') Z-stack images (0.25 μm/optical slice) acquired at 63x magnification with a confocal microscope. Scale bars (A-A''') and (C-C'''): 10μm; (B'-B'''') and (D'-D''''): 2μm.

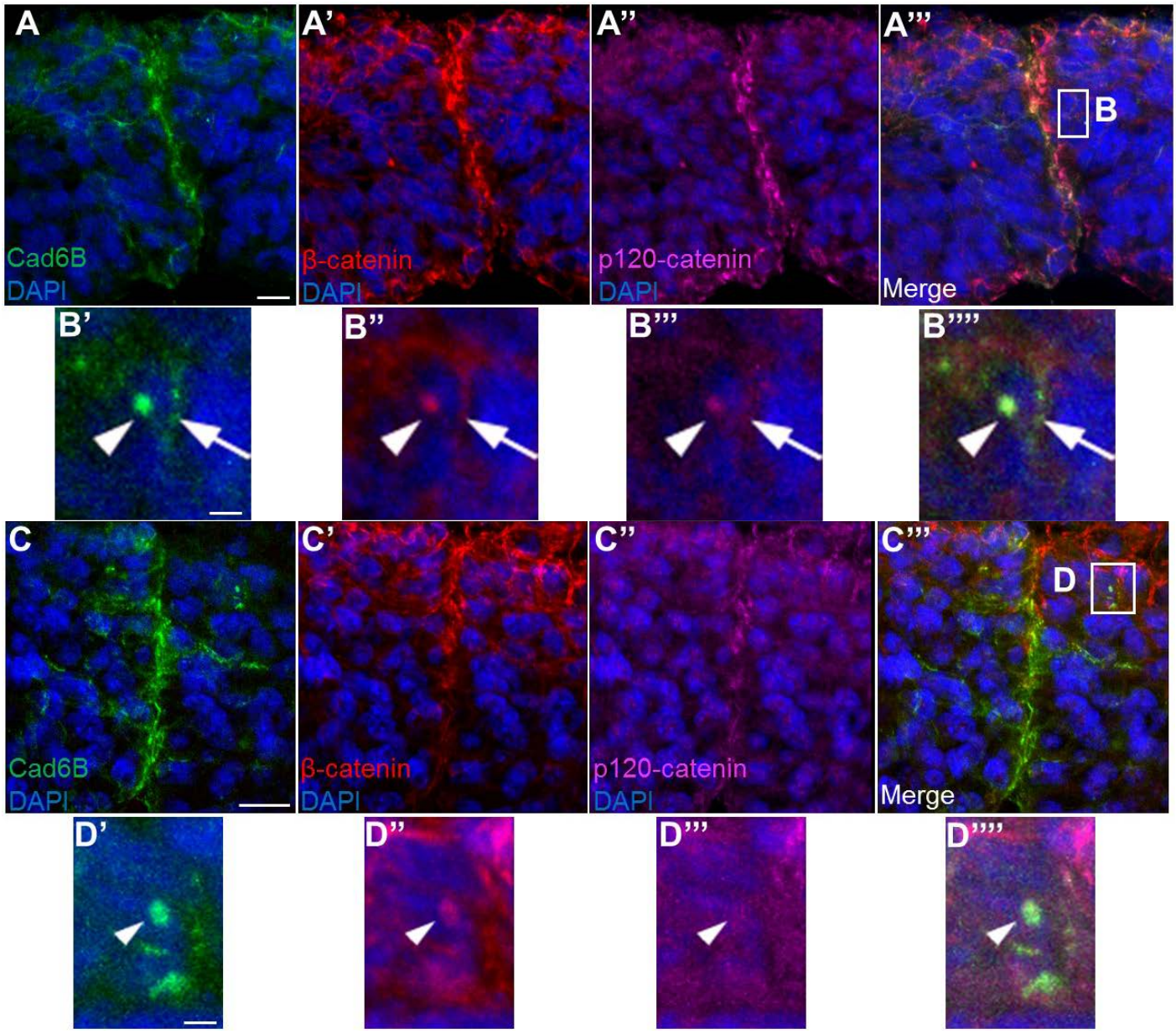
A
A'
A''
A'''
B
Cad6B
DAPI
β-catenin
DAPI
p120-catenin
DAPI
Merge
B'
B''
B'''
B''''
C
C'
C''
C'''
D
Cad6B
DAPI
β-catenin
DAPI
p120-catenin
DAPI
Merge
D'
D''
D'''
D''''

5.4. Inhibition of dynamin abrogates EMT and leads to the accumulation of Cad6B-positive intracellular puncta in cranial neural crest cells

To test these hypothesized mechanisms and elucidate the nature of Cad6B internalization in neural crest cells, we pharmacologically inhibited endocytosis and macropinoctyosis in neural crest cell explants. We first assessed a role for dynamin, which releases vesicles from the plasma membrane during both clathrin-mediated endocytosis and clathrin-independent mechanisms such as macropinocytosis (Jarrett et al., 2002; Orth et al., 2002; Palacios et al., 2002; Cao et al., 2007), by treating explants with Dynasore, a dynamin inhibitor (Macia et al., 2006). Our results show that, compared to DMSO-treated control explants (Fig. 5.4A-A" and B'-B'''; arrows indicate membrane staining), inhibition of dynamin blocks neural crest cell EMT and migration (observed in 5/5 explants compared to 8/8 control explants which underwent EMT and migrated normally; Fig. 5.5B) and leads to the accumulation of multiple, large intracellular Cad6B (NT6B)-positive puncta that at times co-localize with p120-catenin (Fig. 5.4C-C" and D'-D''', arrowheads).

Figure 5.4. Addition of Dynasore results in large puncta of Cad6B on the membrane and in the cytoplasm. Vehicle (0.5% DMSO, A-A") (n = 8 explants) and 100μM Dynasore (C-C") (n = 5 explants) were added to the media of explanted cranial dorsal neural folds. Explants were then incubated to allow for EMT to occur, fixed and immunostained for Cad6B (NT6B; green) and p120-catenin (red). (B'-B''') and (D-D''') are higher magnification views of the boxed region in (A") and (C") respectively. Arrows and arrowheads represent Cad6B (NT6B) and p120-catenin co-staining at the membrane and cytoplasm, respectively. Carets point to Cad6B (NT6B)-positive, p120-catenin-negative puncta. Panels represent the 3D composite of 39 (A-B''') and 66 (C-D''') Z-stack images (0.25 μm/optical slice) acquired at 63x maginification with a confocal microscope. Scale bars (A-A") and (C-C"): 10μm, (B'-B''') and (D'-D'''): 5μm.

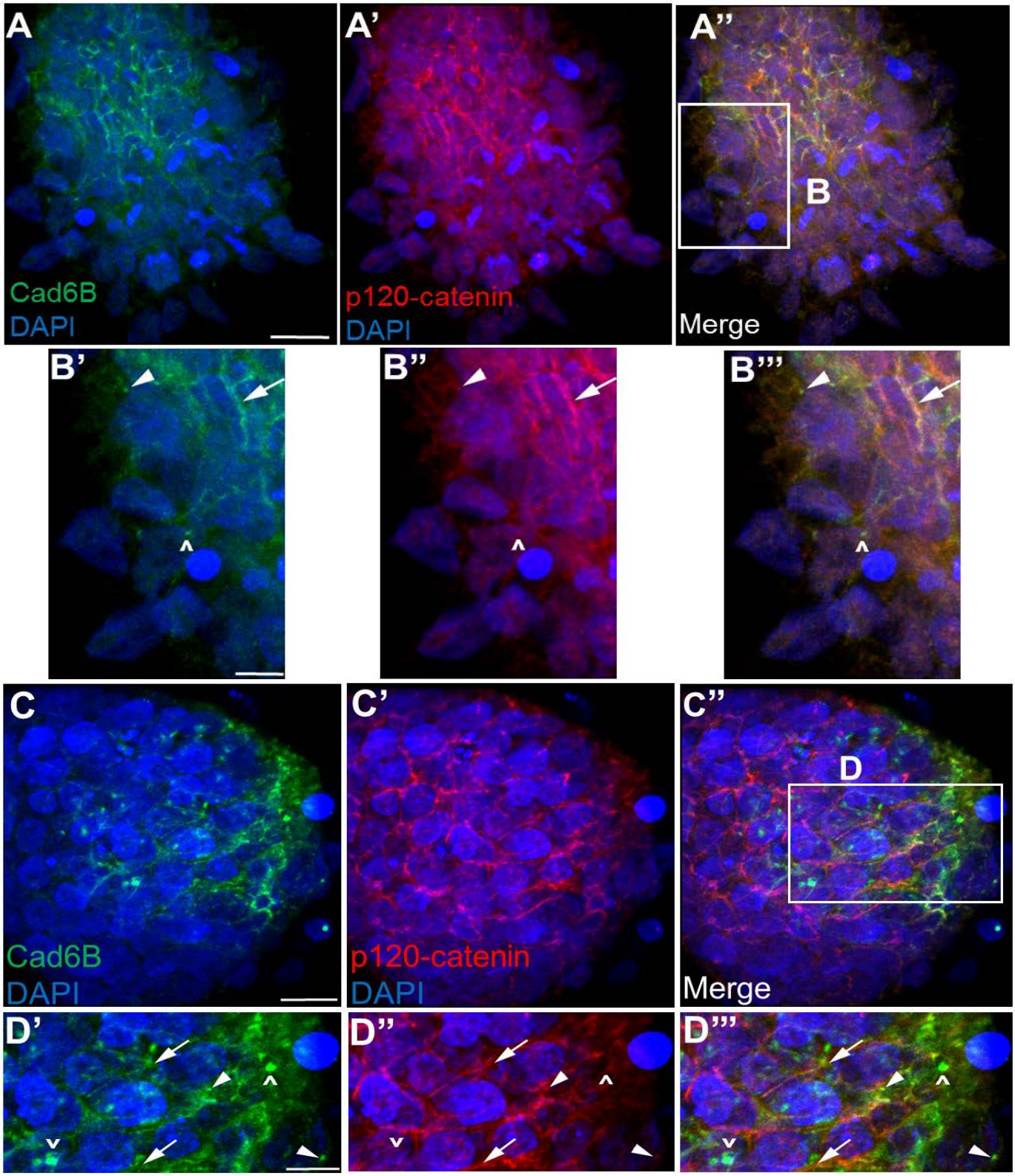
A
Cad6B
DAPI
A'
p120-catenin
DAPI
A''
B
Merge
B'
B''
B'''
C
Cad6B
DAPI
C'
p120-catenin
DAPI
C''
D
Merge
D'
D''
D'''

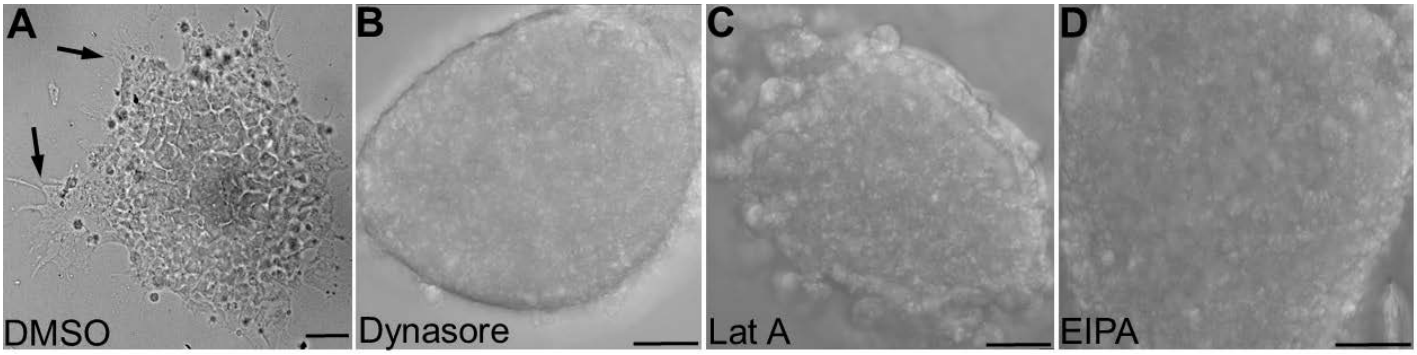

Figure 5.5. Inhibition of actin polymerization, dynamin-mediated internalization or macropinocytosis abolishes EMT in premigratory cranial neural crest cell explants. Vehicle (0.5% DMSO, A; n = 8 explants), 100µM Dynasore (B; n = 5 explants), 30nM Latrunculin A (LatA, C; n = 7 explants), or 50µM EIPA (D; n = 7 explants) were added to the media of explanted cranial dorsal neural folds. Explants were incubated for 3.5 hours to allow for EMT to occur, fixed and imaged under differential interference contrast. Panel (A) represent cranial neural crest cells that have undergone EMT and are migrating, as evidence by the appearance of cell protrusions (arrows). These cells and protrusions are absent in all types of inhibitor-treated explants (B, C, D). Scale bars: 10µm.

5.5. Cad6B undergoes macropinocytosis in cranial neural crest cells

To determine whether macropinocytosis mediates internalization of Cad6B and associated catenins during neural crest cell EMT, we prevented the formation of macropinosomes through two methods. Macropinocytosis is critically dependent on dynamic actin polymerization and depolymerization (Mercer and Helenius, 2009) and indeed, we notice intense actin polymerization occurring near large Cad6B (NT6B)-positive membrane-bound punctum (see Fig.5.6B'-B''', asterisk), suggestive of a macropinocytic event. We inhibited actin polymerization by Latrunculin A (Spector et al., 1983; Mercer and Helenius, 2009) and investigated its effects on the putative macropinocytosis of Cad6B. Latrunculin A treatment negatively affected actin polymerization as evidenced by the marked reduction in phalloidin staining (Fig. 5.6C') compared to DMSO control-treated explants (Fig. 5.6A'). Importantly, addition of Latrunculin A severely decreased the presence/number of Cad6B (NT6B)-containing puncta (Figs. 5.6C-C'' and D'-D'''), with the majority of Cad6B (NT6B) still localized to the plasma membrane (Fig.5.6 D'-D''', arrows), in contrast to what was observed with DMSO-treated control explants (Fig. 5.6A", arrowheads). Nonetheless, we did notice some intracellular Cad6B (NT6B) in Latrunculin A-treated explants (Fig. 5.6D''', arrowheads). Finally, Latrunculin A treatment inhibited EMT (in 7/7 explants examined compared to normal EMT and migration observed in 8/8 control explants; Fig. 5.5C).

Figure 5.6. Inhibition of actin polymerization results in persistence of Cad6B on the plasma membranes of cranial neural crest cells. Vehicle (0.5% DMSO, A-A"; n = 8 explants) or 30nM Latrunculin A (C-C"; n = 7 explants) were added to the media of explanted cranial dorsal neural folds. Explants were then incubated to allow for EMT to occur, fixed and immunostained for Cad6B (NT6B; green) and stained with phalloidin (red). (B'-B''') and (D'-D''') are higher magnification views of the boxed region in (A") and (C") respectively. Arrows represent membrane-localized Cad6B (NT6B), arrowheads point to Cad6B (NT6B)-containing puncta, and the asterisk shows a large Cad6B (NT6B)-positive punctum with intense actin polymerization occurring near it. Panels represent the 3D composite of 37 (A-B''') and 124 (C-D''') Z-stack images (0.25 μm/optical slice) acquired at 63x magnification with a confocal microscope. Scale bars (A-A''') and (C-C'''): 10μm; (B'-B''') and (D'-D'''): 5μm.

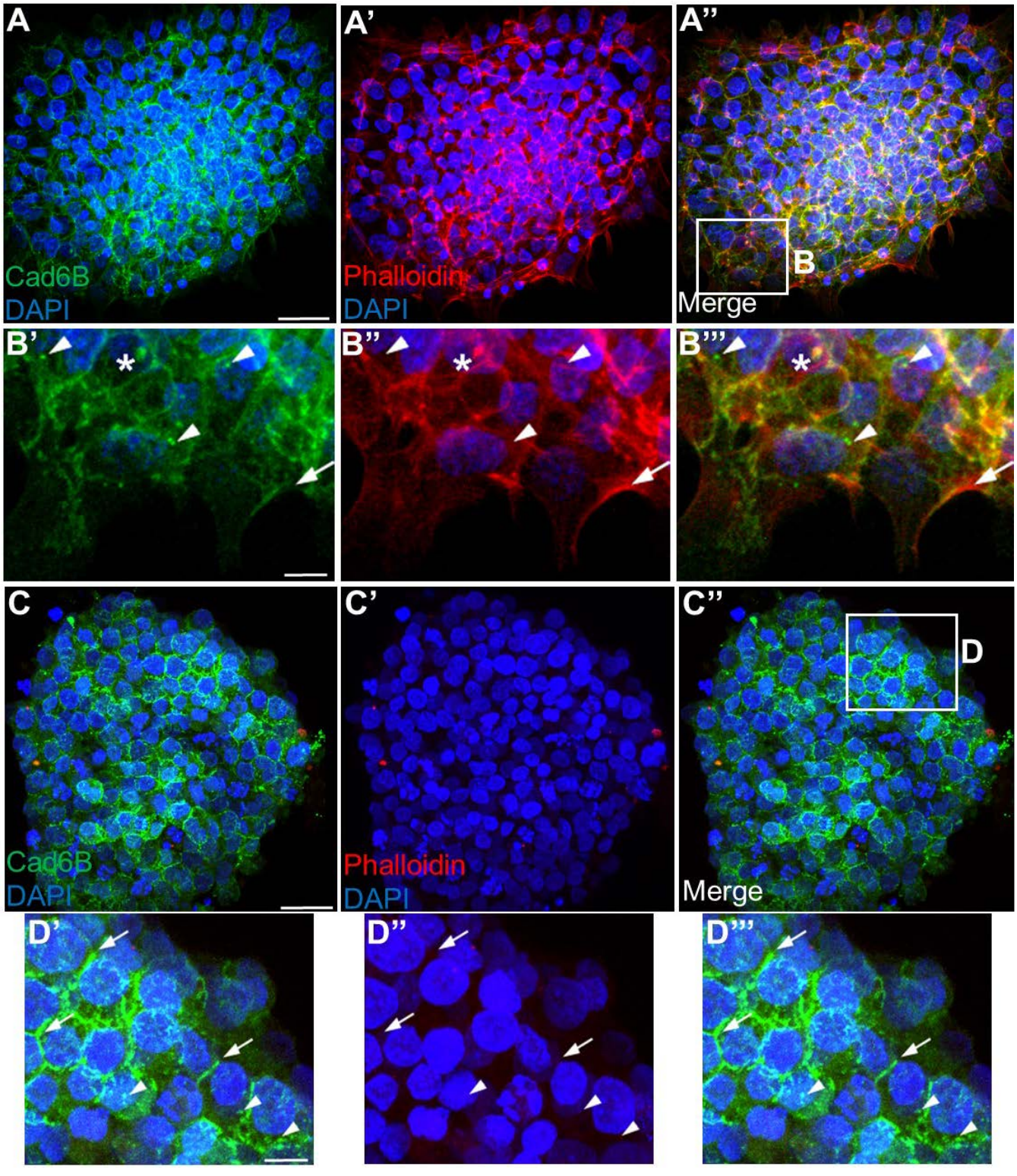
A
Cad6B
DAPI
A'
Phalloidin
DAPI
A''
B
Merge
B'
B''
B'''
C
Cad6B
DAPI
C'
Phalloidin
DAPI
C''
D
Merge
D'
D''
D'''

We next tested the sensitivity of Cad6B internalization to the amiloride EIPA, which prevents maturation of macropinosomes by lowering sub-membraneous pH and inhibiting Rac and Cdc42 activity (Koivusalo et al., 2010) (Figs. 5.7C-C", D'-D'''). EIPA treatment results in the appearance of multiple, large intracellular Cad6B (NT6B) cytoplasmic puncta that co-localize with p120-catenin and also abolishes EMT (Fig. 5.7D'-D''', arrowheads; 7/7 explants show an absence of EMT and migration compared to normal EMT and migration in 8/8 DMSO-treated control explants, see Fig. 5.5D). The size of the accumulated puncta (1.5-3μm, 18 puncta measured from 5 different explants) in this assay is also indicative of macropinocytosis (Swanson, 1989; Hewlett et al., 1994; Schnatwinkel et al., 2004). To further corroborate the EIPA data, we specifically inhibited Rac1 through the chemical inhibitor NSC23766 and observed that it could partially recapitulate the phenotype of EIPA (data not shown).

Figure 5.7. Cad6B is internalized as whole adherens junction complexes in premigratory cranial neural crest cells. Vehicle (0.5% DMSO, A-A", duplicated from Fig. 5.4, as the experiments were performed on the same day; n = 8 explants) and 50μM EIPA (C-C"; n = 7 explants) were added to the media of explanted cranial dorsal neural folds. Explants were then incubated to allow for EMT to occur, fixed and immunostained for Cad6B (NT6B; green) and p120-catenin (red). (B'-B''') and (D-D''') are higher magnification views of the boxed region in (A") and (C") respectively. Arrows and arrowheads represent Cad6B (NT6B) and p120-catenin co-staining at the membrane and cytoplasm, respectively. Carets point to Cad6B (NT6B)-positive, p120-catenin-negative puncta. Panels represent the 3D composite of 39 (A-B''') and 48 (C-D''') Z-stack images (0.25 μm/optical slice) acquired at 63x with a confocal microscope. Scale bars (A-A''') and (C-C'''): 10μm; (B'-B''') and (D'-D'''): 5μm.

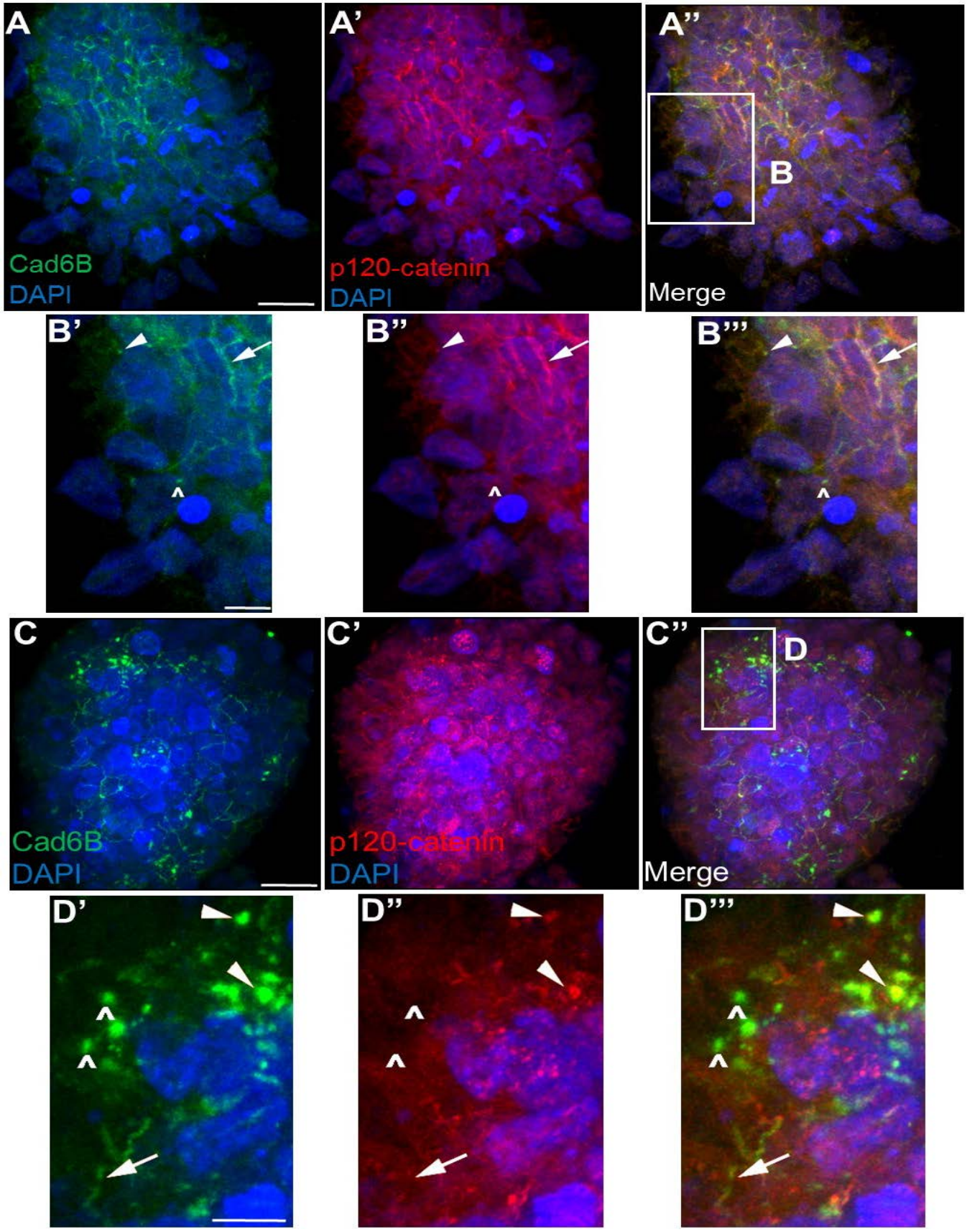
A
Cad6B
DAPI
A'
p120-catenin
DAPI
A''
B
Merge
B'
B''
B'''
C
Cad6B
DAPI
C'
p120-catenin
DAPI
C''
D
Merge
D'
D''
D'''

A more rigorous examination of p120-catenin localization in explants after inhibitor treatment revealed some surprising results. Many of the large Cad6B (NT6B) cytoplasmic puncta observed upon Dynasore (Fig. 5.4D'-D''', carets) or EIPA (Fig. 5.7D'-D''', carets) were in fact p120-catenin-negative, in contrast to our expectation that these putative macropinocytic compartments would possess both Cad6B and p120-catenin as internalized whole adherens junctions. To investigate if these observations were perhaps due to extraneous effects of these inhibitors, we examined Cad6B (NT6B) and p120-catenin co-localization in untreated cells, explants and embryos. Indeed, we noticed in several instances that Cad6B (NT6B) puncta did not co-localize with p120-catenin in untreated cells *in vitro* (Figs. 4.8 B'''', D'''', carets), explants (Fig. 5.4 B''', carets), and embryos *in vivo* (Fig. 5.3D''', arrowheads), implying that they are either endocytic vesicles or that p120-catenin dissociates later from the complex post-macropinocytosis. Moreover, the large NT6B-positive p120-catenin-negtive puncta are unlikely to be ADAM-mediated proteolytic products of Cad6B (the N-terminal extracellular domain) (Schiffmacher et al., 2014), as the N-terminal fragment generated post proteolysis in an *ex vivo* system is likely released into the explant media. Taken together, our results reveal for the first time that Cad6B is internalized during cranial neural crest cell EMT through dynamin-dependent, clathrin-mediated endocytosis and macropinocytosis, with the absence of internalization severely impacting the ability of cranial neural crest cells to undergo EMT and migrate.

5.6. Discussion

Cells dynamically modulate cadherin levels on the plasma membrane through multiple mechanisms (Chapter 1, Section 1.6.2.3), and internalization of cadherins is recognized to be one important means that is critical for development and disease (reviewed in (Kowalczyk and Nanes, 2012)). In premigratory cranial neural crest cells, Cad6B localizes to the cytoplasm, pointing to the possibility that it could be internalized (Chapter 3). We subsequently identified a functional p120-catenin binding motif in the cytoplasmic domain of Cad6B-HA and demonstrated that mutation of critical residues within the core-binding region of p120-catenin enhances Cad6B-HA endocytosis and reduces the stability of Cad6B-HA (Chapter 4). In this Chapter, we sought to investigate the molecular pathway through which Cad6B is internalized, as cadherins are known to removed from the plasma membrane through clathrin-dependent and -independent endocytosis and via macropinocytosis (Le et al., 1999; Akhtar and Hotchin, 2001; Paterson et al., 2003; Bryant et al., 2005; Palacios et al., 2005; Xiao et al., 2005; Bryant et al., 2007; Toyoshima et al., 2007). We chose a strategy that would not only address this question, but also delineate the importance of Cad6B internalization in neural crest EMT.

Our observation that Cad6B (NT6B) co-localizes with clathrin *in vitro* and *in vivo* was immediately suggestive of clathrin-mediated endocytosis and is in line with what is observed for other cadherins (Le et al., 1999; Xiao et al., 2003b; Ivanov et al., 2004; Izumi et al., 2004; Bryant et al., 2005; Gavard and Gutkind, 2006). Retention of Cad6B (NT6B) on the plasma membrane and accumulation in large puncta/vesicles upon addition of Dynasore, a dynamin inhibitor, also supports this mechanism of internalization. Interestingly, however, we noticed several Cad6B (NT6B)-positive, clathrin-negative

puncta, indicating that mechanisms other than clathrin-mediated endocytosis could exist to remove plasma membrane-bound Cad6B. Furthermore, we noticed that these Cad6B (NT6B)-positive puncta were at times immunoreactive for both β-catenin and p120-catenin. Although internalized cadherins have at times been observed to co-localize with β-catenin during endocytosis (Le et al., 1999; Davis et al., 2003; Xiao et al., 2003b; Kam and Quaranta, 2009), co-localization with p120-catenin has only been reported by one group during macropinocytosis of E-cadherin (Bryant et al., 2007). As discussed in Chapter 1 (Section 1.6.2.3.2.4), dissociation of p120-catenin and the resulting exposure of the cadherin AP2 adaptor protein-binding site (which in many cadherins is the dileucine motif) is the classical mechanism by which clathrin mediates endocytosis of cadherins. Indeed, our *in vitro* observations show that p120-catenin masks a critical region of Cad6B-HA, the exposure of which causes enhanced internalization of Cad6B-HA, among other effects (Chapter 4, Sections 4.3-4.8). Thus, the presence of p120-catenin in large Cad6B (NT6B)-positive puncta raises the intriguing possibility that Cad6B could be internalized as whole adherens junction complexes, independent of the binding state of p120-catenin to Cad6B. Such internalization of large volumes of the plasma membrane occurs through a mechanism called macropinocytosis (Falcone et al., 2006).

To corroborate a role for macropinocytosis in reducing surface levels of Cad6B in neural crest cells, inhibitors of macropinocytosis were applied to neural crest cell explants and effects on Cad6B (NT6B) documented. In explants treated with Latrunculin A, a potent inhibitor of actin polymerization that is critical for macropinocytosis (Spector et al., 1983; Mercer and Helenius, 2009), we noted a reduction in Cad6B (NT6B) puncta in neural crest cells. In addition, treatment of explants with EIPA, another macropinocytosis inhibitor,

results in the accumulation of large puncta/vesicles of Cad6B (NT6B) in the cytosol (and associated with the membrane) of premigratory and early migratory neural crest cells, lending further credence to a role for macropinocytosis in Cad6B (NT6B) internalization. Similar large puncta were also noted during Dynasore treatment of explants, implicating dynamin in the pinching off of vesicles and/or macropinosomes during Cad6B internalization. Moreover, treatment with Dynasore, Latrunculin A, and EIPA all blocked neural crest cell EMT and migration in explants, implying that the downregulation of Cad6B through endocytosis and macropinocytosis is critical for EMT. Although the qualitative effect of inhibitors is drastic i.e. appearance of large Cad6B puncta, a quantitative estimate of the difference in the number of Cad6B across treatments is lacking, and methods to quantify the number of puncta in composite 3D z-stack images is currently being investigated. The use of macropinocytosis to remove cadherins from the plasma membrane has only been observed *in vitro* for E-cadherin molecules not actively engaged in cell-cell adhesion (Bryant et al., 2007) and for N-cadherin at the leading edge of migratory cells (Sharma and Henderson, 2007). In another study, Solis et al. (2012) demonstrated that EGF receptor signaling, modulated by reggies/flottilin proteins, promotes E-cadherin macropinocytosis and recycling, thereby regulating cell adhesion (Solis et al., 2012). Although noted *in vitro*, cadherin macropinocytosis has never been demonstrated in an *in vivo* EMT and in any neural crest cell population. As such, our work is the first to report the significance of cadherin macropinocytosis and endocytosis during neural crest cell EMT.

Although treatment with Latrunculin A caused significant retention of Cad6B (NT6B) on cellular plasma membranes, we still noticed small puncta of Cad6B (NT6B),

raising questions as to their nature. Dynamic actin polymerization and de-polymerization is critical not only for macropinocytosis but also for endocytosis (Mooren et al., 2012), but it is less likely that these Cad6B (NT6B)-positive puncta are intracellular endocytic structures because we have substantially blocked the actin polymerization required for endocytosis. Cadherins in adherens junctions are organized into molecular clusters (Tepass and Hartenstein, 1994; Angres et al., 1996; Muller and Wieschaus, 1996; Adams et al., 1998), and the actin cytoskeleton regulates not only the assembly/disassembly of cadherin monomers into clusters but also controls the lateral mobility of these clusters (reviewed in (Collinet and Lecuit, 2013)). Interestingly, actin depolymerization does not dissolve cadherin clusters but instead affects their lateral mobility along the plasma membrane (Cavey et al., 2008). This raises the possibility that the observed puncta in the presence of Latrunculin A could actually be membrane clusters of Cad6B (NT6B) that have failed to undergo endocytosis or macropinocytosis due to the disruption in the actin cytoskeleton. Evidence for this hypothesis is provided by the observation that E-cadherin is organized into local clusters before being endocytosed through the clathrin-mediated pathway in *Drosophila* embryos (Levayer et al., 2011). Indeed, closer examination of several such puncta in the y-z plane of explants treated with Latrunculin A reveals that they are on the cell surface rather than within the cell (data not shown).

In Chapter 4, we were unable to address the importance of Cad6B endocytosis motifs on neural crest cell EMT by expressing Cad6B endocytosis mutants *in vivo*. To demonstrate a correlation between Cad6B internalization and EMT, the effects of inhibitors of endocytosis and macropinocytosis on the EMT process were examined using the explant assay. Taken together, these experiments provide insights into the requirement for Cad6B

endocytosis and macropinocytosis during neural crest cell EMT. The reduction in EMT observed upon inhibition of Cad6B (NT6B) internalization through EIPA or Dynasore (and NSC23766, data not shown) show that Cad6B macropinocytosis and endocytosis could be critical for neural crest cell EMT. However, these chemical inhibitors could have some non-specific effects (reviewed in (Ivanov, 2008)). For example, EIPA can induce reorganization of F-actin in epithelial cells (Lagana et al., 2000) and alter morphology and the intracellular distribution of early and late endosomes in HeLa cells (Fretz et al., 2006). On the other hand, Dynasore has been shown to impair cholesterol trafficking and transcription of sterol-sensitive genes in HeLa cells and macrophages (Girard et al., 2011), and can inhibit caveolar endocytic pathways in some cells (Macia et al., 2006), showing that it can have minor effects on internalization pathways besides those that are clathrin-based. As such, our results are correlative in nature, and further genetic studies are required to establish a role for macropinocytosis and clathrin-mediated endocytosis in the internalization of Cad6B.

Another interesting observation from this study is the localization of p120-catenin with respect to Cad6B (NT6B). Although several Cad6B (NT6B)-containing puncta are also positive for p120-catenin, many puncta lacked p120-catenin, raising questions as to the nature and function of p120-catenin during neural crest cell EMT. As mentioned previously, Cad6B (NT6B)-positive, p120-catenin-negative puncta could either be endocytic vesicles or those wherein p120-catenin has dissociated later from the complex post-macropinocytosis. This latter 'late release' p120-catenin could then perform other signaling roles that directly or indirectly impinge upon neural crest cell EMT (see below

and (Bellovin et al., 2005; Yanagisawa and Anastasiadis, 2006; Cheung et al., 2010; Johnson et al., 2010)).

The discovery of Cad6B macropinocytosis and endocytosis also begs the question as to the factors that stimulate these processes in neural crest cells. Paterson *et al.* (2003) and Sharma and Henderson (2007) have shown a role for the GTPase Arf6 in E-cadherin macropinocytosis (Paterson et al., 2003; Sharma and Henderson, 2007). *Arf1* is the only gene of the Arf family of GTPases that has been analyzed for expression in chick through whole mount *in situ* hybridization, and neural crest cells are devoid of it (GEISHA database; http://geisha.arizona.edu/geisha/index.jsp). Future studies are thus required to determine if another Arf GTPase member is expressed in premigratory cranial neural crest cells that could mediate Cad6B macropinocytosis. Rac1, another classical marker and regulator of macropinocytosis, plays a critical role in E-cadherin macropinocytosis *in vitro* (Bryant et al., 2007). Rac1 is expressed in premigratory and migratory cranial neural crest cells (Kee et al., 2007), but its function in the head is unknown. Conversely, Rac1 is observed only in delaminating and migratory trunk neural crest cells but not premigratory trunk neural crest cells (Shoval and Kalcheim, 2012). Proper spatiotemporal expression of Rac1 at the leading edge of the cells is critical for trunk neural crest cells to initiate migration, as both constitutively active and dominant negative forms of Rac1 inhibit neural crest cell emigration (Shoval and Kalcheim, 2012). Indeed, inhibition of Rac1 through NSC27366 also results in partial recapitulation of EIPA phenotype (data not shown), suggestive of a role of Rac1 in this process. Interestingly, N-cadherin-bound or free p120-catenin inhibits or promotes Rac1 activity, respectively (Grosheva et al., 2001). Given our observation that several Cad6B-postive puncta are negative for p120-catenin, this points to

a possible mechanism wherein p120-catenin regulates both Cad6B endocytosis and macropinocytosis as well as cell motility through Rac1. Another possible scenario could be a reduction in Ca2+ levels in the vicinity of neural crest cells that could directly lead to rapid downregulation of Cad6B, as observed with other cadherins (Pokutta et al., 1994). Studies performed by McKinney and Kulesa (2012) with a genetically-encoded calcium sensor GCaMP3, however, failed to show appreciable change in calcium dynamics in the chick midbrain, indicating that such a mechanism is unlikely (McKinney et al., 2012). Finally, Solis *et al.* (2012) demonstrated that the degree of EGF receptor phosphorylation stimulated by prion protein and reggies/flottilins in turn regulates E-cadherin macropinocytosis (Solis et al., 2012). The expression or function of prion proteins or of the reggies/flottilins in neural crest cells is not known at this time. Because neural crest cell EMT is regulated by a myriad of hierarchical signaling factors, a detailed analysis is therefore required to delineate the precise signals that stimulate Cad6B macropinocytosis and endocytosis.

It is intriguing that cranial neural crest cells employ multiple mechanisms (internalization (this work) and proteolysis (Schiffmacher et al., 2014)) to reduce surface Cad6B levels *en masse* during EMT. One possibility is that these mechanisms are used in different sub-populations of cranial neural crest cells that exist in the dorsal neural tube (Lee et al., 2013; Ridenour et al., 2014). Alternatively, this rapid reduction in Cad6B protein may be necessary to release β-catenin and p120-catenin to the cytosol so that they can perform signaling functions (i.e., transcription, regulation of Rac1 activity) and/or form complexes with other mesenchymal cadherins, such as Cadherin-7 and Cadherin-11 (Nakagawa and Takeichi, 1995; Chalpe et al., 2010), to mediate neural crest cell migration.

Finally, removal of Cad6B from premigratory cranial neural crest cells could be occurring simply to eliminate any physical barriers, such as those provided by adherens junctions, that initially hold premigratory neural crest cells together prior to their delamination and EMT. In summary, we have now demonstrated the existence of a novel macropinocytic and endocytic mechanism to removed Cad6B from the plasma membrane of premigratory cranial neural crest cells, the disruption of which causes a significant loss of neural crest cell EMT and migration.

The broader implications of the existence of redundant mechanisms to remove proteins from the plasma membrane also beg the question on its evolutionary significance. To begin with, it would be interesting to investigate if such a mechanism exists in proto-vertebrate species with proto-neural crest cells, such as amphioxus, hagfish and lampreys. Although they may not possess an equivalent cadherin, investigations could focus on the existence of redundant mechanisms of downregulation of proteins in this proto-neural crest cell population. Nonetheless, it could be hypothesized that redundant mechanisms to regulate multiple proteins apart from cadherins evolved very early during the evolution of chordates. As biological systems became complex, redundant mechanisms may have come forth through convergent evolution to regulate processes that are critical for organismal development. As such, extrapolating from such a possibility points to a situation where loss of Cad6B could be critical for neural crest cell EMT. On the other hand, Cad6B could be a simple transient factor to segregate premigratory neural crest cells from other cells, and once EMT is initiated, the requirement for Cad6B could become unnecessary, prompting the cells to remove this protein through multiple mechanisms. Studies examining the

potential functions of the C-terminal and N-terminal ends of Cad6B will provide critical insight into answering this question.

Chapter 6. Conclusions and Future Directions

6.1. Conclusions

One of the overarching goals of our lab is to understand the role and mechanism of regulation of cellular junction components during cranial neural crest cell EMT. To this end, this dissertation aims to understand the molecular mechanisms underlying the downregulation of the transmembrane cell adhesion protein Cad6B. Specifically, the objective of this dissertation was to investigate if downregulation of Cad6B protein occurs through internalization mediated by endocytosis or other processes. The lab previously identified ADAM-mediated proteolysis as one means by which Cad6B levels are reduced in premigratory cranial neural crest cells, Intrigued by the observation that Cad6B is found in intracellular puncta, however, we hypothesized that Cad6B could get internalized in addition to being cleaved by proteases. To address this hypothesis, we first generated cell lines that stably express Cad6B-HA from a single genomic locus in CHO cells, which lack endogenous cadherins. Using these cell lines and embryo sections, we revealed that Cad6B (NT6B) is localized to the cytoplasm *in vitro* and *in vivo*, suggestive of internalization (Chapter 3). Antibody feeding assays were subsequently performed to show that the Cad6B (NT6B) puncta are endocytic rather than exocytic in nature. We then negated the possibility that addition of Cad6B (NT6B) antibody was stimulating Cad6B internalization by modifying the antibody feeding technique to include a low pH wash, which removed any Cad6B (NT6B) antibody bound to non-internalized (cell surface) Cad6B protein. Thus in Chapter 3 we first established that Cad6B undergoes internalization in premigratory cranial neural crest cells and in cultured cells.

In Chapter 4, we sought to biochemically demonstrate Cad6B internalization *in vitro* and examine its requirement for neural crest cell EMT *in vivo* through the generation

of two Cad6B-HA constructs containing mutations in putative endocytosis motifs. Mutation of the LI residues, which form the dileucine motif, had a minimal influence on Cad6B-HA internalization, interaction with the actin cytoskeleton and stability, but it did affect the localization of β-catenin. In contrast, mutation of the EED residues, which are within the putative p120-catenin binding region of Cad6B, enhanced Cad6B-HA internalization, decreased its interaction with the actin cytoskeleton and its overall stability, and prevented proper localization of both α- and p120-catenin proteins. Although suggestive of a reduced interaction with Cad6B-HA, immunoprecipitation experiments showed no effects on the ability of the EED666AAA-HA mutant to biochemically interact with p120-catenin. We then asked whether the mutants impacted neural crest cell EMT *in vivo*. To this end, we expressed these mutants in premigratory cranial neural crest cells and analyzed embryos for effects on neural crest cell EMT. Surprisingly, expression of the mutants caused no further effects on neural crest migration as compared with expression of wild-type Cad6B-HA. Although it is tempting to conclude that internalization mediated by these motifs does not play any role in neural crest cell EMT, we believe that this is not the case and that instead the technical limitations associated with our system preclude us from evaluating the true effect of these mutants on the EMT process. In summary, our work in Chapter 4 allowed us to functionally validate motifs in the cytoplasmic domain of Cad6B and demonstrate that the EED motif regulates Cad6B internalization.

In Chapter 5, we sought to determine the molecular pathway through which Cad6B is internalized. We noted partial co-localization of Cad6B (NT6B) with clathrin *in vitro* and *in vivo*, indicating that Cad6B likely undergoes some degree of clathrin-mediated endocytosis. The partial co-localization with clathrin, however, suggested the existence of

alternative pathway(s) for internalization of Cad6B. Taking into account our observation that Cad6B (NT6B) puncta were also at times positive for p120-catenin, a protein that normally dissociates from endocytosed cadherins, we strongly suspected that whole membranes containing Cad6B adherens junction complexes were being internalized through macropinocytosis, which has been noted in a few instances for E-cadherin *in vitro* (Paterson et al., 2003; Bryant et al., 2007; Solis et al., 2012). We tested this hypothesis by chemically inhibiting endocytosis and macropinocytosis in neural crest cell explants and analyzing these explants for changes in Cad6B (NT6B) distribution and EMT. Treatment with the actin polymerization inhibitor Latrunculin A, a broad spectrum inhibitor of several internalization pathways including macropinocytosis, resulted in a near complete loss of Cad6B (NT6B) puncta, corresponding with the persistence of plasma membrane-bound Cad6B (NT6B), and a loss of EMT. Further investigations with specific inhibitors such as Dynasore, a dynamin inhibitor, and EIPA, a macropinocytosis inhibitor, revealed the accumulation of large Cad6B (NT6B) puncta characteristic of macropinosomes and the absence of EMT. Taken together, we have now demonstrated for the first time that Cad6B undergoes internalization through a novel dynamin-dependent macropinocytic and clathrin-mediated endocytic pathways, and that this downreguation of Cad6B is critical for cranial neural crest cell EMT.

6.2. Significance

The dissertation has not only advanced our understanding of the molecular regulation of neural crest cell EMT but also adds evidence to the existence of uncommon pathways regulating cadherin proteins in an *in vivo* system. Specifically, this study is the first to

document the downregulation of a cadherin through macropinocytosis during any *in vivo* EMT and in any neural crest cell population. Earlier studies documented cadherin macropinocytosis solely in cell lines and in simulated conditions of cell migration such as wound healing assays (Paterson et al., 2003; Bryant et al., 2007; Solis et al., 2012). Moreover, by demonstrating a severe loss of neural crest cell EMT upon inhibition of macropinocytosis and dynamin-mediated internalization pathways, our work has provided a novel link between a cell biological process (Cad6B internalization) and an essential physiological outcome in vertebrates (neural crest cell EMT). At the molecular level, this dissertation also validates the importance of p120-catenin in regulating cadherin levels on cellular plasma membranes. Furthermore, our lab is the first to show the simultaneous existence, and importance, of both internalization (this dissertation) and proteolysis (Schiffmacher et al., 2014) to reduce levels of a cadherin *in vivo*. The use of macropinocytosis to reduce levels of cell surface cadherins *in vivo* during EMT now opens up interesting questions with respect to the existence and relevance of macropinocytosis in pathogenic conditions that rely upon EMT, such as cancer cell metastasis and fibrosis.

6.3. Future Directions

6.3.1. Coordination of Proteolysis and Internalization of Cad6B

An important question that remains is the temporal and spatial coordination of ADAM-mediated proteolysis and endocytic/macropinocytic internalization of Cad6B during neural crest cell EMT. Indeed, in the Cad6B antibody feeding assays, we notice puncta that are immunoreactive for the C-terminal Cad6B antibody but not for the N-terminal extracellular domain Cad6B antibody (Chapter 3, Fig. 3.7B”), suggesting that these could be C-terminal

Cad6B fragments generated post-ADAM-proteolysis. To test this requires co-treatment of neural crest cell explants with inhibitors of both ADAM proteases (e.g., GM6001, Marimastat) and endocytosis/macropinoctyosis (e.g., EIPA, Dynasore) and examination of Cad6B distribution. The lack of accumulation of large Cad6B puncta in the presence of ADAM inhibitors and EIPA or Dynasore would suggest that proteolytic cleavage is a requisite for endocytosis and/or macropinocytosis to occur. Conversely, ADAM-mediated proteolytic cleavage could be occurring post-endocytosis or –macropinocytosis. One caveat to this approach, however, is that the combinatorial treatment of explants with multiple inhibitors could be toxic. A better strategy might instead be to employ a combination of both genetic (e.g. CRISPR) and chemical disruption of these factors/pathways and evaluation of effects on Cad6B.

6.3.2. The fate of internalized Cad6B

Although we have demonstrated that Cad6B undergoes internalization through endocytosis and macropinocytosis, the fate of internalized Cad6B is still unknown. As described in Chapter 1, Section 1.6.2.3.2.1, internalized cadherins can be recycled to the plasma membrane or degraded in lysosomes. Since Cad6B is not observed in migratory cranial neural crest cells, one hypothesis is that it is likely degraded in lysosomes and/or by the proteasome. Inhibitor strategies in neural crest cell explants could be adopted again as described above, using agents that disrupt lysosomal or proteasomal activity in the presence or absence of endocytosis and macropinocytosis inhibitors, and changes in the distribution of Cad6B examined. Retention of Cad6B puncta in the presence of a lysosomal or

proteasomal inhibitor without an endocytosis/macropinocytosis inhibitor would directly demonstrate that Cad6B is degraded in lysosomes after internalization.

Interestingly, unpublished studies from our lab show that the C-terminal fragment of Cad6B that is generated upon Cad6B cleavage plays important roles in modulating neural crest cell EMT through transcriptional regulation of genes associated with EMT. Once again, it will be interesting to determine the role, if any, of the internalization mechanisms described herein during proteolysis and the generation of this soluble C-terminal Cad6B fragment. In addition, we observed that Cad6B-positive macropinosomes were not always positive for p120-catenin, suggesting that these p120-catenin molecules could be released and in turn play novel signaling roles to promote EMT. Combinatorial chemical inhibition of endocytosis/macropinocytosis and proteolysis/lysosomes will provide interesting results and further address these questions.

6.3.3. Molecular mechanisms regulating Cad6B macropinocytosis

As discussed in Chapter 5, macropinocytosis of cadherins is regulated by multiple factors, including Arf6, Rac1 and reggies/flottilins. Each of these molecules could be tested for their relevance in Cad6B macropinocytosis through the use of dominant active and dominant negative approaches. Indeed, our preliminary data through a chemical inhibitor of Rac1 show that it could potentially play a role in this process. A potential issue here, though, would be the ability to precisely and consistently target neural crest cells that are actively downregulating Cad6B. We hypothesize that expression of dominant active Arf6 or Rac1 would result in the accumulation of large Cad6B puncta, similar to what is

observed in the presence of EIPA. Conversely, expression of dominant negative Arf6 or Rac1 would result in inhibition of macropinocytosis and a loss of Cad6B puncta.

6.3.4. Other components of Cad6B-positive macropinosomes

The observation that whole Cad6B-containing adherens junctions undergo macropinocytosis opens up intriguing questions with respect to the composition of these Cad6B-positive macropinosomes. Do they contain other components of premigratory cranial neural crest cell adherens junctions, such as N- and/or E-cadherin? Our lab has also noted that loss of tight junction components is critical for neural crest cell EMT (Wu et al., 2011; Fishwick et al., 2012), so it would be interesting to determine whether tight junctions in premigratory cranial neural crest cells are internalized through similar pathways (Bruewer et al., 2005). Immunofluorescence could be performed for the known repertoire of cadherins and tight junction proteins expressed in premigratory cranial neural crest cells, such as N- and E-cadherin and claudin-1 (Dady et al., 2012; Fishwick et al., 2012), to address this question.

6.3.5. Upstream factors stimulating endocytosis and macropinocytosis

Once the molecular factor(s) controlling Cad6B macropinocytosis have been elucidated, the next step would be to determine the upstream signal(s) that stimulates this process. Clues to the identify of potential regulators emerge from studies examining the role of Annexin A1 in phagosomes during phagocytosis, a process similar to macropinocytosis (Patel et al., 2011). Here, the authors showed that Annexin A1 promotes F-actin polymerization near phagosomes in the presence of calcium. Furthermore, another

Annexin, Annexin A6, promotes clathrin-coated pit assembly by directly binding to the μ subunit of the AP2 adaptor protein (Creutz and Snyder, 2005). Interestingly, prior work from our lab showed that overexpression and knockdown of Annexin A6 in premigratory cranial neural crest cells causes premature loss and persistence of Cad6B, respectively (Wu and Taneyhill, 2012). Given our unpublished observations that Wnt regulates Annexin A6, and that *Snail2* is a Wnt target gene that is upregulated during cranial neural crest cell EMT, a mechanism that ultimately results in *en masse* downregulation of Cad6B can now be postulated (i.e., through Snail2 repression of *cad6B* at the transcriptional level and Cad6B protein post-translational proteolysis and internalization, the latter all regulated by Annexin A6). This hypothesis could be tested simply by overexpressing Annexin A6 in premigratory cranial neural crest cells, explanting premigratory neural crest cells and observing whether the number of the Cad6B puncta changes. A potential hurdle to this experiment could be the potential rapid downregulation of Cad6B upon overexpression of Annexin A6, thereby making it difficult to adequately capture the macropinosomes through confocal imaging. Knockdown of Annexin A6 could be employed as an alternative, as in this treatment macropinosomes should still form on the membrane but would fail to pinch off into the cytoplasm due to lack of F-actin polymerization. As a result, large Cad6B puncta may be observed, similar to what was noted after EIPA or Dynasore treatment.

6.3.6. Identification of additional Cad6B endocytosis motifs

Although we determined that Cad6B possesses a functional p120-catenin binding motif in its cytoplasmic domain, we were unable to observe any adverse effects on internalization of Cad6B upon mutation of the putative dileucine motif. Moreover, mutating the EED

residues also did not cause a complete abrogation of Cad6B-p120-catenin interaction biochemically. Considering the fact that loss of p120-catenin binding causes enhanced internalization of Cad6B, and that p120-catenin masks the dileucine motif recognized by AP2 adaptor proteins of the clathrin-mediated pathway, we can speculate that unknown motifs still exist within the region protected by p120-catenin in Cad6B, and that there are additional residues important for Cad6B-p120-catenin interaction. Cad6B constructs with individual and combinatorial point mutations in the Cad6B cytoplasmic domain must be generated and tested for difference in endocytosis to determine the exact motif(s) that is responsible for clathrin-mediated endocytosis.

6.3.7. Relevance of Cad6B internalization during neural crest cell EMT at other axial levels

Another question that requires addressing is the validity of these internalization mechanisms with respect to the regulation of Cad6B in neural crest cell populations at other axial levels, such as in the trunk and hindbrain. As described in Chapter 1, Section 1.6.2.2, Cad6B is not downregulated in the trunk but instead persists until early emigration and migration of neural crest cells into the mesenchyme (Park and Gumbiner, 2010), and migratory hindbrain neural crest cells also express Cad6B (T. Jen and A. Schiffmacher, HHMI project, unpublished). Although this suggests that the mechanisms underlying the downregulation of Cad6B could be different, our unpublished observations *in vivo* do provide evidence of Cad6B puncta in these other neural crest cell populations. Therefore, it is attractive to propose conservation of Cad6B internalization (and perhaps proteolysis)

mechanisms in these other neural crest cell populations, albeit with these post-translational processes being regulated differently in the hindbrain and trunk than in the crania.

In conclusion, this dissertation reveals that premigratory midbrain neural crest cells of the chick embryo downregulate the adherens junction protein Cad6B through a novel and uncommon pathway of macropinocytosis, in addition to clathrin-mediated endocytosis, and that disruption of these pathways inhibits neural crest cell EMT. This work provides important insights into the dynamic regulation of cadherins that is requisite for cell migration not only during neural crest cell EMT but also during normal embryonic development, tissue repair and pathological conditions. Our approach has direct biological relevance because it uses both *in vitro* and *in vivo* assays to establish cadherin internalization. Importantly, our data also integrate cell biology and physiology by revealing how a *cellular event*, the active down-regulation of a membrane protein, results in a *physiological event*, neural crest cell EMT and migration. Finally, our results urge for a critical rethink for how *in vivo* EMTs occur, including whether such uncommon pathways of protein internalization regulate EMTs associated with both development and disease.

Appendices

Appendix I

Table A1. Tested antibodies to endosomal markers that do not recognize their cognate antigen in chick tissue.

Antibody	Compartment	Company and catalog number	Immunogen	Percentage identity with chick antigen
EEA1	Early endosome	Abcam ab2900	Human; Around residues 1350	97%
Rab4	Early endosome	Millipore 07-655	Human; Full-length Rab4	98%
Rab7a	Late endosome	Abcam ab77993	Human; Amino acids 90-140	99%
Caveolin1	Caveolin-positive	Abcam ab2910	Human; Amino acids 1-17	76%
Rab11	Recycling endosome	Millipore 05-853	Human; Amino acids 86-207	99%
LAMP1	Lysosome	SCBT sc-8098	Human; C-terminus	95%

Fixation and permeabilization conditions tested:

1. 4% PFA for 20 minutes at room temperature or overnight at 4˚C. Permeabilization with 0.2% TX100 in TBS for 10 minutes at room temperature.
2. -20˚C 100% MeOH for 10 minutes at -20˚C; no permeabilization.
3. Ice-cold 5% Acetic Acid/ 95% Ethanol for 10 minutes at 4˚C; no permeabilization.

Appendix II: Endosomal marker-fluorescent protein fusions tested in the chick embryo.

The following constructs (obtained from Dr. Iqbal Hamza) were expressed in the chick embryo at trace levels (1μg/μl) along with sub-phenotypic levels of Cad6B-HA in the pCI-H2B-RFP backbone (0.8 μg/μl), with the following observations noted. Exogenous Cad6B-HA was introduced because of the challenges faced in detecting endogenous co-localization events in a small population of neural crest cells that is rapidly downregulating Cad6B.

Table A2. Endosomal marker-fluorescent protein fusions tested in the chick embryo and their co-localization with exogenous Cad6B-HA.

Expression construct	**Gene**	**Expression pattern**	**Distribution with respect to exogenously-expressed Cad6B**
pCLC-YFP	Human light chain clathrin	Ubiquitous (Fig. A2.1)	N/A
pCaveolin-GFP	Dog caveolin-1	Punctate	Co-localization (Fig. A2.2)
pGPI-GFP	GPI-GFP	Ubiquitous on the membrane	Ubiquitious membrane co-localization with Cad6B
pEGFP-N2-Lgp120	Rat LAMP1 (lysosome)	Punctate	No co-localization
pRab4-YFP	Dog Rab4 (Early endosome)	Ubiquitous	N/A
pRab5-YFP	Dog Rab5 (Early endosome)	Punctate	Co-localization
pRab7-YFP	Dog Rab7 (Late endosome)	Ubiquitous	N/A
pRab11-YFP	Dog Rab11 (Recycling endosome)	Ubiquitous	N/A
pUb-GFP	Ubiquitin	Ubiquitous	N/A

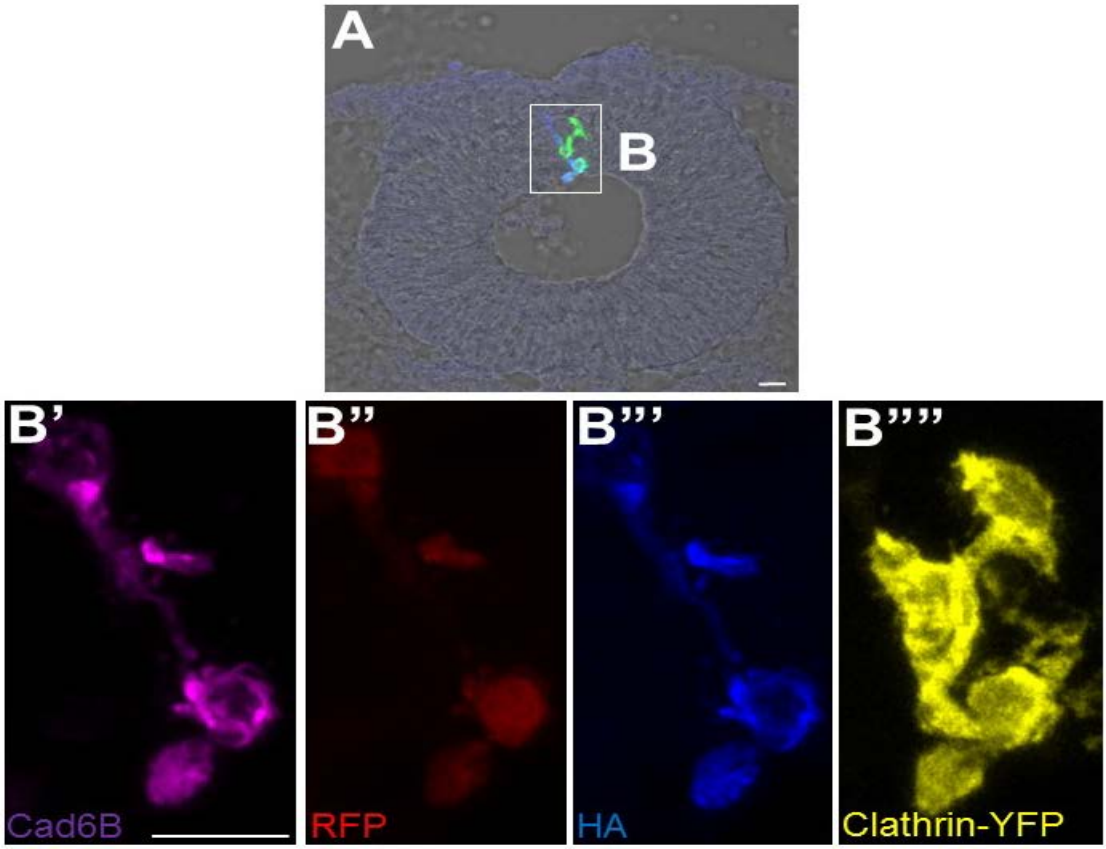

Figure A2.1. Example of expression constructs that exhibit non-specific localization in the chick. (A) Sub-phenotypic levels of clathrin-YFP and Cad6B-HA expression constructs were introduced into chick premigratory cranial neural crest cells. Embryos were incubated to EMT stages, fixed and immunostained for Cad6B, HA, and RFP. (B'-B'''') are higher magnification view of the boxed region in (A), where the exogenous constructs are expressed and neural crest cells are delaminating and undergoing EMT. The localization of clathrin-YFP is non-specific and thus appears diffuse throughout cells. Immunostaining for endogenous clathrin, however, reveals puncta that are at times positive for Cad6B *in vivo* (Figs. 5.1, 5.2). Similar localization patterns were observed for other constructs, as listed in Table A1. The images in (B'-B'''') represent the 3D composite of several Z-stack images acquired with a confocal microscope. Scale bars: 10μm.

Exogenous Cad6B-HA co-localized with caveolin1-eGFP in chick delaminating cranial neural crest cells (Fig. A2.2), suggesting that Cad6B could be internalized through caveolin-mediated endocytosis. Co-localization, however, was not observed *in vitro* in FlpInwtC6B-HA cell lines (Fig. A2.3) or on neural crest cell explants (Fig. A2.4), suggesting that the observed co-localization of exogenously-expressed Cad6B-HA and caveolin-1 could be due to elevated levels of these proteins (caveolin antibody failed to detect its cognate antigen in the chick tissue).

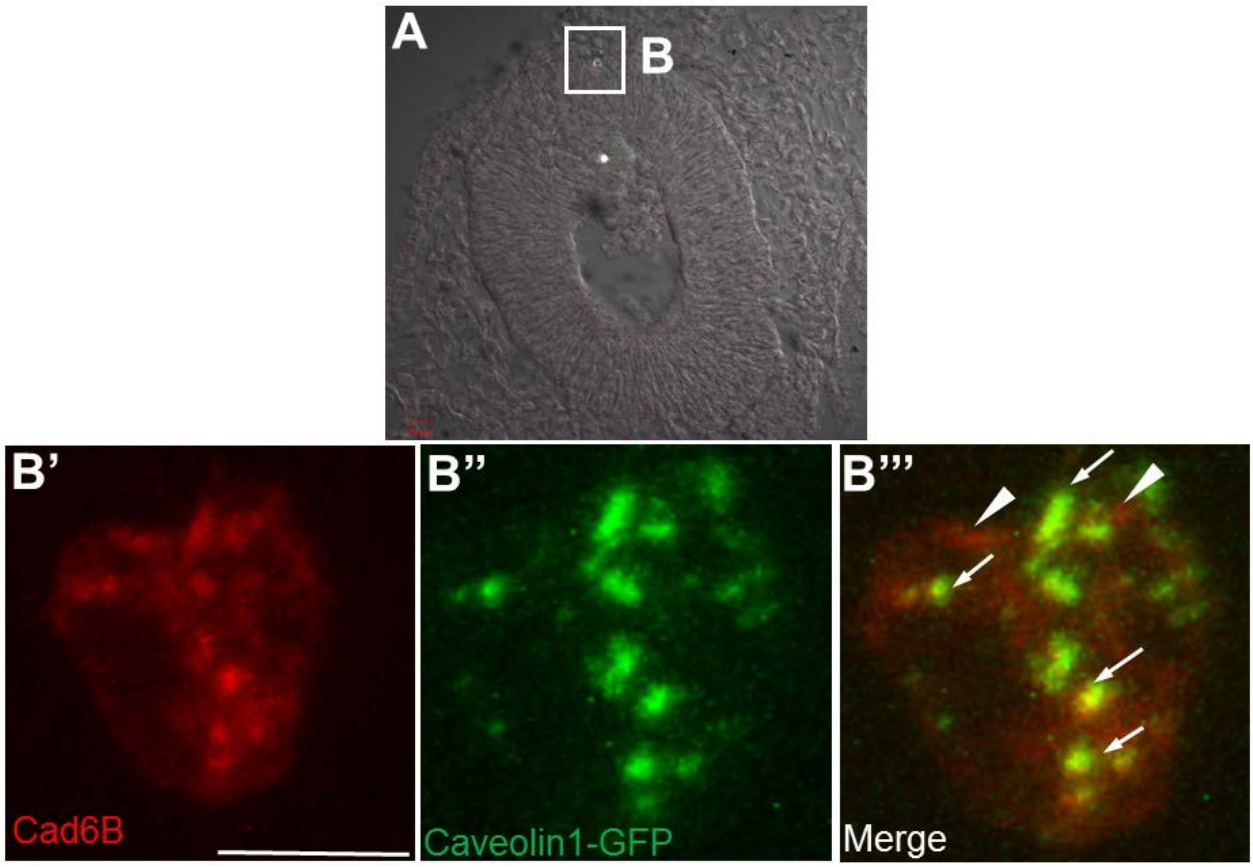

Figure A2.2. Exogenous Cad6B co-localizes with exogenous caveolin1-eGFP. (A) Sub-phenotypic levels of caveolin1-GFP and Cad6B-HA expression constructs were introduced into chick premigratory cranial neural crest cells. The embryos were incubated to EMT stages, fixed and then immunostained for Cad6B, HA and RFP. (B'-B''') are higher magnification view of the boxed region in (A), where the exogenous constructs are expressed and neural crest cells are delaminating and undergoing EMT. Exogenous Cad6B-HA partially co-localizes with caveolin1-eGFP (arrows and arrowheads represent co-localized and non-co-localized puncta, respectively). The images in (B'-B''') represent the 3D composite of several Z-stack images acquired with a confocal microscope. Scale bar: 5μm.

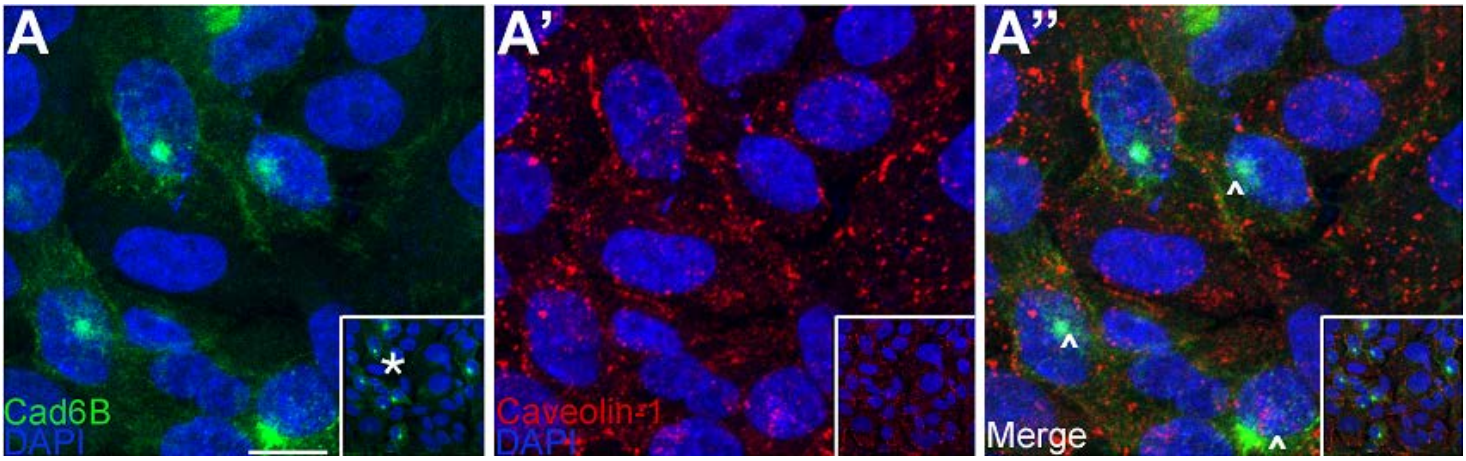

Figure A2.3. Cad6B-HA does not co-localize with endogenous caveolin-1 in FlpInwtC6B cells. FlpInwtC6B-HA cells were fixed and immunostained for endogenous Cad6B (NT6B; green) and caveolin-1 (red). Carets indicate Cad6B (NT6B) puncta that do not co-localize with caveolin-1. Images represent the 3D composite of several Z-stack images acquired with a confocal microscope. Inset boxes in (A-A") show the original image at 63x, with the asterisks in (A) indicating the location of the higher magnification field of view shown in the main panels. Scale bars: 10μm. Image reproduced from (Padmanabhan R, Taneyhill LA, under re-review at J Cell Sci).

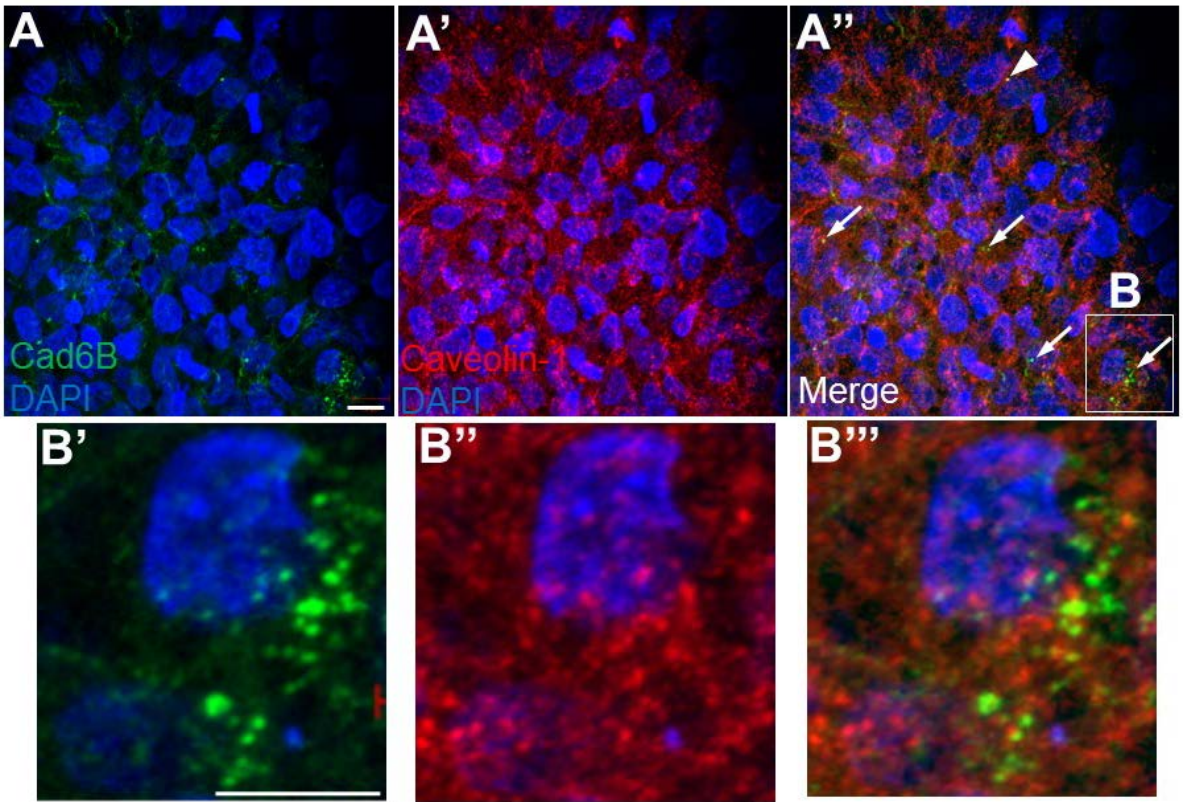

Figure A2.4. Cad6B does not co-localize with caveolin-1 in neural crest cell explant cultures. (A) Cranial dorsal neural folds possessing premigratory neural crest cells were explanted onto chamber slides, allowed to undergo EMT, fixed and immunostained for endogenous Cad6B (NT6B; green) and caveolin-1 (red). (B'-B''') are higher magnification views of the boxed region in (A''). Caveolin-1 in general does not co-localize with Cad6B (NT6B) (arrows in A'), but is rarely seen co-localizing (arrowheads in A). Images represent the 3D composite of several Z-stack images acquired with a confocal microscope. Scale bars: 10μm.

Appendix III: Mosaic nature of electroporation of the combination of Cad6B morpholino and wild-type or endocytosis-mutant Cad6B expression constructs.

Electroporation of Cad6B morpholinos, along with a wild-type or endocytosis mutant Cad6B-HA expression construct, is uneven, and both the number and location of cells receiving this combination are stochastic (Fig. A3.1)

Figure A3.1. Mosaic nature of electroporation of the combination of Cad6B morpholino (MO) and Cad6B-HA expression construct (wild-type or endocytosis mutant). 0.5mM Cad6B MO along with 1.5μg/μL pCIH2BRFP-Cad6B-HA or mutant Cad6B-HA expression construct was introduced unilaterally into premigratory neural crest cells, and embryos were harvested at stages when neural crest cells are undergoing EMT and cryosectioned transversely to reveal electroporation efficiency. Shown here are representative transverse sections of embryos with varying efficiencies of electroporation, irrespective of the construct electroporated. (A-A") represents an example where only Cad6B morpholino is electroporated (arrows), and (B-B") shows an example where only the expression construct is electroporated. (C-C") denotes an example where only cells in the dorsal neural tube cells are electroporated (arrows), and (D-D") is an example where only the dorsolateral and ventral cells of the neural tube are electroporated (arrows). Scale: 10μm.

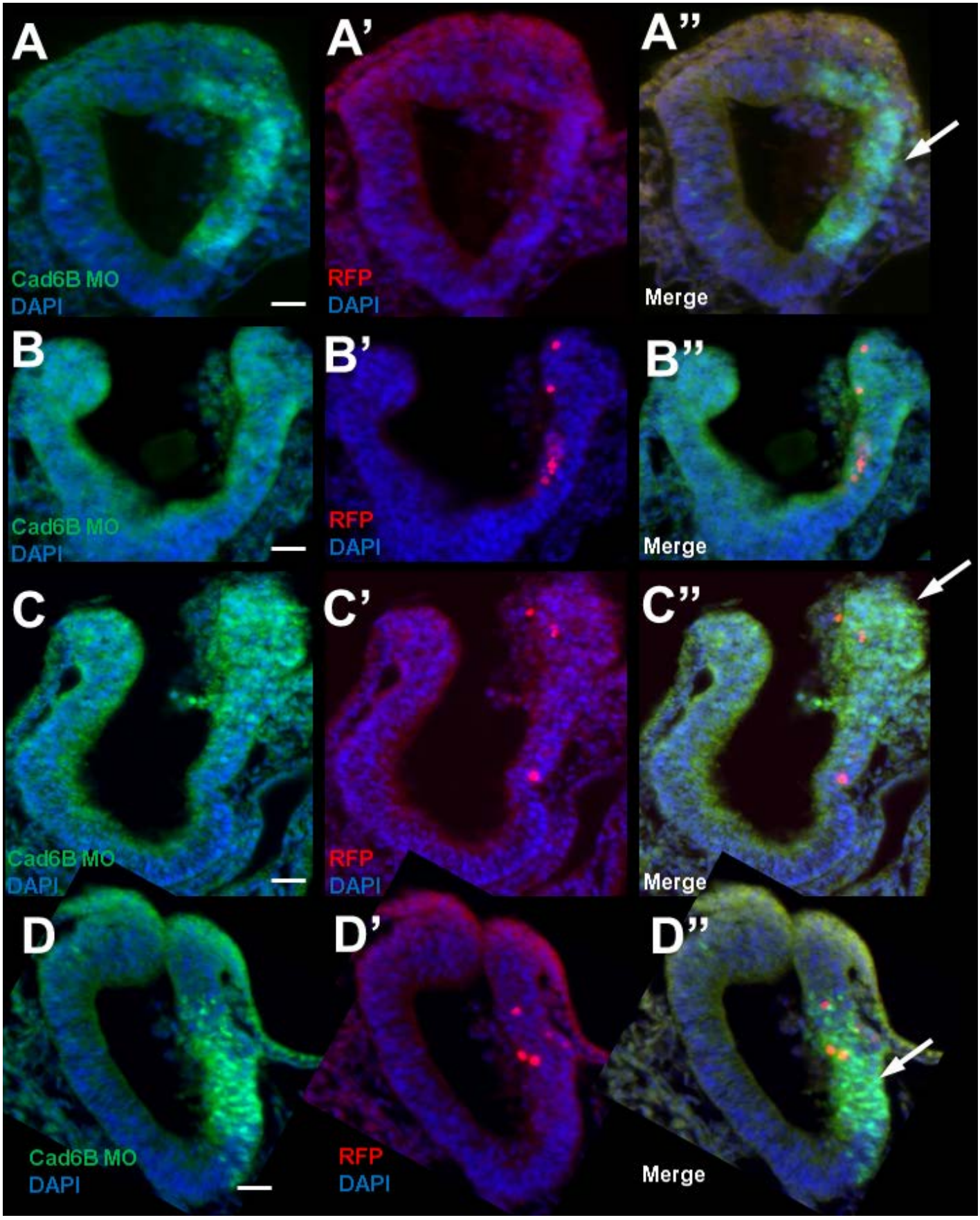
A
A'
A''
Cad6B MO
DAPI
RFP
DAPI
Merge
B
B'
B''
Cad6B MO
DAPI
RFP
DAPI
Merge
C
C'
C''
Cad6B MO
DAPI
RFP
DAPI
Merge
D
D'
D''
Cad6B MO
DAPI
RFP
DAPI
Merge

Bibliography

Adams, C. L., Chen, Y. T., Smith, S. J. and Nelson, W. J. (1998). Mechanisms of epithelial cell-cell adhesion and cell compaction revealed by high-resolution tracking of E-cadherin-green fluorescent protein. *The Journal of cell biology* **142**, 1105-1119.

Akhtar, N. and Hotchin, N. A. (2001). RAC1 regulates adherens junctions through endocytosis of E-cadherin. *Molecular biology of the cell* **12**, 847-862.

Angres, B., Barth, A. and Nelson, W. J. (1996). Mechanism for transition from initial to stable cell-cell adhesion: kinetic analysis of E-cadherin-mediated adhesion using a quantitative adhesion assay. *The Journal of cell biology* **134**, 549-557.

Arancibia-Carcamo IL, F. B., Moss SJ, Kittler JT. (2006). Studying the Localization, Surface Stability and Endocytosis of Neurotransmitter Receptors by Antibody Labeling and Biotinylation Approaches. In *The Dynamic Synapse: Molecular Methods in Ionotropic Receptor Biology* (ed. K. J. a. M. SJ), pp. 91: Taylor & Francis Group, LLC.

Bagheri-Fam, S., Barrionuevo, F., Dohrmann, U., Gunther, T., Schule, R., Kemler, R., Mallo, M., Kanzler, B. and Scherer, G. (2006). Long-range upstream and downstream enhancers control distinct subsets of the complex spatiotemporal Sox9 expression pattern. *Developmental biology* **291**, 382-397.

Bateman, J. and Van Vactor, D. (2001). The Trio family of guanine-nucleotide-exchange factors: regulators of axon guidance. *Journal of cell science* **114**, 1973-1980.

Batlle, E., Sancho, E., Franci, C., Dominguez, D., Monfar, M., Baulida, J. and Garcia De Herreros, A. (2000). The transcription factor snail is a repressor of E-cadherin gene expression in epithelial tumour cells. *Nature cell biology* **2**, 84-89.

Beel, A. J. and Sanders, C. R. (2008). Substrate specificity of gamma-secretase and other intramembrane proteases. *Cellular and molecular life sciences : CMLS* **65**, 1311-1334.

Bellovin, D. I., Bates, R. C., Muzikansky, A., Rimm, D. L. and Mercurio, A. M. (2005). Altered localization of p120 catenin during epithelial to mesenchymal transition of colon carcinoma is prognostic for aggressive disease. *Cancer research* **65**, 10938-10945.

Benmerah, A. and Lamaze, C. (2007). Clathrin-coated pits: vive la difference? *Traffic* **8**, 970-982.

Betancur, P., Bronner-Fraser, M. and Sauka-Spengler, T. (2010). Assembling neural crest regulatory circuits into a gene regulatory network. *Annual review of cell and developmental biology* **26**, 581-603.

BK, H. (2009). The Neural Crest and Neural Crest Cells in Vertebrate Development and Evolution: Springer.

Bolande, R. P. (1997). Neurocristopathy: its growth and development in 20 years. *Pediatric pathology & laboratory medicine : journal of the Society for Pediatric Pathology, affiliated with the International Paediatric Pathology Association* **17**, 1-25.

Bonifacino, J. S. and Traub, L. M. (2003). Signals for sorting of transmembrane proteins to endosomes and lysosomes. *Annual review of biochemistry* **72**, 395-447.

Borchers, A., David, R. and Wedlich, D. (2001). Xenopus cadherin-11 restrains cranial neural crest migration and influences neural crest specification. *Development* **128**, 3049-3060.

Braga, V. M., Del Maschio, A., Machesky, L. and Dejana, E. (1999). Regulation of cadherin function by Rho and Rac: modulation by junction maturation and cellular context. *Molecular biology of the cell* **10**, 9-22.

Bremm, A., Walch, A., Fuchs, M., Mages, J., Duyster, J., Keller, G., Hermannstadter, C., Becker, K. F., Rauser, S., Langer, R. et al. (2008). Enhanced activation of epidermal growth factor receptor caused by tumor-derived E-cadherin mutations. *Cancer research* **68**, 707-714.

Breviario, F., Caveda, L., Corada, M., Martin-Padura, I., Navarro, P., Golay, J., Introna, M., Gulino, D., Lampugnani, M. G. and Dejana, E. (1995). Functional properties of human vascular endothelial cadherin (7B4/cadherin-5), an endothelium-specific cadherin. *Arteriosclerosis, thrombosis, and vascular biology* **15**, 1229-1239.

Brieher, W. M., Yap, A. S. and Gumbiner, B. M. (1996). Lateral dimerization is required for the homophilic binding activity of C-cadherin. *The Journal of cell biology* **135**, 487-496.

Bronner-Fraser, M., Wolf, J. J. and Murray, B. A. (1992). Effects of antibodies against N-cadherin and N-CAM on the cranial neural crest and neural tube. *Developmental biology* **153**, 291-301.

Bruewer, M., Utech, M., Ivanov, A. I., Hopkins, A. M., Parkos, C. A. and Nusrat, A. (2005). Interferon-gamma induces internalization of epithelial tight junction proteins via a macropinocytosis-like process. *FASEB journal : official publication of the Federation of American Societies for Experimental Biology* **19**, 923-933.

Bryant, D. M., Wylie, F. G. and Stow, J. L. (2005). Regulation of endocytosis, nuclear translocation, and signaling of fibroblast growth factor receptor 1 by E-cadherin. *Molecular biology of the cell* **16**, 14-23.

Bryant, D. M., Kerr, M. C., Hammond, L. A., Joseph, S. R., Mostov, K. E., Teasdale, R. D. and Stow, J. L. (2007). EGF induces macropinocytosis and SNX1-modulated recycling of E-cadherin. *Journal of cell science* **120**, 1818-1828.

Cain, C. C., Sipe, D. M. and Murphy, R. F. (1989). Regulation of endocytic pH by the Na+,K+-ATPase in living cells. *Proceedings of the National Academy of Sciences of the United States of America* **86**, 544-548.

Canfield, W. M., Johnson, K. F., Ye, R. D., Gregory, W. and Kornfeld, S. (1991). Localization of the signal for rapid internalization of the bovine cation-independent mannose 6-phosphate/insulin-like growth factor-II receptor to amino acids 24-29 of the cytoplasmic tail. *The Journal of biological chemistry* **266**, 5682-5688.

Cano, A., Perez-Moreno, M. A., Rodrigo, I., Locascio, A., Blanco, M. J., del Barrio, M. G., Portillo, F. and Nieto, M. A. (2000). The transcription factor snail controls epithelial-mesenchymal transitions by repressing E-cadherin expression. *Nature cell biology* **2**, 76-83.

Casciola-Rosen, L. A. and Hubbard, A. L. (1992). Lumenal labeling of rat hepatocyte early endosomes. Presence of multiple membrane receptors and the Na+,K(+)-ATPase. *The Journal of biological chemistry* **267**, 8213-8221.

Cavey, M., Rauzi, M., Lenne, P. F. and Lecuit, T. (2008). A two-tiered mechanism for stabilization and immobilization of E-cadherin. *Nature* **453**, 751-756.

Chalpe, A. J., Prasad, M., Henke, A. J. and Paulson, A. F. (2010). Regulation of cadherin expression in the chicken neural crest by the Wnt/beta-catenin signaling pathway. *Cell adhesion & migration* **4**, 431-438.

Cheung, L. W., Leung, P. C. and Wong, A. S. (2010). Cadherin switching and activation of p120 catenin signaling are mediators of gonadotropin-releasing hormone to promote tumor cell migration and invasion in ovarian cancer. *Oncogene* **29**, 2427-2440.

Cheung, M., Chaboissier, M. C., Mynett, A., Hirst, E., Schedl, A. and Briscoe, J. (2005). The transcriptional control of trunk neural crest induction, survival, and delamination. *Developmental cell* **8**, 179-192.

Chiasson, C. M., Wittich, K. B., Vincent, P. A., Faundez, V. and Kowalczyk, A. P. (2009). p120-catenin inhibits VE-cadherin internalization through a Rho-independent mechanism. *Molecular biology of the cell* **20**, 1970-1980.

Chiasson CM, K. A. (2008). Cadherin Trafficking and Junction Dynamics. In *Cell Junctions: Adhesion, Development, and Disease* (ed. K. A. LaFlamme SE), pp. 251-270: Wiley.

Citi, S., Sabanay, H., Jakes, R., Geiger, B. and Kendrick-Jones, J. (1988). Cingulin, a new peripheral component of tight junctions. *Nature* **333**, 272-276.

Coles, E. G., Taneyhill, L. A. and Bronner-Fraser, M. (2007). A critical role for Cadherin6B in regulating avian neural crest emigration. *Developmental biology* **312**, 533-544.

Collinet, C. and Lecuit, T. (2013). Stability and dynamics of cell-cell junctions. *Progress in molecular biology and translational science* **116**, 25-47.

Cordenonsi, M., D'Atri, F., Hammar, E., Parry, D. A., Kendrick-Jones, J., Shore, D. and Citi, S. (1999). Cingulin contains globular and coiled-coil domains and interacts with ZO-1, ZO-2, ZO-3, and myosin. *The Journal of cell biology* **147**, 1569-1582.

Crane, J. F. and Trainor, P. A. (2006). Neural crest stem and progenitor cells. *Annual review of cell and developmental biology* **22**, 267-286.

Creutz, C. E. and Snyder, S. L. (2005). Interactions of annexins with the mu subunits of the clathrin assembly proteins. *Biochemistry* **44**, 13795-13806.

D'Atri, F. and Citi, S. (2001). Cingulin interacts with F-actin in vitro. *FEBS letters* **507**, 21-24.

D'Atri, F., Nadalutti, F. and Citi, S. (2002). Evidence for a functional interaction between cingulin and ZO-1 in cultured cells. *The Journal of biological chemistry* **277**, 27757-27764.

Dady, A., Blavet, C. and Duband, J. L. (2012). Timing and kinetics of E- to N-cadherin switch during neurulation in the avian embryo. *Developmental dynamics : an official publication of the American Association of Anatomists* **241**, 1333-1349.

Davidson, L. A. and Keller, R. E. (1999). Neural tube closure in Xenopus laevis involves medial migration, directed protrusive activity, cell intercalation and convergent extension. *Development* **126**, 4547-4556.

Davis, M. A., Ireton, R. C. and Reynolds, A. B. (2003). A core function for p120-catenin in cadherin turnover. *The Journal of cell biology* **163**, 525-534.

Deardorff, M. A., Tan, C., Saint-Jeannet, J. P. and Klein, P. S. (2001). A role for frizzled 3 in neural crest development. *Development* **128**, 3655-3663.

Delva, E., Jennings, J. M., Calkins, C. C., Kottke, M. D., Faundez, V. and Kowalczyk, A. P. (2008). Pemphigus vulgaris IgG-induced desmoglein-3 endocytosis and desmosomal disassembly are mediated by a clathrin- and dynamin-independent mechanism. *The Journal of biological chemistry* **283**, 18303-18313.

Detrick, R. J., Dickey, D. and Kintner, C. R. (1990). The effects of N-cadherin misexpression on morphogenesis in Xenopus embryos. *Neuron* **4**, 493-506.

Dixon, J., Jones, N. C., Sandell, L. L., Jayasinghe, S. M., Crane, J., Rey, J. P., Dixon, M. J. and Trainor, P. A. (2006). Tcof1/Treacle is required for neural crest cell formation and proliferation deficiencies that cause craniofacial abnormalities. *Proceedings of the National Academy of Sciences of the United States of America* **103**, 13403-13408.

Douarin NM, D. E. (2014). The Neural Crest, a Fourth Germ Layer of the Vertebrate Embryo: Significance in Chordate Evolution. In *Neural Crest Cells: Evolution, Development and Disease* (ed. P. Trainor), pp. 4-22: Elsevier.

Duband, J. L. (2010). Diversity in the molecular and cellular strategies of epithelium-to-mesenchyme transitions: Insights from the neural crest. *Cell adhesion & migration* **4**, 458-482.

Duband, J. L. and Thiery, J. P. (1982). Distribution of fibronectin in the early phase of avian cephalic neural crest cell migration. *Developmental biology* **93**, 308-323.

Duband, J. L., Volberg, T., Sabanay, I., Thiery, J. P. and Geiger, B. (1988). Spatial and temporal distribution of the adherens-junction-associated adhesion molecule A-CAM during avian embryogenesis. *Development* **103**, 325-344.

Dutton, K. A., Pauliny, A., Lopes, S. S., Elworthy, S., Carney, T. J., Rauch, J., Geisler, R., Haffter, P. and Kelsh, R. N. (2001). Zebrafish colourless encodes sox10 and specifies non-ectomesenchymal neural crest fates. *Development* **128**, 4113-4125.

Erickson, C. A. and Weston, J. A. (1983). An SEM analysis of neural crest migration in the mouse. *Journal of embryology and experimental morphology* **74**, 97-118.

Etchevers, H. C., Amiel, J. and Lyonnet, S. (2006). Molecular bases of human neurocristopathies. *Advances in experimental medicine and biology* **589**, 213-234.

Fairchild, C. L., Conway, J. P., Schiffmacher, A. T., Taneyhill, L. A. and Gammill, L. S. (2014). FoxD3 regulates cranial neural crest EMT via downregulation of tetraspanin18 independent of its functions during neural crest formation. *Mechanisms of development* **132**, 1-12.

Falcone, S., Cocucci, E., Podini, P., Kirchhausen, T., Clementi, E. and Meldolesi, J. (2006). Macropinocytosis: regulated coordination of endocytic and exocytic membrane traffic events. *Journal of cell science* **119**, 4758-4769.

Fanning, A. S., Jameson, B. J., Jesaitis, L. A. and Anderson, J. M. (1998). The tight junction protein ZO-1 establishes a link between the transmembrane protein occludin and the actin cytoskeleton. *The Journal of biological chemistry* **273**, 29745-29753.

Feldmann, T., Glukmann, V., Medvenev, E., Shpolansky, U., Galili, D., Lichtstein, D. and Rosen, H. (2007). Role of endosomal Na+-K+-ATPase and cardiac steroids in the regulation of endocytosis. *American journal of physiology. Cell physiology* **293**, C885-896.

Ferreri, D. M., Minnear, F. L., Yin, T., Kowalczyk, A. P. and Vincent, P. A. (2008). N-cadherin levels in endothelial cells are regulated by monolayer maturity and p120 availability. *Cell communication & adhesion* **15**, 333-349.

Fingleton, B. (2006). Matrix metalloproteinases: roles in cancer and metastasis. *Frontiers in bioscience : a journal and virtual library* **11**, 479-491.

Fishwick, K. J., Neiderer, T. E., Jhingory, S., Bronner, M. E. and Taneyhill, L. A. (2012). The tight junction protein claudin-1 influences cranial neural crest cell emigration. *Mechanisms of development*.

Fretz, M., Jin, J., Conibere, R., Penning, N. A., Al-Taei, S., Storm, G., Futaki, S., Takeuchi, T., Nakase, I. and Jones, A. T. (2006). Effects of Na+/H+ exchanger inhibitors on subcellular localisation of endocytic organelles and intracellular dynamics of protein transduction domains HIV-TAT peptide and octaarginine. *Journal of controlled release : official journal of the Controlled Release Society* **116**, 247-254.

Fuchs, R., Schmid, S. and Mellman, I. (1989). A possible role for Na+,K+-ATPase in regulating ATP-dependent endosome acidification. *Proceedings of the National Academy of Sciences of the United States of America* **86**, 539-543.

Fujimori, T., Miyatani, S. and Takeichi, M. (1990). Ectopic expression of N-cadherin perturbs histogenesis in Xenopus embryos. *Development* **110**, 97-104.

Fujita, Y., Krause, G., Scheffner, M., Zechner, D., Leddy, H. E., Behrens, J., Sommer, T. and Birchmeier, W. (2002). Hakai, a c-Cbl-like protein, ubiquitinates and induces endocytosis of the E-cadherin complex. *Nature cell biology* **4**, 222-231.

Furuse, M. (2010). Molecular basis of the core structure of tight junctions. *Cold Spring Harbor perspectives in biology* **2**, a002907.

Garcia-Castro, M. I., Marcelle, C. and Bronner-Fraser, M. (2002). Ectodermal Wnt function as a neural crest inducer. *Science* **297**, 848-851.

Gavard, J. and Gutkind, J. S. (2006). VEGF controls endothelial-cell permeability by promoting the beta-arrestin-dependent endocytosis of VE-cadherin. *Nature cell biology* **8**, 1223-1234.

Germanguz, I., Lev, D., Waisman, T., Kim, C. H. and Gitelman, I. (2007). Four twist genes in zebrafish, four expression patterns. *Developmental dynamics : an official publication of the American Association of Anatomists* **236**, 2615-2626.

Giannotta, M., Trani, M. and Dejana, E. (2013). VE-cadherin and endothelial adherens junctions: active guardians of vascular integrity. *Developmental cell* **26**, 441-454.

Girard, E., Paul, J. L., Fournier, N., Beaune, P., Johannes, L., Lamaze, C. and Vedie, B. (2011). The dynamin chemical inhibitor dynasore impairs cholesterol trafficking and sterol-sensitive genes transcription in human HeLa cells and macrophages. *PloS one* **6**, e29042.

Goodman, F. R. (2003). Congenital abnormalities of body patterning: embryology revisited. *Lancet* **362**, 651-662.

Grazia Lampugnani, M., Zanetti, A., Corada, M., Takahashi, T., Balconi, G., Breviario, F., Orsenigo, F., Cattelino, A., Kemler, R., Daniel, T. O. et al. (2003).

Contact inhibition of VEGF-induced proliferation requires vascular endothelial cadherin, beta-catenin, and the phosphatase DEP-1/CD148. *The Journal of cell biology* **161**, 793-804.

Grosheva, I., Shtutman, M., Elbaum, M. and Bershadsky, A. D. (2001). p120 catenin affects cell motility via modulation of activity of Rho-family GTPases: a link between cell-cell contact formation and regulation of cell locomotion. *Journal of cell science* **114**, 695-707.

Gumbiner, B., Lowenkopf, T. and Apatira, D. (1991). Identification of a 160-kDa polypeptide that binds to the tight junction protein ZO-1. *Proceedings of the National Academy of Sciences of the United States of America* **88**, 3460-3464.

Hall. (2008). The neural crest and neural crest cells: discovery and significance for theories of embryonic organization. *Journal of Bioscience* **33**, 781-793.

Hamburger, V. and Hamilton, H. L. (1992). A series of normal stages in the development of the chick embryo. 1951. *Developmental dynamics : an official publication of the American Association of Anatomists* **195**, 231-272.

Haskins, J., Gu, L., Wittchen, E. S., Hibbard, J. and Stevenson, B. R. (1998). ZO-3, a novel member of the MAGUK protein family found at the tight junction, interacts with ZO-1 and occludin. *The Journal of cell biology* **141**, 199-208.

Hatta, K. and Takeichi, M. (1986). Expression of N-cadherin adhesion molecules associated with early morphogenetic events in chick development. *Nature* **320**, 447-449.

Hay, E. D. (1995). An overview of epithelio-mesenchymal transformation. *Acta anatomica* **154**, 8-20.

Hay, E. D. (2005). The mesenchymal cell, its role in the embryo, and the remarkable signaling mechanisms that create it. *Developmental dynamics : an official publication of the American Association of Anatomists* **233**, 706-720.

Hayashida, K., Bartlett, A. H., Chen, Y. and Park, P. W. (2010). Molecular and cellular mechanisms of ectodomain shedding. *Anatomical record* **293**, 925-937.

Hewlett, L. J., Prescott, A. R. and Watts, C. (1994). The coated pit and macropinocytic pathways serve distinct endosome populations. *The Journal of cell biology* **124**, 689-703.

Hong, C. S., Park, B. Y. and Saint-Jeannet, J. P. (2008). Fgf8a induces neural crest indirectly through the activation of Wnt8 in the paraxial mesoderm. *Development* **135**, 3903-3910.

Hong, S., Troyanovsky, R. B. and Troyanovsky, S. M. (2010). Spontaneous assembly and active disassembly balance adherens junction homeostasis. *Proceedings of the National Academy of Sciences of the United States of America* **107**, 3528-3533.

Hopwood, N. D., Pluck, A. and Gurdon, J. B. (1989). A Xenopus mRNA related to Drosophila twist is expressed in response to induction in the mesoderm and the neural crest. *Cell* **59**, 893-903.

Hoshino, T., Sakisaka, T., Baba, T., Yamada, T., Kimura, T. and Takai, Y. (2005). Regulation of E-cadherin endocytosis by nectin through afadin, Rap1, and p120ctn. *The Journal of biological chemistry* **280**, 24095-24103.

Ikenouchi, J., Matsuda, M., Furuse, M. and Tsukita, S. (2003). Regulation of tight junctions during the epithelium-mesenchyme transition: direct repression of the gene expression of claudins/occludin by Snail. *Journal of cell science* **116**, 1959-1967.

Ikenouchi, J., Furuse, M., Furuse, K., Sasaki, H., Tsukita, S. and Tsukita, S. (2005). Tricellulin constitutes a novel barrier at tricellular contacts of epithelial cells. *The Journal of cell biology* **171**, 939-945.

Inoue, T., Chisaka, O., Matsunami, H. and Takeichi, M. (1997). Cadherin-6 expression transiently delineates specific rhombomeres, other neural tube subdivisions, and neural crest subpopulations in mouse embryos. *Developmental biology* **183**, 183-194.

Ireton, R. C., Davis, M. A., van Hengel, J., Mariner, D. J., Barnes, K., Thoreson, M. A., Anastasiadis, P. Z., Matrisian, L., Bundy, L. M., Sealy, L. et al. (2002). A novel role for p120 catenin in E-cadherin function. *The Journal of cell biology* **159**, 465-476.

Ishiyama, N., Lee, S. H., Liu, S., Li, G. Y., Smith, M. J., Reichardt, L. F. and Ikura, M. (2010). Dynamic and static interactions between p120 catenin and E-cadherin regulate the stability of cell-cell adhesion. *Cell* **141**, 117-128.

Itasaki, N., Bel-Vialar, S. and Krumlauf, R. (1999). 'Shocking' developments in chick embryology: electroporation and in ovo gene expression. *Nature cell biology* **1**, E203-207.

Ivanov. (2008). Pharmacological Inhibition of Endocytic Pathways: Is It Specific Enough to Be Useful? In *Exocytosis and Endocytosis* (ed. I. AI), pp. 15-33: Humana Press.

Ivanov, A. I., Nusrat, A. and Parkos, C. A. (2004). Endocytosis of epithelial apical junctional proteins by a clathrin-mediated pathway into a unique storage compartment. *Molecular biology of the cell* **15**, 176-188.

Izumi, G., Sakisaka, T., Baba, T., Tanaka, S., Morimoto, K. and Takai, Y. (2004). Endocytosis of E-cadherin regulated by Rac and Cdc42 small G proteins through IQGAP1 and actin filaments. *The Journal of cell biology* **166**, 237-248.

Jadot, M., Canfield, W. M., Gregory, W. and Kornfeld, S. (1992). Characterization of the signal for rapid internalization of the bovine mannose 6-phosphate/insulin-like growth factor-II receptor. *The Journal of biological chemistry* **267**, 11069-11077.

Jesuthasan, S. (1996). Contact inhibition/collapse and pathfinding of neural crest cells in the zebrafish trunk. *Development* **122**, 381-389.

Jhingory, S., Wu, C. Y. and Taneyhill, L. A. (2010). Novel insight into the function and regulation of alphaN-catenin by Snail2 during chick neural crest cell migration. *Developmental biology* **344**, 896-910.

Johnson, E., Seachrist, D. D., DeLeon-Rodriguez, C. M., Lozada, K. L., Miedler, J., Abdul-Karim, F. W. and Keri, R. A. (2010). HER2/ErbB2-induced breast cancer cell migration and invasion require p120 catenin activation of Rac1 and Cdc42. *The Journal of biological chemistry* **285**, 29491-29501.

Jones, N. C., Lynn, M. L., Gaudenz, K., Sakai, D., Aoto, K., Rey, J. P., Glynn, E. F., Ellington, L., Du, C., Dixon, J. et al. (2008). Prevention of the neurocristopathy Treacher Collins syndrome through inhibition of p53 function. *Nature medicine* **14**, 125-133.

Jovic, M., Sharma, M., Rahajeng, J. and Caplan, S. (2010). The early endosome: a busy sorting station for proteins at the crossroads. *Histology and histopathology* **25**, 99-112.

Kalluri, R. and Weinberg, R. A. (2009). The basics of epithelial-mesenchymal transition. *The Journal of clinical investigation* **119**, 1420-1428.

Kam, Y. and Quaranta, V. (2009). Cadherin-bound beta-catenin feeds into the Wnt pathway upon adherens junctions dissociation: evidence for an intersection between beta-catenin pools. *PloS one* **4**, e4580.

Kamei, T., Matozaki, T., Sakisaka, T., Kodama, A., Yokoyama, S., Peng, Y. F., Nakano, K., Takaishi, K. and Takai, Y. (1999). Coendocytosis of cadherin and c-Met coupled to disruption of cell-cell adhesion in MDCK cells--regulation by Rho, Rac and Rab small G proteins. *Oncogene* **18**, 6776-6784.

Karafiat, V., Dvorakova, M., Krejci, E., Kralova, J., Pajer, P., Snajdr, P., Mandikova, S., Bartunek, P., Grim, M. and Dvorak, M. (2005). Transcription factor c-Myb is involved in the regulation of the epithelial-mesenchymal transition in the avian neural crest. *Cellular and molecular life sciences : CMLS* **62**, 2516-2525.

Kartenbeck, J., Schmelz, M., Franke, W. W. and Geiger, B. (1991). Endocytosis of junctional cadherins in bovine kidney epithelial (MDBK) cells cultured in low Ca2+ ion medium. *The Journal of cell biology* **113**, 881-892.

Kashef, J., Kohler, A., Kuriyama, S., Alfandari, D., Mayor, R. and Wedlich, D. (2009). Cadherin-11 regulates protrusive activity in Xenopus cranial neural crest cells upstream of Trio and the small GTPases. *Genes & development* **23**, 1393-1398.

Kee, Y., Hwang, B. J., Sternberg, P. W. and Bronner-Fraser, M. (2007). Evolutionary conservation of cell migration genes: from nematode neurons to vertebrate neural crest. *Genes & development* **21**, 391-396.

Kerosuo, L. and Bronner-Fraser, M. (2012). What is bad in cancer is good in the embryo: importance of EMT in neural crest development. *Seminars in cell & developmental biology* **23**, 320-332.

Keyte, A. and Hutson, M. R. (2012). The neural crest in cardiac congenital anomalies. *Differentiation; research in biological diversity* **84**, 25-40.

Kintner, C. (1992). Regulation of embryonic cell adhesion by the cadherin cytoplasmic domain. *Cell* **69**, 225-236.

Kourtidis, A., Ngok, S. P. and Anastasiadis, P. Z. (2013). p120 catenin: an essential regulator of cadherin stability, adhesion-induced signaling, and cancer progression. *Progress in molecular biology and translational science* **116**, 409-432.

Kowalczyk, A. P. and Nanes, B. A. (2012). Adherens junction turnover: regulating adhesion through cadherin endocytosis, degradation, and recycling. *Sub-cellular biochemistry* **60**, 197-222.

Kowalczyk AP, G. K. (2014). Structure, Function, and Regulation of Desmosomes. In *Progresss in Molecular Biology and Translational Science: The Molecular Biology of Cadherins* (ed. V. R. F), pp. 95-119: Elsevier.

Krispin, S., Nitzan, E., Kassem, Y. and Kalcheim, C. (2010). Evidence for a dynamic spatiotemporal fate map and early fate restrictions of premigratory avian neural crest. *Development* **137**, 585-595.

LaBonne, C. and Bronner-Fraser, M. (1998). Neural crest induction in Xenopus: evidence for a two-signal model. *Development* **125**, 2403-2414.

LaBonne, C. and Bronner-Fraser, M. (2000). Snail-related transcriptional repressors are required in Xenopus for both the induction of the neural crest and its subsequent migration. *Developmental biology* **221**, 195-205.

Lagana, A., Vadnais, J., Le, P. U., Nguyen, T. N., Laprade, R., Nabi, I. R. and Noel, J. (2000). Regulation of the formation of tumor cell pseudopodia by the Na(+)/H(+) exchanger NHE1. *Journal of cell science* **113 (Pt 20)**, 3649-3662.

Larue, L., Ohsugi, M., Hirchenhain, J. and Kemler, R. (1994). E-cadherin null mutant embryos fail to form a trophectoderm epithelium. *Proceedings of the National Academy of Sciences of the United States of America* **91**, 8263-8267.

Le, T. L., Yap, A. S. and Stow, J. L. (1999). Recycling of E-cadherin: a potential mechanism for regulating cadherin dynamics. *The Journal of cell biology* **146**, 219-232.

Lee, R. T., Nagai, H., Nakaya, Y., Sheng, G., Trainor, P. A., Weston, J. A. and Thiery, J. P. (2013). Cell delamination in the mesencephalic neural fold and its implication for the origin of ectomesenchyme. *Development* **140**, 4890-4902.

Levayer, R., Pelissier-Monier, A. and Lecuit, T. (2011). Spatial regulation of Dia and Myosin-II by RhoGEF2 controls initiation of E-cadherin endocytosis during epithelial morphogenesis. *Nature cell biology* **13**, 529-540.

Levenberg, S., Yarden, A., Kam, Z. and Geiger, B. (1999). p27 is involved in N-cadherin-mediated contact inhibition of cell growth and S-phase entry. *Oncogene* **18**, 869-876.

Lewis, J. L., Bonner, J., Modrell, M., Ragland, J. W., Moon, R. T., Dorsky, R. I. and Raible, D. W. (2004). Reiterated Wnt signaling during zebrafish neural crest development. *Development* **131**, 1299-1308.

Liang, D., Wang, X., Mittal, A., Dhiman, S., Hou, S. Y., Degenhardt, K. and Astrof, S. (2014). Mesodermal expression of integrin alpha5beta1 regulates neural crest development and cardiovascular morphogenesis. *Developmental biology*.

Liem, K. F., Jr., Tremml, G. and Jessell, T. M. (1997). A role for the roof plate and its resident TGFbeta-related proteins in neuronal patterning in the dorsal spinal cord. *Cell* **91**, 127-138.

Liem, K. F., Jr., Tremml, G., Roelink, H. and Jessell, T. M. (1995). Dorsal differentiation of neural plate cells induced by BMP-mediated signals from epidermal ectoderm. *Cell* **82**, 969-979.

Linker, C., Bronner-Fraser, M. and Mayor, R. (2000). Relationship between gene expression domains of Xsnail, Xslug, and Xtwist and cell movement in the prospective neural crest of Xenopus. *Developmental biology* **224**, 215-225.

Lister, J. A., Cooper, C., Nguyen, K., Modrell, M., Grant, K. and Raible, D. W. (2006). Zebrafish Foxd3 is required for development of a subset of neural crest derivatives. *Developmental biology* **290**, 92-104.

Liu, J., Kesiry, R., Periyasamy, S. M., Malhotra, D., Xie, Z. and Shapiro, J. I. (2004). Ouabain induces endocytosis of plasmalemmal Na/K-ATPase in LLC-PK1 cells by a clathrin-dependent mechanism. *Kidney international* **66**, 227-241.

Liu, J., Liang, M., Liu, L., Malhotra, D., Xie, Z. and Shapiro, J. I. (2005). Ouabain-induced endocytosis of the plasmalemmal Na/K-ATPase in LLC-PK1 cells requires caveolin-1. *Kidney international* **67**, 1844-1854.

Lochter, A., Galosy, S., Muschler, J., Freedman, N., Werb, Z. and Bissell, M. J. (1997). Matrix metalloproteinase stromelysin-1 triggers a cascade of molecular alterations that leads to stable epithelial-to-mesenchymal conversion and a premalignant phenotype in mammary epithelial cells. *The Journal of cell biology* **139**, 1861-1872.

Lu, Z., Ghosh, S., Wang, Z. and Hunter, T. (2003). Downregulation of caveolin-1 function by EGF leads to the loss of E-cadherin, increased transcriptional activity of beta-catenin, and enhanced tumor cell invasion. *Cancer cell* **4**, 499-515.

Macia, E., Ehrlich, M., Massol, R., Boucrot, E., Brunner, C. and Kirchhausen, T. (2006). Dynasore, a cell-permeable inhibitor of dynamin. *Developmental cell* **10**, 839-850.

Maeda, M., Johnson, E., Mandal, S. H., Lawson, K. R., Keim, S. A., Svoboda, R. A., Caplan, S., Wahl, J. K., 3rd, Wheelock, M. J. and Johnson, K. R. (2006). Expression of inappropriate cadherins by epithelial tumor cells promotes endocytosis and degradation of E-cadherin via competition for p120(ctn). *Oncogene* **25**, 4595-4604.

Mansouri, M., Rose, P. P., Moses, A. V. and Fruh, K. (2008). Remodeling of endothelial adherens junctions by Kaposi's sarcoma-associated herpesvirus. *Journal of virology* **82**, 9615-9628.

Marambaud, P., Wen, P. H., Dutt, A., Shioi, J., Takashima, A., Siman, R. and Robakis, N. K. (2003). A CBP binding transcriptional repressor produced by the PS1/epsilon-cleavage of N-cadherin is inhibited by PS1 FAD mutations. *Cell* **114**, 635-645.

Marambaud, P., Shioi, J., Serban, G., Georgakopoulos, A., Sarner, S., Nagy, V., Baki, L., Wen, P., Efthimiopoulos, S., Shao, Z. et al. (2002). A presenilin-1/gamma-secretase cleavage releases the E-cadherin intracellular domain and regulates disassembly of adherens junctions. *The EMBO journal* **21**, 1948-1956.

Marchant, L., Linker, C., Ruiz, P., Guerrero, N. and Mayor, R. (1998). The inductive properties of mesoderm suggest that the neural crest cells are specified by a BMP gradient. *Developmental biology* **198**, 319-329.

Maretzky, T., Reiss, K., Ludwig, A., Buchholz, J., Scholz, F., Proksch, E., de Strooper, B., Hartmann, D. and Saftig, P. (2005). ADAM10 mediates E-cadherin shedding and regulates epithelial cell-cell adhesion, migration, and beta-catenin translocation. *Proceedings of the National Academy of Sciences of the United States of America* **102**, 9182-9187.

Martinsen, B. J. and Bronner-Fraser, M. (1998). Neural crest specification regulated by the helix-loop-helix repressor Id2. *Science* **281**, 988-991.

Mayor, R. and Theveneau, E. (2013). The neural crest. *Development* **140**, 2247-2251.

Mayor, R., Morgan, R. and Sargent, M. G. (1995). Induction of the prospective neural crest of Xenopus. *Development* **121**, 767-777.

Mayor, R., Guerrero, N. and Martinez, C. (1997). Role of FGF and noggin in neural crest induction. *Developmental biology* **189**, 1-12.

McGuire, J. K., Li, Q. and Parks, W. C. (2003). Matrilysin (matrix metalloproteinase-7) mediates E-cadherin ectodomain shedding in injured lung epithelium. *The American journal of pathology* **162**, 1831-1843.

Meng, W. and Takeichi, M. (2009). Adherens junction: molecular architecture and regulation. *Cold Spring Harbor perspectives in biology* **1**, a002899.

Mercer, J. and Helenius, A. (2009). Virus entry by macropinocytosis. *Nature cell biology* **11**, 510-520.

Mese, G., Richard, G. and White, T. W. (2007). Gap junctions: basic structure and function. *The Journal of investigative dermatology* **127**, 2516-2524.

Miranda, K. C., Khromykh, T., Christy, P., Le, T. L., Gottardi, C. J., Yap, A. S., Stow, J. L. and Teasdale, R. D. (2001). A dileucine motif targets E-cadherin to the basolateral cell surface in Madin-Darby canine kidney and LLC-PK1 epithelial cells. *The Journal of biological chemistry* **276**, 22565-22572.

Miyashita, Y. and Ozawa, M. (2007a). Increased internalization of p120-uncoupled E-cadherin and a requirement for a dileucine motif in the cytoplasmic domain for endocytosis of the protein. *The Journal of biological chemistry* **282**, 11540-11548.

Miyashita, Y. and Ozawa, M. (2007b). A dileucine motif in its cytoplasmic domain directs beta-catenin-uncoupled E-cadherin to the lysosome. *Journal of cell science* **120**, 4395-4406.

Mooren, O. L., Galletta, B. J. and Cooper, J. A. (2012). Roles for actin assembly in endocytosis. *Annual review of biochemistry* **81**, 661-686.

Mosesson, Y., Mills, G. B. and Yarden, Y. (2008). Derailed endocytosis: an emerging feature of cancer. *Nature reviews. Cancer* **8**, 835-850.

Muller, H. A. and Wieschaus, E. (1996). armadillo, bazooka, and stardust are critical for early stages in formation of the zonula adherens and maintenance of the polarized blastoderm epithelium in Drosophila. *The Journal of cell biology* **134**, 149-163.

Nakagawa, S. and Takeichi, M. (1995). Neural crest cell-cell adhesion controlled by sequential and subpopulation-specific expression of novel cadherins. *Development* **121**, 1321-1332.

Nakagawa, S. and Takeichi, M. (1998). Neural crest emigration from the neural tube depends on regulated cadherin expression. *Development* **125**, 2963-2971.

Nanes, B. A., Chiasson-MacKenzie, C., Lowery, A. M., Ishiyama, N., Faundez, V., Ikura, M., Vincent, P. A. and Kowalczyk, A. P. (2012). p120-catenin binding masks an endocytic signal conserved in classical cadherins. *The Journal of cell biology* **199**, 365-380.

Navarro, P., Ruco, L. and Dejana, E. (1998). Differential localization of VE- and N-cadherins in human endothelial cells: VE-cadherin competes with N-cadherin for junctional localization. *The Journal of cell biology* **140**, 1475-1484.

Nelms BL, L. P. (2010). Transcriptional Control of Neural Crest Development. In *Colloquium Series on Developmental Biology*: Morgan & Claypool Life Sciences.

Nichols, D. H. (1981). Neural crest formation in the head of the mouse embryo as observed using a new histological technique. *Journal of embryology and experimental morphology* **64**, 105-120.

Nieman, M. T., Kim, J. B., Johnson, K. R. and Wheelock, M. J. (1999). Mechanism of extracellular domain-deleted dominant negative cadherins. *Journal of cell science* **112 (Pt 10)**, 1621-1632.

Nieto, M. A. (2002). The snail superfamily of zinc-finger transcription factors. *Nature reviews. Molecular cell biology* **3**, 155-166.

Nieto, M. A., Sargent, M. G., Wilkinson, D. G. and Cooke, J. (1994). Control of cell behavior during vertebrate development by Slug, a zinc finger gene. *Science* **264**, 835-839.

Nikitina, N., Sauka-Spengler, T. and Bronner-Fraser, M. (2008). Dissecting early regulatory relationships in the lamprey neural crest gene network. *Proceedings of the National Academy of Sciences of the United States of America* **105**, 20083-20088.

O'Donnell, M., Hong, C. S., Huang, X., Delnicki, R. J. and Saint-Jeannet, J. P. (2006). Functional analysis of Sox8 during neural crest development in Xenopus. *Development* **133**, 3817-3826.

Oda, H. and Takeichi, M. (2011). Evolution: structural and functional diversity of cadherin at the adherens junction. *The Journal of cell biology* **193**, 1137-1146.

Orpen, N., Goodman, R., Bowker, C. and Lakhoo, K. (2003). Intralobar pulmonary sequestration with congenital cystic adematous malformation and rhabdomyomatous dysplasia. *Pediatric surgery international* **19**, 610-611.

Overduin, M., Harvey, T. S., Bagby, S., Tong, K. I., Yau, P., Takeichi, M. and Ikura, M. (1995). Solution structure of the epithelial cadherin domain responsible for selective cell adhesion. *Science* **267**, 386-389.

Palacios, F., Tushir, J. S., Fujita, Y. and D'Souza-Schorey, C. (2005). Lysosomal targeting of E-cadherin: a unique mechanism for the down-regulation of cell-cell adhesion during epithelial to mesenchymal transitions. *Molecular and cellular biology* **25**, 389-402.

Pandey, K. N. (2009). Functional roles of short sequence motifs in the endocytosis of membrane receptors. *Frontiers in bioscience* **14**, 5339-5360.

Park, K. S. and Gumbiner, B. M. (2010). Cadherin 6B induces BMP signaling and de-epithelialization during the epithelial mesenchymal transition of the neural crest. *Development* **137**, 2691-2701.

Park, K. S. and Gumbiner, B. M. (2012). Cadherin-6B stimulates an epithelial mesenchymal transition and the delamination of cells from the neural ectoderm via LIMK/cofilin mediated non-canonical BMP receptor signaling. *Developmental biology* **366**, 232-243.

Passos-Bueno, M. R., Ornelas, C. C. and Fanganiello, R. D. (2009). Syndromes of the first and second pharyngeal arches: A review. *American journal of medical genetics. Part A* **149A**, 1853-1859.

Patel, D. M., Ahmad, S. F., Weiss, D. G., Gerke, V. and Kuznetsov, S. A. (2011). Annexin A1 is a new functional linker between actin filaments and phagosomes during phagocytosis. *Journal of cell science* **124**, 578-588.

Paterson, A. D., Parton, R. G., Ferguson, C., Stow, J. L. and Yap, A. S. (2003). Characterization of E-cadherin endocytosis in isolated MCF-7 and chinese hamster ovary cells: the initial fate of unbound E-cadherin. *The Journal of biological chemistry* **278**, 21050-21057.

Perez-Alcala, S., Nieto, M. A. and Barbas, J. A. (2004). LSox5 regulates RhoB expression in the neural tube and promotes generation of the neural crest. *Development* **131**, 4455-4465.

Periyasamy, S. M., Liu, J., Tanta, F., Kabak, B., Wakefield, B., Malhotra, D., Kennedy, D. J., Nadoor, A., Fedorova, O. V., Gunning, W. et al. (2005). Salt loading induces redistribution of the plasmalemmal Na/K-ATPase in proximal tubule cells. *Kidney international* **67**, 1868-1877.

Piloto, S. and Schilling, T. F. (2010). Ovo1 links Wnt signaling with N-cadherin localization during neural crest migration. *Development* **137**, 1981-1990.

Pokutta, S., Herrenknecht, K., Kemler, R. and Engel, J. (1994). Conformational changes of the recombinant extracellular domain of E-cadherin upon calcium binding. *European journal of biochemistry / FEBS* **223**, 1019-1026.

Pon, Y. L., Auersperg, N. and Wong, A. S. (2005). Gonadotropins regulate N-cadherin-mediated human ovarian surface epithelial cell survival at both post-translational and transcriptional levels through a cyclic AMP/protein kinase A pathway. *The Journal of biological chemistry* **280**, 15438-15448.

Pond, L., Kuhn, L. A., Teyton, L., Schutze, M. P., Tainer, J. A., Jackson, M. R. and Peterson, P. A. (1995). A role for acidic residues in di-leucine motif-based targeting to the endocytic pathway. *The Journal of biological chemistry* **270**, 19989-19997.

Pujuguet, P., Del Maestro, L., Gautreau, A., Louvard, D. and Arpin, M. (2003). Ezrin regulates E-cadherin-dependent adherens junction assembly through Rac1 activation. *Molecular biology of the cell* **14**, 2181-2191.

Qian, X., Karpova, T., Sheppard, A. M., McNally, J. and Lowy, D. R. (2004). E-cadherin-mediated adhesion inhibits ligand-dependent activation of diverse receptor tyrosine kinases. *The EMBO journal* **23**, 1739-1748.

Radice, G. L., Rayburn, H., Matsunami, H., Knudsen, K. A., Takeichi, M. and Hynes, R. O. (1997). Developmental defects in mouse embryos lacking N-cadherin. *Developmental biology* **181**, 64-78.

Ragland, J. W. and Raible, D. W. (2004). Signals derived from the underlying mesoderm are dispensable for zebrafish neural crest induction. *Developmental biology* **276**, 16-30.

Rappoport, J. Z. (2008). Focusing on clathrin-mediated endocytosis. *The Biochemical journal* **412**, 415-423.

Reiprich, S., Stolt, C. C., Schreiner, S., Parlato, R. and Wegner, M. (2008). SoxE proteins are differentially required in mouse adrenal gland development. *Molecular biology of the cell* **19**, 1575-1586.

Reiss, K., Maretzky, T., Ludwig, A., Tousseyn, T., de Strooper, B., Hartmann, D. and Saftig, P. (2005). ADAM10 cleavage of N-cadherin and regulation of cell-cell adhesion and beta-catenin nuclear signalling. *The EMBO journal* **24**, 742-752.

Ridenour, D. A., McLennan, R., Teddy, J. M., Semerad, C. L., Haug, J. S. and Kulesa, P. M. (2014). The neural crest cell cycle is related to phases of migration in the head. *Development* **141**, 1095-1103.

Rodriguez, D., Morrison, C. J. and Overall, C. M. (2010). Matrix metalloproteinases: what do they not do? New substrates and biological roles identified by murine models and proteomics. *Biochimica et biophysica acta* **1803**, 39-54.

Rogers, C. D., Saxena, A. and Bronner, M. E. (2013). Sip1 mediates an E-cadherin-to-N-cadherin switch during cranial neural crest EMT. *The Journal of cell biology* **203**, 835-847.

Sadaghiani, B. and Thiebaud, C. H. (1987). Neural crest development in the Xenopus laevis embryo, studied by interspecific transplantation and scanning electron microscopy. *Developmental biology* **124**, 91-110.

Saint-Jeannet, J. P., He, X., Varmus, H. E. and Dawid, I. B. (1997). Regulation of dorsal fate in the neuraxis by Wnt-1 and Wnt-3a. *Proceedings of the National Academy of Sciences of the United States of America* **94**, 13713-13718.

Sakai, D., Suzuki, T., Osumi, N. and Wakamatsu, Y. (2006). Cooperative action of Sox9, Snail2 and PKA signaling in early neural crest development. *Development* **133**, 1323-1333.

Sakai, D., Tanaka, Y., Endo, Y., Osumi, N., Okamoto, H. and Wakamatsu, Y. (2005). Regulation of Slug transcription in embryonic ectoderm by beta-catenin-Lef/Tcf and BMP-Smad signaling. *Development, growth & differentiation* **47**, 471-482.

Sandoval, I. V., Martinez-Arca, S., Valdueza, J., Palacios, S. and Holman, G. D. (2000). Distinct reading of different structural determinants modulates the dileucine-

mediated transport steps of the lysosomal membrane protein LIMPII and the insulin-sensitive glucose transporter GLUT4. *The Journal of biological chemistry* **275**, 39874-39885.

Sasai, N., Mizuseki, K. and Sasai, Y. (2001). Requirement of FoxD3-class signaling for neural crest determination in Xenopus. *Development* **128**, 2525-2536.

Sauka-Spengler, T. and Bronner-Fraser, M. (2008). A gene regulatory network orchestrates neural crest formation. *Nature reviews. Molecular cell biology* **9**, 557-568.

Sauka-Spengler, T. and Bronner, M. (2010). Snapshot: neural crest. *Cell* **143**, 486-486 e481.

Schiffmacher, A. T., Padmanabhan, R., Jhingory, S. and Taneyhill, L. A. (2014). Cadherin-6B is proteolytically processed during epithelial-to-mesenchymal transitions of the cranial neural crest. *Molecular biology of the cell* **25**, 41-54.

Schnatwinkel, C., Christoforidis, S., Lindsay, M. R., Uttenweiler-Joseph, S., Wilm, M., Parton, R. G. and Zerial, M. (2004). The Rab5 effector Rabankyrin-5 regulates and coordinates different endocytic mechanisms. *PLoS biology* **2**, E261.

Schulz, B., Pruessmeyer, J., Maretzky, T., Ludwig, A., Blobel, C. P., Saftig, P. and Reiss, K. (2008). ADAM10 regulates endothelial permeability and T-Cell transmigration by proteolysis of vascular endothelial cadherin. *Circulation research* **102**, 1192-1201.

Sharma, M. and Henderson, B. R. (2007). IQ-domain GTPase-activating protein 1 regulates beta-catenin at membrane ruffles and its role in macropinocytosis of N-cadherin and adenomatous polyposis coli. *The Journal of biological chemistry* **282**, 8545-8556.

Shoval, I. and Kalcheim, C. (2012). Antagonistic activities of Rho and Rac GTPases underlie the transition from neural crest delamination to migration. *Developmental dynamics : an official publication of the American Association of Anatomists* **241**, 1155-1168.

Sleeman, J. P. and Thiery, J. P. (2011). SnapShot: The epithelial-mesenchymal transition. *Cell* **145**, 162 e161.

Solis, G. P., Schrock, Y., Hulsbusch, N., Wiechers, M., Plattner, H. and Stuermer, C. A. (2012). Reggies/flotillins regulate E-cadherin-mediated cell contact formation by affecting EGFR trafficking. *Molecular biology of the cell* **23**, 1812-1825.

Soo, K., O'Rourke, M. P., Khoo, P. L., Steiner, K. A., Wong, N., Behringer, R. R. and Tam, P. P. (2002). Twist function is required for the morphogenesis of the cephalic neural tube and the differentiation of the cranial neural crest cells in the mouse embryo. *Developmental biology* **247**, 251-270.

Spector, I., Shochet, N. R., Kashman, Y. and Groweiss, A. (1983). Latrunculins: novel marine toxins that disrupt microfilament organization in cultured cells. *Science* **219**, 493-495.

Stevenson, B. R., Siliciano, J. D., Mooseker, M. S. and Goodenough, D. A. (1986). Identification of ZO-1: a high molecular weight polypeptide associated with the tight junction (zonula occludens) in a variety of epithelia. *The Journal of cell biology* **103**, 755-766.

Steventon, B., Araya, C., Linker, C., Kuriyama, S. and Mayor, R. (2009). Differential requirements of BMP and Wnt signalling during gastrulation and neurulation define two steps in neural crest induction. *Development* **136**, 771-779.

Stewart, R. A., Arduini, B. L., Berghmans, S., George, R. E., Kanki, J. P., Henion, P. D. and Look, A. T. (2006). Zebrafish foxd3 is selectively required for neural crest specification, migration and survival. *Developmental biology* **292**, 174-188.

Strobl-Mazzulla, P. H. and Bronner, M. E. (2012). A PHD12-Snail2 repressive complex epigenetically mediates neural crest epithelial-to-mesenchymal transition. *The Journal of cell biology* **198**, 999-1010.

Swanson, J. A. (1989). Phorbol esters stimulate macropinocytosis and solute flow through macrophages. *Journal of cell science* **94 (Pt 1)**, 135-142.

Tai, C. Y., Mysore, S. P., Chiu, C. and Schuman, E. M. (2007). Activity-regulated N-cadherin endocytosis. *Neuron* **54**, 771-785.

Takai, Y., Ikeda, W., Ogita, H. and Rikitake, Y. (2008). The immunoglobulin-like cell adhesion molecule nectin and its associated protein afadin. *Annual review of cell and developmental biology* **24**, 309-342.

Takeichi, M. (1991). Cadherin cell adhesion receptors as a morphogenetic regulator. *Science* **251**, 1451-1455.

Taneyhill, L. A. (2008). To adhere or not to adhere: the role of Cadherins in neural crest development. *Cell adhesion & migration* **2**, 223-230.

Taneyhill, L. A., Coles, E. G. and Bronner-Fraser, M. (2007). Snail2 directly represses cadherin6B during epithelial-to-mesenchymal transitions of the neural crest. *Development* **134**, 1481-1490.

Taneyhill LA, P. R. (2014). The Cell Biology of Neural Crest Cell Delamination and EMT. In *Neural Crest Cells: Evolution, Development and Disease* (ed. P. Trainor), pp. 51-66: Elsevier.

Teng, L., Mundell, N. A., Frist, A. Y., Wang, Q. and Labosky, P. A. (2008). Requirement for Foxd3 in the maintenance of neural crest progenitors. *Development* **135**, 1615-1624.

Tepass, U. and Hartenstein, V. (1994). The development of cellular junctions in the Drosophila embryo. *Developmental biology* **161**, 563-596.

Theveneau, E. and Mayor, R. (2012). Neural crest delamination and migration: from epithelium-to-mesenchyme transition to collective cell migration. *Developmental biology* **366**, 34-54.

Theveneau, E., Duband, J. L. and Altabef, M. (2007). Ets-1 confers cranial features on neural crest delamination. *PloS one* **2**, e1142.

Thiery, J. P., Duband, J. L. and Delouvee, A. (1982). Pathways and mechanisms of avian trunk neural crest cell migration and localization. *Developmental biology* **93**, 324-343.

Thiery, J. P., Acloque, H., Huang, R. Y. and Nieto, M. A. (2009). Epithelial-mesenchymal transitions in development and disease. *Cell* **139**, 871-890.

Thisse, C., Thisse, B., Schilling, T. F. and Postlethwait, J. H. (1993). Structure of the zebrafish snail1 gene and its expression in wild-type, spadetail and no tail mutant embryos. *Development* **119**, 1203-1215.

Toyoshima, M., Tanaka, N., Aoki, J., Tanaka, Y., Murata, K., Kyuuma, M., Kobayashi, H., Ishii, N., Yaegashi, N. and Sugamura, K. (2007). Inhibition of tumor growth and metastasis by depletion of vesicular sorting protein Hrs: its regulatory role on E-cadherin and beta-catenin. *Cancer research* **67**, 5162-5171.

Troyanovsky, S. (2005). Cadherin dimers in cell-cell adhesion. *European journal of cell biology* **84**, 225-233.

Vallin, J., Girault, J. M., Thiery, J. P. and Broders, F. (1998). Xenopus cadherin-11 is expressed in different populations of migrating neural crest cells. *Mechanisms of development* **75**, 171-174.

Vallin, J., Thuret, R., Giacomello, E., Faraldo, M. M., Thiery, J. P. and Broders, F. (2001). Cloning and characterization of three Xenopus slug promoters reveal direct regulation by Lef/beta-catenin signaling. *The Journal of biological chemistry* **276**, 30350-30358.

Van de Putte, T., Maruhashi, M., Francis, A., Nelles, L., Kondoh, H., Huylebroeck, D. and Higashi, Y. (2003). Mice lacking ZFHX1B, the gene that codes for Smad-interacting protein-1, reveal a role for multiple neural crest cell defects in the etiology of Hirschsprung disease-mental retardation syndrome. *American journal of human genetics* **72**, 465-470.

Van Dyke, R. W. (2004). Heterotrimeric G protein subunits are located on rat liver endosomes. *BMC physiology* **4**, 1.

van Roy, F. (2014). Beyond E-cadherin: roles of other cadherin superfamily members in cancer. *Nature reviews. Cancer* **14**, 121-134.

Vandewalle, C., Comijn, J., De Craene, B., Vermassen, P., Bruyneel, E., Andersen, H., Tulchinsky, E., Van Roy, F. and Berx, G. (2005). SIP1/ZEB2 induces EMT by repressing genes of different epithelial cell-cell junctions. *Nucleic acids research* **33**, 6566-6578.

Villanueva, S., Glavic, A., Ruiz, P. and Mayor, R. (2002). Posteriorization by FGF, Wnt, and retinoic acid is required for neural crest induction. *Developmental biology* **241**, 289-301.

Wang, Q., Lu, T. L., Adams, E., Lin, J. L. and Lin, J. J. (2013). Intercalated disc protein, mXinalpha, suppresses p120-catenin-induced branching phenotype via its interactions with p120-catenin and cortactin. *Archives of biochemistry and biophysics* **535**, 91-100.

Wang, Z., Sandiford, S., Wu, C. and Li, S. S. (2009). Numb regulates cell-cell adhesion and polarity in response to tyrosine kinase signalling. *The EMBO journal* **28**, 2360-2373.

Watanabe, T., Sato, K. and Kaibuchi, K. (2009). Cadherin-mediated intercellular adhesion and signaling cascades involving small GTPases. *Cold Spring Harbor perspectives in biology* **1**, a003020.

Waterhouse, A. M., Procter, J. B., Martin, D. M., Clamp, M. and Barton, G. J. (2009). Jalview Version 2--a multiple sequence alignment editor and analysis workbench. *Bioinformatics* **25**, 1189-1191.

Wheelock, M. J., Buck, C. A., Bechtol, K. B. and Damsky, C. H. (1987). Soluble 80-kd fragment of cell-CAM 120/80 disrupts cell-cell adhesion. *Journal of cellular biochemistry* **34**, 187-202.

Wheelock, M. J., Shintani, Y., Maeda, M., Fukumoto, Y. and Johnson, K. R. (2008). Cadherin switching. *Journal of cell science* **121**, 727-735.

White JM, B. L., DeSimone DW, Tomczuk M, and Wolfsberg TG. (2005). Introduction to the ADAM family. In *The ADAM Family of Proteases: Proteases in Biology and Disease* (ed. H. N. a. L. V), pp. 1-28. Dordrecht, The Netherlands: Springer.

Wilkie, A. O. and Morriss-Kay, G. M. (2001). Genetics of craniofacial development and malformation. *Nature reviews. Genetics* **2**, 458-468.

Wilson, P. A. and Hemmati-Brivanlou, A. (1995). Induction of epidermis and inhibition of neural fate by Bmp-4. *Nature* **376**, 331-333.

Wittchen, E. S., Haskins, J. and Stevenson, B. R. (1999). Protein interactions at the tight junction. Actin has multiple binding partners, and ZO-1 forms independent complexes with ZO-2 and ZO-3. *The Journal of biological chemistry* **274**, 35179-35185.

Wu, C. Y. and Taneyhill, L. A. (2012). Annexin a6 modulates chick cranial neural crest cell emigration. *PloS one* **7**, e44903.

Wu, C. Y., Jhingory, S. and Taneyhill, L. A. (2011). The tight junction scaffolding protein cingulin regulates neural crest cell migration. *Developmental dynamics : an official publication of the American Association of Anatomists* **240**, 2309-2323.

Wu, J., Yang, J. and Klein, P. S. (2005). Neural crest induction by the canonical Wnt pathway can be dissociated from anterior-posterior neural patterning in Xenopus. *Developmental biology* **279**, 220-232.

Xiao, K., Allison, D. F., Kottke, M. D., Summers, S., Sorescu, G. P., Faundez, V. and Kowalczyk, A. P. (2003a). Mechanisms of VE-cadherin processing and degradation in microvascular endothelial cells. *The Journal of biological chemistry* **278**, 19199-19208.

Xiao, K., Allison, D. F., Buckley, K. M., Kottke, M. D., Vincent, P. A., Faundez, V. and Kowalczyk, A. P. (2003b). Cellular levels of p120 catenin function as a set point for cadherin expression levels in microvascular endothelial cells. *The Journal of cell biology* **163**, 535-545.

Xiao, K., Garner, J., Buckley, K. M., Vincent, P. A., Chiasson, C. M., Dejana, E., Faundez, V. and Kowalczyk, A. P. (2005). p120-Catenin regulates clathrin-dependent endocytosis of VE-cadherin. *Molecular biology of the cell* **16**, 5141-5151.

Xie, L. Q., Bian, L. J., Li, Z., Li, Y., Li, Z. X. and Li, B. (2010). Altered expression of E-cadherin by hepatocyte growth factor and effect on the prognosis of nasopharyngeal carcinoma. *Annals of surgical oncology* **17**, 1927-1936.

Yanagisawa, M. and Anastasiadis, P. Z. (2006). p120 catenin is essential for mesenchymal cadherin-mediated regulation of cell motility and invasiveness. *The Journal of cell biology* **174**, 1087-1096.

Yonemura, S. (2011). Cadherin-actin interactions at adherens junctions. *Current opinion in cell biology* **23**, 515-522.

Zhu, A. J. and Watt, F. M. (1996). Expression of a dominant negative cadherin mutant inhibits proliferation and stimulates terminal differentiation of human epidermal keratinocytes. *Journal of cell science* **109 (Pt 13)**, 3013-3023.